# A STUDY OF DIFFERENTIAL EQUATIONS POSSESSING EITHER TIME-VARYING COEFFICIENTS OR WEAK NONLINEARITIES. APPLICATION TO AN AEROTHERMOELASTIC PROBLEM

by

Eugene John Brunelle, Jr.

B.S.E. (Aero.) The University of Michigan, 1954
M.S.E. (Aero.) The University of Michigan, 1955

Submitted in Partial Fulfillment
of the Requirements for the
Degree of Doctor of Science

at the

MASSACHUSETTS INSTITUTE OF TECHNOLOGY
January, 1962

Signature of Author _____
Department of Aeronautics and
Astronautics, 1 January 1962

Certified by _____
Thesis Supervisor

Accepted by _____
Chairman, Departmental Committee
on Graduate Students

# A STUDY OF DIFFERENTIAL EQUATIONS POSSESSING EITHER TIME-VARYING COEFFICIENTS OR WEAK NONLINEARITIES. APPLICATION TO AN AEROTHERMOELASTIC PROBLEM

by

Eugene John Brunelle, Jr.

Submitted to the Department of Aeronautics and Astronautics on 1 January 1962 in partial fulfillment of the requirements for the degree of Doctor of Science.

## ABSTRACT

Part I of this thesis presents an engineering approach to the one and two degree of freedom study of both linear differential equations with time-varying coefficients and autonomous differential equations with constant coefficients containing weak nonlinearities. Approximate solutions of varying complexity and hence accuracy are presented for these equations and the results are qualitatively compared. In order to provide a convenient reference analysis for assessing aeroelastic examples of time-varying and nonlinear system behavior, a portion of this report is devoted to presenting the general features of a constant coefficient aeroelastic process in a nonclassical manner.

Part II of this thesis investigates the equations representing the dynamic, torsion-bending motion of a wing which is one major component of an ultra-high performance manned vehicle. Preliminary work required for this investigation is included as an integral part of

the report. This preliminary work includes the derivation of various impulse responses using the results of exact two-dimensional linearized supersonic aerodynamic theory for an accelerating unsteady supersonic rigid chord airfoil, and a derivation for the torsional stiffness loss of an aircraft wing that includes the effects of a specified time-dependent wall temperature due to the given flight mission and that includes the effects of mid-plane stretching.

The computer studies consider a "super X-15" type wing performing two specified flight missions and provide answers in the form of pitch and plunge impulse response time histories. The "exact" solutions are compared with two approximate solutions. The results of the comparisons indicate that a quasi-steady aerothermoelastic analysis is adequate for all manned vehicles of the foreseeable future. This statement does not apply to the dynamic stability analysis (rigid-body) of these vehicles since their lower rigid-body frequencies permit a moderate to strong coupling between the governing equations and their time-varying coefficients.

Thesis Supervisor: Raymond L. Bisplinghoff

Title: Professor of Aeronautics and Astronautics

## ACKNOWLEDGEMENTS

The author wishes to express his appreciation to the following persons: Professor Raymond L. Bisplinghoff who supervised the thesis, Mr. Doyle McClure and Mr. Garabed Zartarian who taught the author the principles of accelerating unsteady supersonic aerodynamics, Mrs. Evelyn Mack who programmed and supervised the intricate IBM 704 calculations, and Mrs. Grace Arnesen who so ably typed the manuscript.

Acknowledgement is made to the MIT Computation Center for its work, done as Problem M815.

A major portion of this thesis was prepared under the auspices of DSR Project 8132, sponsored by the Air Research and Development Command, United States Air Force, Wright Air Development Division, Contract No. AF33 (616)-6185, Project No. 1370, Task No. 13478.

# TABLE OF CONTENTS

Figures (Cont'd) — Page No.

Figures (Cont'd) Page No.

Figures (Cont'd) Page No.

Figures (Cont'd) — Page No.

## LIST OF PRINCIPAL SYMBOLS FOR PART I

| | |
|---|---|
| $a(t)$ | amplitude function |
| $a$ | free stream speed of sound |
| $b$ | semi-chord of airfoil |
| $\bar{h}$ | translational vertical displacement (positive down) |
| $m$ | mass/unit length |
| $p^n$ | $n^{\text{th}}$ time derivative $\frac{d^n}{dt^n}$ |
| $r_\alpha$ | radius of gyration |
| $t$ | time |
| $\widetilde{u^r(t_1)}$ | ensemble average of the $r^{\text{th}}$ power of u at time $t = t_1$ |
| $w(x,t)$ | transverse beam displacement (positive up) |
| $x,y$ | dimensionless displacement coordinates with respect to the length 2b |
| $x_o$ | dimensionless distance from the leading edge to the elastic axis |
| $x_1$ | dimensionless distance from the leading edge to the aileron hinge |
| $x_\alpha$ | dimensionless distance from the elastic axis to the center of gravity |
| $EI(x,t)$ | flexural rigidity |
| $F_z(x,t)$ | externally applied transverse force |
| $I_\alpha$ | wing cross-section moment of inertia about the elastic axis |

## LIST OF PRINCIPAL SYMBOLS FOR PART I (Continued)

| | |
|---|---|
| $I_\beta$ | aileron cross-section moment of inertia about the aileron hinge line |
| $\mathcal{Q}(t,\tau)$ | impulse response function |
| $L_i, \mathcal{L}_i$ | linear differential operators with time-varying coefficients |
| $M(x,t)$ | bending moment |
| $M_j(t)$ | generalized mass |
| $S(x,t)$ | shear |
| $S_\alpha$ | wing cross-section static unbalance about the elastic axis |
| $S_\beta$ | aileron cross-section static unbalance about the aileron hinge line |
| $T(x,t)$ | system period |
| $U$ | airspeed |
| $W[u_1,(t),u_2(t)]$ | Wronskian of the functions $u_1(t)$ and $u_2(t)$ |
| $W_i(x)$ | natural beam mode shapes |
| $\alpha$ | angle of attack (positive nose up) |
| $\beta$ | aileron deflection angle (positive trailing edge down) |
| $\delta(t-\tau)$ | Dirac delta function |
| $\mu$ | small parameter, mass density ratio |
| $\rho_\infty$ | free stream density |

## LIST OF PRINCIPAL SYMBOLS FOR PART I (Continued)

| | |
|---|---|
| $\tau$ | dummy time variable |
| $\varphi(t)$ | phase angle function |
| $\varphi_i(x)$ | normalized natural beam mode shapes |
| $\varphi_{uu}(t_1, t_2)$ | auto-correlation function |
| $\varphi_{uv}(t_1, t_2)$ | cross-correlation function |
| $\Psi$ | total phase angle |
| $\omega$ | oscillation frequency |
| $\omega_\alpha$ | wing pitching oscillation frequency |
| $\omega_\beta$ | aileron pitching oscillation frequency |
| $\omega_h$ | wing plunging oscillation frequency |
| $\underset{\sim}{\Xi}(t)$ | generalized force |
| $\Phi_{uu}(\omega)$ | power spectral density |
| $\Omega$ | frequency ratio |

## LIST OF PRINCIPAL SYMBOLS FOR PART II

| | |
|---|---|
| $a_\infty$ | free stream speed of sound |
| $b$ | airfoil semi-chord |
| $c_m$ | specific heat of the wing material |
| $h(t)$ | flight mission altitude |
| $\bar{h}(t)$ | vertical displacement of airfoil (plunging motion) |
| $h(y)$ | wing thickness |
| $h^*$ | heat transfer coefficient |
| $p_u$ $(L)$ | upper (lower) wing surface pressure |
| $p^n = \frac{d^n}{dt^n}$ | $n^{\underline{th}}$ order differential operator |
| $t$ | time; streamwise space variable for three dimensional wing |
| $w_a(x,t)$ | upwash on the airfoil surface |
| $x$ | dimensionless length with respect to 2b |
| $x_o$ | dimensionless distance from leading edge to elastic axis |
| $x_1$ | dimensionless distance from leading edge to aileron hinge line |
| $x,y,z$ | space variables |
| $A$ | value of constant forward acceleration |
| $\mathcal{F} = \frac{bA}{a_\infty^2}$ | Froude number |
| $GJ$ | iso-thermal torsional stiffness |

LIST OF PRINCIPAL SYMBOLS FOR PART II (Continued)

| | |
|---|---|
| $GJ_{EFF}$ | effective torsional stiffness |
| $I_\alpha$ | wing cross-section moment of inertia about the elastic axis |
| $L$ | wing lift |
| $L_c(\tau, t-\tau)$ | lift due to impulsive plunging motion |
| $L_\ell(\tau, t-\tau)$ | lift due to impulsive pitch rate about the airfoil leading edge |
| $M$ | Mach number |
| $\overline{M}$ | wing cross-section mass |
| $M^*(t)$ | thermal moment resultant acting on wing cross-section |
| $M_c(\tau, t-\tau)$ | moment due to impulsive plunging motion |
| $M_\ell(\tau, t-\tau)$ | moment due to impulsive pitch rate about the airfoil leading edge |
| $M_{x_o}$ | wing moment about the elastic axis |
| $M_{x_1}$ | wing moment about the aileron hinge line |
| $S_\alpha$ | wing cross-section static unbalance about the elastic axis |
| $T(y, z, t)$ | wing temperature at a point y, z at time t |
| $T_w(y, z, t)$ | wing equilibrium wall temperature |
| $T^*(t)$ | thermal force resultant acting on a wing cross-section |
| $\tau$ | torque due to thermal gradients and pre-twist |
| $\tau_t$ | total torque (Saint-Venant plus thermally induced torque) |
| $U$ | airspeed |

## LIST OF PRINCIPAL SYMBOLS FOR PART II (Continued)

| | |
|---|---|
| $\alpha_{(t)}$ | airfoil angle of attack |
| $\beta_{(t)}$ | aileron angle of attack relative to $\alpha(t)$ |
| $\gamma$ | specific heat |
| $\delta(t-\tau)$ | unit impulse function (Dirac delta function) |
| $\epsilon$ | width of upwash band on three dimensional wing |
| $\epsilon_x$ | total strain in X direction, including thermal effects |
| $\zeta, \eta, \tau$ | dummy integration variables |
| $\rho_m$ | wing mass density |
| $\rho_\infty$ | free stream density |
| $\sigma_x$ | total stress in X direction including thermal effects |
| $\varphi(x)$ | wing twist distribution |
| $\varphi(x,z,t)$ | velocity potential |
| $\omega_h$ | wing plunging oscillation frequency |
| $\omega_\alpha$ | wing pitching oscillation frequency |
| $\omega_\beta$ | aileron pitching oscillation frequency |
| $\textcircled{H}(t,y)$ | non-dimensional wing temperature |

# OBJECT

The object of this thesis is twofold. Firstly, to present an engineering approach to the one and two degree of freedom study of both linear differential equations with time-varying coefficients and autonomous differential equations with constant coefficients containing weak nonlinearities; secondly, to study the effects of time-varying parameters on the aerothermoelastic response of a high performance aircraft wing executing any given flight mission and to thus make recommendations concerning the least complicated analysis that adequately represents the wing motion.

# CHAPTER 1

# INTRODUCTION

Presently available methods of analyzing an aeroelastic system require that the physical system be represented by a set of linear simultaneous equations with constant coefficients. Although this requirement is apparently quite restrictive, experience has shown that this simple mathematical representation has been very satisfactory in predicting aeroelastic stability and response phenomena. The prime reasons for the success of this simplified mathematical representation are twofold. Firstly, the effects of nonlinearities have been virtually absent in the usual small deflection motion of most aircraft (or at worst the nonlinear effects assumed importance only after instability occurred in a linearized manner) thus obviating, from a conservative standpoint, the more involved mathematical representation.

Secondly, thrust/drag ratios of even modern operational aircraft are small enough to prevent large accelerations. Sequentially, the absence of large accelerations prevents large rates of fuel consumption and, usually, large rates of change in ambient state parameters (pressure, density, and temperature) and stiffness parameters. Hence, on qualitative physical grounds, it is reasonable to expect that the above mentioned simplified mathematical representation would be adequate.

However, consideration of highly accelerating anti-missile missiles and boost-glide vehicles operating in a high speed, high temperature environment raises serious questions as to the appli-

cability of the linear constant coefficient analysis, since it is easy to envision either large deflection motions due to combinations of high q and large transient stiffness losses, and/or large rates of change of mass, stiffness, and state parameters.

Therefore, it is the objective of Part I of this thesis to set forth an engineering approach to the one and two degree of freedom study of both simultaneous linear differential equations with time-varying coefficients and simultaneous autonomous differential equations with constant coefficients containing weak nonlinearities. In order to provide a convenient reference analysis for assessing aeroelastic examples of time-varying and nonlinear system behavior, Chapter 2 presents the general features of the constant coefficient aeroelastic process in a nonclassical manner. Chapters 3 and 4 then discuss equations with time-varying coefficients and Chapter 5 discusses equations with weak nonlinearities.

Part II of this thesis is concerned with formulating and analyzing, to several degrees of approximation, the bending-torsion response problem of a wing such as might be found on an ultra-high performance manned aircraft. To this end, Chapter 6 presents the required structural theory including aerothermoelastic effects in some detail, as well as presenting two alternate unsteady accelerating flow aerodynamic theories.

Chapters 7 and 8 present the details of the response problem and its solutions. The various solutions are then compared and discussed.

# PART I

## THEORETICAL CONSIDERATIONS

# CHAPTER 2

# TRANSIENT MOTION ANALYSIS OF CONSTANT COEFFICIENT SUPERSONIC AEROELASTIC SYSTEMS

## 2.1 Introduction

Although much effort has been concentrated on solving aeroelastic response and flutter problems during the last three decades, very little has been done to present the general aeroelastic features of even the simple typical section. This type of investigation has been primarily retarded by the complicated aerodynamic representations necessary to describe the lift and moment due to arbitrary motion.

However, as pointed out by Ashley and Zartarian (Ref. 1), the advent of piston theory aerodynamics removes this difficulty when considering a wide portion of the supersonic region, and in fact recasts the equations of motion into a form most suitable for obtaining the general features of the aeroelastic process. The first step in presenting these features consists of considering the degenerate system equations as the airspeed U approaches first zero and then infinity. This then permits the system to be classified as one of several types. The second step, for any specific system, involves computing the loci of all system roots using the airspeed U as a "gain" parameter. This is usually a rapid process, and when supplemented with a few additional computations yields a complete representation of the system's damped normal aeroelastic modes, the associated damping ratios and frequencies as well as a method for explicitly determining the violence with which the flutter mode

and the divergence mode appear. Hence, all the necessary information is available to perform any and all stability and response investigations. Furthermore, this essentially exact process permits one to make observations about the conditions under which simplified flutter theories such as the one advanced by Pines are valid, as well as fulfilling the original purpose of setting forth a convenient reference analysis for assessing supersonic aeroelastic examples including time-varying and nonlinear system behavior.

Before proceeding with the analysis it must be noted that, since piston theory is applicable only for a specified supersonic Mach number range, the locus of roots corresponding to velocities below and above this Mach number range are not quantitatively correct. However, with this in mind, no difficulties in interpreting the analysis should occur. It also should be noted that the airspeed U is not the only "gain" parameter available for computing the loci of the system roots. In fact any quantity one desires may be used for this purpose. For example, the density $\rho_\infty$ or the static unbalance $x_\alpha$ might have been chosen. However, even a cursory examination reveals that there is no computational advantage of using one quantity rather than another, so that the use of the airspeed U as the gain parameter simply reflects the author's preference for this quantity.

## 2.2 Presentation of the Equations of Motion, the Characteristic Equations of the Two Degree of Freedom Subsystems and the Examination of the Degenerate System Equations as $U \rightarrow 0$ and $U \rightarrow \infty$.

Incorporating the lift and moment expressions as given by the piston theory development of Chapter 6, the zero-thickness typical section equations of motion with three degrees of freedom (Figure 1) are given by,

$$(A_{11}p^2 + A_{12}p + A_{13})\bar{h} + (A_{14}p^2 + A_{15}p + UA_{16})\alpha + (A_{17}p^2 + A_{18}p + UA_{19})\beta = 0$$

$$(A_{21}p^2 + A_{22}p + A_{23})\bar{h} + (A_{24}p^2 + A_{25}p + A_{26} + UA_{26}^*)\alpha + (A_{27}p^2 + A_{28}p + UA_{29})\beta = 0$$

$$(A_{31}p^2 + A_{32}p + A_{33})\bar{h} + (A_{34}p^2 + A_{35}p + UA_{36})\alpha + (A_{37}p^2 + A_{38}p + A_{39} + UA_{39}^*)\beta = 0 \qquad (2-1)$$

where $p = \frac{d}{dt}$ and the $A_{ij}$'s have the following forms,

$A_{11} = m$ $\quad A_{21} = S_\alpha$ $\quad A_{31} = S_\beta$

$A_{12} = 4b\rho_\infty a_\infty$ $\quad A_{22} = 4b^2\rho_\infty a_\infty c$ $\quad A_{32} = 4b^2\rho_\infty a_\infty \ell$

$A_{13} = m\omega_h^2$ $\quad A_{23} = 0$ $\quad A_{33} = 0$

$A_{14} = S_\alpha$ $\quad A_{24} = I_\alpha$ $\quad A_{34} = I^*$

$A_{15} = 4b^2\rho_\infty a_\infty c$ $\quad A_{25} = -4b^3\rho_\infty a_\infty d$ $\quad A_{35} = \frac{8}{3}b^3\rho_\infty a_\infty Q_0$

$A_{16} = 4b\rho_\infty a_\infty$ $\quad A_{26} = I_\alpha\omega_\alpha^2$ $\quad A_{36} = 4b^2\rho_\infty a_\infty \ell$

$A_{26}^* = 4b^2\rho_\infty a_\infty c$

$A_{17} = S_\beta$ $\quad A_{27} = I^*$ $\quad A_{37} = I_\beta$

$A_{18} = 4b^2\rho_\infty a_\infty r^2$ $\quad A_{28} = \frac{8}{3}b^3\rho_\infty a_\infty Q_0$ $\quad A_{38} = \frac{16}{3}b^3\rho_\infty a_\infty Q_1$

$A_{19} = 4b\rho_\infty a_\infty r$ $\quad A_{29} = 4b^2\rho_\infty a_\infty r(c + x_1)$

$A_{39} = \omega_\beta^2 I_\beta$

$A_{39}^* = 4b^2\rho_\infty a_\infty r^2$

and additionally,

$$c = 1 - 2x_0 \qquad \ell = 1 - x_1(2 + x_1)$$

$$d = 4x_0(1 - x_0) - 4/3 \qquad Q_0 = 2 + x_1(x_1^2 - 3) - 3x_0(1 - x_1)^2$$

$$I^* = I_\beta + 2S_\beta b(x_1 - x_0) \qquad Q_1 = 1 - x_1^3 - 3x_1(1 - x_1)$$

$$r = 1 - x_1$$

With these equations established, it is now possible to examine the system behavior by probing the system's characteristic equation. However, in order to clearly present the tools used in examining the system, attention will be focused on the subsystem characteristic equations describing the bending-torsion, the bending-aileron, and the torsion-aileron motions as listed below. Again, denoting $\frac{d^n}{dt^n}$ by $p^n$, one has

Bending-Torsion Characteristic Equation:

$$(A_{11}p^2 + A_{12}p + A_{13})(A_{24}p^2 + A_{25}p + A_{26} + A_{26}^*U) - (A_{14}p^2 + A_{15}p + UA_{16})(A_{21}p + A_{22})p = 0 \qquad (2-2)$$

Bending-Aileron Characteristic Equation:

$$(A_{11}p^2 + A_{12}p + A_{13})(A_{37}p^2 + A_{38}p + A_{39} + A_{39}^*U) - (A_{17}p^2 + A_{18}p + A_{19}U)(A_{31}p + A_{32})p = 0 \qquad (2-3)$$

Torsion-Aileron Characteristic Equation:

$$(A_{24}p^2 + A_{25}p + A_{26} + A_{26}^*U)(A_{37}p^2 + A_{38}p + A_{39} + A_{39}^*U)$$

$$- (A_{27}p^2 + A_{28}p + A_{29}U)(A_{34}p^2 + A_{35}p + A_{36}U) = 0 \qquad (2-4)$$

Briefly, the procedure is now to first let $U \rightarrow 0$ and determine the roots of the resulting system and then secondly let $U \rightarrow \infty$ and determine all finite roots of this resulting system. These roots, symbolically denoted as $\left\{ \sigma(U) + j\omega(U) \right\}_{\substack{U \rightarrow 0 \\ \text{or} \\ U \rightarrow \infty}}$ **, are plotted on a complex $\sigma$, $j\omega$ plane. Then using some techniques developed by W. R. Evans for control-system analysis (for example, see Reference 2) it is very easy to find the angles at which the loci of roots in the complex plane depart from their values at $U = 0$ (hereafter called "asymptotes at $\infty$"). These rapid calculations immediately give a qualitative description of how the loci of the system roots will behave in the complex plane as U is increased from 0 to $\infty$.

At this point it is instructive to look at the degenerate equations contained in Eq. (2 - 2) and Eq. (2 - 4). Note that Eq. (2 - 3) is not considered separately since it has exactly the same form as Eq. (2 - 2). As $U \rightarrow 0$ both equations retain their fourth-degree character and yield four roots for each equation. These roots will be complex conjugate pairs. The resulting forms are shown in Eqs. (2 - 5) and (2 - 6).

---

** This symbolism assumes that all other system constants are determined and only U is a variable.

Bending-Torsion Characteristic Equation as $U \longrightarrow 0$

$$(A_{11}p^2 + A_{12}p + A_{13})(A_{24}p^2 + A_{25}p + A_{26}) - (A_{14}p + A_{15})(A_{21}p + A_{22})p^2 = 0 \qquad (2-5)$$

Torsion-Aileron Characteristics Equation as $U \longrightarrow 0$

$$(A_{24}p^2 + A_{25}p + A_{26})(A_{37}p^2 + A_{38}p + A_{39}) - (A_{27}p + A_{28})(A_{34}p + A_{35})p^2 = 0 \qquad (2-6)$$

Similarly, as $U \longrightarrow \infty$, the resulting forms are shown below.

Bending-Torsion Characteristic Equation as $U \longrightarrow \infty$

$$(A_{26}^* A_{11} - A_{16}A_{21})p^2 + A_{26}^* A_{13} = 0 \qquad (2-7)$$

Torsion-Aileron Characteristic Equation as $U \longrightarrow \infty$

$$\lim_{U \to \infty} \left\{ (A_{24}A_{39}^* + A_{37}A_{26}^* - A_{27}A_{36} - A_{29}A_{34})p^2 + (A_{25}A_{39}^* + A_{38}A_{26}^* - A_{28}A_{36} - A_{29}A_{35})p + (A_{26}A_{39}^* + A_{39}A_{26}^*) + (A_{26}^* A_{39}^* - A_{29}A_{36})U \right\} = 0 \qquad (2-8)$$

It is to be noted from the two equations above that finite as well as infinite roots can exist, the sum of both types being equal to the degree of the original characteristic equation in question. Furthermore, the magnitudes of the various $A_{ij}$'s determine whether the finite roots are real, imaginary, complex, or if in fact they exist at all. For completeness, special mention must be made about the form of Eq. (2 - 8). This form implies that if $(A_{26}*A_{39}* - A_{29}A_{36})$ is equal to zero, then two finite roots exist. Conversely, if this term is not equal to zero (as will be the usual case), then all roots are infinite as $U \rightarrow \infty$. One now knows where the loci of roots start and terminate as a function of some given $A_{ij}$'s. As discussed previously, when supplemented with the "break-away angles" and the "asymptotes at $\infty$", an excellent qualitative estimate of the system behavior is thus obtained. Hence, it is felt that a meaningful classification of the physical systems represented is to state the type of system roots that arise as $U \rightarrow \infty$.

In the next section, two examples are presented so that step-by-step inspection may be made of the ideas presented in this section as well as obtaining the actual modes, frequencies, damping ratios, and flutter and divergence sensitivities.

## 2.3 Investigation of the System Roots for Two Bending-Torsion Aeroelastic Systems

In order to facilitate computations the following definitions are introduced:

$$\epsilon^* = \frac{a_\infty}{\mu b \omega_\alpha} \qquad h = \bar{h}/b \qquad x_\alpha = S_\alpha/mb$$

$$t^* = \omega_\alpha t \text{ where } t \text{ is real time} \qquad \mu = m/4p_\infty b^2 \qquad r_\alpha^2 = I_\alpha/mb^2$$

$$p^n = \frac{d^n}{dt^n} = \omega_\alpha^n \frac{d^n}{dt^{*n}} \qquad \Omega^2 = (\omega_h/\omega_\alpha)^2 \qquad U^* = U/b\omega_\alpha$$

$$= \omega_\alpha^n s^n$$

With this notation, Eq. (2 - 2) can be written as follows:

$$-\left(\frac{r_\alpha}{x_\alpha}\right)^2 (s^2 + \epsilon^* s + \Omega^2)\left(s^2 - \frac{\epsilon^* d}{r_\alpha^2} s + 1\right) + s^2\left(s + \frac{\epsilon^* c}{x_\alpha}\right)^2 + \frac{\epsilon^* U^*}{x^2_\alpha}\left[(x_\alpha - c)s^2 - \Omega^2 c\right] = 0 \qquad (2 - 9)$$

Notice that the term $(x_\alpha - c)s^2 - \Omega^2 c$ entirely controls the behavior of the system as $U \rightarrow \infty$; the dimensional counterparts of c and $x_\alpha$ (bc and $bx_\alpha$) within this term having the following physical meanings. The quantity bc represents the distance from the elastic axis to the midchord (the midchord being almost coincident with the aerodynamic center for supersonic aircraft) and the quantity $bx_\alpha$ represents the distance from the elastic axis to the center of gravity. These quantities are thus measures of the aerodynamic coupling and the mass coupling present in the system, respectively. Hence the above term demonstrates that the system behavior is significantly influenced by whether $c(x_\alpha - c)^{-1} \gtreqless 0$. In fact, in a later section it will be hypothesized that only for systems in which $c \cong x_\alpha$, in which the roots initially approach one another, and in which $\epsilon^*$ is not a large number does the so-called Pines' method have any predictable success in approximating bending-torsion flutter speeds and frequencies. Referring to Figure 2, the boxed-in rectangular portion of the $x_\alpha$, $x_0$ plane represents fairly typical values of these variables for modern aircraft, while the sloping line represents the $x_\alpha = c$ condition. Thus the shaded area represents the region in which our hypothesis predicts the validity of Pines' method.

Returning to the main theme of this section, the two examples chosen have identical parameters except those that involve $x_0$ and $x_\alpha$. These systems will be labelled (A) and (B) and analyzed in separate subsections that follow.

2.3.1 Analysis of System A

The constants involved in system A are

$x_0 = .40$ $\quad\quad$ $\mu = 50$

$x_\alpha = .20$ $\quad\quad$ $b = 4$

$r_\alpha^2 = .25$ $\quad\quad$ $a_\infty = 972$

$b\omega_\alpha / a_\infty = .238$ $\quad\quad$ $\Omega^2 = .25$

thus Eq. (2 - 9) becomes

$$-6.25(s^2 + .084s + .25)(s^2 + .1254s + 1) + s^2(s + .084)^2 - .105U^* = 0 \qquad (2\text{-}10)$$

Following the usual procedure in the "root locus" technique the terms not containing U* are factored by a rapid graphical technique to yield,

$$(s + .043 \pm .496i)(s + .066 \pm 1.115i) + .02U^* = 0 \qquad (2 - 11)$$

Hence the roots at U = 0 are given by the two bracket terms and the roots at U = ∞ are obviously infinite. Once again utilizing the "root locus" technique, a graph may be obtained of the actual system roots as a function of the airspeed U. The result is shown in Figure 3. Notice that the loci of roots yield the frequency and damping terms, as illustrated in Figure 4, for the damped, normal, aeroelastic modes of the system. Now by cross-plotting the damping ratio $\zeta$ versus the airspeed U, the degree of violence with which the flutter mode becomes established is illustrated in Figure 5. It is seen that the rate of damping loss increases rapidly as $U \rightarrow U_{flutter}$. This indicates a violent flutter, since a small increment in airspeed

above the flutter speed then predicates a substantial growth of the wing oscillation amplitudes in a very short time.

Finally, it is also possible to calculate the mode shapes for any given U. This is accomplished by first considering $\alpha$ as a unit vector $e^{io}$ and then obtaining the root $p = \sigma + j\omega$ for a particular value of U, from Figure 3. This information is then substituted into one of the equations of motion, either the h or the $\alpha$ equation, which then will contain only the h vector as an unknown. The solution for the h term is then straightforward. For example, picking two values of airspeed, say 1950 ft/sec and 2840 ft/sec, the associated roots (corresponding to the eventually unstable locus shown in Figure 3) are $p = -.035 \pm .680\,i$ and $p = \pm .802\,i$. Substituting this information into one of the equations of motion and letting $\alpha = e^{io}$, the values of the h vector can be found and hence the mode shape can be determined for each case. The results of this procedure are shown in Figure 6. It is noticed that the modal contents (h, $\alpha$, and the phase angle between them) change as a function of the U as well as the system roots.

At this point all information regarding the stability of the system has been obtained and all the information necessary to compute response problems is contained in Figure 3. System B is now considered.

### 2.3.2 Analysis of System B

The constants involved in System B are

| | |
|---|---|
| $x_0 = .55$ | $\mu = 50$ |
| $x_\alpha = -.10$ | $b = 4$ |
| $r_\alpha^2 = .25$ | $a_\infty = 972$ |
| $b\omega_\alpha/a_\infty = .238$ | $\Omega^2 = .25$ |

thus Eq. (2 - 9) becomes

$$-25(s^2 + .084s + .25)(s^2 + .1142s + 1) + s^2(s + .084)^2 + .210U^* = 0 \qquad (2 - 12)$$

After factoring the terms not containing $U^*$, Eq. (2 - 12) becomes

$$24(s + .057 \pm 1.02i)(s + .042 \pm .491i) - .210U^* = 0 \qquad (2 - 13)$$

Now as in example A, the roots at $U = 0$ are given by the two bracket terms and the roots at $U = \infty$ are similarly infinite. However, there is a sign difference in the $U^*$ term in Eq. (2 - 11) and Eq. (2 - 13), hence, the manner in which the roots approach infinity as $U \rightarrow \infty$ is completely different. This effect is clearly shown when the system roots are plotted as a function of U. Figure 7 presents this information. Notice that in this case the frequencies of the damped, normal aeroelastic modes always move away from each other until one locus intersects the real axis. At this point, this locus splits and one branch crosses the origin when $U = 6612$ ft/sec. This airspeed is the divergence speed. Hence for any airspeed greater than $U = 6612$ ft/sec, this wing will exhibit an exponential type unstable motion until failure occurs or until some unaccounted for nonlinear interaction restrains the wing in some nondestructive fashion.

In summary, this section has presented two examples which demonstrate how the general features of an aeroelastic system may be obtained if piston theory aerodynamics is applicable. However, (although the development is not shown here) it is found that if Jones' approximation to the Wagner function is incorporated with a Duhammel integral representation, the same general methods of solution apply to the incompressible cases although the amount of labor required is sharply increased.

## 2.4 Discussion of Flutter Analyses that Utilize Zero-Damping Approximations.

In recent years, the importance of damping terms in various types of flutter analyses has been investigated by several authors. The investigations have had varying degrees of success. On the more successful side, the neglecting of damping terms in the panel flutter problem by Hedgepeth (Ref. 3) and a host of other authors has led to consistently accurate results for all high mass-density ratio configurations. On the other hand, the analogous method presented by Pines (Ref. 4) for the analysis of wing-like surfaces often leads to inaccurate results simply because this theory provides no method of assessing when the assumptions and hence the results are inaccurate. However, if this information could be provided then a truly useful zero-damping analysis for wing-like surfaces could be put forth. To this end Dugundji and Crisp (Ref. 5) have observed that, as in the panel flutter case, a large mass-density ratio is a necessary requirement for the success of the zero-damping analysis of wing-like surfaces and in their own words ".... it appears that the frequency coalescence behavior (Pines' method) is useful only when very little damping coupling is present compared to either stiffness or inertia couplings. Its success in panel flutter seems due to this fact, for other systems such as bending-torsion flutter, its use can be misleading".

It is now suggested, by using some physical intuition with the help of the root loci system representation and by inspection of the characteristic equations of the binary subsystems (bending-torsion, etc.), that the observations of Dugundji and Crisp can be refined.

First of all, there is the effect of the mass-density ratio $\mu$ which is incorporated in the $\epsilon^*$ term of the present terminology.

As given before $\epsilon^* \sim \mu^{-1}$. By inspecting the bending-torsion characteristic equation, Eq. (2 - 9), it is seen that a high mass-density ratio, hence a small $\epsilon^*$, definitely predicts a very slightly damped system. One might then be tempted to assert, since the zero damping root loci in the complex plane are simply the vertical axis projections of the actual root loci with small but finite damping, that this large $\mu$ condition is indeed sufficient (as in the panel flutter case) to insure accurate flutter point calculations. To this end, Table 1 summarizes some bending-torsion flutter calculations utilizing first an exact solution and secondly the zero-damping solution. All examples were for systems with a mass-density ratio $\mu$ equal to 50. Inspection of this table demonstrates that a small $\epsilon^*$ (a large $\mu$) may be a necessary condition for accurate flutter point calculations but it is certainly <u>not</u> a sufficient condition. In attempting to present the correct "sufficient conditions" it is necessary to digress a bit. This digression begins by noticing that a torsion-aileron system is generically just an extremely simple panel structure. Thus the mechanisms that insure good results for zero-damping panel flutter analyses should be inherent in the torsion-aileron characteristic equation. Apparently, these mechanisms should appear in the torsion-aileron equation as a departure from the general form of the bending-torsion and bending-aileron equations. Thus looking at the torsion-aileron characteristic equation Eq. (2 - 8 ) it is noticed, contrary to the other binary subsystems general behaviors, that as $U \rightarrow \infty$ the system roots always* approach infinity. Furthermore since the zero damping solutions require a "frequency coalescence" the break-away angles at $U = 0$ always point the two loci

---

* As discussed previously, this statement neglects the very unusual case in which the term $(A_{26}^* A_{39} - A_{29} A_{36})$ is equal to zero.

towards one another. This fact then leads one to hypothesize that zero-damping analyses are valid only if the roots of the system under consideration approach infinity, or at least are very large, as $U \rightarrow \infty$, and additionally, that the break-away angles direct the two loci towards one another. When considering bending-torsion examples, the condition of large roots as $U \rightarrow \infty$ is seen from Eq. (2 - 9) to be $x_\alpha \cong c$. Now returning to the contents of Table 1, it is seen that the only non-trivial case in which a zero-damping analysis is reasonably accurate is indeed the case in which $x_\alpha = c$ (i.e. $x_\alpha = .2$, $x_0 = .4$), and the two loci approach one another before turning to approach infinity. This case is the System A of section 2.3.1. Notice that System B of section 2.3.2 also fulfills the small $\epsilon^*$ condition and the $x_\alpha = c$ condition but does not satisfy the requirement that the break-away angles direct the two loci towards each other. Needless to say, the above hypothesis must be more carefully checked by the results of many worked examples, but it is felt that the present evidence is convincing enough to warrant its presentation at this time.

# CHAPTER 3

# SOME SOLUTION TECHNIQUES FOR ONE AND TWO DEGREE OF FREEDOM SYSTEMS WITH TIME-VARYING COEFFICIENTS

## 3.1 Introduction

It is the intent of this chapter to present, for the benefit of the aeroelastician (or any other "engineering-type"), a collection of well known mathematical techniques which are useful for the approximate* solution of engineering problems involving linear differential equations with time-varying coefficients. More specifically, this collection consists of techniques for studying (1) a second order linear differential equation with time-varying coefficients, (2) a linear partial differential equation with separable time-varying coefficients, and (3) a system of second order linear differential equations with time-varying coefficients.

## 3.2 The One Degree of Freedom System with Time-Varying Coefficients

The general form of the equation considered in this section is

$$\frac{d^2y}{dt^2} + a_1(t)\frac{dy}{dt} + a_2(t)y = h(t) \qquad (3-1)$$

Following a classical procedure (for example see Ref. 6), the homogeneous solution of Eq. (3 - 1) is assumed to be of the form $y = A^* e^{\int^t [v(\tau) - a_1(\tau)/2]d\tau}$ where $A^*$ is a constant associated with each linearly independent solution of $v(\tau)$ and where $v(\tau)$ is some

---

* As is to be expected exact solutions are not possible except in very special and rarely occurring cases; hence the emphasis on approximate solutions.

as yet undetermined function. Substituting this relation into the homogeneous form of Eq. (3 - 1), it is found that the following equation in $v(\tau)$ must be satisfied.

$$v^2(\tau) + \frac{dv(\tau)}{d\tau} = R(\tau) \qquad (3 - 2)$$

where

$$R(\tau) = (a_1/2)^2 + \frac{d(a_1/2)}{d\tau} - a_2$$

A special, obvious set of solutions, denoted by $v_0$'s, can be obtained for Eq. (3 - 2) if $R(\tau)$ is a constant. Thus if $R(\tau)$ is equal to some positive number $a^2$, one has

$$\begin{aligned} v_0/a &= \tanh a\tau \;;\; v_0^2 < a^2 \\ v_0/a &= \operatorname{ctnh} a\tau \;;\; v_0^2 > a^2 \end{aligned} \qquad (3 - 3)$$

and

$$v_0 = \sqrt{R} = a \qquad (3 - 4)$$

while on the other hand, if $R(\tau)$ is equal to some negative number $-a^2$, one has

$$v_0/a = \tan(-a\tau) \qquad (3 - 5)$$

$$v_0 = \sqrt{R} = ia \qquad (3 - 6)$$

A little thought demonstrates that Eqs. (3 - 3) have a negligible influence on the solution of Eq. (3 - 1) except when $R \to 0$ in which case Eqs. (3 - 3) merge with the solution obtained by formally setting $R = 0$ in Eq. (3 - 2). In other words, the $v_0 = a \tanh a\tau$ solution becomes $v_0 \to 0$ as $R \to 0$ and the $v_0 = a \operatorname{ctnh} a\tau$ solution becomes $v_0 \to \frac{1}{\tau}$ as $R \to 0$.

Furthermore, it is seen that Eq. (3-6) is physically inadmissible, thus the only solution of consequence (when $R \neq 0$) is $v_0 = \sqrt{R}$ for R either positive or negative. Following the steps indicated in Ref. 6 it can be shown that if $(dv_0/d\tau)^2/8v_0^4 \ll 1$, the approximate homogeneous solution of Eq. (3-1) is given by

$$y(t) = \begin{cases} [Ae^{\int^t v_0(\tau)d\tau} + Be^{-\int^t v_0(\tau)d\tau}]e^{-\frac{1}{2}\int^t [\frac{dv_0/d\tau}{v_0(\tau)} + a_1(\tau)]d\tau} & ; R > 0 \quad (3\text{-}7) \\ [At + B]e^{-\int^t a_1(\tau)/2\, d\tau} & ; R = 0 \quad (3\text{-}8) \\ [A\cos \int^t i v_0(\tau)d\tau + B \sin \int^t i v_0(\tau)d\tau]e^{-\frac{1}{2}\int^t [\frac{dv_0/d\tau}{v_0(\tau)} + a_1(\tau)]d\tau} & ; R < 0 \quad (3\text{-}9) \end{cases}$$

where i is the unit imaginary vector and A and B are arbitrary constants to be determined by initial conditions. Notice that Eqs. (3-7), (3-8), and (3-9) are generalizations of the constant coefficient solutions for an overdamped, critically damped, and underdamped system respectively. In summary it is seen, for the time-varying coefficient problem, that the spring and damping time-derivatives contribute to the instantaneous frequency and damping ratio of the solution. Thus some engineering problems require the use of this solution (see Ref. 7) while the quasi-steady approximation is quite accurate in other cases, for example as in Ref. 8.

Finally, using the standard variation of parameters technique, the total approximate solution of Eq. (3-1 is given by

$$y(t) = \int^t h(\eta)\,[u_1(\eta)u_2(t) - u_2(\eta)u_1(t)]\,W^{-1}[u_1(\eta), u_2(\eta)]d\eta + c_1u_1(t) + c_2u_2(t) \quad (3\text{-}10)$$

where $u_1(t)$ and $u_2(t)$ are the linearly independent homogeneous solutions of Equation (3-1), $c_1$ and $c_2$ are as yet undetermined coefficients, and $W[u_1(t), u_2(t)]$ is the Wronskian of $u_1(t)$ and $u_2(t)$.

## 3.3 Comments on Work, Presented by Various Authors, Complementary to the Present Effort

In the past few years, several authors have suggested some approximate solutions of one degree of freedom linear differential equations with time-varying coefficients to specifically cope with various aeronautical problems. All solutions are traceable to some variant of the classical approach used in Section 3.2. However, the different notations and the varying degrees of accuracy of these solutions makes it desirable to briefly discuss each method in a unified notation so that comparisons can be obtained.

Additionally, a few comments are supplied concerning statements by some of the authors.

### 3.3.1 Garber's Method

In a recent paper (Reference 7) Garber presents an iterative solution based on an approximate solution of the general equation $\ddot{y} + a_1(t)\dot{y} + a_2(t)y = 0$. This is the only method, that the author has found, that improves on the original approximate solution. The procedure is as follows. Assume a solution of the form $y(t) = Ae^{\int \lambda(t)dt}$, thus the original equation is replaced by a non-linear operator equation of the form $\dot{\lambda} + \lambda^2 + a_1\lambda + a_2 = 0$. $\lambda$ is assumed to be a complex quantity so that $\lambda = \sigma + j\omega$. This expression is put into the operator equation thus yielding two equations. They are,

$$\sigma = -(a_1/2) - \dot{\omega}/2\omega \qquad (3-11)$$

$$\omega^2 = a_2 - (a_1/2)^2 - \dot{a}_1/2 + 3(\dot{\omega}/2\omega)^2 - \ddot{\omega}/2\omega \qquad (3-12)$$

The solution of the equation is then

$$y(t) = [e^{-1/2\int^t a_1 dt} / \omega^{1/2}][A_1 \cos\int^t \omega dt + A_2 \sin\int^t \omega dt] \qquad (3-13)$$

All that remains is to find $\omega$ from Eq. (3 - 12). This is accomplished by performing an iteration solution of the form

$$\omega_{i+1}^2 = a_2 - (a_1/2)^2 - (\dot{a}_1/2) + 3(\dot{\omega}_i/2\omega i)^2 - \ddot{\omega}_i/2\omega i \qquad (i = 0,1,2,\ldots) \qquad (3-14)$$

where

$$\omega_1 = a_2 - (a_1/2)^2 - (\dot{a}_1/2)$$

3.3.2 Collar's Treatment

In 1957 Collar published one of the first papers (Ref. 9) dealing with the stability of accelerating aeronautical systems. One of the many sections of this paper was entitled "A Useful Formal Solution", in which another variant of the classical approximate solution was given. Translating Collar's solution into the notation of the present work yields the result that

$$y(t) = A a_2^{-1/4} e^{-1/2\int^t a_1 d\tau} \cos\left\{B + \int^t a_2^{1/2}\, d\tau\right\}$$

The solution as given in Section 3.2 of this work is

$$y(t) = Ae^{-1/2 \int^{t} [\frac{\partial v_0/\partial \tau}{v_0} + a_1] d\tau} \cos\left\{B + \int^{t} iv_0 d\tau\right\}$$

Thus an equivalence of these two solutions requires that

$$a_2^{-1/4} = e^{-1/2 \int^{t} \frac{\partial v_0/\partial \tau}{v_0} d\tau} \tag{3-15}$$

$$a_2^{1/2} = iv_0 \tag{3-16}$$

Noting that $iv_0 = [a_2 - (\frac{a_1}{2})^2 - \frac{1}{2}(da_1/d\tau)]^{1/2}$ and that

$$e^{-1/2 \int \frac{\partial v_0/\partial \tau}{v_0} d\tau} = e^{\ell n\, v_0^{-1/2}} = v_0^{-1/2} = [a_2 - (\frac{a_1}{2})^2 - \frac{1}{2}(da_1/d\tau)]^{-1/4}$$

it is seen that both Equations (3-15) and (3-16) are approximately fulfilled when $a_2 >> (a_1^2/4) + \frac{1}{2}(da_1/d\tau)$

### 3.3.3 Squire's Objections

In a recent note (Ref. 10) Squire claims that the approximate solution of our much discussed equation neglects a term $(I'/4I)^2$ where $I'(\tau)$ in our notation is simply the $-\frac{dR(\tau)}{d\tau}$ of section 3.2. Furthermore, he claims that this neglected term becomes dominant as $I \longrightarrow 0$.

Now, although $(I'/4I)^2$ is neglected, as Squire states, it is perfectly consistent with the truncated binomial series expansion as given in Ref. 6 which leads to our solutions for $y(t)$. Additionally, if one more term of this expansion were included, Squire's result and that of Eq. (3 - 7) or Eq. (3 - 9) would be identical. Furthermore as $I \longrightarrow 0$, Squire neglects the $v_0/a = \text{ctnh } a\tau$ solution given by Eq. (3 - 3) so that our <u>exact</u> $y(t)$ solution for $R = 0$ is obviously superior to the result of Squire.

### 3.5.4 Reed's Observations

In one section of a recent paper (Ref. 11) Reed presents an approximate solution of an undamped single degree of freedom system whose natural frequency is increasing at a large rate. He then notes that the effect of increasing frequency is to make the solutions (i.e., $x$, $\dot{x}$, $\ddot{x}$) of this undamped system behave as both "stable and unstable" depending upon the particular solution being observed. This result has startled many casual readers of Reed's work, but in fact even a <u>quasi-steady</u> analysis of this system yields the same general conclusions. To this end, consider a conservative constant coefficient system $\ddot{x} + \omega^2 x = 0$. Multiplying this equation by $\dot{x}$ and integrating, the following energy equation results,

$$x^2 + \omega^2 x^2 = \epsilon^2 \qquad (3 - 17)$$

where $\epsilon^2$ is a term proportional to the energy in the system.

Solving the original system equation and applying the initial conditions $x(0) = X$ and $\dot{x}(0) = V$, the result is

$$x = X \cos \omega t + \frac{V}{\omega} \sin \omega t \tag{3-18}$$

Now since Equation (3-17) is valid for any time, the $t = 0$ form of this equation is $V^2 + \omega^2 X^2 = \epsilon^2$. For simplicity, if either V or X is chosen to be zero, it can be easily demonstrated that the absolute values of the amplitudes of $x$, $\dot{x}$ and $\ddot{x}$ are given by

$$\begin{aligned} |x| &= \epsilon\omega^{-1} \\ |\dot{x}| &= \epsilon \\ |\ddot{x}| &= \epsilon\omega \end{aligned} \tag{3-19}$$

or expressing $|\dot{x}|$ and $|\ddot{x}|$ in terms of $|x|$,

$$\begin{aligned} |\dot{x}| &= \omega\,|x| \\ |\ddot{x}| &= \omega^2\,|x| \end{aligned} \tag{3-20}$$

Notice that the desired trend is now exhibited in both Equations (3-19) and (3-20). For example, referring to Equation (3-18), if the amount of energy ($\sim \epsilon^2$) in the system remains constant, then increasing the system frequency on a quasi-steady basis will decrease the amplitude of $x$, will not affect the amplitude of $\dot{x}$ and will increase the amplitude of $\ddot{x}$.

## 3.4 A Partial Differential Beam Equation with Separable Space-Time Coefficients

Using the technique presented in Section 3.2 for approximately solving a second-order equation with time-varying coefficients, it is then possible to solve the problem of a partial differential equation with separable* coefficients. In order to simultaneously present a

---

*This implies that all coefficients $c_i(x,t)$ in the given equation can be expressed as a product of terms $\bar{c}_i(x)\tilde{c}_i(t)$.

possible engineering application and to demonstrate the method of solution, a forced lateral beam vibration problem (in which transverse shear and rotary inertia effects are negligible) is treated. Referring to Figure 8, the dynamics of an element of a slender beam, neglecting rotary inertia, is described by

$$\frac{\partial}{\partial t}(m\dot{w})\,dx = \frac{\partial S}{\partial x}\,dx + F_z(x,t)dx \qquad \text{(vertical force summation)}$$

$$S\,dx + \frac{\partial M}{\partial x}dx = 0 \qquad \text{(moment summation)}$$

Note that the vertical force summation equation assumes that the mass lost by the system has a zero residual momentum component in the z direction. Obviously this condition does not always occur when representing physical problems, but for our illustrative purposes nothing essential is lost in presenting the system, and hence the analysis, in this simplified form.

Combining the above equations and neglecting shear deformation leads to the following equation of motion.

$$m\ddot{w} + \dot{m}\dot{w} + \frac{\partial^2}{\partial x^2}\left(EI\frac{\partial^2 w}{\partial x^2}\right) = F_z(x,t) \qquad (3\text{-}21)$$

Explicitly denoting the separable coefficients as

$$EI(x,t) = \overline{EI}(x)\,\widetilde{EI}(t)$$
$$m(x,t) = \overline{m}(x)\,\widetilde{m}(t)$$

and assuming a separable solution $w(x,t) = \phi(x)T(t)$, the homogeneous counterpart of Equation (3-21) reduces to two equations as given below.

$$\frac{\partial^2}{\partial x^2}\left[\overline{EI}\,\frac{\partial^2 \phi}{\partial x^2}\right] + \bar{m} K^2 \phi = 0 \qquad (3\text{-}22)$$

$$\ddot{T} + (\tilde{\bar{m}}/\tilde{\bar{m}})\dot{T} + K^2(\tilde{\overline{EI}}/\tilde{\bar{m}})T = 0 \qquad (3\text{-}23)$$

where $-K^2$ is the separation constant.

Notice that Equation (3-22) has the same form as the separated space equation associated with a beam motion equation with time-invariant coefficients. Thus the concept of vibration modes is preserved, the orthogonality relations $\int_0^\ell \phi_p \phi_q \bar{m}\, dx = \delta_{pq} \int_0^\ell \phi_q^2 \bar{m}\, dx$ are still valid, and as Equation (3-23) shows, the T coordinates can be approximately calculated by the technique of Section 3.2.

The solution of the forced equation (Equation (3-21) in its entirety) can be expressed in the form $w(x,t) = \sum_{i=1}^{\infty} \phi_i(x)\, \zeta_i(t)$ where $\zeta_i(t)$ are the generalized coordinates given by the following equation obtained by well-known methods.

$$\ddot{\zeta}_i + (\tilde{\bar{m}}/\tilde{\bar{m}})\,\dot{\zeta}_i + (\tilde{\overline{EI}}/\tilde{\bar{m}})\,K_i^2\,\zeta_i = (\tilde{\bar{m}} M_i)^{-1} \Xi_i \qquad (3\text{-}24)$$

where $M_i = \int_0^\ell \bar{m}\, \phi_i^2\, dx \equiv i^{\text{th}}$ generalized mass

$$\Xi_i = \int_0^\ell F_z\, \phi_i\, dx \equiv i^{\text{th}} \text{ generalized force}$$

If $F_z$ is not dependent on the beam motion then each $i^{\text{th}}$ equation of the set represented by Equation (3-24) can be solved independently of the other equations. When this occurs, the approximate methods

of Section 3.2 may be employed. However, if $F_z$ is motion dependent, all equations represented by Equation (3-24) may be coupled; thus a simultaneous solution is then required. This situation is discussed in the following section with special reference to a two degree of freedom system.

## 3.5 The Two Degree of Freedom System with Time-Varying Coefficients

This section presents a routine operator method for uncoupling a linear, homogeneous, second order, two degree of freedom set of equations. Obviously, this uncoupling procedure could be carried out by cross-differentiation and elimination operations. However, the proposed method proves to be an interesting and unusual exercise in constructing non-commutative operators that will uncouple a set of equations. Additionally, the well-ordered form of the operator method is advantageous when performing approximate calculations.*

Consider a general homogeneous coupled set of linear differential equations given as

$$L_1(x) + L_2(y) = 0$$
$$L_3(x) + L_4(y) = 0 \qquad (3\text{-}25)$$

where,

$$L_1 = A_2(t)\, d^2/dt^2 + A_1(t)\, d/dt + A_0(t)$$
$$L_2 = B_2(t)\, d^2/dt^2 + B_1(t)\, d/dt + B_0(t)$$
$$L_3 = C_2(t)\, d^2/dt^2 + C_1(t)\, d/dt + C_0(t) \qquad (3\text{-}26)$$
$$L_4 = D_2(t)\, d^2/dt^2 + D_1(t)\, d/dt + D_0(t)$$

---

*This is pointed out in the discussion of "discrete-time" solutions occurring in the next section.

and the $A_i$, $B_i$, $C_i$, and $D_i$ ( i = 0, 1, 2) are known functions of time. Since the $L_i$ (i = 1, 2, 3, 4) have time dependent coefficients, $L_iL_j \neq L_jL_i$ ( $i \neq j$), so that these $L_i$ operators are non-commutative and hence the usual methods for uncoupling simultaneous differential equations with constant coefficients are not applicable. Thus, it is necessary to synthesize a set of operators $\mathscr{L}_i$ (i = 1, 2, 3, 4) such that Equation (3-25) can be uncoupled.

To this end the following operator operations are performed on Equation (3-25).

$$\mathscr{L}_4 [L_1(x) + L_2(y)] = 0 \tag{3-27}$$

$$\mathscr{L}_2 [L_3(x) + L_4(y)] = 0 \tag{3-28}$$

$$\mathscr{L}_3 [L_1(x) + L_2(y)] = 0 \tag{3-29}$$

$$\mathscr{L}_1 [L_3(x) + L_4(y)] = 0 \tag{3-30}$$

Subtracting Equation (3-28) from Equation (3-27) and Equation (3-30) from Equation (3-29) yields,

$$\begin{aligned} \mathscr{L}_4 [L_1(x) + L_2(y)] - \mathscr{L}_2 [L_3(x) + L_4(y)] &= 0 \\ \mathscr{L}_3 [L_1(x) + L_2(y)] - \mathscr{L}_1 [L_3(x) + L_4(y)] &= 0 \end{aligned} \tag{3-31}$$

and upon rearranging these equations,

$$\begin{aligned} [\mathscr{L}_4L_1 - \mathscr{L}_2L_3]x + [\mathscr{L}_4L_2 - \mathscr{L}_2L_4]y &= 0 \\ [\mathscr{L}_3L_1 - \mathscr{L}_1L_3]x + [\mathscr{L}_3L_2 - \mathscr{L}_1L_4]y &= 0 \end{aligned} \tag{3-32}$$

Thus, if the $\mathcal{L}_i$ can be found such that

$$\mathcal{L}_4 L_2 = \mathcal{L}_2 L_4$$
$$\mathcal{L}_3 L_1 = \mathcal{L}_1 L_3 \tag{3-33}$$

Equation (3-32) can be reduced to uncoupled equations of the form

$$L_5(x) = 0$$
$$L_6(y) = 0 \tag{3-34}$$

where

$$L_5 = \mathcal{L}_4 L_1 - \mathcal{L}_2 L_3$$
$$L_6 = \mathcal{L}_3 L_2 - \mathcal{L}_1 L_4$$

Notice that if the $L_i$ lose their time-varying character they must necessarily be identical to the $\mathcal{L}_i$. This observation suggests that even in the time-varying case the <u>form</u> of the $\mathcal{L}_i$ should be identical to the $L_i$. Acting on this observation the $\mathcal{L}_i$ are given the following form

$$\mathcal{L}_1 = a_2(t)\, d^2/dt^2 + a_1(t)\, d/dt + a_0(t)$$
$$\mathcal{L}_2 = b_2(t)\, d^2/dt^2 + b_1(t)\, d/dt + b_0(t)$$
$$\mathcal{L}_3 = c_2(t)\, d^2/dt^2 + c_1(t)\, d/dt + c_0(t) \tag{3-35}$$
$$\mathcal{L}_4 = d_2(t)\, d^2/dt^2 + d_1(t)\, d/dt + d_0(t)$$

where $a_i$, $b_i$, $c_i$, and $d_i$ are as yet <u>unknown</u> functions of time.

Substituting Equation (3-35) into Equation (3-33) yields the two following relations.

$$(d_2\, d^2/dt^2 + d_1\, d/dt + d_0)\,(B_2\, d^2/dt^2 + B_1\, d/dt + B_0)$$

$$= (b_2\, d^2/dt^2 + b_1\, d/dt + b_0)\,(D_2\, d^2/dt^2 + D_1\, d/dt + D_0) \tag{3-36}$$

$$(c_2\, d^2/dt^2 + c_1\, d/dt + c_0)\,(A_2\, d^2/dt^2 + A_1\, d/dt + A_0)$$

$$= (a_2\, d^2/dt^2 + a_1\, d/dt + a_0)\,(C_2\, d^2/dt^2 + C_1\, d/dt + C_0)$$

Expanding Equation (3-36) and equating the coefficients of similar derivatives yields the two following matrix equations which will determine the coefficients of the $\mathcal{L}_i$ operators.

$$\begin{bmatrix} 0 & 0 & D_2 & 0 & 0 & -B_2 \\ 0 & D_2 & (2\dot{D}_2+D_1) & 0 & -B_2 & -(2\dot{B}_2+\dot{B}_1) \\ D_2 & (\dot{D}_2+D_1) & (\ddot{D}_2+2\dot{D}_1+D_0) & -B_2 & -(\dot{B}_2+B_1) & -(\ddot{B}_2+2\dot{B}_1+B_0) \\ D_1 & (\dot{D}_1+D_0) & (\ddot{D}_1+2\dot{D}_0) & -B_1 & -(\dot{B}_1+B_0) & -(\ddot{B}_1+2\dot{B}_0) \\ D_0 & \dot{D}_0 & \ddot{D}_0 & -B_0 & -\dot{B}_0 & -\ddot{B}_0 \end{bmatrix} \begin{bmatrix} b_0 \\ b_1 \\ b_2 \\ d_0 \\ d_1 \\ d_2 \end{bmatrix} = \begin{bmatrix} 0 \\ 0 \\ 0 \\ 0 \\ 0 \\ 0 \end{bmatrix} \tag{3-37}$$

$$\begin{bmatrix} 0 & 0 & C_2 & 0 & 0 & -A_2 \\ 0 & C_2 & (2\dot{C}_2+C_1) & 0 & -A_2 & -(2\dot{A}_2+A_1) \\ C_2 & (\dot{C}_2+C_1) & (\ddot{C}_2+2\dot{C}_1+C_0) & -A_2 & -(\dot{A}_2+A_1) & -(\ddot{A}_2+2\dot{A}_1+A_0) \\ C_1 & (\dot{C}_1+C_0) & (\ddot{C}_1+2\dot{C}_0) & -A_1 & -(\dot{A}_1+A_0) & -(\ddot{A}_1+2\dot{A}_0) \\ C_0 & \dot{C}_0 & \ddot{C}_0 & -A_0 & -\dot{A}_0 & -\ddot{A}_0 \end{bmatrix} \begin{bmatrix} a_0 \\ a_1 \\ a_2 \\ c_0 \\ c_1 \\ c_2 \end{bmatrix} = \begin{bmatrix} 0 \\ 0 \\ 0 \\ 0 \\ 0 \\ 0 \end{bmatrix}$$

(3-38)

A Gauss-Jordan reduction process will demonstrate that the above 5x6 matrix equations possess non-trivial solutions, which is equivalent to stating that any <u>one</u> operator coefficient in each of the above equations may be arbitrarily chosen. For instance, if the choice that $a_2 = A_2$ and that $d_2 = D_2$ is made, Equations (3-37) and (3-38) reduce to the following relations: $b_2 = B_2$, $c_2 = C_2$, and

$$\begin{bmatrix} 0 & D_2 & 0 & -B_2 \\ D_2 & (\dot{D}_2+D_1) & -B_2 & -(\dot{B}_2+B_1) \\ D_1 & (\dot{D}_1+D_0) & -B_1 & -(\dot{B}_1+B_0) \\ D_0 & \dot{D}_0 & -B_0 & -\dot{B}_0 \end{bmatrix} \begin{bmatrix} b_0 \\ b_1 \\ d_0 \\ d_1 \end{bmatrix} = D_2 \begin{bmatrix} 2\dot{B}_2+B_1 \\ \ddot{B}_2+2\dot{B}_1+B_0 \\ \ddot{B}_1+2\dot{B}_0 \\ \ddot{B}_0 \end{bmatrix} - B_2 \begin{bmatrix} 2\dot{D}_2+D_1 \\ \ddot{D}_2+2\dot{D}_1+D_0 \\ \ddot{D}_1+2\dot{D}_0 \\ \ddot{D}_0 \end{bmatrix}$$

(3-39)

$$\begin{bmatrix} 0 & C_2 & 0 & -A_2 \\ C_2 & \dot{(C_2+C_1)} & -A_2 & -\dot{(A_2+A_1)} \\ C_1 & \dot{(C_1+C_0)} & -A_1 & -\dot{(A_1+A_0)} \\ C_0 & \dot{C}_0 & -A_0 & -\dot{A}_0 \end{bmatrix} \begin{bmatrix} a_0 \\ a_1 \\ c_0 \\ c_1 \end{bmatrix} = C_2 \begin{bmatrix} \dot{2A_2+A_1} \\ \ddot{A_2+2A_1+A_0} \\ \ddot{A_1+2A_0} \\ \ddot{A}_0 \end{bmatrix} - A_2 \begin{bmatrix} \dot{2C_2+C_1} \\ \ddot{C_2+2C_1+C_0} \\ \ddot{C_1+2C_0} \\ \ddot{C}_0 \end{bmatrix} \tag{3-40}$$

Solving Equation (3-39) and (3-40) for the remaining $a_i$, $b_i$, $c_i$, and $d_i$ defines the $\mathcal{L}_i$ operators completely, hence the $L_5$ and $L_6$ operators may be computed thus yielding the uncoupled equations for x and y. The uncoupled equations will be of the form,

$$\nu_4(t)\frac{d^4x}{dt^4} + \nu_3(t)\frac{d^3x}{dt^3} + \nu_2(t)\frac{d^2x}{dt^2} + \nu_1(t)\frac{dx}{dt} + \nu_0(t)\,x = 0 \tag{3-41}$$

$$\nu_4^*(t)\frac{d^4y}{dt^4} + \nu_3^*(t)\frac{d^3y}{dt^3} + \nu_2^*(t)\frac{d^2y}{dt^2} + \nu_1^*(t)\frac{dy}{dt} + \nu_0^*(t)\,y = 0$$

The $\nu_i$ and the $\nu_i^*$ could be written out explicitly (for example, see Reference 12) but this lengthy procedure is not done here since, when making approximate calculations, it is most convenient to work directly from Equations (3-39) and (3-40). This point is discussed in Section 3.6. Now, since each equation given by Equation (3-41) is linear and of fourth order, each equation will possess four linearly independent solutions so that the x and y general solutions may be expressed as

$$x(t) = \sum_{i=1}^{4} f_i \, v_i(t)$$
$$y(t) = \sum_{i=1}^{4} g_i \, w_i(t) \qquad (3\text{-}42)$$

where the $v_i(t)$ and the $w_i(t)$ are linearly independent solutions and the $f_i$ and $g_i$ are arbitrary constants. The particular solution of these equations requires that all eight of the constants $f_i$ and $g_i$ be determined by specifying the functions x, y, and their first three derivatives at some initial time $t_0$. However, the particular solution of the parent equations, Equation (3-25), requires that only the functions x, y, and their first derivatives be specified at some initial time $t_0$. Thus in order to obtain particular solutions of Equation (3-42) that are also solutions of Equation (3-25) it is necessary that firstly, the same basic initial conditions (i.e., $x(t_0)$, $y(t_0)$, $\dot{x}(t_0)$, $\dot{y}(t_0)$) be specified for Equation (3-42) as for Equation (3-25) and that secondly, the initial values of the second and third derivatives of x and y be found in terms of the initial x,y values and their first derivatives. These remaining unknown initial values are found, in terms of the x,y initial values and their first derivatives, by a power series technique applied to the parent equations, Equation (3-25), only at the initial time $t = t_0$. The essentials of this technique are presented in Appendix I.

## 3.6 Approximate Solutions of the Fourth Order Uncoupled Equations with Time-Varying Coefficients

Two immediately obvious approximate solutions of Equations (3-41) are of the "frozen*-time" variety, the term "frozen-time"

*This term was apparently coined by L. Zadeh. See Reference 13.

implying that at some time $t_0$ the coefficients of the differential equations are evaluated and the analysis proceeds as if one had a constant coefficient system. That is, instead of solving the equation $\sum_{i=0}^{4} \nu_i(t) \frac{d^i x}{dt^i} = 0$ for all time, the equation $\sum_{i=0}^{4} \nu_i(t_0) \frac{d^i x}{dt^i} = 0$ is solved in some limited time region that includes $t_0$ as the lower limit. The extent of the time region in which the solution is valid clearly depends on the time-varying behavior of the coefficients. Hence the usefulness of the frozen-time solutions of Equation (3-41) depends on the details of the $\nu_i(t)$ and the $\nu_i^*(t)$ time behavior. These details are now examined and the two approximate solutions and their complex plane representations are presented.

The expanded forms of the $\nu_i$ (and also the $\nu_i^*$) reveal that it is always possible to group the terms comprising each $\nu_i$ (and also each $\nu_i^*$) into two sub-groups, the first sub-group containing <u>only</u> products of the originally known time-functions $A_i$, $B_i$, $C_i$, $D_i$ and the second sub-group containing products of the originally known time-functions $A_i$, $B_i$, $C_i$, $D_i$ <u>and</u> an assortment of their time derivatives. The first sub-group will be referred to as the "quasi-steady" term, denoted by ${}_q\nu_i$ (and also ${}_q\nu_i^*$) and the second sub-group will be referred to as the "discrete-time increment" term, denoted by ${}_d\nu_i$ (and ${}_d\nu_i^*$). Therefore it is seen that $\nu_i = {}_q\nu_i + {}_d\nu_i$ and $\nu_i^* = {}_q\nu_i^* + {}_d\nu_i^*$. Note that as the original $A_i$, $B_i$, $C_i$, $D_i$ gradually lose their time-varying character and approach constant values it is necessarily true that ${}_d\nu_i \to 0$ and ${}_d\nu_i^* \to 0$. Thus, as was expected, the ${}_q\nu_i$ and the ${}_q\nu_i^*$ are equal when their sub-terms are constants. However, since the forms of the ${}_q\nu_i$ (and the ${}_q\nu_i^*$) remain the same

even when their terms are time-varying, it is then true that ${}_q\nu_i(t) \equiv {}_q\nu_i^*(t)$. Thus when ${}_q\nu_i(t) \gg {}_d\nu_i(t)$ and ${}_q\nu_i^*(t) \gg {}_d\nu_i^*(t)$, the x and y solutions shown by Equation (3-41) are, to an excellent approximation, described by the same time functions; that is, $v_i(t) \cong w_i(t)$ for $i = 1,2,3,4$. Additionally if the $\nu_i$ and $\nu_i^*$ coefficients change by only a few percent during the time required for the system to complete a natural oscillation cycle#, an approximate frozen-time solution that retains just the quasi-steady terms (${}_q\nu_i$ and ${}_q\nu_i^*$) will adequately describe the actual system solutions. This solution is naturally called the quasi-steady solution. When performing the quasi-steady solution calculations, the fact that $\mathcal{L}_i \equiv L_i$ is immediately used thus rendering the numerical work almost trivial. Now if the above inequalities are not valid but the $\nu_i(t)$ and the $\nu_i^*(t)$ yet change by only a few percent during the specified cycle time, a second type of frozen-time solution is still valid. This solution freezes the $\nu_i$ and the $\nu_i^*$ coefficients in their entirety (that is, the quasi-steady term and the discrete-time increment term) and will be referred to as the discrete-time solution. The x and y solutions shown by Equation (3-41) are now not composed of the same time functions, thus there is a possibility that the x solution may exhibit

---

#It is seen that in most cases of interest the ${}_q\nu_i(t) \gg {}_d\nu_i(t)$ and the ${}_q\nu_i^*(t) \gg {}_d\nu_i^*(t)$ conditions will automatically insure that the quasi-steady solution is valid. Therefore, unless the time required for the system to complete one natural oscillation cycle is unusually long, the validity of a quasi-steady solution is assured by the conditions that ${}_q\nu_i(t) \gg {}_d\nu_i(t)$ and that ${}_q\nu_i^*(t) \gg {}_d\nu_i^*(t)$. In order to estimate the $\nu_i$ (and similarly the $\nu_i^*$) percentage changes, let $\Delta(t_0)$ denote the $\nu_i(t)$ percentage change per specified unit time. The required expression for $\Delta(t_0)$ is then $\Delta(t_0) = 200\pi[\partial \nu_i/\partial t]_{t=t_0}/\Omega(t_0)\nu_i(t_0)$ where $\Omega^2(t_0)$ is the smaller of the terms $A_0/A_2$ or $D_0/D_2$ (the uncoupled natural frequencies squared) given in Equation (3-25).

an instantaneous stability behavior entirely different than that of the y solution.

When performing the discrete-time solution calculations experience has shown that it is much easier to invert the matrix relations given by Equation (3-39) and Equation (3-40) to obtain the $\mathcal{L}_i$ coefficients (and eventually the $\nu_i$ and the $\nu_i^*$ terms) than to "plug-in" values in the expanded version of the $\nu_i$ and the $\nu_i^*$ terms. This method also results in a routine procedure with several convenient check points for discovering errors.

The final topic to be discussed is the complex plane representation of the frozen-time solutions. Strictly speaking, the complex plane representation of a system with time-varying coefficients is not possible, but when the frozen-time solutions of this section are valid this type of representation is permissible and in fact useful. The usefulness of this representation is obviously its ability to show the essential features of the system for any value of time. Borrowing some of the techniques described in Chapter 2, the methods for obtaining the complex plane plots for first the quasi-steady solution and then the discrete-time solution are now described.

### 3.6.1 Complex Plane Representation of the Quasi-Steady Solution

After first choosing a series of times at which the system is to be examined, plot the complex plane loci for each of the chosen times as a function of some parameter (for an aero-elastic system this parameter might be the relative wind velocity) U using the quasi-steady approximation for the equations. The results of this procedure are shown in Figure 9 for one locus of the complete solution. The second step is to choose a desired parameter-time

relationship U(t), or several relationships if an evaluation of the effects of changing U(t) is desired. It is then possible to plot, with the aid of Figure 9, the actual system locus for any specified U(t). This result is shown in Figure 10 for two values of U(t).

### 3.6.2 Complex Plane Representation of the Discrete-Time Solution.

Since the x and y solutions are now not composed of the same time functions there will be one set of complex plane loci for the x solution and another set of loci for the y solution. The method of obtaining the complex plane plots is similar to that described in Section 3.6.1 except that now the number of plots required has increased two-fold. Two actual system loci corresponding to an x and a y solution are displayed in Figure 11 for two values of U(t).

# CHAPTER 4

# COMMENTS ON THE STABILITY ANALYSIS OF TIME-VARYING SYSTEMS AND AN INTRODUCTION TO NON-STATIONARY RANDOM PROCESSES

## 4.1 Introduction

The preceding chapter has discussed solutions, solution features, and techniques for treating one and two degree of freedom systems possessing time-varying coefficients. However, as perhaps the reader has noticed, the topic of stability has been tacitly neglected. It is demonstrated in this chapter that a different treatment of this topic may be necessary, if a system varies rapidly with time, since the concept of stability loses its analytical attractiveness and must in fact be replaced with a more meaningful criterion. The new criterion is shown to be necessarily statistical in nature; hence, most of this chapter is devoted to presenting the background material necessary to formulate problems within the framework of a non-stationary random process. The closing portion of this chapter discusses aircraft problems of a non-stationary random character.

## 4.2 Stability, and Time-Varying Systems

As an introduction to the anomalies arising from a stability analysis of a system with time-varying coefficients, it is instructive to consider the simple time-varying system shown in Figure 12. All system coefficients have some prescribed, continuous time variation

and additionally it is assumed that the spring and damping coefficients can assume negative as well as positive values if necessary. Now, at different levels of sophistication, the homogeneous behavior of this system is sought by two methods. Both methods are approximate, however the first method treats the system as a succession of constant coefficient systems (the so-called quasi-steady approximation), whereas the second method emphasizes the time-varying character of the coefficients (the method presented in Section 3.2) and is hence a more nearly exact treatment. Additionally, both methods assume that at some time $\tau$ the perturbation displacement and velocity, identically zero until time $\tau$, are assigned initial values which satisfy the usual tacit assumption of all stability analyses that their magnitudes permit no permanent deformation or failure of the system to occur at time $\tau$.

Proceeding, Figure 13 displays the types of oscillatory homogeneous behavior admissible when using the first method described above. As usual, the instantaneous stability of this system at any time $\tau$ (due to the quasi-steady assumption of the first method) is determined by noting whether the amplitude of the oscillatory motion is increasing, remaining constant, or decreasing. This type of analysis, were it valid, leaves no doubt as to whether or not the system would eventually fail in its free vibration motion. In other words, there is a one-to-one correspondence between (a) stability and structural soundness and between (b) instability and eventual destruction, provided that the initial condition magnitudes are not too large (as we have already assumed). Note that these relationships are the basic reasons for the dominant role that stability analyses have assumed

in the analysis of linear differential systems with constant coefficients; since, if a system possesses any degree of stability, then the system automatically possesses structural soundness when executing its homogeneous response.*

However, using the more nearly exact second method, a significant change in the character of the system response occurs: the envelope of the homogeneous system response is in general non-monotonic. This fact severely alters the relationships (a) and (b) as is shown in the following discussion. Referring to Figure 14, where possible time history segments of the homogeneous system response due to a displacement initial condition A are shown, attention is to be focused on the dotted line indicating the dimensionless system amplitude corresponding to the boundary between safe and unsafe stress levels, as well as the regions created by the intersections of this dotted line and the homogeneous response envelopes. Note that this dotted line is not horizontal since frequency changes with time, thus correspondingly altering the maximum permissible amplitude level. Furthermore, as A decreases, the dotted line translates upward as also indicated by the dashed lines in Figure 14. The significance of each region (for $A = A_1$) is tabulated below.

Region 1 - Failure cannot occur but depending on the time $\tau$, the instantaneous state of the system can be stable, unstable or neutrally stable.

Region 2 - The system fails as it enters this region, hence motion cannot exist beyond the first encounter with this region. However, note that a formal stability analysis carried out for this region at some time $\tau$ could yield a system state of stability, instability or neutral stability.

---

*Merrick, in Reference 14, has interesting comments on this subject.

Region 3 - The system fails as it enters this region and a stability analysis yields an unstable state. Note that if the amplitude A of the initial condition is changed, regions 1 through 3 may appear, disappear or change their time intervals of existence.

## 4.3 Introduction to Non-Stationary Random Processes

It has been demonstrated in Section 4.2 that if a system possesses strongly time-varying coefficients, such that non-monotonic impulse responses (homogeneous solutions) are possible, then a stability analysis does not yield the information necessary to assess the system's usefulness as in the case of a constant coefficient system. Furthermore, it has been shown that a knowledge of the initial condition magnitude to be imposed on the system at any given time is also important to assess the system's usefulness. However, since no rational method exists for explicitly determining the magnitudes of initial condition inputs throughout the life span of most systems, the next best description of the expected inputs must be statistical in nature. This unavoidable fact then clearly suggests that the behavior of the time-varying system is best described by determining MS outputs (MS denotes mean square) due to random type inputs. This information, along with estimates of the probabilities of exceeding the MS values by specified amounts etc., will also provide the input information necessary to conduct accumulative damage studies. It must be recognized that, in general, the system and the system's input will have non-stationary characteristics. Thus it is necessary to discuss some of the properties of non-stationary random processes*

---

*Some of the ensuing presentation follows that of Reference 15.

before attempting the analysis of the time-varying system. The averaging properties of a non-stationary random process will be discussed first.

Let a non-stationary random process u(t) be repeated many times. Thus the resulting ensemble of this process over some given time interval may appear as shown in Figure 15. At any time, say $t = t_1$, the ensemble average of this process is given by

$$\tilde{\tilde{u}}(t_1) = \lim_{N\to\infty} N^{-1} \sum_{i=1}^{N} u_i(t_1) \equiv \int_{-\infty}^{\infty} u P_1(u,t_1)du \tag{4-1}$$

where $P_1(u,t_1)$ is the so-called first probability distribution at $t = t_1$. In fact, the mean of the $r^{\text{th}}$ power (sometimes called the $r^{\text{th}}$ moment of the first probability distribution) of the process at $t_1$, is given by a simple generalization of Equation (4-1).

$$\tilde{\tilde{u^r}}(t_1) = \lim_{N\to\infty} N^{-1} \sum_{i=1}^{N} u_i^r(t_1) \equiv \int_{-\infty}^{\infty} u^r P_1(u,t_1)du \tag{4-2}$$

Note that if $\tilde{\tilde{u^r}}(t)$ is equal to some fixed value for all values of t, then the process is stationary random and is thus equivalent (by invoking the ergodic hypothesis) to the more familiar time average

$$\overline{u^r} = \lim_{T\to\infty} (2T)^{-1} \int_{-T}^{T} u^r(t)dt \tag{4-3}$$

Using the ensemble averaging technique described above, the correlation functions of a non-stationary random process can be defined. For instance, if $\varphi_{uu}(t_1, t_2)$ is the autocorrelation coefficient of some ensemble of processes $u_i(t)$ then using Equation (4-1) the following relation results

$$\varphi_{uu}(t_1, t_2) = \widetilde{u(t_1)u(t_2)} = \lim_{N\to\infty} N^{-1} \sum_{i=1}^{\infty} u_i(t_1)u_i(t_2)$$

$$= \int_{-\infty}^{\infty} \int_{-\infty}^{\infty} u_1 u_2 P_2(u_1, t_1; u_2, t_2) du_1 du_2 \qquad (4-4)$$

where $P_2(u_1, t_1; u_2, t_2)$ is the so-called second probability distribution. In a similar fashion, the cross-correlation coefficient of two ensembles of processes $u_i(t)$ and $v_j(t)$ is given by

$$\varphi_{uv}(t_1, t_2) = \widetilde{u(t_1)v(t_2)} = \lim_{N\to\infty} N^{-1} \sum_{i=1}^{\infty} u_i(t_1)v_i(t_2)$$

$$= \int_{-\infty}^{\infty} \int_{-\infty}^{\infty} uv P_2(u, t_1; v, t_2) du\, dv \qquad (4-5)$$

Since it may be desirable to have some qualitative feeling for the properties of $\varphi_{uu}$ and $\varphi_{uv}$, some of their more interesting properties are listed below.

$$\varphi_{uu}(t_1, t_2) = \varphi_{uu}(t_2, t_1) \qquad (4-6)$$

$$\varphi_{uu}(t_1, t_1) = \widetilde{u^2(t_1)} \tag{4-7}$$

$$\varphi_{uu}(t_1, t_2) \leq \frac{1}{2}\left\{\varphi_{uu}(t_1, t_1) + \varphi_{uu}(t_2, t_2)\right\} \tag{4-8}$$

$$\lim_{\tau \to 0} \frac{\partial \varphi_{uu}}{\partial \tau}(t_1, t_1 + \tau) = \widetilde{u(t_1)\frac{\partial u(t_1)}{\partial t_1}} \equiv 0 \tag{4-9}$$

$$\varphi_{uv}(t_1, t_2) \neq \varphi_{uv}(t_2, t_1) \tag{4-10}$$

$$\varphi_{uv}(t_1, t_2) = \varphi_{vu}(t_2, t_1) \tag{4-11}$$

Additionally $\varphi_{uv}$ is not necessarily maximum when either $t_1 = t_2$ or $t_2 = t_1$. Note that Equations (4-6), (4-7), (4-9), (4-10), and (4-11) follow directly from the definitions of the auto- and cross-correlation function. Equation (4-8) needs proof and is supplied below.

Proof for Equation (4-8)

With a little manipulation, plus or minus the product $u_i(t_1)u_i(t_2)$ may be written as

$$\pm u_i(t_1)u_i(t_2) = \frac{1}{2}\left\{\left[u_i(t_1) \pm u_i(t_2)\right]^2 - u_i^2(t_1) - u_i^2(t_2)\right\}$$

An ensemble average of this quantity then yields,

$$\pm \varphi_{uu}(t_1, t_2) = \frac{1}{2}\left\{\widetilde{\left[u_i(t_1) \pm u_i(t_2)\right]^2} - \varphi_{uu}(t_1, t_1) - \varphi_{uu}(t_2, t_2)\right\}$$

Re-arranging and taking the absolute value

$$\left| \frac{\varphi_{uu}(t_1,t_1) + \varphi_{uu}(t_2,t_2)}{2} - \frac{1}{2}\widetilde{[u_i(t_1) \pm u_i(t_2)]^2} \right| = \left| \varphi_{uu}(t_1,t_2) \right|$$

Hence it follows that

$$\left| \varphi_{uu}(t_1,t_2) \right| \leq \frac{\varphi_{uu}(t_1,t_1) + \varphi_{uu}(t_2,t_2)}{2}$$

Additionally it is interesting to note the stationary random counterpart of this statement which is obtained by noting that $\varphi_{uu}(t_1,t_1) = \varphi_{uu}(t_2,t_2)$. Thus for a stationary random process it is seen that $\varphi_{uu}(0) \geq \left| \varphi_{uu}(t_1) \right|$, as is well known. Now proceeding to the next topic of this section, the generalized power spectral density technique as applied to the non-stationary random process will be discussed.

For a stationary random process the power spectral density is defined as

$$\Phi_{uu}(\omega) = \frac{1}{\pi} \int_{-\infty}^{\infty} \varphi_{uu}(\tau) e^{-i\omega\tau} d\tau \qquad (4\text{-}12)$$

where the inverse relation is given as

$$\varphi_{uu}(\tau) = \frac{1}{2} \int_{-\infty}^{\infty} \Phi_{uu}(\omega) e^{i\omega\tau} d\omega \qquad (4\text{-}13)$$

where $t_2 - t_1 = \tau$

If a formal extension of this definition to include non-stationary random processes is attempted, Equation (4-12) is generalized to the following form.

$$\Phi_{uu}(\omega, t_1) = \frac{1}{\pi} \int_{-\infty}^{\infty} \varphi_{uu}(t_1, t_1 + \tau) e^{i\omega(t_1 + \tau)} d(t_1 + \tau) \qquad (4\text{-}14)$$

However, since $\Phi_{uu}(\omega, t_1)$, as given above implicitly depends on all other times $t_1 + \tau$, this concept is not meaningful for general non-stationary processes. Apparently, its usefulness lies only in treating weakly non-stationary random inputs or actual stationary random inputs. Notice that if a system is non-stationary due to only time-varying system coefficients, then the power spectral density technique for determining MS outputs is applicable as will now be shown. Assuming a stationary random input correlation function $\varphi_{xx}$, it is desired to first find the output correlation function $\varphi_{uu}$. This is accomplished in the following manner. First find the system output u(t) for two different values of time by using the superposition integral technique. Hence if x ($\tau$) is the input and $W(t, \tau)$ is the system impulse response, the two outputs $u(t_1)$ and $u(t_2)$ are given by

$$u(t_1) = \int_{-\infty}^{t_1} W(t_1, \tau)\, x(\tau) d\tau \qquad (4\text{-}15)$$

$$u(t_2) = \int_{-\infty}^{t_2} W(t_2, \tau)\, x(\tau) d\tau \qquad (4\text{-}16)$$

Multiplying these two equations together, supplying proper dummy variables, and ensemble averaging both sides of the resulting equation yields the desired output correlation function $\varphi_{uu}$.

$$\varphi_{uu}(t_1, t_2) = \int_{-\infty}^{t_1} W(t_1, \tau_1)d\tau_1 \int_{-\infty}^{t_2} W(t_2, \tau_2)\, \varphi_{xx}(\tau_2 - \tau_1)d\tau_2 \qquad (4\text{-}17)$$

Now substituting the relation

$$\varphi_{xx}(t_2 - t_1) = \frac{1}{2} \int_{-\infty}^{\infty} \Phi_{xx}(\omega)e^{j\omega(t_2 - t_1)}d\omega$$

into Equation (4-17) yields the results that

$$\varphi_{uu}(t_1, t_2) = \frac{1}{2} \int_{-\infty}^{\infty} \Phi_{xx}(\omega)d\omega \int_{-\infty}^{t_1} W(t_1, \tau_1)e^{-j\omega\tau_1}\, d\tau_1 \int_{-\infty}^{t_2} W(t_2, \tau_2)e^{j\omega\tau_2}\, d\tau_2 \qquad (4\text{-}18)$$

Furthermore using the basic relation between the transfer function $Y(j\omega, t)$ of a system and the system's impulse response which is expressed as

$$Y(j\omega, t) = \int_{-\infty}^{t} W(t, \tau)e^{-j\omega(t-\tau)}d\tau$$

Equation (4-18) then becomes

$$\varphi_{uu}(t_1, t_2) = \frac{1}{2} \int_{-\infty}^{\infty} \Phi_{xx}(\omega)\, Y^*(j\omega, t_1)\, Y(j\omega, t_2)e^{j\omega(t_2 - t_1)}d\omega \qquad (4\text{-}19)$$

where $Y^*(j\omega, t_1)$ is the conjugate of $Y(j\omega, t_1)$.
Now as $t_1 \longrightarrow t_2$ Equation (4-19) yields the result:

$$\widetilde{u^2(t)} = \frac{1}{2} \int_{-\infty}^{\infty} \Phi_{xx}(\omega) \left| Y(j\omega, t) \right|^2 d\omega \qquad (4\text{-}20)$$

This result clearly demonstrates that a variable-coefficient system acted upon by a stationary random input can have its MS non-stationary random output expressed in terms of the input power spectral density and the system's time dependent transfer function. Notice that the success of this method depends entirely on the stationary random character of the input. When the input does not possess this character it will be necessary to formulate the problem of finding the non-stationary random output of a system entirely in the time domain. This formulation is now described.

The system under consideration has time-varying coefficients and is acted upon by a non-stationary random input. To be as general as possible, the system is as shown in Figure 16. Any output error time history is given by

$$\epsilon(t) = \int_{-\infty}^{t} W(t,\tau) f_i(\tau) d\tau - f_d(t)$$

since

$$f_o(t) = \int_{-\infty}^{t} W(t,\tau) f_i(\tau) d\tau$$

Hence

$$\epsilon(t_1)\epsilon(t_2) = \int_{-\infty}^{t_1} W(t_1,\tau_1) f_i(\tau_1) d\tau_1 \int_{-\infty}^{t_2} W(t_2,\tau_2) f_i(\tau_2) d\tau_2 + f_d(t_1) f_d(t_2)$$

$$- f_d(t_1) \int_{-\infty}^{t_2} W(t_2,\tau_2) f_i(\tau_2) d\tau_2 - f_d(t_2) \int_{-\infty}^{t_1} W(t_1,\tau_1) f_i(\tau_1) d\tau_1$$

(4-21)

Ensemble averaging Equation (4-21) on both sides,

$$\varphi_{\epsilon\epsilon}(t_1,t_2) = \int_{-\infty}^{t_1}\int_{-\infty}^{t_2} W(t_1,\tau_1)W(t_2,\tau_2)\varphi_{ii}(\tau_1,\tau_2)d\tau_1 d\tau_2 + \varphi_{dd}(t_1,t_2)$$

$$- \int_{-\infty}^{t_2} W(t_2,\tau_2)\varphi_{di}(t_1,\tau_2)d\tau_2 - \int_{-\infty}^{t_1} W(t_1,\tau_1)\varphi_{di}(t_2,\tau_1)d\tau_1 \qquad (4\text{-}22)$$

Now letting $t_1 \rightarrow t_2$ in Equation (4-22), the desired MS error is given by

$$\widetilde{\epsilon^2}(t) = \int_{-\infty}^{t}\int_{-\infty}^{t} W(t,\tau_1)W(t,\tau_2)\varphi_{ii}(\tau_1,\tau_2)d\tau_1 d\tau_2 + \varphi_{dd}(t,t)$$

$$- 2\int_{-\infty}^{t} W(t,\tau_2)\varphi_{di}(t,\tau_2)d\tau_2 \qquad (4\text{-}23)$$

Notice that if no correlation exists between the total input (signal and noise) and the desired output, then the term $-2\int_{-\infty}^{t} W(t,\tau_2)\varphi_{di}(t,\tau_2)d\tau_2$ is identically equal to zero. Thus knowing the input autocorrelation function and the system weighting function (assuming that $\varphi_{dd} = \varphi_{di} = 0$) the output error autocorrelation function and the mean square error output are determined.

The above-mentioned quantities provide interesting information about the system but it would also be interesting to know what is the probability of an output occurring that is k times the MS value and what is the probable number of times per unit time that an output exceeds the value $\zeta$. Tsien (Reference 16) presents the derivation of these quantities for a <u>stationary</u> random process, following the lead of Bienaymé, Chebyshev, Gauss, and Rice. See References 17 and 18. Fortunately,

the results of these derivations may be recast into their non-stationary random counterparts with little difficulty. For example, if the form of the first probability distribution function $P_1(u,t)$ is known, then the probability of the magnitude of the random function u exceeding the value K is given by

$$P\left[|u(t) - \widetilde{u(t)}| \geq K\right] = 1 - \int_{-K}^{K} P_1(u,t)\,du \qquad (4\text{-}24)$$

If the first probability distribution is assumed to be Gaussian and K is expressed as a multiple of the variance at some time $t_0$ (i.e., $K = k\sigma(t_0)$ Equation (4-24) becomes

$$P\left[\,|u(t) - \widetilde{u(t)}| \geq k\,\sigma(t_0)\,\right] = 1 - \int_{-k\sigma_*(t)}^{k\sigma_*(t)} \frac{e^{-\eta^2/2}}{2} \qquad (4\text{-}25)$$

where $\sigma_*(t) = \dfrac{\sigma(t_0)}{\sigma(t)}$. Furthermore, if $k \gg 1$, then an asymptotic expansion of the error function[#] yields the result

---

[#] It must be pointed out that Tsien's statement (Reference 16, p. 126) "it is easily shown that $P\left[|y-\bar{y}| \geq k\sigma\right] \approx \dfrac{e^{-k^2/2}}{k\sqrt{2\pi}}$ for $k \gg 1$" is not correct. The factor $1/\sqrt{2\pi}$ should be replaced by $\sqrt{\frac{2}{\pi}}$. Furthermore, he states that for k = 3 the probability is .002 which is not what one obtains from using his erroneous formula, or the corrected formula for that matter. The following table summarizes the correct and the incorrect results of this stationary random probability calculation.

| Method Used or Source | $P\left[|y-\bar{y}| \geq 3\sigma\right]$ |
|---|---|
| Cramer's Table II (Ref. 17, p. 274) | 0.00270 |
| Correct first order asymptotic expansion | 0.00296 |
| Correct third order asymptotic expansion | 0.00274 |
| Tsien's value as stated in his text | 0.00200 |
| Tsien's first order asymptotic expansion | 0.00148 |

$$P\left[\left|u(t) - \tilde{\tilde{u}}(t)\right| \geq k\sigma(t_0)\right] \approx \sqrt{\frac{2}{\pi}} \frac{e^{-\frac{k^2\sigma_*^2(t)}{2}}}{k\sigma_*(t)} \cdot \left[1 - \sum_{n=1}^{\infty}(-1)^n[k\sigma_*(t)]^{-2n}\prod_{m=1}^{n}(2m-1)\right] \tag{4-26}$$

where the first order approximation is usually sufficient. If the form of the first probability distribution is not known except that it is uni-modal[#] and symmetric about $\tilde{\tilde{u}}(t)$, then a generalized form of Gauss's inequality states,

$$P\left[\left|u(t) - \tilde{\tilde{u}}(t)\right| \geq k\sigma(t_0)\right] \leq \frac{4}{9k^2\sigma_*^2(t)} \tag{4-27}$$

Finally, if nothing is known about the form of the first probability distribution, a generalized form of the Bienaymé-Chebyshev inequality states,

$$P\left[\left|u(t) - \tilde{\tilde{u}}(t)\right| \geq k\sigma(t_0)\right] \leq \frac{1}{k^2\sigma_*^2(t)} \tag{4-28}$$

It is interesting to note that if the probability for the response $u(t) - \tilde{\tilde{u}}(t)$ to exceed a given value $k\sigma(t_0)$ is $P(t)$, then the probable number of random inputs in which one will cause a response exceeding $k\sigma(t_0)$ is

$$S(t) = \frac{1}{P(t)} \tag{4-29}$$

---

[#]A physical example of a non-uni-modal distribution is provided by Mott-Smith (Reference 19) who demonstrates that the distribution of molecular velocities in a strong shock wave in a gas is bi-modal.

Proceeding to another topic, let $Q(\zeta,t)$ be the probable number of times per unit time the random function will exceed the value $u = \zeta$ at some time t. The expression for $Q(\zeta,t)$ is found to be

$$Q(\zeta,t) = \frac{1}{2}\int_{-\infty}^{\infty} P_2(\zeta,t;u',t)\,|u'|\,du' \tag{4-30}$$

where $u' = \frac{\partial u}{\partial t}$. Moreover, keeping in mind Equation (4-9), one may infer that $P_2(\zeta,t;u',t) \equiv P_1(\zeta,t)\,P_1(u',t)$. This permits Equation (4-30) to be written as

$$Q(\zeta,t) = \frac{1}{2}P_1(\zeta,t)\int_{-\infty}^{\infty} P_1(u',t)\,|u'|\,du' \tag{4-31}$$

If it happens that $P_1(u',t)$ is symmetrical Equation (4-31) then simplifies to

$$Q(\zeta,t) = P_1(\zeta,t)\int_{0}^{\infty} P_1(u',t)\,|u'|\,du' \tag{4-32}$$

It is then a trivial matter (left to any motivated or curious reader) to present the forms that $Q(\zeta,t)$ would assume if $P_1(u',t)$ were Gaussian with a variance $\sigma'(t)$ and then if $P_1(\zeta,t)$ were Gaussian with a variance $\sigma(t)$ and then if both $P_1(u',t)$ and $P_1(\zeta,t)$ were assumed Gaussian.

Thus ends the introduction to non-stationary random processes.

## 4.4 An Aeronautical Application Depending on the Non-Stationary Random Process

During the last decade an ever-growing amount of success and confidence has been associated with the stationary random analysis of a variety of aircraft problems representable by constant coefficient

systems.[#] Seemingly then, any number of a variety of aircraft problems representable by time-varying coefficient systems could be successfully analyzed by non-stationary random techniques. The desirability for such applications is furthered by the conclusions of Section 4.3 where an attempt to replace the "stability" analysis of a time-varying coefficient system by a more meaningful type of analysis directly led one to consider a non-stationary random description of the system. These applications of non-stationary random techniques to aircraft problems were thought to have been previously unused. However, in the specific area of aircraft landing loads analysis, an outstanding paper by Fung (Reference 24), which had been published late in 1955, was found as this chapter was being finished. Additionally, in 1960, Thorson and Bohne (Reference 25) treated time-varying coefficient missile and aircraft problems as continuous sums of stationary random sub-problems, and in 1961 Bieber (Reference 26) presented a non-stationary random analysis for obtaining the rigid-body structural load response of a vertical-rising ballistic missile to an environment of atmospheric disturbances.

Having dispensed with the motivational and cronological aspects, the professed purpose of this section is to demonstrate how a relatively simple non-stationary random aeronautical problem is formulated, to present the important problem parameters and to indicate how the solution is effected.[##] The problem chosen is a

---

[#] Four excellent presentations of these applications, as well as a complete listing of references, are those of Bisplinghoff, et al (References 20 and 21), and Fung (References 22 and 23).

[##] Actually, Acker (Reference 27) has made some calculations, based on the problem to be outlined in this section, in a thesis supervised by the author. The results are quite interesting and some attention will be accorded them at the end of this section.

study of the MS vertical acceleration and the vertical acceleration auto-correlation functions possessed by a supersonic, forward accelerating, rigid chord airfoil restrained in pitch. It will be observed that this problem has a classical stationary random counterpart when the forward speed is constant. See Reference 23. Denoting the vertical acceleration impulse response due to a unit impulse in upwash as $\ddot{W}$, the vertical acceleration time history $\ddot{h}$ for a given upwash $w(\tau)$ can be expressed as

$$\ddot{h}(t) = \int_{-\infty}^{t} \ddot{W}(t-\tau) w(\tau) d\tau \tag{4-33}$$

The use of piston theory aerodynamics yields the following value of $\ddot{W}$

$$\ddot{W}(t-\tau) = \epsilon_0^2 e^{-\epsilon_0 (t-\tau)} \tag{4-34}$$

where

$\epsilon_0 = 4b\rho_\infty a_\infty / m$

$b$ = airfoil semi-chord

$\rho_\infty$ = free stream density

$a_\infty$ = free stream speed of sound

$m$ = airfoil mass per unit span

Ensemble averaging the product of two terms given by Equation (4-33), that is $\ddot{h}(t_1)\,\ddot{h}(t_2)$, using the $\ddot{W}$ of Equation (4-34), and employing the von Kármán-Howarth result for the vertical turbulence auto-correlation function $\varphi_{ww}$, as given by Liepmann (Reference 28), results in the following basic expression,

$$\varphi_{\ddot{h}\,\ddot{h}}(t_1,t_2) = \epsilon_0^4 \overline{w^2}\, e^{-\epsilon_0(t_1+t_2)} \int_{-\infty}^{t_1}\int_{-\infty}^{t_2}\left[1-\frac{|\Delta x|}{L}\right]e^{-\frac{|\Delta x|}{L}+\epsilon_0(\tau_1+\tau_2)}\,d\tau_1 d\tau_2 \tag{4-35}$$

where

$\varphi_{\ddot{h}\,\ddot{h}}(t_1,t_2)$ = airfoil vertical acceleration auto-correlation function

$\overline{w^2}$ = mean square turbulence intensity

$L$ = integral scale of turbulence

$|\Delta x| = |x_2 - x_1|$ = space coordinate difference (absolute value)

This expression may also be used to calculate the mean square airfoil vertical acceleration by letting $t_2 \rightarrow t_1$, remembering that $\overline{\ddot{h}^2(t_1)} \equiv \varphi_{\ddot{h}\,\ddot{h}}(t_1,t_1)$. At this point Equation (4-35) may represent either a stationary random process or a non-stationary random process depending on the relation between $|\Delta x|$ and the time coordinates $\tau_1$ and $\tau_2$. In other words if the airfoil has a constant forward velocity, $|\Delta x|$ will be linearly related to the time scale $|\tau_2 - \tau_1|$ so that $\varphi_{\ddot{h}\,\ddot{h}}(t_1,t_2)$ will depend on only the difference $t_2 - t_1 = \tau$. Hence $\varphi_{\ddot{h}\,\ddot{h}}(\tau)$ will be a stationary random quantity. On the other hand, if the airfoil is accelerating forward, $|\Delta x|$ will be non-linearly related to the time scale so that $\varphi_{\ddot{h}\,\ddot{h}}(t_1,t_2)$ will be a <u>non-stationary</u> random quantity. This last situation commands our attention. Thus, it is assumed for time less than zero, that the airfoil is flying at a constant supersonic velocity $v_0$. At time zero the airfoil experiences an impulse in jerk[#], so that a constant acceleration "a" results for all time greater than or equal to zero. With the acceleration time history so defined, the term $\frac{|\Delta x|}{L}$ is given in non-dimensional form by the following relation.

---

[#]Jerk = the time rate of change of acceleration.

When $-\infty \leq \sigma_1 \leq 0$

$$\frac{|\Delta x|}{L} = \frac{|\Delta x|_1}{L} = \begin{cases} \sigma_1 - \sigma_2 & ; -\infty \leq \sigma_2 \leq \sigma_1 \\ \sigma_2 - \sigma_1 & ; \sigma_1 \leq \sigma_2 \leq 0 \\ \sigma_2 - \sigma_1 + \frac{\mathcal{F}}{2}\sigma_2^2 & ; 0 \leq \sigma_2 \leq \theta_2 \end{cases} \tag{4-36}$$

When $0 \leq \sigma_1 \leq \theta_1$

$$\frac{|\Delta x|}{L} = \frac{|\Delta x|_2}{L} = \begin{cases} \sigma_1 - \sigma_2 + \frac{\mathcal{F}}{2}\sigma_1^2 & ; -\infty \leq \sigma_2 \leq 0 \\ \sigma_1 - \sigma_2 + \frac{\mathcal{F}}{2}(\sigma_1^2 - \sigma_2^2) & ; 0 \leq \sigma_2 \leq \sigma_1 \\ \sigma_2 - \sigma_1 + \frac{\mathcal{F}}{2}(\sigma_2^2 - \sigma_1^2) & ; \sigma_1 \leq \sigma_2 \leq \theta_2 \end{cases} \tag{4-37}$$

where

$$\left.\begin{aligned} \sigma_i &= v_0 \tau_i / L \\ \theta_i &= v_0 t_i / L \end{aligned}\right\} \quad i = 1, 2$$

$\mathcal{F} = \frac{aL}{v_0}$ = Froude number

$v_0$ = initial velocity

a = value of airfoil's constant forward acceleration for time greater than zero

Additionally, by letting,

$$\beta = \epsilon_0 L / v_0 = [\mu M_0]^{-1}\left(\frac{L}{b}\right)$$

$\mu = m/4b^2\rho_\infty \equiv$ mass density ratio

$M_0 = v_0/a_\infty \equiv$ initial Mach number

$$\varphi_{dd}^{*}(\theta_1, \theta_2) = \varphi_{dd}\left(\frac{\theta_1 L}{v_0}, \frac{\theta_2 L}{v_0}\right) \quad ; d = \ddot{h}, \zeta''$$

$$\zeta = h/L$$

$$\ddot{h} = \frac{\partial^2 h}{\partial t^2}$$

$$\zeta'' = \frac{\partial^2 \zeta}{\partial \theta^2}$$

it is easy to show that Equation (4-35) can be non-dimensionalized, in two interesting alternate forms, as presented below in Equation (4-38).

$$\left.\begin{aligned} &\underline{\text{FORM I :}} \quad \left[\left(\frac{\overline{w^2}}{L}\right)\left(\frac{v_0^2}{L}\right)\right]^{-1} \varphi_{\ddot{h}\ddot{h}}^{**}(\theta_1, \theta_2) \\ &\underline{\text{FORM II :}} \quad \left[\frac{\overline{w^2}}{v_0^2}\right]^{-1} \varphi_{\zeta''\zeta''}^{*}(\theta_1, \theta_2) \end{aligned}\right\} = F(\theta_1, \theta_2, \beta, \mathcal{F})\beta^4 e^{-\beta(\theta_1+\theta_2)} \tag{4-38}$$

where

$$F(\theta_1, \theta_2, \beta, \mathcal{F}) = \int_{-\infty}^{\theta_1}\int_{-\infty}^{\theta_2}\left[1 - \frac{|\Delta x|}{L}\right]e^{-\frac{|\Delta x|}{L} + \beta(\sigma_1+\sigma_2)}\, d\sigma_1\, d\sigma_2 \tag{4-39}$$

The domain of integration and two typical integration paths are shown in Figure 17. As given in FORM I, $\varphi_{\ddot{h}\ddot{h}}^{**}(\theta_1, \theta_2)$ is a <u>dimensional</u> auto-correlation function expressed in terms of non-dimensional arguments $\theta_1$ and $\theta_2$ for a fixed $\mathcal{F}$ and $\beta$. Thus the left hand side of FORM I must be divided by two acceleration terms in order to be non-dimensional. These acceleration terms ($\frac{\overline{w^2}}{L}$ and $\frac{v_0^2}{L}$) are

proportional to the constant accelerations that would be required to traverse a distance equal to the integral scale of turbulence by starting at x = 0 with zero velocity and arriving at x = L with the velocity $\sqrt{\overline{w^2}}$ or $v_0$. In FORM II, $\varphi^*_{\zeta''\zeta''}(\theta_1, \theta_2)$ is a non-dimensional auto-correlation function expressed in terms of non-dimensional arguments $\theta_1$ and $\theta_2$ for a fixed $\mathcal{F}$ and $\beta$. It is seen that $\varphi^*_{\zeta''\zeta''}(\theta_1, \theta_2)$ is directly proportional to $\overline{w^2}$. The effect of $\mathcal{F}$ and some of the $\beta$ effects are contained in the F function. In general, the effect of positive $\mathcal{F}$ is to increase the value of $\overline{\dot{h}^2}$ and to skew the $\varphi^*_{\dot{h}\dot{h}}(\theta_1, \theta_1 + \theta)$ curve[#] to the left about $\theta = 0$. For negative $\mathcal{F}$, the converse is expected to be true. Since $F(\theta_1, \theta_2, \beta, \mathcal{F})$ is a well behaved function of its arguments the overall effect of $\beta$ is given by the expression $\beta^4 e^{-\beta(\theta_1 + \theta_2)}$ which provides the physically expected results that when either $\beta \to 0$ or $\beta \to \infty$, $\varphi^*_{\dot{h}\,\dot{h}}(\theta_1, \theta_2) \to 0$. Acker's calculations (Reference 27), which were carried out for a specific wing, state properties, and two values of constant acceleration (50g and 100g), agree with the above generalized predictions and arrive at mean square accelerations (for a = 50g) about 13% over the corresponding $\mathcal{F} = 0$ quasi-stationary random case.

A useful goal, arising from the solution of the above problem and some knowledge of the first probability distribution functions given in Section 3.3, would be the prediction of structural failure of the wing during any specified mission. This failure information could be used in place of qualitatively using disturbance growth and growth-rate information (time-varying stability indicators) to determine safe or unsafe behavior. This action appears desirable since, as discussed in Section 3.2, there appears to be no really satisfactory method of interpreting time-varying stability information if the coefficients[##] of the system are changing rapidly.

---

[#] Note that for convenience $\theta_2$ is represented as $\theta_1 + \theta$.

[##] In the example presented above, the deterministic counterpart would involve a time-varying coefficient problem; the state parameters being the time-varying quantities.

# CHAPTER 5

## WEAKLY NON-LINEAR AUTONOMOUS EQUATIONS OF INTEREST TO THE AEROELASTICIAN AND A TECHNIQUE FOR THEIR SOLUTION

### 5.1 Introduction; A Concise History of Non-Linear Mechanics

During the period 1882-1893 the classical researches and publications of Lindstedt (Reference 29), Poincaré (References 30,31), and Liapounoff (Reference 32) cast the foundations of non-linear mechanics. In fact, the two basic methods of approach emerging from these works still persist in modern treatments of non-linear mechanics. These methods may be described as the topological methods and the quantitative methods of successive approximations. The topological methods study trajectories in a phase space, hence permitting a comprehensive appreciation and understanding of all possible motions of the system. The penalty one pays for this "broad picture" is that numerical calculations are difficult to extract from this type of analysis. In sharp contrast, the quantitative methods severely restrict the scope of one's understanding of the system but they do permit numerical solutions to be made. Poincaré contributed fundamental ideas in each of these basic methods, thus he is often referred to as "the father of non-linear mechanics". However, the quantitative approach of Lindstedt brilliantly overcame the "secular term" difficulties experienced by Poincaré and thus logically formed the basis of the quantitative works of van der Pol (in the 20's) and of Kryloff and Bogoliuboff (in the 30's). During the period 1893-1931, a few isolated contributions of merit were presented by such people as Bendixon, Liénard, and van der Pol. See References 33, 34, and 35. Beginning in 1932 and extending through the 30's, Kryloff

and Bogoliuboff (References 36, 37, 38, 39, 40, 41, 42) and Mandelstam and Papelexi (References 43, 44) prodigiously carried out numerous applications based on slightly modified approaches of earlier authors. The Kryloff-Bogoliuboff approach was based on the original work of Lindstedt (and a co-worker Gyldén) as noted previously, while the Mandelstam-Papelexi approach was patterned after the original work of Poincaré. Following this pioneering period of emphasis on applications sampled from the various scientific disciplines, the interest of an increasing number of mathematicians, physicists and engineers was stimulated. Thus contributions to the non-linear mechanics literature appeared at an accelerating pace, the emphasis of these contributions now concentrating on such topics as the existence and stability of non-linear periodic motions (limit cycles) for a given class of equations or an engineering solution of the quantitative aspects of limit cycle analysis. A compendium of national and foreign works from this period to the present may be obtained by reference to the series of monographs edited by Lefschetz (Reference 45), the extensive bibliography of Ku (Reference 46), the classical survey text of Minorsky (Reference 47), recent contributions appearing in Prikladnaia Mathematika I Mekhanika (References 48, 49, 50, 51, 52, 53, 54), and the recent books of Cesari (Reference 55), Malkin (Reference 56), and of Bogoliuboff and Mitropolsky (Reference 57).*

## 5.2 Weakly Non-Linear Solution Techniques that Satisfy the Aeroelastician's Needs

Remaining cognizant of the techniques implicitly contained in the capsule history given in the previous section, attention is now

---

*The author is indebted to Professor W. D. Hayes (Princeton University) for alerting him to the existence and, more importantly, the scope of these last two texts.

focused on aeroelastic applications only. Thus given a problem in non-linear aeroelasticity one must first ask what types of answers are required. That is, is one interested in the numerical values of flutter amplitudes and frequencies, the existence of certain periodic solutions (that is, the existence of non-linear flutter), the stability of the possible periodic solutions, or perhaps the detailed transient motion of the aerodynamic surface in question due to some input occurring at velocities not necessarily equal to the flutter speeds? Depending on what information is desired the solution technique may vary. For example, Fung (Reference 58) and Shen (Reference 59) find the Kryloff-Bogoliuboff "averaging" technique to be very useful in settling the questions of existence and stability of non-linear flutter motions in panels and wings respectively, as well as in the determination of numerical values for flutter frequency and velocity as functions of amplitude. Runyan, Andrews, and Woolston (Reference 60) employ the analog technique (and many servo-multipliers) to obtain their answers. If the detailed transient motion due to some input is sought it is obvious that the "electronic marvel" technique of Runyan, Andrews and Woolston is quite capable of solving the problem. However, the available analytical approaches leave something to be desired. For example, the method Kryloff and Bogoliuboff does not correctly account for strong linear damping terms in the system it represents, hence the non-linear perturbations are effected about an approximate solution of the linearized equation. This fact is not important when treating the gross properties of a periodic motion such as the frequency and amplitude of a limited flutter motion, as verified by the studies of Fung (Reference 58) and Shen (Reference 59), but it is extremely important when dealing with the transient motion of

a system whose detailed motion is predominately influenced by linear springs and dampers, and secondarily by weakly non-linear elements. Noticing that transient aeroelastic problems are of the latter nature, one may expect that the method of Kryloff and Bogoliuboff will not fulfill the needs of an aeroelastician interested in transient motion aeroelastic problems. During the last two decades many attempts have been made to improve or supplant the method of Kryloff and Bogoliuboff. Unfortunately, the successful attempts have been only for those applications in which properties of periodic motions of the system are desired. As a typical* example, the much respected recent works of Cesari (Reference 61) and Hale (References 62, 63, 64) are concerned with discussing the solution technique, the stability and the existence of periodic solutions of weakly non-linear differential systems. Other typical examples are the works of Laricheva (Reference 49) and of Plotnikova (Reference 53). Laricheva investigates equations of the type,

$$\beta_{11}\ddot{x}_1 + \beta_{12}\ddot{x}_2 + \alpha_{11}x_1 + \alpha_{12}x_2 = \mu f_1(\dot{x}_1, \dot{x}_2)$$

$$\beta_{12}\ddot{x}_1 + \beta_{22}\ddot{x}_2 + \alpha_{12}x_1 + \alpha_{22}x_2 = \mu f_2(\dot{x}_1, \dot{x}_2)$$

hence, the aeroelastically important linear damping terms $\gamma_{11}\dot{x}_1$, $\gamma_{12}\dot{x}_2$, $\gamma_{12}\dot{x}_1$, and $\gamma_{22}\dot{x}_2$ are not accounted for. Additionally, Laricheva seeks only periodic solutions. Plotnikova investigates equations of the type,

---

*The reader need not be a priori convinced of this stated typicality. However, a careful search of the references given will force this opinion upon the reader.

$$\ddot{x} + ax + by = f_1(t) + \mu F_1(x, \dot{x}, y, \dot{y})$$

$$\ddot{y} + cx + dy = f_2(t) + \mu F_2(x, \dot{x}, y, \dot{y})$$

thereby neglecting inertia coupling as well as any form of important linear damping.

Since the aeroelastic system behavior of interest in this thesis depends on strong linear damping terms as well as the weakly non-linear terms, the representations given by the literature are not adequate for our purposes. Thus it is the intent of the next two sections to introduce an improved analysis for the one degree of freedom weakly non-linear problem with strong linear damping and to present the framework for a two degree of freedom weakly non-linear problem which includes the effects of complete linear couplings.

## 5.3 An Approximate Analytical Method for Treating Equations of the Type $\ddot{x} + 2\beta\dot{x} + \omega^2 x + \mu f(x, \dot{x}) = 0$

In an attempt to eliminate the weakness inherent in the Kryloff-Bogoliuboff formulation, the following equation is now considered and subsequently analyzed.

$$\ddot{x} + 2\beta\dot{x} + \omega^2 x + \mu f(x, \dot{x}) = 0 \tag{5-1}$$

As $\mu \longrightarrow 0$ the solution of Equation (5-1) for $x$ and $\dot{x}$ approach the linear solutions given by

$$x = ae^{-\beta t} \sin(\omega^* t + \varphi) \tag{5-2}$$

$$x = ae^{-\beta t} \left\{ \omega^* \cos(\omega^* t + \varphi) - \beta \sin(\omega^* t + \varphi) \right\} \tag{5-3}$$

where $\omega^* = \omega\sqrt{1 - (\beta/\omega)^2}$

Now formally considering the case in which $-1 << \beta << 1$, the $x$ and $\dot{x}$ linear solutions are approximated by

$$x = a \sin(\omega^* t + \varphi) \tag{5-4}$$

$$\dot{x} = a\omega^* \cos(\omega^* t + \varphi) - a\beta \sin(\omega^* t + \varphi) \tag{5-5}$$

This artifice has fictitiously restored the harmonic form of $x$ and $\dot{x}$ but has retained the phase lag term in the $\dot{x}$ expression. It is this phase lag term that will contribute to the accuracy of the final solution, while the fictitious harmonic form prevents any mathematical difficulties from arising when applying the modified variation of parameters method. In fact it will be seen that the variation of parameters technique will <u>restore</u> the full range of linear damping right up to, but not including, a critically damped case $(\omega/\beta = 1)$.

Now, assuming that $a$ and $\varphi$ are slowly varying functions of time for the case when $\mu \neq 0$ but small, the calculation proceeds. Differentiating Equation (5-4) yields,

$$\dot{x} = \dot{a} \sin \psi + a\omega^* \cos \psi + a\dot{\varphi} \cos \psi \tag{5-6}$$

where $\psi = \omega^* t + \varphi$

Equating Equation (5-5) to Equation (5-6) yields the following condition.

$$\dot{a} \sin \psi + a\dot{\varphi} \cos \psi + a\beta \sin \psi = 0 \tag{5-7}$$

Differentiating Equation (5-5) yields,

$$\ddot{x} = -\beta\dot{a} \sin \psi - a\omega^* \beta \cos \psi - a\dot{\varphi} \beta \cos \psi + \dot{a}\omega^* \cos \psi$$
$$- a\omega^{2*} \sin \psi - a\omega^* \dot{\varphi} \sin \psi \tag{5-8}$$

Now substituting Equations (5-4), (5-5), and (5-8) into Equation (5-1) yields the following condition.

$$-\beta\dot{a}\sin\Psi - a\omega^*\beta\cos\Psi - a\dot{\varphi}\,\beta\cos\Psi + \dot{a}\omega^*\cos\Psi - a\omega^{*2}\sin\Psi$$

$$- a\omega^*\dot{\varphi}\sin\Psi + 2a\beta\omega^*\cos\Psi - 2a\beta^2\sin\Psi + \omega^{*2}a\sin\Psi$$

$$+ \mu f^*(x,\dot{x}) = 0 \qquad (5\text{-}9)$$

where $f^*(x,\dot{x}) \equiv f(a\sin\Psi\,,\ a\omega^*\cos\Psi - a\beta\sin\Psi)$.

After simplification due to cancellations and identity relations, Equation (5-9) becomes,

$$\dot{a}\omega^*\cos\Psi - a\omega^*\dot{\varphi}\sin\Psi = -a\beta\omega^*\cos\Psi - \mu f^*(x,\dot{x}) \qquad (5\text{-}10)$$

Now Equations (5-7) and (5-10) supply the information necessary to solve for $\dot{a}$ and $\dot{\varphi}$. That is,

$$\begin{bmatrix} \omega^*\cos\Psi - a\omega^*\sin\Psi \\ \sin\Psi \qquad a\cos\Psi \end{bmatrix} \begin{Bmatrix} \dot{a} \\ \dot{\varphi} \end{Bmatrix} = -\begin{Bmatrix} a\beta\omega^*\cos\Psi + \mu f^*(x,\dot{x}) \\ a\beta\sin\Psi \end{Bmatrix} \qquad (5\text{-}11)$$

Solving Equation (5-11) for $\dot{a}$ and $\dot{\varphi}$ yields

$$\dot{a} = -\beta a - [\mu/\omega^*]f^*(x,\dot{x})\cos\Psi \qquad (5\text{-}12)$$

$$\dot{\varphi} = [\mu/a\omega^*]f^*(x,\dot{x})\sin\Psi \qquad (5\text{-}13)$$

Noticing that the non-linear terms in Equations (5-12) and (5-13) are periodic with a period $2\pi/\omega^*$ and that $\dot{a}$ and $\dot{\varphi}$ are proportional to the small parameter $\mu$, it appears reasonable to assume a and $\varphi$ are slowly varying functions of time over any given period. Hence they may be considered, to the first approximation, as constants on the right-hand sides of Equations (5-12) and (5-13), thus allowing Fourier expansion of these right-hand sides. Hence $f^*(x,\dot{x})\cos\psi$ and $f^*(x,\dot{x})\sin\psi$ are represented as,

$$f^*(x,\dot{x})\cos\psi = K_0(a) + \sum_{n=1}^{\infty} [K_n(a)\cos n\psi + L_n(a)\sin n\psi] \qquad (5\text{-}14)$$

$$f^*(x,\dot{x})\sin\psi = P_0(a) + \sum_{n=1}^{\infty} [P_n(a)\cos n\psi + Q_n(a)\sin n\psi]$$

where $K_0(a) = (2\pi)^{-1} \int_0^{2\pi} f(a\sin\psi, a\omega\cos\psi)\cos\psi\, d\psi$

$$P_0(a) = (2\pi)^{-1} \int_0^{2\pi} f(a\sin\psi, a\omega\cos\psi)\sin\psi\, d\psi$$

$$K_n(a) = \pi^{-1} \int_0^{2\pi} f(a\sin\psi, a\omega\cos\psi)\cos\psi\cos n\psi\, d\psi$$

$$L_n(a) = \pi^{-1} \int_0^{2\pi} f(a\sin\psi, a\omega\cos\psi)\cos\psi\sin n\psi\, d\psi$$

$$P_n(a) = \pi^{-1} \int_0^{2\pi} f(a\sin\psi, a\omega\cos\psi)\sin\psi\cos n\psi\, d\psi$$

$$Q_n(a) = \pi^{-1} \int_0^{2\pi} f(a\sin\psi, a\omega\cos\psi)\sin\psi\sin n\psi\, d\psi$$

Since we have assumed a and $\varphi$ constant over one period, all terms for $n \geq 1$ vanish and the solution to the original non-linear equation, Equation (5-1), is given as

$$x = a \sin (\omega^* t + \varphi) \tag{5-16}$$

where $\dot{a} = -\beta a - (\mu/\omega^*) K_0 (a)$

$$\dot{\varphi} = (\mu/a\omega^*) P_0 (a) \tag{5-17}$$

$$K_0 (a) = (2\pi)^{-1} \int_0^{2\pi} f^*(x,\dot{x}) \cos\psi \, d\psi$$

$$P_0 (a) = (2\pi)^{-1} \int_0^{2\pi} f^*(x,\dot{x}) \sin\psi \, d\psi$$

To check the limiting behavior of this equation as $\mu \rightarrow 0$, it suffices to observe Equations (5-12) and (5-13) when the $\mu \rightarrow 0$ limit is taken. Thus,

$$\lim_{\mu \rightarrow 0} (\dot{a}) = -\beta a$$

and (5-18)

$$\lim_{\mu \rightarrow 0} (\dot{\varphi}) = 0$$

Integrating these expressions,

$$a = A_0 e^{-\beta t}$$

$$\varphi = \text{const.} \tag{5-19}$$

Hence the form of Equation (5-16) becomes

$$x = A_0 e^{-\beta t} \sin(\omega^* t + \varphi) \tag{5-20}$$

which is the correct linear solution.

As another indication of the improved approximate transient solutions obtained by the method of this sub-section, the classical van der Pol equation given as,

$$\ddot{x} + x + \mu(x^2 - 1)\dot{x} = 0$$

was solved for two values of $\mu$ (.2 and .4) by an "exact" numerical integration technique, by the Kryloff-Bogoliuboff technique, and finally by the technique presented in this sub-section. The results of these calculations are presented as phase plane plots in Figures 18 through 23.

Notice that the phase plane plots obtained by using the method presented in this sub-section possess nearly the same ovaloid spiral shapes, hence phase velocities, that characterize the exact solutions even at distances close to the limit cycle. On the other hand, the phase plane plots obtained by using the Kryloff-Bogoliuboff method always have a very definite circular spiral shape so that the phase velocities of this solution and the exact solution will match only in four small sectors for each transient cycle in the phase space. Furthermore, comparing the positions of the symbols (0) that denote equal time intervals ($\sim$1.6 sec.) on the phase plane plots, it is seen that the Kryloff-Bogoliuboff solution at first leads* and lags about the exact solution and eventually lags at an increasing rate as the limit cycle is approached. In comparison the solution plot of this section at first possesses a slowly growing phase lead, in fact almost negligible until the approach to the limit cycle is over half completed, and then grows rapidly in the remaining two or three cycles that bring the trace into coincidence with the limit cycle. As an aside, it was found that both methods predict the limit cycle amplitude and frequency quite well. The point to stress however is that the method of this section is much superior to the Kryloff-Bogoliuboff method in predicting the phase velocity during the entire

*Only in the $\mu$ = .4 case does the Kryloff-Bogoliuboff solution exhibit the initial lead-lag condition. For $\mu$ = .2 just the increasing lag feature is exhibited.

transient approach to the limit cycle and predicts the actual phase quite accurately over the first 60 to 70% of the approach. Potentially, then, the method of this section is of use to aeroelasticians interested in transient motion problems. Obviously if an aeroelastic analog to the van der Pol equation existed, no one would be interested in the transient behavior since limit-cycle flutter will occur for any initial position of the system in the phase space. A system in which transient motion is of interest would be one in which the linearized analysis about the phase plane origin yielded a stable focus or a stable node. In other words a "hard"excitation must be given the system before it will exhibit a limit-cycle flutter. Any excitation less severe than the prescribed "hard" excitation, which would be a function of the airspeed U, would result in a non-linear inward motion towards the origin of the phase space. For example in Reference 60 it was found that at a velocity U, less than the linearized flutter speed of a wing, a certain finite amplitude excitation is required to cause flutter. This required amplitude decreases* as U increases until finally, at U equal to the linear flutter speed, the required amplitude is zero. If this problem were to be linearized about the phase space origin one would indeed find the stable focus or stable node motion near the origin for any velocity U less than the linear flutter speed. Hence, transient motion analysis is of interest in this case. Since this case involves two degrees of freedom, the method of this section must be extended to treat two-dimensional problems. This is done in the next section.

---

*This says physically that the change in the system parameter U changes the character of the phase space such that the amplitude and shape of the limit cycle nearest the origin diminishes until it degenerates to the point at the origin when U is equal to the linear flutter speed.

## 5.4 An Approximate Analytical Method for Treating Equations with Full Linear Couplings as well as Weakly Non-Linear Coupling Terms

The system of equations considered in this section is

$$\begin{aligned} L_1 x + L_2 y &= \mu \mathcal{X} \\ L_3 x + L_4 y &= \mu Y \end{aligned} \tag{5-21}$$

where $L_i = a_i P^2 + b_i P + \omega_i^2 \quad ; i = 1,2,3,4$

and the $\mathcal{X}$ and Y are composed of $x, \dot{x}$ and $y, \dot{y}$ non-linear combinations (e.g., $\dot{y}^2 x + y^3 \dot{x}^2$, $\ddot{y}x$, etc.). When $\mu = 0$, the x and y uncoupled equations are represented as

$$\begin{aligned} (L_2 L_3 - L_4 L_1)\, x &= 0 \\ (L_2 L_3 - L_4 L_1)\, y &= 0 \end{aligned} \tag{5-22}$$

where, in a normalized form, the operator $(L_2 L_3 - L_4 L_1)$ may be expressed as

$$(L_2 L_3 - L_4 L_1) = (p^2 + 2\nu_1 p + \Omega_1^2)(p^2 + 2\nu_2 p + \Omega_2^2) \tag{5-23}$$

Thus the exact solutions of the linear uncoupled set, if damped oscillatory motion ensues, are

$$\begin{aligned} x &= a e^{-\nu_1 t} \sin(\Omega_1 t + \varphi_{1a}) + b e^{-\nu_2 t} \sin(\Omega_2 t + \varphi_{2b}) \\ y &= c e^{-\nu_1 t} \sin(\Omega_1 t + \varphi_{1c}) + d e^{-\nu_2 t} \sin(\Omega_2 t + \varphi_{2d}) \end{aligned} \tag{5-24}$$

Now using the artifice explained in the previous section, the $\nu_i$ are initially restricted to the condition $-1 << \nu_i << 1$, such that $e^{-\nu_i t} \cong 1$. Thus the assumed forms of the x solution and its derivatives, in the case with $\mu$ small but not equal to zero, are given as*

$$x = a \sin(\Omega_1 t + \varphi_{1a}) + b \sin(\Omega_2 t + \varphi_{2b}) \tag{5-25}$$

$$\dot{x} = a\Omega_1 \cos(\Omega_1 t + \varphi_{1a}) - a\nu_1 \sin(\Omega_1 t + \varphi_{1a}) \tag{5-26}$$

$$+ b\Omega_2 \cos(\Omega_2 t + \varphi_{2b}) - b\nu_2 \sin(\Omega_2 t + \varphi_{2b})$$

$$\ddot{x} = -a\Omega_1^2 \sin(\Omega_1 t + \varphi_{1a}) - b\Omega_2^2 \sin(\Omega_2 t + \varphi_{2b}) \tag{5-27}$$

$$- 2a\nu_1\Omega_1 \cos(\Omega_1 t + \varphi_{1a}) - 2b\nu_2\Omega_2 \cos(\Omega_2 t + \varphi_{2b})$$

$$\dddot{x} = 3a\nu_1\Omega_1^2 \sin(\Omega_1 t + \varphi_{1a}) + 3b\nu_2\Omega_2^2 \sin(\Omega_2 t + \varphi_{2b}) \tag{5-28}$$

$$- a\Omega_1^3 \cos(\Omega_1 t + \varphi_{1a}) - b\Omega_2^3 \cos(\Omega_2 t + \varphi_{2b})$$

Thus using the variation of parameters technique and considering a, b, $\varphi_{1a}$ and $\varphi_{2b}$ to be time functions, the following set of algebraic equations** are derived.

$$\begin{bmatrix} k_{11} & k_{12} & k_{13} & k_{14} \\ k_{21} & k_{22} & k_{23} & k_{24} \\ k_{31} & k_{32} & k_{33} & k_{34} \\ k_{41} & k_{42} & k_{43} & k_{44} \end{bmatrix} \begin{Bmatrix} \dot{a} \\ \dot{b} \\ a\dot{\varphi}_{1a} \\ b\dot{\varphi}_{2b} \end{Bmatrix} = \begin{Bmatrix} k_1 \\ k_2 \\ k_3 \\ k_4 \end{Bmatrix} \tag{5-29}$$

---

*The y solutions obviously have a similar form.

**Note that the equations governing $\dot{c}$, $\dot{d}$, $d\dot{\varphi}_{1c}$, and $d\dot{\varphi}_{2d}$ are similar to those given in Equation (5-29).

where

$$k_{11} = (\sin \Psi_{1a}) \qquad k_{12} = (\sin \Psi_{2b})$$

$$k_{21} = (\Omega_1 \cos \Psi_{1a} - \nu_1 \sin \Psi_{1a}) \qquad k_{22} = (\Omega_2 \cos \Psi_{2b} - \nu_2 \sin \Psi_{2b})$$

$$k_{31} = (-\Omega_1^2 \sin \Psi_{1a} - 2\nu_1 \Omega_1 \cos \Psi_{1a}) \qquad k_{32} = (-\Omega_2^2 \sin \Psi_{2b} - 2\nu_2 \Omega_2 \cos \Psi_{2b})$$

$$k_{41} = (A \sin \Psi_{1a} - \Omega_1^3 \cos \Psi_{1a}) \qquad k_{42} = (B \sin \Psi_{2b} - \Omega_2^3 \cos \Psi_{2b})$$

$$k_{13} = (\cos \Psi_{1a}) \qquad k_{14} = (\cos \Psi_{2b})$$

$$k_{23} = (-\Omega_1 \sin \Psi_{1a} - \nu_1 \cos \Psi_{1a}) \qquad k_{24} = (-\Omega_2 \sin \Psi_{2b} - \nu_2 \cos \Psi_{2b})$$

$$k_{33} = (-\Omega_1^2 \cos \Psi_{1a} + 2\nu_1 \Omega_1 \sin \Psi_{1a}) \qquad k_{34} = (-\Omega_2^2 \cos \Psi_{2b} + 2\nu_2 \Omega_2 \sin \Psi_{2b})$$

$$k_{43} = (A \cos \Psi_{1a} + \Omega_1^3 \sin \Psi_{1a}) \qquad k_{44} = (B \cos \Psi_{2b} + \Omega_2^3 \sin \Psi_{2b})$$

$$k_1 = -a\nu_1 \sin \Psi_{1a} - b\nu_2 \sin \Psi_{2b}$$

$$k_2 = -a\nu_1 \Omega_1 \cos \Psi_{1a} - b\nu_2 \Omega_2 \cos \Psi_{2b}$$

$$k_3 = a\nu_1 \Omega_1^2 \sin \Psi_{1a} + b\nu_2 \Omega_2^2 \sin \Psi_{2b}$$

$$k_4 = a(C_a \cos \Psi_{1a} - S_a \sin \Psi_{1a}) + b(C_b \cos \Psi_{2b} - S_b \sin \Psi_{2b}) + \eta\chi$$

$$\eta = \mu/(a_2 a_3 - a_4 a_1)$$

$$\Psi_{1a} = \Omega_1 t + \varphi_{1a} \qquad A = 3\nu_1 \Omega_1^2$$

$$\Psi_{2b} = \Omega_2 t + \varphi_{2b} \qquad B = 3\nu_2 \Omega_2^2$$

$$C_a = \nu_1 \Omega_1^3 - 8\nu_1^2 \nu_2 \Omega_1 \qquad C_b = \nu_2 \Omega_2^3 - 8\nu_2^2 \nu_1 \Omega_2$$

$$S_a = 6\nu_1^2 \Omega_1^2 - 2\nu_1^2 \Omega_2^2 + 4\nu_1 \nu_2 \Omega_1^2 - 4\nu_1 \nu_2 \Omega_1^2$$

$$S_b = 6\nu_2^2 \Omega_1^2 - 2\nu_2^2 \Omega_1^2 + 4\nu_1 \nu_2 \Omega_2^2 - 4\nu_1 \nu_2 \Omega_2^2$$

The first step in solving these equations is to compute the determinant of the system matrix. After much labor, all the sine and cosine terms combine in such a manner as to cancel one another, thus eliminating any time variable from the value of the determinant. The resulting value of the determinant is

$$|D| = \Omega_1 \Omega_2 [2(\Omega_1^2 + \Omega_2^2)(\nu_1 + \nu_2)^2 - 8(\nu_1^2 \Omega_1^2 + \nu_2^2 \Omega_2^2) - (\Omega_1^2 - \Omega_2^2)^2] \quad (5\text{-}30)$$

Next, solving Equation (5-29) and a corresponding one for the y solution components, the differential equations for a, b, c, d, $a\dot{\varphi}_{1a}$, $b\dot{\varphi}_{2b}$, $c\dot{\varphi}_{1c}$, and $d\dot{\varphi}_{2d}$ may be written.

$$\begin{aligned}\dot{a}|D| = {} & -\eta\chi(p_{01}\cos\Psi_{1a} + p_{10}\sin\Psi_{1a}) + (p_1 + p_2\sin^2\Psi_{1a} + p_3\cos^2\Psi_{1a} \\ & + p_4\sin\Psi_{1a}\cos\Psi_{1a})a + ([p_5\sin\Psi_{2b} + p_6\cos\Psi_{2b}]\sin\Psi_{1a} \\ & + [p_7\sin\Psi_{2b} + p_8\cos\Psi_{2b}]\cos\Psi_{1a})b \end{aligned} \quad (5\text{-}31)$$

$$\begin{aligned}\dot{b}|D| = {} & -\eta\chi(q_{01}\cos\Psi_{2b} + q_{10}\sin\Psi_{2b}) + (q_2\sin^2\Psi_{2b} + q_3\cos^2\Psi_{2b} \\ & + q_4\sin\Psi_{2b}\cos\Psi_{2b})b + ([q_5\sin\Psi_{2b} + q_6\cos\Psi_{2b}]\sin\Psi_{1a} \\ & + [q_7\sin\Psi_{2b} + q_8\cos\Psi_{2b}]\cos\Psi_{1a})a \end{aligned} \quad (5\text{-}32)$$

$$\begin{aligned}a\dot{\varphi}_{1a}|D| = {} & -\eta\chi(\bar{p}_{01}\cos\Psi_{1a} + \bar{p}_{10}\sin\Psi_{1a}) + (\bar{p}_2\sin^2\Psi_{1a} + \bar{p}_3\cos^2\Psi_{1a} \\ & + \bar{p}_4\sin\Psi_{1a}\cos\Psi_{1a})a + ([\bar{p}_5\sin\Psi_{2b} + \bar{p}_6\cos\Psi_{2b}]\sin\Psi_{1a} \\ & + [\bar{p}_7\sin\Psi_{2b} + \bar{p}_8\cos\Psi_{2b}]\cos\Psi_{1a})b \end{aligned} \quad (5\text{-}33)$$

$$\begin{aligned}b\dot{\varphi}_{2b}|D| = {} & -\eta\chi(\bar{q}_{01}\cos\Psi_{2b} + \bar{q}_{10}\sin\Psi_{2b}) + (\bar{q}_2\sin^2\Psi_{2b} + \bar{q}_3\cos^2\Psi_{2b} \\ & + \bar{q}_4\sin\Psi_{2b}\cos\Psi_{2b})b + ([\bar{q}_5\sin\Psi_{2b} + \bar{q}_6\cos\Psi_{2b}]\sin\Psi_{1a} \\ & + [\bar{q}_7\sin\Psi_{2b} + \bar{q}_8\cos\Psi_{2b}]\cos\Psi_{1a})a \end{aligned} \quad (5\text{-}34)$$

$$\dot{c}|D| = -\eta Y(r_{01}\cos\Psi_{1c} + r_{10}\sin\Psi_{1c}) + (r_2\sin^2\Psi_{1c} + r_3\cos^2\Psi_{1c} + r_4\sin\Psi_{1c}\cos\Psi_{1c})c + ([r_5\sin\Psi_{2d} + r_6\cos\Psi_{2d}]\sin\Psi_{1c} + [r_7\sin\Psi_{2d} + r_8\cos\Psi_{2d}]\cos\Psi_{1c})d \quad (5\text{-}35)$$

$$\dot{d}|D| = -\eta Y(s_{01}\cos\Psi_{2d} + s_{10}\sin\Psi_{2d}) + (s_2\sin^2\Psi_{2d} + s_3\cos^2\Psi_{2d} + s_4\sin\Psi_{2d}\cos\Psi_{2d})d + ([s_5\sin\Psi_{2d} + s_6\cos\Psi_{2d}]\sin\Psi_{1c} + [s_7\sin\Psi_{2d} + s_8\cos\Psi_{2d}]\cos\Psi_{1c})c \quad (5\text{-}36)$$

$$\dot{c\varphi}_{1c}|D| = -\eta Y(\bar{r}_{01}\cos\Psi_{1c} + \bar{r}_{10}\sin\Psi_{1c}) + (\bar{r}_2\sin^2\Psi_{1c} + \bar{r}_3\cos^2\Psi_{1c} + \bar{r}_4\sin\Psi_{1c}\cos\Psi_{1c})c + ([\bar{r}_5\sin\Psi_{2d} + \bar{r}_6\cos\Psi_{2d}]\sin\Psi_{1c} + [\bar{r}_7\sin\Psi_{2d} + \bar{r}_8\cos\Psi_{2d}]\cos\Psi_{1c})d \quad (5\text{-}37)$$

$$\dot{d\varphi}_{2d}|D| = -\eta Y(\bar{s}_{01}\cos\Psi_{2d} + \bar{s}_{10}\sin\Psi_{2d}) + (\bar{s}_2\sin^2\Psi_{2d} + \bar{s}_3\cos^2\Psi_{2d} + \bar{s}_4\sin\Psi_{2d}\cos\Psi_{2d})d + ([\bar{s}_5\sin\Psi_{2d} + \bar{s}_6\cos\Psi_{2d}]\sin\Psi_{1c} + [\bar{s}_7\sin\Psi_{2d} + \bar{s}_8\cos\Psi_{2d}]\cos\Psi_{1c})c \quad (5\text{-}38)$$

where $C_c = C_a \qquad C_d = C_b \qquad S_c = S_a \qquad S_d = S_b$

$$p_{01} = \Omega_2\left\{\Omega_2^2 - \Omega_1^2 - 2\nu_2(\nu_1 - \nu_2)\right\}$$

$$p_{10} = 2\Omega_1\Omega_2(\nu_1 - \nu_2)$$

$$q_{01} = -\Omega_1\left\{\Omega_2^2 - \Omega_1^2 + 2\nu_1(\nu_2 - \nu_1)\right\}$$

$$q_{10} = 2\Omega_1\Omega_2(\nu_2 - \nu_1)$$

$$\bar{p}_{01} = 2\Omega_1\Omega_2\,(\nu_1 - \nu_2)$$

$$\bar{p}_{10} = -\Omega_2\left\{\Omega_2^{\,2} - \Omega_1^{\,2} - 2\nu_2\,(\nu_1 - \nu_2)\right\}$$

$$\bar{q}_{01} = 2\Omega_1\Omega_2\,(\nu_2 - \nu_1)$$

$$\bar{q}_{10} = -\Omega_1\left\{\Omega_2^{\,2} - \Omega_1^{\,2} + 2\nu_1(\nu_2 - \nu_1)\right\}$$

$$r_{01} = \Omega_2\left\{\Omega_2^{\,2} - \Omega_1^{\,2} - 2\nu_2(\nu_1 - \nu_2)\right\}$$

$$r_{10} = 2\Omega_1\Omega_2(\nu_1 - \nu_2)$$

$$s_{01} = \Omega_1\left\{\Omega_2^{\,2} - \Omega_1^{\,2} + 2\nu_1(\nu_2 - \nu_1)\right\}$$

$$s_{10} = 2\Omega_1\Omega_2(\nu_2 - \nu_1)$$

$$\bar{r}_{01} = 2\Omega_1\Omega_2(\nu_1 - \nu_2)$$

$$\bar{r}_{10} = -\Omega_2\left\{\Omega_2^{\,2} - \Omega_1^{\,2} - 2\nu_2(\nu_1 - \nu_2)\right\}$$

$$\bar{s}_{01} = 2\Omega_1\Omega_2(\nu_2 - \nu_1)$$

$$\bar{s}_{10} = -\Omega_1\left\{\Omega_2^{\,2} - \Omega_1^{\,2} - 2\nu_1(\nu_1 - \nu_2)\right\}$$

Notice that no definitions have been given for the $p_i$, $q_i$, $\bar{p}_i$, $\bar{q}_i$, $r_i$, $s_i$, $\bar{r}_i$, and $\bar{s}_i$, where i = 1,2,3,4. Expressions could have been written down* for these quantities but this would have been an unnecessary step as is now pointed out. Suppose that $\eta \longrightarrow 0$. Then, after applying an averaging process to eliminate the trigonometric terms, equations 5-31 through 5-38 are first order linear differential equations describing the behavior of $\dot{a}, \dot{b}, \ldots \dot{\varphi}_{1a}, \ldots \dot{\varphi}_{2d}$ in terms of

*For example see Chapter 6 of Reference 12.

a, b, c, and d. However, we can find these equations directly from the solution of the original linear coupled equations. That is, from Equation 5-21 with $\eta \sim \mu = 0$. Hence the deleted definitions. Thus, when averaging Equations 5-31 through 5-38 over a cycle, one actually carries out the averaging process for the terms multiplied by an $\eta$ (the non-linear terms), but merely replaces all other terms by their linear equation counterparts. For example, the averaged counterpart of Equation 5-31 would appear as

$$\dot{a}\,|D| = -\eta F(a,b,\ldots,\dot{a},\ldots d) + k_1 a + k_2 b$$

where F is a non-linear function equal to the first term of the Fourier expansion of $\chi(p_{01}\cos\Psi_{1a} + p_{10}\sin\Psi_{1a})$, and $k_1$ and $k_2$ are constants determined from the direct solution of Equation 5-21. The Fourier series expansion may be effected by first expanding products such as $\cos^m\Omega_1 \sin^n\Omega_1 \cos^\ell\Omega_2 \sin^t\Omega_2$ into the form $\sum\sum_{rs}\{A_{rs}\cos(r\Omega_1 \pm s\Omega_2) + B_{rs}\sin(r\Omega_1 \pm s\Omega_2)\}$. As an aside note that when $\chi$ has no y or $\dot{y}$ dependence and when Y has no x or $\dot{x}$ dependence, Equations 5-31 through 5-38 split into two uncoupled sets of equations. That is, Equations 5-31 through 5-34 and Equations 5-35 through 5-38. At this point all that remains is to specify $\chi$ and Y, carry out the averaging process in the manner already explained, and solve the resulting first order equations for the amplitude and phase parameters which will then be inserted into Equation 5-24. This is a tedious but nevertheless practical process which, in summary, provides the aeroelastician with a method for treating the transient motion described by two simultaneous differential equations with complete linear couplings and weak non-linear couplings.

# PART II

## AEROTHERMOELASTIC APPLICATIONS

# CHAPTER 6

# PRESENTATION OF THE REQUIRED AERODYNAMIC AND AEROTHERMOELASTIC THEORIES

## 6.1 Introduction

The object of Part II of this thesis is to formulate and investigate the equations representing the dynamic, torsion-bending motion of a wing which is one major component of an ultra-high performance manned vehicle that is performing some specified flight mission(s). A necessary step in obtaining this object is the derivation of the terms required to compute the time-varying coefficients of the governing equations. The derivation of these terms is necessary for the following reasons. Firstly, it is noted that a highly accelerated flight mission performed at supersonic speeds may introduce flight conditions that invalidate the well-known solution (Reference 65) for the torsional stiffness loss of an aircraft wing. The introduced conditions make it necessary to include the effects of a specified time-dependent wall temperature due to the given flight mission and to include the effects of large wing deformations due to the large magnitude transient thermal stresses produced by the given flight mission. Secondly, it is noted that although "piston theory" aerodynamics is widely in use throughout the aeronautical industry, its use as a mathematical representation for arbitrary motion may be unfamiliar. Thus a short compendium of arbitrary

motion piston theory expressions for lift and moment will be useful to the reader. Thirdly, in order to provide an aerodynamic theory that does not yield the simplified quasi-steady results of piston theory and additionally accounts for the direct effects of acceleration, it is necessary to consider the exact two-dimensional linearized aerodynamic theory for an accelerating unsteady supersonic airfoil. The well-known foundations of this exact theory are briefly recounted and then the theory is utilized to obtain lift and moment responses to impulsive upwashes of two varieties.

Thus the following three sub-sections present the material necessary to determine the time-varying coefficients that will be used in the latter portions of this thesis.

## 6.2 Loss of Torsional Stiffness due to Aerodynamic Heating, Including the Effects of Mid-Plane Stretching, Finite Acceleration and Varying State Values

In recent years several articles (References 65, 66, 67) have appeared concerning the loss of wing torsional stiffness due to aerodynamic (kinetic) heating. The solution most widely known to the members of the aeronautical profession however, adopts a mathematical model that considers an infinite acceleration to attain some final Mach number. Thus a constant wall temperature exists during the time that the wing is undergoing a torsional stiffness loss. Additionally, this model is based on the small deflection theory of elasticity. Since this model may be inadequate for the supersonic velocity, finite acceleration flight missions envisioned, the important features of Reference 67 are incorporated into the model presented in this subsection as well as a means for including the effects of arbitrary finite acceleration and varying state (density, etc.) values.

To this end, consider a plate-like wing as shown in Figure 24, which is assumed to have an x-direction uniaxial stress and strain distribution. Utilizing the finite bending theory of thin plates, the total strain in the x-direction is given by

$$\epsilon_x = \epsilon_{0x} - \zeta \frac{\partial^2 w_0}{\partial x^2} + \frac{1}{2}\left\{\frac{\partial w_0}{\partial x}\right\}^2 \tag{6.1}$$

where

$\epsilon_{0x}$ = mid-plane strain at $\zeta = 0$.

$\zeta \frac{\partial^2 w_0}{\partial x^2}$ = strain due to bending

$\frac{1}{2}\left\{\frac{\partial w_0}{\partial x}\right\}^2$ = strain due to finite transverse displacement

Now assuming that the mid-plane strain is given as $\epsilon_{0x} = \delta + \beta y$, where $\delta$ and $\beta$ are as yet undetermined time-dependent coefficients, and by using Singer's approximation for $w_0 = kxy$,* where k is the angle of twist per unit length, the total strain is given as

$$\epsilon_x = \delta + \beta y + \frac{1}{2} k^2 y^2 \tag{6.2}$$

*Reference 67 demonstrates that this extremely simple formula yields at most 5% errors in deflections when compared with exact solutions.

Hence the total stress, including thermal gradients, is given as

$$\sigma_x(y,z,t) = E\left\{\delta + \beta y + \frac{1}{2}k^2y^2 - \alpha\left[T(y,z,t) - T_w(y,z,o)\right]\right\} \tag{6.3}$$

where

E = Modulus of elasticity

$T(y,z,t)$ = actual wing temperature at $(y,z,)$ during time t

$T_w(y,z,o)$ = a reference temperature, chosen to be the wing equilibrium temperature at t = 0

In order to insure zero force and moment resultants at all wing cross-sections it is required that

$$\int_A \sigma_x \, dA = 0$$

$$\int_A y\sigma_x \, dA = 0 \tag{6.4}$$

where A is the cross-sectional area.

However, the choice of the $w_o$ function and the additional assumption of a thermally thin wing dictates that $\frac{\partial \sigma_x}{\partial z} = 0$ throughout the wing, thus Equation (6.4) is replaced by the following simpler statement.

$$\int_{-b}^{b} h\sigma_x \, dy = 0$$

$$\int_{-b}^{b} hy\sigma_x \, dy = 0 \tag{6.5}$$

where $h = h(y)$ is the local wing thickness. Now if $E = E(t)$ at most, the introduction of Equation (6.3) into Equation (6.5) yields the results

$$\begin{bmatrix} A & A^* \\ A^* & Iy \end{bmatrix} \begin{bmatrix} \delta \\ \beta \end{bmatrix} = \begin{bmatrix} \alpha T^* - \frac{k^2}{2} Iy \\ \alpha M^* - \frac{k^2}{2} \Psi \end{bmatrix} \tag{6.6}$$

where

$$A = \int_{-b}^{b} h dy = \text{cross-sectional area}$$

$$A^* = \int_{-b}^{b} hy dy \ ( = o \text{ for a symmetrical cross-section})$$

$$I_y = \int_{-b}^{b} hy^2 dy = \text{moment of inertia}$$

$$\Psi = \int_{-b}^{b} hy^3 dy \ ( = o \text{ for a symmetrical cross-section})$$

$$T^*(t) = \int_{-b}^{b} h[T(t,y) - T_w(0)]dy = \text{thermal force}$$

$$M^*(t) = \int_{-b}^{b} hy\,[T(t,y) - T_w(0)]dy = \text{thermal moment}$$

Solving Equation (6.6) yields the following results:

$$\delta(t) = (AI_y - A^{*2})^{-1} \left\{ \alpha[I_y T^*(t) - A^* M^*(t)] + \frac{k^2}{2} [A^* \Psi - I_y^{\,2}] \right\}$$

$$\beta(t) = (AI_y - A^{*2})^{-1} \left\{ \alpha[AM^*(t) - A^* T^*(t)] + \frac{k^2}{2} [A^* I_y - A\Psi] \right\} \tag{6.7}$$

At this point, $\sigma_x(y,t)$ is completely determined once k and $T(t,y) - T_w(0)$ have been specified. The next step in the calculation is to relate the stress distribution to the ensuing loss in torsional stiffness. Following the simplified development given in Reference 65, attention is focused on Figure 25 which pictures a longitudinal "fiber" originally in the position A-B of a wing structure located at a distance r from the axis of twist, which has been given an incremental twist of magnitude $\frac{d\varphi}{dx}dx$; thus the fiber is now in the position A'-B'. If the stress $\sigma_x$ is still axially aligned with the fiber, now in the position A'-B', it is seen that a small component of this stress acts in the plane of the wing cross-section. This stress component is given by $\sigma_x r \frac{d\varphi}{dx}$. Thus the incremental twisting moment about the axis of twist is given as $d\tau = \sigma_x r^2 \frac{d\varphi}{dx} dA$. Integration over the cross-section yields the result

$$\tau = \frac{d\varphi}{dx} \int_A \sigma_x r^2 \, dA \tag{6.8}$$

When Equation (6.8) is added to the usual Saint-Venant torque, the total torque $\tau_t$ becomes

$$\tau_t = \left\{ GJ + \int_A \sigma_x r^2 \, dA \right\} \frac{d\varphi}{dx} \tag{6.9}$$

It is immediately seen that the bracket term is physically just an effective torsional stiffness which will be denoted by $GJ_{eff}$. Thus,

$$GJ_{eff} = GJ + \int_A \sigma_x r^2 \, dA \tag{6.10}$$

Where GJ is now more descriptively termed an iso-thermal torsional stiffness and will be denoted by $GJ_{iso\text{-}thermal}$. The next reduction is to incorporate $GJ_{eff}$ into an expression for the square of a wing torsional frequency $\omega^2_\alpha$ since this is the term in which the stiffness appears in the equations of motion. This is accomplished by utilizing the Rayleigh method. Thus, for a constant cross-section wing of semi-span L, $\omega^2_\alpha$ is given by

$$\omega^2_\alpha = \frac{GJ_{eff}}{I_\alpha} \int_0^L \left(\frac{d\varphi}{dx}\right)^2 dx \Big/ \int_0^L \varphi^2 \, dx$$

where $\varphi$ is simply chosen as

$$\varphi = \sin \frac{\pi x}{2L}$$

Thus, a simple integration yields the result that

$$\omega^2_\alpha(t) = \frac{\pi^2 \, GJ_{eff}(t)}{4L^2 I_\alpha} \tag{6.11}$$

The last step in the calculation of $\omega^2_\alpha(t)$ is to determine the temperature distribution time history of the wing. Assuming a solid, thermally-thin wing which possesses no heat conduction in either the chordwise or spanwise directions, the heat balance equation governing the temperature at any chordwise distance y is given by

$$\frac{\partial \Theta}{\partial t} + F\Theta = F\mathcal{D} \tag{6.12}$$

with the initial condition

$$\Theta(0,y) = 0$$

where

$$\Theta(t,y) = \frac{T(t,y) - T_w(0)}{T_w(T^*) - T_w(0)}$$

$$\Omega(t) = \frac{T_w(t) - T_w(0)}{T_w(T^*) - T_w(0)}$$

$$F(t,y) = \frac{2h^*(t,y)}{\rho_m c_m h(y)}$$

$h^*$ = heat-transfer coefficient

$\rho_m$ = mass density of the wing

$c_m$ = specific heat of the wing

$h(y)$ = wing thickness

$T(t,y)$ = wing temperature

$T_w(t)$ = wall temperature

$T_w(0)$ = equilibrium wall temperature at $t = 0$

$T_w(T^*)$ = final equilibrium wall temperature at $t = T^*$

Fortunately, Equation (6.12) is a first order linear differential equation in $\Theta(t,y)$ with time-varying coefficients. Furthermore, y plays only the role of a parameter. Utilizing a standard technique, the left-hand side of Equation (6.12) is made an exact differential by multiplying the entire equation by an appropriate integrating factor $\nu$. This integrating factor is given by $\nu = e^{\int^t F(\zeta,y)d\zeta}$. The solution for $\Theta(t,y)$ then becomes,

$$\Theta(t,y) = e^{-\int^t F(\zeta,y)d\zeta}\left\{\text{const.} + \int^t F(\eta,y)\Omega(\eta)e^{\int^\eta F(\xi,y)d\xi}d\eta\right\} \qquad (6.13)$$

where the constant term is determined by the condition

$$\Theta(0,y) = 0$$

Thus, once a particular flight mission is specified and the wing properties are given, the required square of the torsional frequency $\omega^2_\alpha(t)$ can be calculated.

## 6.3 Arbitrary Motion Piston Theory

The conception and development of piston theory is concisely framed by a quote of Runyan and Morgan (Reference 68) who observed that, "This procedure was originally suggested by Hayes (Reference 69), was used by Lighthill (Reference 70) to check the results of Van Dyke at high Mach number, and later was elaborated on and applied to the flutter problem by Ashley and Zartarian (Reference 1)." One of several interesting topics discussed in the classic paper of Ashley and Zartarian was that of using piston theory assumptions in formulating lift and moment expressions for arbitrary airfoil motions.

Referring to Figure 26 and noting that (1) lift is defined positive downward (2) moment about the elastic axis is defined positive nose up and (3) moment about the aileron hinge line is defined positive trailing edge down, these expressions for the zero-thickness lift and moments are given by

$$-L = 4b\rho_\infty a_\infty \dot{\bar{h}} + 4b\rho_\infty a_\infty U\alpha + 4b^2\rho_\infty a_\infty (1-2x_0)\dot{\alpha} + 4b\rho_\infty a_\infty U(1-x_1)\beta + 4b^2\rho_\infty a_\infty (1-x_1)^2\dot{\beta} \tag{6.14}$$

$$M_{x_1} = 4b^2\rho_\infty a_\infty (x_1[2+x_1]-1)\dot{\bar{h}} + 4b^2\rho_\infty a_\infty U(x_1[2+x_1]-1)\alpha + \frac{8}{3}b^3\rho_\infty a_\infty (3x_0[1-x_1]^2 - x_1[x_1^2-3]-2)\dot{\alpha} - 4b^2\rho_\infty a_\infty U(1-x_1)^2\beta - \frac{16}{3}b^3\rho_\infty a_\infty ([1-x_1^3]-3x_1[1-x_1])\dot{\beta} \tag{6.15}$$

$$M_{x_0} = 4b^2\rho_\infty a_\infty(2x_0 - 1)\dot{\bar{h}} + 4b^2\rho_\infty a_\infty U(2x_0 - 1)\alpha + 4b^3\rho_\infty a_\infty[4x_0(1-x_0)-\frac{4}{3}]\dot{\alpha}$$

$$+ 4b^2\rho_\infty a_\infty U(1-x_1)(2x_0-1-x_1)\beta + \frac{8}{3}b^3\rho_\infty a_\infty(3x_0[1-x_1]^2-x_1[x_1^2-3]-2)\dot{\beta} \qquad (6.16)$$

where

b = airfoil semi-chord

$x_0$ = dimensionless distance from leading edge to elastic axis

$x_1$ = dimensionless distance from leading edge to aileron hinge line

$(\dot{\ }) = \frac{d(\ )}{dt}$

$\rho_\infty$ = free stream density

$a_\infty$ = free stream speed of sound

U = airspeed

$\bar{h}(t)$ = dimensional plunging motion

$\alpha(t)$ = airfoil angle of attack

$\beta(t)$ = aileron angle of attack relative to the angle

and it has been tacitly assumed that the airfoil has an aerodynamically unbalanced flap so that $\epsilon = 0$.

## 6.4 Exact Two-Dimensional Linearized Aerodynamic Theory for an Accelerating Unsteady Supersonic Airfoil

The preceding sub-section has dealt with a theory that utilizes an instantaneous point function relationship between the vertical component of the airfoil velocity and the pressure at any point on a two-simensional wing. This relationship has been found to be quite satisfactory for constant flow velocity problems in which the flow velocity

is within a rather wide range of supersonic speeds. At the lower supersonic speeds however, the piston theory concept yields less accurate results since the time history of the airfoil downwash contributes appreciably to the pressure expressions. Additionally, the piston theory concept is unable to show the direct effects of airfoil forward acceleration in any velocity regime. In order to overcome these possible deficiences, this sub-section introduces the exact two-dimensional linearized aerodynamic theory for an accelerating unsteady supersonic airfoil. This introduction will then permit a comparison of this more exact theory with the linearized version of piston theory. Since it is not possible, in general, to obtain exact solutions for the theory alluded to in this sub-section, it was decided to solve the relatively easy problem that leads to the determination of the various impulse responses of the airfoil. As will be seen these impulse responses provide a clear indication of the effects of both the time history of the airfoil motion and the forward acceleration as well as providing the kernel functions necessary for an integral formulation of the lift and moment expressions for arbitrary motion. This work is facilitated by utilizing a remarkable analogy that exists between a two-dimensional accelerating unsteady airfoil problem (see Figure 27) and a three-dimensional steady flow airfoil problem in which the main stream Mach number is fixed at $M = \sqrt{2}$ (See Figure 28). The details of this analogy are well-known and may be reviewed by referring to a report by Lomax et al (Reference 71) and to a monograph by Miles (Reference 72). Utilizing this analogy it is possible to treat the entire forward speed range, subsonic and supersonic, of the two-dimensional airfoil flying at a constant altitude. However, since a subsonic forward speed requires that the three-dimensional "analogy" wing possess subsonic leading and trailing

edges, the computational labor (for example see References 73 and 74) becomes prohibitive. For this reason, the present investigation was limited to speeds of sonic and supersonic magnitudes. Rigorously speaking, the theory of this section is valid only for constant altitude flight. However, the results and discussion contained in Appendix II show that except at $M \leq 1$ the variable altitude cases may be very satisfactorily treated by simply considering the state variables as given functions of time.

At this point all the necessary mathematical tools are implicitly available (in References 71 and 72) to calculate the time-varying pressure distribution on the two-dimensional supersonic airfoil by first obtaining the pressure distribution on the steady flow three-dimensional analogy wing and then appropriately transforming the results. As previously explained the pressure distributions and eventually the integrated lifts and moments, will be obtained that correspond to the various upwash impulse responses of the two-dimensional airfoil. For the rigid chord airfoil, two upwash impulse responses, corresponding to impulsive plunging motion and to impulsive pitch rate motion (i.e., constant and linear chordwise variation in instantaneous upwash), are required to represent motion dependent forces. The determination of these upwash impulse responses requires careful integration techniques since the already singular integrals inherent in the formulation are further complicated by the required singular upwash distributions. Thus a finite band of upwash will be used in formulating the expressions for the upwash responses and then a limiting process will be used to rigorously determine the true impulse responses. When this limiting process is applied, many integration regions on the three-dimensional analogy wing (these

regions being defined by intersections of various Mach lines) vanish, thus these vanishing regions must be examined to make sure that they leave no residual contributions to the pressure distribution. This work, as well as the rest of the details required to obtain the various upwash impulse responses, is quite lengthy. Since an outline of the procedure for obtaining the upwash impulse responses is given in Appendix III, just the final results of this procedure are now presented for a rigid chord* airfoil with a constant forward acceleration.

Lift and Moment Due to Upwash Caused by Impulsive Plunging

$$L_c(\tau,x') = \begin{cases} -4b\rho_\infty a_\infty \delta(x') & \text{Region I} \\ -\frac{4}{\pi} b\rho_\infty a_\infty \sqrt{1-\left(\frac{1-F(\tau,x')}{x'}\right)^2} & \text{Region II} \\ 0 & \text{Region III} \end{cases} \tag{6.17}$$

$$M_c(\tau,x') = \begin{cases} -4b^2\rho_\infty a_\infty [\,\delta(x') - x'] & \text{Region I} \\ -\frac{8}{\pi} b^2\rho_\infty a_\infty \left[\frac{x'}{2}\cos^{-1}\left(\frac{-1+F(\tau,x')}{x'}\right) - \right. & \text{Region II} \\ \left. \frac{1+F(\tau,x')}{2}\sqrt{1-\left(\frac{1-F(\tau,x')}{x'}\right)^2}\,\right] & \\ 0 & \text{Region III} \end{cases} \tag{6.18}$$

*As will be seen in Appendix III, upwash distributions of higher power in the chordwise variable present no difficulties, thus flexible chord airfoils may also be treated by this technique.

Lift and Moment Due to Upwash Caused by an Impulsive Pitch Rate About the Leading Edge

$$L_\ell(\tau,x')=\begin{cases} -4b\rho_\infty a_\infty\left[\delta(x')/2 + x'/2\right] & \text{Region I} \\ -\frac{4}{\pi}b\rho_\infty a_\infty\left[\frac{x'}{2}\cos^{-1}\left(\frac{-1+F(\tau,x')}{x'}\right) + \frac{1-F(\tau,x')}{2}\sqrt{1-\left(\frac{1-F(\tau,x')}{x'}\right)^2}\right] & \text{Region II} \\ 0 & \text{Region III} \end{cases} \tag{6.19}$$

$$M_\ell(\tau,x')=\begin{cases} 8b^2\rho_\infty a_\infty\left\{\frac{\delta(x')}{3}+\frac{x'}{2}F(\tau,x')\right\} & \text{Region I} \\ -\frac{8}{\pi}b^2\rho_\infty a_\infty\left\{\frac{(x')^2}{3}\left[1-\left(\frac{1-F(\tau,x')}{x'}\right)^2\right]^{3/2}\right. & \\ \left. -F(\tau,x')\left[\frac{1-F(\tau,x')}{2}\sqrt{1-\left(\frac{1-F(\tau,x')}{x'}\right)^2}+\frac{x'}{2}\cos^{-1}\left(\frac{-1+F(\tau,x')}{x'}\right)\right]\right\} & \text{Region II} \\ 0 & \text{Region III} \end{cases} \tag{6.20}$$

where $F(\tau,x') = [M_0(\tau)][t-\tau] + \mathcal{F}[t-\tau]^2$

$x' = t-\tau$

$\mathcal{F} = bA/a_\infty^2$ = Froude number

A = Value of the constant forward acceleration

$\delta(x')$ = Unit impulse function (Dirac delta function)

$( )_c$ Refers to constant upwash condition due to impulsive plunging

$( )_\ell$ Refers to linearly varying upwash condition due to impulsive pitch rate about the leading edge

Region I is given by

$$\tau \leq t \leq \tau - \frac{M_0+1}{2\mathcal{F}} + \sqrt{\left\{\frac{M_0+1}{2\mathcal{F}}\right\}^2 + \frac{1}{\mathcal{F}}} \tag{6.21}$$

Region II is given by

$$\tau - \frac{M_0+1}{2\mathcal{F}} + \sqrt{\left\{\frac{M_0+1}{2\mathcal{F}}\right\}^2 + \frac{1}{\mathcal{F}}} \leq t \leq \tau - \frac{M_0-1}{2\mathcal{F}} + \sqrt{\left\{\frac{M_0-1}{2\mathcal{F}}\right\}^2 + \frac{1}{\mathcal{F}}} \tag{6.22}$$

Region III is given by

$$t \geq \tau - \frac{M_0-1}{2\mathcal{F}} + \sqrt{\left\{\frac{M_0-1}{2\mathcal{F}}\right\}^2 + \frac{1}{\mathcal{F}}}$$

If a non-constant forward acceleration is to be considered, it is only necessary to re-define the $F(\tau, t-\tau)$ term and the integration regions. Thus for non-constant acceleration beginning at $t=\tau=0$, the only changes in the above equations are given as

$$F(\tau, t-\tau) = -\frac{1}{a_\infty}\left[\int_0^\tau U(\zeta)d\zeta - \int_0^t U(\zeta)d\zeta\right]$$

Region I is given by $0 \leq t \leq t_4$

Region II is given by $t_4 \leq t \leq t_6$ (6.23)

Region III is given by $t \geq t_6$

where $t_4$ and $t_6$ are given by the following implicit relations

$$t_4 - \tau = 1 - F(\tau, t_4 - \tau)$$

$$t_6 - \tau = -1 + F(\tau, t_6 - \tau) \tag{6.24}$$

In order to obtain an indication of the effects of airfoil time history and forward acceleration, Figures 29 through 32 present the lift and moment impulse responses for instantaneous Mach numbers $M_0(\tau)$ equal to 1.0, 1.5, and 2.0. Zero, moderate and very large accelerations are considered in each case by choosing Froude numbers equal to 0, $1 \times 10^{-2}$, and $1 \times 10^{-1}$. These Froude numbers correspond to accelerations of 0, 300, and 3000g for a 1 foot semi-chord airfoil or to accelerations of 0, 30, and 300g for a 10 foot semi-chord airfoil. Additionally, the influence of very large deceleration ( $\mathfrak{F} = -1 \times 10^{-1}$) is shown for Mach number $M_0(\tau) = 2$. Figures 29 through 32 reveal the following features about the lift and moment impulse responses:

A. The portions of the lift and moment impulse responses containing the delta functions are independent of Mach number and acceleration. In fact they are equal to the impulse responses calculated by piston theory aerodynamics.

B. The influence of increasing the Mach number $M_0(\tau)$ and/or the acceleration ($\sim\mathfrak{F}$) is to cause the lift and moment impulse responses to attenuate more rapidly.

C. Except at Mach number $M_0(\tau) \tilde{=} 1$ the influence of acceleration is microscopic compared to the influence of the Mach number $M_0(\tau)$.

D. Increasing the Mach number $M_0(\tau)$ brings the present theory rapidly into close agreement with the simpler piston theory results.

Additionally, Figures 29 through 32 imply that it is advantageous to distinguish between the influence of the quasi-steady variation of Mach number (which is the time history effect) and the direct influence of the acceleration (which is embodied in the $\mathcal{F}$ terms); since, once it is shown that the quasi-steady variation of Mach number dominates the direct acceleration effects, then the two-dimensional airfoil calculations are somewhat simplified and (perhaps more important for future work) some justification is established for treating the accelerating finite span wing in an approximate quasi-steady manner. In fact, Figures 29 through 32 do show that, except for $M_0(\tau) \cong 1$, even the large acceleration cases ( $\mathcal{F} = 1 \times 10^{-1}$) are approximated very well by assuming $\mathcal{F} = 0$ and by just considering the quasi-steady variation of $M_0(\tau)$. Additionally, for a Mach number $M_0(\tau) > 2.5$, even the effect of $M_0(\tau)$ is very small so that piston theory aerodynamics begins to be an accurate representation.

When considering a problem in which arbitrary motion is involved, the lift and moment impulse responses calculated in Equations(6.17) through (6.20) are the kernel functions for the integral relations that determine the lift and moment due to a given arbitrary motion. Referring to Figure 33, which illustrates the notation used in describing the airfoil's perturbed flight path, the integral relations for the lift and moment about the leading edge due to a given arbitrary motion are given by:

$$L(t) = \int_{-\infty}^{t^+} L_c(\tau, x')[\dot{\bar{h}}(\tau) + U(\tau)\alpha(\tau)]d\tau + \int_{-\infty}^{t^+} L_\ell(\tau, x')\dot{\theta}(\tau)d\tau \qquad (6.25)$$

$$M(t) = \int_{-\infty}^{t^+} M_c(\tau, x')[\dot{\bar{h}}(\tau) + U(\tau)\alpha(\tau)]d\tau + \int_{-\infty}^{t^+} M_\ell(\tau, x')\dot{\theta}(\tau)d\tau \qquad (6.26)$$

Thus, the presentation of the exact two-dimensional linearized aerodynamic theory for an accelerating unsteady supersonic airfoil is completed.

Finally, as a thought towards further work, it is suggested that a useful approximation of the exact linearized theory may be constructed by considering the lift and moment impulse responses as a collection of weighted pulses. This would reduce the above integrals, Equations (6.25) and (6.26), to difference - differential elements. Thus when these relations are substituted into the equations of motion for some system, the system is described by a coupled set of difference - differential equations. The solution of this set of equations, perhaps by Laplace transform methods, may be less time-consuming than solving the original set of integro-differential equations that describe the system's behavior. The success of this method obviously depends on having a large value of the ratio of the characteristic time period of the unsteady motion to the time increment required for the impulse load (lift or moment) response to go to zero; since, if this ratio is large, the effect of an impulse or of a finite load time history on the system will be practically identical. However, if this condition is not met it simply means that more pulses must be used to more accurately describe the load impulse responses. Clearly if the required number of pulses is too large, the original integro-differential equations may still be attractive.

However, referring again to Figures 29 through 32 it is seen that the time increment required for the impulse load responses to go to zero (excepting the M = 1 case) is of the order of $2b \times 10^{-3}$ to $2b \times 10^{-2}$ sec., where b is the airfoil semi-chord measured in feet.

Thus, at most, two pulses (in addition to the "piston theory pulse") should be adequate for a wide class of problems. Referring to Figures 34 and 35 it is readily seen how the load time history areas are replaced by an "equivalent area" impulse centered at the x'-centroids of the original load time history areas. The distances of the centroids from the x' = 0 axis as well as the original areas may be plotted as a function of Mach number $M_0(\tau)$ with the Froude number $\mathcal{F}$ as a parameter. See Figure 36. However, as mentioned previously, probably only the $\mathcal{F} = 0$ curve need be used when $M_0(\tau) \not\approx 1$. If successful, this "multi-pulse" piston theory should facilitate response and flutter calculations in the Mach number range from slightly above 1.0 to slightly above 2.5 where the usual piston theory begins to be an accurate representation.

At this point the presentation and discussion of the required aerodynamic and aerothermoelastic theories terminates, the remaining two chapters being devoted to an example of high-speed vibratory wing response.

# CHAPTER 7

## THE PURPOSE, DEFINITION AND DESCRIPTION OF THE COMPUTATIONAL EFFORTS

This chapter states the purpose of the ensuing computational effort, briefly defines the problem to be analyzed, describes the equations representing the problem and then discusses the methods of solving the problem. The definition of the problem includes a presentation of the flight missions chosen and a summary of the geometrical and structural properties of the wing associated with the vehicle chosen to perform the flight missions. The calculations necessary for expressing the time-varying coefficients of the above-mentioned equations are also displayed graphically. Finally, the equations of motion are presented and the methods utilized in the computational routines are explained. A short summary of IBM 704 calculation times is presented in Appendix IV to give the reader some idea of the "run-time" magnitudes required to perform a study of this general type.

The purpose of the ensuing computational effort is to answer, as completely as possible, the following questions.

(A) When are time-varying coefficients of importance in aeroelastic applications?

(B) Do these instances of importance (if any) correspond to aircraft performing flight missions of practical importance?

(C) Given a specific type of flight mission and aircraft, what is the least complicated theory that may be confidently used for analysis purposes?

(D) Will in fact the answer to (C) be that a quasi-steady linear analysis is adequate for a large variety of flight missions and aircraft?

Emphasis has been placed on the possibility of an affirmative answer for question (D) since this fact would permit the aeroelastician to utilize, with confidence, a standard analysis technique for the study of a large class of aircraft performing their various flight missions.

Although it is desired to answer questions (A) through (D) for all types of aeronautical vehicles, the enormous amount of computational effort required to calculate even one exact* reference solution for a problem involving time-varying coefficients necessitates that the different types of aircraft considered and their numerous possible flight missions must be severely limited so that the computational work can be completed using reasonable amounts of time and funds. Accordingly, it was decided to concentrate on manned vehicles operating within the atmosphere. Furthermore, in order to make the computations as useful as possible, two flight missions will be chosen that could conceivably represent the upper bound performance of manned vehicles of the foreseeable future. This choice of flight missions should insure clear indications of how approximately the time-varying system coefficients may be treated and still yield the correct system behavior.

Flight within the atmosphere yields definite bounds on the flight missions possible due to temperature-induced material limitations and the specification of a human occupant yields an upper bound on the g loading time history that can be endured by the pilot.

---

*The term "exact" here implies the use of the most accurate theories presented in Chapter 6.

For example, Reference 75 presents the maximum Mach number-altitude trajectories permissible (assuming reasonable material properties) due to kinetic heating and high q loadings, while Reference 76 displays the human time-tolerance intervals at different g loadings for various body orientations. Considering the above bounds imposed on the flight missions, a consistent choice of a manned vehicle would be one of a "super X-15" variety or of a boost-glide type which will perform the following two assumed flight missions.

The vehicle starts from a slightly supersonic speed (M = 1.05) at 35,000 feet and initiates a vertical climb which culminates in an altitude of about 140,000 feet and a final Mach number M = 8; after which time the vehicle remains at a constant altitude and Mach number. The two flight missions are distinguished only by the acceleration time histories used during the vertical climb. The first time history is a constant 9g acceleration while the second time history is an $\alpha/2(1-\cos \beta t)$ type acceleration with $\alpha$ and $\beta$ adjusted so that the time to climb, the final altitude and the final Mach number are approximately equal. The variables summarizing these two flight missions are now presented as functions of time, and are also given in graphical form in Figures 37 through 40. Additionally, the variation of the dynamic pressure q versus altitude h is shown for the 9g acceleration case in Figure 41.

Flight Trajectory Summary for the 9g Vertical Acceleration

$$h(t) = \begin{cases} 35000 + 144.9t^2 + 1018t \text{ Ft.}; & 0 \leq t \leq 23.26 \text{ sec.} \\ 137074 \text{ Ft.} ; & t \geq 23.26 \text{ sec.} \end{cases} \tag{7.1}$$

$$M(t) = \begin{cases} 1.05 + .2985t ; & 0 \leq t \leq 23.26 \text{ sec.} \\ 8.00 ; & t > 23.26 \text{ sec.} \end{cases} \tag{7.2}$$

$$\rho_\infty(h(t)) = .0034e^{-h(t)/22,000} \text{ slugs/ft.}^3 \tag{7.3}$$

The wall temperature is not an analytical function of time and is therefore expressed in tabular form.

| $T_w(t)$ deg. R. | t sec. |
|---|---|
| 471 | 0 |
| 850 | 5 |
| 960 | 6 |
| 1305 | 10 |
| 1450 | 13 |
| 1500 | 15 |
| 1540 | 20 |
| 1530 | 23 |
| 1525 | 25 |

(7.4)

Flight Trajectory Summary for the $\alpha/2(1-\cos \beta t)$ Vertical Acceleration

$$\alpha = 540$$
$$\beta = .2513 \tag{7.5}$$

$$h(t) = \begin{cases} 30723 + 4277 \cos (.2513t) + 1018t \\ \qquad + 135\, t^2 \text{ Ft}; \quad 0 \leq t \leq 25 \text{ sec.} \\ 144825 \text{ Ft.} \qquad ; \quad t \geq 25 \text{ sec.} \end{cases} \tag{7.6}$$

$$M(t) = \begin{cases} 1.05 - 1.1065 \sin (.2513t) + .2780t; \quad 0 \leq t \leq 25 \text{ sec.} \\ 8 \qquad ; \quad t \geq 25 \text{ sec.} \end{cases} \tag{7.7}$$

$$\rho_\infty(h(t)) = .0034e^{-h(t)/22,000} \text{ slugs/ft.}^3 \tag{7.8}$$

| $T_w(t)$ deg. R. | t sec. | |
|---|---|---|
| 471 | 0 | |
| 530 | 5 | |
| 577 | 6 | |
| 1108 | 10 | |
| 1490 | 13 | (7.9) |
| 1630 | 15 | |
| 1680 | 20 | |
| 1600 | 23 | |
| 1490 | 25 | |

Summary of the Geometrical and Structural Properties of the Vehicle Wing

The wing geometry is described in Figure 42. Although the planform is rectangular the wing area, wing weight, etc., are roughly the same as the unclassified estimates (available in periodicals) made for the X-15. Structurally the wing is represented by a 3% unsymmetrical (fore and aft) double wedge stainless steel multi-cell thick skin cross-section. The number of cells is not determined since this then allows the required freedom in choosing the iso-thermal fundamental torsional frequency. This freedom in choosing $\omega\alpha_{\text{iso-thermal}}$ is necessary since a wing must be found that is just slightly stable (but not unstable) when analyzed by quasi-steady techniques over some portion of the flight mission. This slightly stable configuration gives some "sensitivity" to the results calculated using non-quasi-steady analyses. In view of these remarks $\omega_\alpha^2$ is found by using a modified form of Equation 6.11

$(\omega_{\alpha\ \text{iso-thermal}}^2 = K^2 \dfrac{\pi^2}{(2L)^2 I\alpha} \cdot GJ(0)^*_{\text{linear}})$ where $K^2$ is adjusted to give an adequate value of $\omega_{\alpha\ \text{iso-thermal}}^2$. After some mathematical experimenting it is found that $K^2 \cong 4.00$, which appears to be quite high. However, this value of $K^2$ corresponds to adding only about .015 to the existing airfoil thickness ratio. Hence this artifice produces the required changes well within the error bounds of a design analysis.

Using the assumed values,

$\overline{M} = 5.8230$ slugs/ft.

$I_\alpha = 14.216$ slug ft.$^2$

$S_\alpha = -3.6394$ slug ft.

$\left(\frac{\omega h}{\omega \alpha}\right)^2 = .20$

$c = 2b = 6.25$ ft.

$L = 8$ ft.

it is found that

$\omega_\alpha^2(t) = .01085\ GJ(t)$

$GJ(0)_{\text{linear}} = 5.932 \times 10^6$ #ft.$^2$

$\omega_{\alpha\ \text{iso-thermal}}^2(0) = 6.44 \times 10^4$ rad.$^2$/sec.$^2$

$\omega_{h\ \text{iso-thermal}}^2(0) = 1.288 \times 10^4$ rad.$^2$/sec.$^2$

By assuming no degradation of elastic properties at <u>constant</u> elevated temperatures,

$\omega_{h\ \text{iso-thermal}}^2(0) \equiv \omega_h^2(t).$

---

*$GJ(0)_{\text{linear}}$ denotes the value of GJ at t = 0 when no <u>non-linear mid-plane stretching effect</u> is included.

Now by using equation 6.10 the $GJ_{eff}$ may be calculated with just one modification. Equation 6.10 was derived assuming a solid wing, thus some correction must be made for the fact that the wing to be analyzed has a cellular structure. The desired correction has been made by introducing a thermal stress efficiency factor $\eta$ into the equation for GJ(t) so that this result is now given, referring to Figure 43, as

$$GJ(t) = GJ(0) = 2\eta \int_{.55C}^{0} \sigma_x y^2 t_1(y)dy + 2\eta \int_{0}^{.45C} \sigma_x y^2 t_2(y)dy \quad \#ft.^2$$

where $\sigma_x$ is given by Equation 6.3.

Again after a limited amount of mathematical experimenting, $\eta$ was assigned a value of $\eta = .5000$. Additionally when assessing $\sigma_x$ it is necessary to specify the initial twist rate k that introduces the non-linearity into the analysis. Figure 44 shows the effect of k on GJ(t) for both flight missions and for three values of k.

As can be seen from Figure 44, large reductions in torsional stiffness do not take place. This is primarily due to the fact that, at the altitudes considered, the heat transfer coefficient $h^*$ is quite small since it is directly proportional to the $4/5^{ths}$ power of the atmospheric density.

## SUMMARY OF CALCULATION PROCEDURES AND METHODS OF SOLVING THE PROBLEM

The calculations described in this sub-section were designed to numerically solve the system of Equations 7.10 and 7.11 with an accuracy of four or five significant figures. Since the solution of these equations depends on what aerodynamic theory is used to

describe the lift and moment, what flight mission is chosen, and how exactly (or how approximately) the effects of the time-varying coefficients are treated, it is obvious that several solutions of varying "exactness" will ensue and that, possibly, each solution may be best obtained by a different calculation procedure. Furthermore, since it is not known a priori how markedly the solutions utilizing the time-varying coefficients and/or the various aerodynamic theories will differ from the damped sinusoidal sums that are characteristic of the quasi-steady solutions, the more exact solutions must be the responses to some suitable set of inputs such that these solutions reveal a significant amount of information about the effects of the time-varying coefficients and the various aerodynamic theories. Clearly, several choices must be now made as to what inputs are to be used, at what times during the flight mission should these inputs be initiated, how long after these input initiations should the response be recorded, how many different approximate solutions are to be attempted, and as to what techniques should be used to obtain the various approximate solutions. These choices are described in the following paragraphs.

Suitable inputs are obtained by using perturbation impulsive loadings ($\dot{\underline{h}}$ or $\dot{\alpha}$) at some time $\tau$. One advantage of impulsive inputs is their correspondence to velocity initial conditions for a given system. Hence it is possible to obtain the homogeneous response of the system at time t due to specified velocity initial conditions at time $\tau$. The above reference to perturbation is underlined since it is to be understood that the system response is comprised of two parts. The first part being that response due to intentional control and throttle movements throughout the flight mission; the

second part being the response to the chosen perturbation inputs occurring at time(s) $\tau$. This further implies that the response of interest in this report, the perturbation response, is zero until $t = \tau$. Thus given a flight mission, and a perturbation input at time $\tau_i$ (the i denotes that there may be several values of $\tau$ at which one would like to investigate the effects of the input), one will obtain i traces of $\bar{h}$ and $\alpha$ perturbation motions, each trace being zero until $t = \tau_i$. These $\bar{h}$ and $\alpha$ motions are combinations of the damped normal aeroelastic modes (if they exist) of the system, thus unless one mode predominates in the description of either $\bar{h}$ or $\alpha$ it may be difficult to draw quantitative conclusions about the effective damping ratios of the system, although qualitative conclusions are easily obtained. In the special case of the quasi-steady analysis utilizing piston theory aerodynamics, it is much easier to calculate the frequencies and damping ratios directly with no consideration given to the total $\bar{h}$ and $\alpha$ motion. Had time permitted, the quasi-steady response to $\dot{\bar{h}}$ and $\dot{\alpha}$ impulsive inputs would have provided a more direct correlation with the other calculations.

The large amounts of time required, on even such an efficient high-speed machine as the IBM 704 computer, to calculate the response time histories made it imperative to sparingly choose the times of input initiations and the duration of the recorded response. Thus the cases involving piston theory aerodynamics were studied for inputs at 0, 2, 4, ..., 28, 30 seconds, with each time history having a one second duration and the cases involving the exact unsteady accelerating aerodynamics were studied for inputs at 0, 2, 4, 6, and 8 seconds, with each time history having a one-half second duration.

The solutions involving piston theory aerodynamics were found by first treating the time-varying coefficients exactly and then by using a quasi-steady analysis for the times t = 0, 2, 4,..., 28, 30 seconds.

When considering the solutions involving the exact unsteady accelerating aerodynamics the results of a preliminary calculation involving the determination of lift and moment responses to impulsive pitch and plunge inputs indicated, for the accelerations involved in the given flight missions and for the stated Mach number range $1.05 \leq M \leq 8$, that the direct effect of the Froude number $\mathcal{F}$ was negligible. Hence the $\mathcal{F} = 0$ approximation is used with excellent justification for all the exact unsteady accelerating aerodynamics relations. Furthermore, it was decided to first compare the results of the more critical flight mission (more critical in the sense of simultaneous high q and high $\mathcal{F}$ occurring) with the simpler piston theory solutions and then to determine if the less* critical flight mission should be considered. This decision and its aftermath is discussed in Chapter 8. The calculation procedures for these exact solutions and the approximate procedures are now described in some detail.

The equations treated, referring to Figure 26, are

$$\ddot{\bar{h}}(t) + \frac{S_o}{\bar{M}} \ddot{\alpha}(t) + \omega_h^2 \bar{h}(t) = - L(t)/\bar{M} \qquad (7.10)$$

---

*One might argue that the "less critical" flight mission, the 9g case, would demonstrate more unsteady accelerating aerodynamics effects in the Mach number region 1.05-1.5 than would the "most critical" flight mission. The argument is of course correct except that the Froude number $\mathcal{F}$ for a 9g acceleration of the airfoil in question at 35,000 ft. altitude is $\mathcal{F} \cong 10^{-3}$. This value of $\mathcal{F}$ predicates small effects even in the low supersonic range $1.05 \leq M \leq 1.5$.

$$S_o/I_o \ddot{\bar{h}}(t) + \ddot{\alpha}(t) + \omega_\alpha^2 \alpha(t) = M_o(t)/I_o \tag{7.11}$$

where

$M$ = mass = 5.8230 slugs

$I_o \equiv I_\alpha$ = 14.216 slug ft.$^2$

$S_o \equiv S_\alpha$ = -3.6394 slug ft.

Now for an unsteady supersonic aerodynamic solution $L(t)$ and $M_a(t)$ are given by

$$L(t) = \int_0^{t^+} L_c(\tau, t-\tau) U(\tau) \left[\frac{\dot{\bar{h}}(\tau)}{U(\tau)} + \alpha(\tau)\right] d\tau$$

$$+ \int_0^{t^+} L_\ell(\tau, t-\tau) \dot{\alpha}(\tau) d\tau \tag{7.12}$$

$$M_a(t) = \int_0^{t^+} M_c(\tau, t-\tau) U(\tau) \left[\frac{\dot{\bar{h}}(\tau)}{U(\tau)} + \alpha(\tau)\right] d\tau$$

$$+ \int_0^{t^+} M_\ell(\tau, t-\tau) \dot{\alpha}(\tau) d\tau \tag{7.13}$$

while for a piston theory solution:

$$L(t) = \frac{\rho_\infty(t)}{2} U^2(t) S\left[\frac{4}{M(t)} \left(\frac{\dot{\bar{h}}(t)}{U(t)} + \alpha(t)\right) + \left(\frac{4}{M(t)} \left(\frac{1}{2} - a\right)\right.\right.$$

$$\left.\left. - (\gamma + 1) \frac{A_w}{c^2}\right) \frac{c \dot{\alpha}(t)}{U(t)}\right] \tag{7.14}$$

$$M_a(t) = \frac{\rho_\infty(t)}{2} U^2(t)\, Sc\Big[\Big(\frac{4}{M(t)}\Big(a - \frac{1}{2}\Big) + (\gamma+1)\frac{A_w}{c^2}\Big(\frac{\dot{\bar{h}}(t)}{U(t)} + \alpha(t)\Big)\Big)$$

$$+ \Big(\frac{4}{M(t)}\Big\{a - a^2 - \frac{1}{3}\Big\} - (\gamma+1)\Big(\frac{2aA_w}{c^2} - \frac{2M_w}{c^3}\Big)\Big)\frac{c\dot{\alpha}(t)}{U(t)}\Big] \qquad (7.15)$$

where

$A_w$ = total wing cross-section area

$M_w$ = first area-moment of total wing cross-section about the leading edge

The piston theory solution of the problem was found first, as the differential equations could be solved numerically with an accuracy of five significant figures and could be compared with a difference equation solution of the same set. This comparison is important, since it gives the basis for a statement of accuracy concerning the difference equations used to solve the unsteady aerodynamics set of equations. A preliminary study was done to determine whether operational calculus methods could be employed to reduce the exact solution of the unsteady aerodynamics set to a feasible IBM 704 problem. Results of this study showed that an estimated minimum of 100 hours of machine time would be necessary for this solution due to the presence of changing functions of $(t-\tau, \tau)$ under the integral sign. Therefore, the decision to use difference equation approximations was made since the comparison of the exact solution with the difference equation solution of the piston theory formulation showed that 4 to 5 significant figure accuracy could be obtained by using a $\Delta t$ of .001 sec. and by approximating the true value of $\bar{h}(t)$ and $\alpha(t)$ at the end of the first .001 second interval by the piston theory exact solution values.

The entire study as described was done for an acceleration of ng = 270 (1 - cos .2513t) letting $\mathcal{F} = 0$ and the complete piston theory and quasi-steady study was done for an acceleration of ng = 9g. Each of these accelerations was broken up into two cases. Case 1 is a time history following a unit impulse on $\dot{\bar{h}}(t)$ at time $t_o$ where $\dot{\alpha}(t_o) = 0$; Case assumes $\dot{\bar{h}}(t_o) = 0$ and $\dot{\alpha}(t_o) = 1.0$.

Before the main body of calculations could be started, a suitable k had to be found (as mentioned previously). By finding GJ(t) in a separate preliminary calculation, it was determined that k = .006 was a reasonable choice. Then GJ(t) was approximated by a series of cubic equations yielding five significant figures for use in solving Equations (7.10) and (7.11).

Substituting the given values into Equations (7.10) and (7.11) the piston theory system for both ng's becomes:

$$\ddot{\bar{h}}(t) - .625\,\ddot{\alpha}(t) = -2084.4\rho_\infty(t)\left\{\dot{\bar{h}}(t) - .3125\,\dot{\alpha}(t)\right\}$$

$$- 1.288 \times 10^4\,\bar{h}(t) - 2084.4\,\rho_\infty(t)U(t)\alpha(t) \qquad (7.16)$$

$$-.256\ddot{\bar{h}}(t) + \ddot{\alpha}(t) = 853.77\rho_\infty(t)\left\{.3125\dot{\bar{h}}(t) - 3.3529\,\dot{\alpha}(t)\right\}$$

$$+ \left\{266.80\rho_\infty(t)U(t) - \omega_\alpha^{\,2}(t)\right\}\alpha(t) \qquad (7.17)$$

As stated previously, these equations were first solved numerically and then the finite difference form of these equations were solved for several time histories in order that the aforementioned

comparison could be made. Additionally, this set of equations was solved in a quasi-steady manner, for times t = 0, 2, 4, ..., 23, 30 seconds. This quasi-steady calculation was performed in the classical manner by letting $p^n = \frac{d^n}{dt^n}$ in the Equations 7.16 and 7.17 and then solving for the roots of the resultant quartic in p. One thus obtains four sets of roots in the form a ± ib and c ± id, where a and c are proportional to the instantaneous (quasi-steady) damping ratios $\zeta$ of the system and b and d are the instantaneous frequencies of the system.

To treat the unsteady supersonic aerodynamics solution Equations 7.10 and 7.11 were written in operational form:

$$\ddot{x}_i(t) - L^*_{ii}(t)\{x_i(t)\} - L^*_{ij}\{x_j(t)\} = f_i^*(t)$$

$$+ g_i^*(t) \int_0^{t^+} [\tilde{K}^*_{ii}(\tau, t-\tau)x_i(\tau) + \tilde{K}^*_{ij}(\tau, t-\tau)x_j(\tau)$$

$$+ \bar{K}^*_{ii}(\tau, t-\tau)\dot{x}_i(\tau) + \bar{K}^*_{ij}(\tau, t-\tau)\dot{x}_j(\tau)]d\tau \qquad i,j = 1,2 \quad i \neq j \qquad (7.18)$$

where 1 denotes the $\bar{h}$ motion and 2 denotes the $\alpha$ motion and

$$L^*_{ii}(t) = a^*_{ii}(t)\frac{d}{dt} + b^*_{ii}(t)$$

$$L^*_{ij}(t) = d^*_{ij}(t)\frac{d^2}{dt^2} + a^*_{ij}(t)\frac{d}{dt} + b^*_{ij}(t)$$

It is most convenient to remove the dirac portion of the expression from under the integral sign yielding Equation 7.19, where $\tilde{C}_{k\ell}$ and $\bar{C}_{k\ell}$ are the coefficients of the dirac portion of the kernel multiplying $X_\ell$ and $\dot{X}_\ell$ respectively, and $\tilde{K}_{k\ell}$ and $\bar{K}_{k\ell}$ are the kernels with the dirac portion removed.

$$\ddot{x}_i(t) = L^*_{ii}(t)\{x_i(t)\} + L^*_{ij}(t)\{x_j(t)\} + g^*_i(t)\left[\tilde{C}_{ii}x_i(t) + \tilde{C}_{ij}x_j(t) + \bar{C}_{ii}\dot{x}_i(t) + \bar{C}_{ij}\dot{x}_j(t)\right] + f^*_i(t) + g^*_i(t)\int_0^t \left[\tilde{K}_{ii}x_i(\tau) + \tilde{K}_{ij}x_j(\tau) + \bar{K}_{ii}\dot{x}_i(\tau) + \bar{K}_{ij}\dot{x}_j(\tau)\right]d\tau \qquad (7.19)$$

where

$$f^*_i(t) = 0 \qquad a^*_{ii} = a^*_{ij} = 0$$

$$d^*_{12} = -S_o/\bar{M} \qquad d^*_{21} = -S_o/I_o$$

$$b^*_{11} = -\omega^2_h \qquad b^*_{22} = -\omega^2_\alpha \qquad b_{ij} = 0$$

$$g^*_1 = -S/c\bar{M} \qquad g^*_2 = S/cI_o$$

$$\tilde{C}_{11} = \tilde{C}_{21} = 0 \qquad \tilde{C}_{12} = 2\rho_\infty a_\infty cU \qquad \tilde{C}_{22} = 2\rho_\infty a_\infty c^2 U(a-\tfrac{1}{2})$$

$$\bar{C}_{11} = 2\rho_\infty a_\infty c \qquad \bar{C}_{12} = 2\rho_\infty a_\infty c^2(\tfrac{1}{2} - a) \qquad \tilde{K}_{11} = \tilde{K}_{21} = 0$$

$$\bar{C}_{21} = 2\rho_\infty a_\infty c^2(a - \tfrac{1}{2}) \qquad \bar{C}_{22} = -2\rho_\infty a_\infty c^3(\tfrac{1}{3} - a + a^2)$$

$$\tilde{K}_{12} = \begin{cases} 0 & ;\ 0 \le x' \le x'_2 \\ \frac{2}{\pi}\rho_\infty a^2_\infty U\sqrt{1 - \left(\frac{1-f}{x'}\right)^2} & ;\ x'_2 < x';\ f \le 1 + x' \\ 0 & ;\ f \ge 1 + x' \end{cases}$$

$$\tilde{K}_{22} = \begin{cases} \rho_\infty a_\infty^2 c U x' \\ \frac{2}{\pi}\rho_\infty a_\infty^2 c U \left[\frac{x'}{2}\cos^{-1}\left(\frac{f-1}{x'}\right) + \left(a - \frac{1+f}{2}\right)\sqrt{1 - \left(\frac{1-f}{x'}\right)^2}\right] \\ 0 \end{cases}$$

$$x' = \frac{a_\infty}{c}(t-\tau)$$

$$f = f(x', \tau) = M(\tau)x'$$

$$x'_2 = [1 + M(\tau)]^{-1}$$

$$\bar{K}_{11} = \begin{cases} 0 & ; 0 \le x' \le x'_2 \\ \frac{2}{\pi}\rho_\infty a_\infty^2 \sqrt{1 - \left(\frac{1-f}{x'}\right)^2} & ; x'_2 < x',\ f < 1 + x' \\ 0 & ; f \ge 1 + x' \end{cases}$$

$$\bar{K}_{21} = \begin{cases} \rho_\infty a_\infty^2 c x' \\ \frac{2}{\pi}\rho_\infty a_\infty^2 c \left\{\frac{x'}{2}\cos^{-1}\left(\frac{f-1}{x'}\right) + \left(a - \frac{1+f}{2}\right)\sqrt{1 - \left(\frac{1-f}{x'}\right)^2}\right\} \\ 0 \end{cases}$$

$$\bar{K}_{12} = \begin{cases} \rho_\infty a_\infty^2 c x' \\ \frac{2}{\pi}\rho_\infty a_\infty^2 c \left\{\frac{x'}{2}\cos^{-1}\left(\frac{f-1}{x'}\right) + \left(\frac{1-f}{2} - a\right)\sqrt{1 - \left(\frac{1-f}{x'}\right)^2}\right\} \\ 0 \end{cases}$$

$$\bar{K}_{22} = \begin{cases} -\rho_\infty a_\infty^2 c_\infty^2 f x' \\ \frac{2}{\pi}\rho_\infty a_\infty^2 c_\infty^2 \left\{ -f\left[\frac{x'}{2}\cos^{-1}\left(\frac{f-1}{x'}\right)\right] + \left[\frac{f(f-1)}{2} + a(1-a)\right]\sqrt{1-\left(\frac{1-f}{x'}\right)^2} \right. \\ \qquad \left. + \frac{x'^2}{3}\left[1-\left(\frac{1-f}{x'}\right)^2\right]^{3/2} \right\} \\ 0 \end{cases}$$

By using central difference approximations, set

$$\dot{x}_n(t) \cong \frac{x_{n+1}(t) - x_{n-1}(t)}{2(t_{n+1} - t_n)} = \frac{x_{n+1}(t) - x_{n-1}(t)}{2\Delta}$$

$$\ddot{x}_n(t) \cong \frac{x_{n+1}(t) - 2\,x_n(t) + x_{n-1}(t)}{\Delta^2}$$

and replacing the above integral by

$$I_{ijn} \equiv g_i \sum_{k=0}^{n-1} W_k \left[\tilde{K}_{ii}(t_k,\, t_n - t_k)x_k^{(i)} + \tilde{K}_{ij}(t_k,\, t_n - t_k)x_k^{(j)}\right.$$

$$+ \bar{K}_{ii}(t_k,\, t_n - t_k)\left(\frac{x_{k+1}^{(i)} - x_{k-1}^{(i)}}{2\Delta}\right)$$

$$\left. + \bar{K}_{ij}(t_k,\, t_n - t_k)\left(\frac{x_{k+1}^{(j)} - x_{k-1}^{(j)}}{2\Delta}\right)\right]$$

(where $W_k$ is the weighting factor corresponding to the trapezoidal rule of numerical integration) one obtains the difference equations,

$$\beta_{iin}x^{(i)}_{n+1} + \beta_{ijn}x^{(j)}_{n+1} = \Gamma_{iin}x^{(i)}_{n} + \Gamma_{ijn}x^{(j)}_{n} + \Delta_{iin}x^{(i)}_{n-1}$$

$$+ \Delta_{ijn}x^{(j)}_{n-1} + I_{ijn} \qquad (7.20)$$

where

$i \neq j$

$$\beta_{iin} = \frac{1}{\Delta^2} - \frac{a^*_{iin}}{2\Delta} - \frac{g^*_i C_{ijn}}{2\Delta}$$

$$\beta_{ijn} = -\frac{d^*_{ijn}}{\Delta^2} - \frac{a^*_{ijn}}{2\Delta} - \frac{g^*_i \bar{C}_{ijn}}{2\Delta}$$

$$\Gamma_{iin} = \frac{2}{\Delta^2} + b^*_{iin} + g^*_i \tilde{C}_{iin}$$

$$\Gamma_{ijn} = \frac{-2d_{ijn}}{\Delta^2} + b^*_{ijn} + g^*_i \tilde{C}_{ijn}$$

$$\Delta_{iin} = \frac{1}{\Delta^2} - \frac{a^*_{iin}}{2\Delta} - \frac{g^*_i \bar{C}_{ii}}{2\Delta}$$

$$\Delta_{ijn} = \frac{d^*_{ijn}}{\Delta^2} - \frac{a^*_{ijn}}{2\Delta} - \frac{g^*_i \bar{C}_{ij}}{2\Delta}$$

$$\Delta = t_n - t_{n-1}$$

To start the solution of these difference equations Case 1 and Case 2 initial conditions were used, the values from the piston theory solution at $t_o$ + .001 sec. (the piston theory solution = the unsteady aerodynamics solution to five significant figures at $t_o$ + .001 sec.), and the exact derivatives at $t = t_o$ rather than the difference approximations. These measures were taken to insure at least 4 figures of accuracy in the results, since it was found that a sizeable error can be introduced by using the stated difference equation between $t_o$ and $t_o$ + .001 sec.

Since the GJ(t) calculation, the piston theory differential equation solution, and the difference equation solution utilizing the exact unsteady accelerating aerodynamic theory were all done by means of an IBM 704, programs written in the Share Assembly language are available for future use by interested people or agencies. Problems similarly formulated with different parameters could be solved by making only minor modifications to the existing programs.

# CHAPTER 8

## PRESENTATION AND DISCUSSION OF THE SOLUTIONS

Once the calculations described in Chapter 7 have been completed the resulting plethora of information must be presented in an organized fashion such that the answers to questions (A) through (D)*, posed in the first page of Chapter 7 of this thesis may be obtained. To this end, the impulse response time histories $\bar{h}$ and $\alpha$ were examined over their full time range and then grouped into the following two categories. The first category contained $\bar{h}$ and $\alpha$ time histories, utilizing piston theory aerodynamics, for the two acceleration time histories and both Case 1 and Case 2 inputs. The second category contained $\bar{h}$ and $\alpha$ time histories, utilizing first piston theory aerodynamics and then unsteady accelerating aerodynamics, which were examined over the time interval $0 \leq t \leq 8$ seconds for the ng = 270(1-cos.2513t) acceleration time history and both Case 1 and Case 2 inputs. Note that the $\bar{h}$ and $\alpha$ time histories grouped in the above two categories are exact solutions of the problem within the framework of the mathematical model chosen for the aerodynamics, etc. Thus these time histories yield the most accurate response curves of the aircraft wing. A third grouping of information was formed by compiling the quasi-steady frequency calculations, as well as the

---

*For the chosen class of "manned vehicles".

instantaneous frequencies obtained from the exact solutions utilizing first piston theory aerodynamics and then unsteady accelerating aerodynamics, over the entire time range for both acceleration time histories. This bloc of information obviously yields the crudest possible, and most easily obtainable, description of the wing motion.* At this point, the "best" and the "worst" solutions are available for inspection. Note that if additional solutions intermediate to the "best" and "worst" are required, the theories developed in Part I of this thesis are then applicable. The need for these additional solutions must be a consequence of a poor correlation between the "worst" and the "best" solution, therefore the comparison of these latter solutions should be first pursued.

Since Groups 1, 2, and 3 contain so much data,** these data were re-examined and then sorted, within each group, into their essential and non-essential elements;*** the essential elements of each group being presented in this thesis. The essential elements of the first, second, and third groups are contained in Figures 51 through 66, Figures 67 through 78, and Tables 2 through 6, respectively.

---

* In order to directly compare the quasi-steady portion of the group three information with groups one and two, a quasi-steady analysis of the wing response due to Case 1 and Case 2 inputs should have been made. However, time limitations dictated the approach pursued above.

** Necessarily so, because the only feasible calculational procedure dictated a step by step (time-wise) method as described in Chapter 7 of this thesis.

*** Non-essential being used here to indicate a redundant or repetitive type of information.

Thus Figures 51 through 66 present $\bar{h}$ and $\alpha$ time histories utilizing piston theory aerodynamics near the times $t = t_o$ and $t \cong t_o + .45$ seconds, where $t_o$ = 0, 10, 20, and 30 seconds, for the two acceleration time histories and the Case 1 and 2 inputs. This group of information should demonstrate whether the $\bar{h}$ and $\alpha$ impulse responses are similar to the general type* of impulse response $W(\tau, t-\tau)$ for a time-varying system or if indeed they are more nearly like the impulse response $W(t-\tau)$ for a constant coefficient system. The above-mentioned demonstrations may be carried out by noting the behavior of the delayed trace at $t \cong t_o + .45$ seconds with respect to the trace observed just after the application of the impulsive input at $t = t_o$.

Figures 67 through 78 present comparisons between the $\bar{h}$ and $\alpha$ time histories obtained by first using piston theory aerodynamics and then using unsteady accelerating aerodynamics in the exact analysis. The $t_o$ time range for these comparisons is concentrated in the early portions of the ng = 270(1-cos.2513t) flight mission since it is in this time interval that the greatest solution differences should appear due to the two aerodynamic theory representations. This group of information should establish the relative merits of using the "more accurate" (but computationally difficult) unsteady accelerating aerodynamic theory as

---

*Denote $t-\tau$ by s. Thus the waveform of the general type of impulse response $W(\tau, s)$, associated with a system describable in terms of time-varying coefficient differential equations, depends on the time $\tau$ at which the impulse is applied as well as the elapsed time s. In other words, if a plot of $W(\tau_1, s)$ were compared with a plot of $W(\tau_2, s)$ such that the $\tau_1$ point and the $\tau_2$ point were coincident, the waveforms would not be identical. This is in sharp contrast to the waveform of an impulse response associated with a system described in terms of constant coefficient differential equations, in which such a comparison would show identical waveforms so that only a dependence on s is demonstrated. A similar description of this elementary concept is given by Laning and Battin on page 182 of Reference 15.

opposed to using the "less accurate" (but computationally simpler) piston theory aerodynamics.

Tables 2 through 6 present comparisons between the quasi-steady and the instantaneous frequencies over the entire time range. This group of information should give supporting evidence to the trends established by an analysis of Figures 51 through 78.

Now that the usefulness and purpose of the above three groups of information has been delineated the conclusions obtained from these groups may be presented.

Figures 51 through 66 generally demonstrate, in any given time interval, that the $\bar{h}$ and $\alpha$ time histories exhibit the usual characteristics of a constant coefficient system coupled mode response. One of a few exceptions to this general statement is Figure 57 in which the $\alpha$ time history is seen to grow slightly for $t_o \cong 10.45$ seconds. However this growth may be predicted on a quasi-steady basis since at this particular time GJ and $\rho_\infty$ are beginning to show reasonable decreases. It is thus correct to state that the coupled $\bar{h}$ and $\alpha$ impulse responses are <u>not</u> similar to the general type of impulse response $W(\tau, t-\tau)$ but are indeed very nearly like the constant coefficient system impulse responses $W(t-\tau)$.

Figures 67 through 78 demonstrate that there is <u>no</u> justification for employing the unsteady accelerating aerodynamics (linear) theory instead of the second-order piston theory aerodynamics.

Finally, an inspection of Tables 2 through 6 reveals that in most cases the quasi-steady frequencies and the instantaneous frequencies are almost identical. The worst frequency correlation, which occurs in only a few cases, is of the order of 5%.

Thus evidences of the time-varying coefficients are seen but they are small. It is seen that the omission of the ng = 9g calculations suggested in the last page of Chapter 7 proved to be the correct procedure since the more critical ng = 270(1-cos.2513t) flight mission produced such unspectacular results.

The answers to questions (A) through (D) posed at the beginning of Chapter 7 may now be answered by the following statements.

(A) Time-varying coefficients are of little importance in the aeroelastic analysis of manned aircraft.

(B) It is suggested that time-varying coefficients would be of importance in the aeroelastic analysis of an anti-missile missile, etc.

(C) Quasi-steady analysis appears to be still a remarkably good method of analysis. It is suggested that a more complete quasi-steady analysis should be made, however, to obtain both the frequencies and mode shapes as well as the response to some specified impulsive input. This procedure insures knowledge of the pertinent amplitude growths.

# APPENDIX I

## DETERMINATION OF THE $f_i$ AND $g_i$ CONSTANTS FROM THE SPECIFIED INITIAL CONDITIONS $x(t_0)$, $y(t_0)$, $\dot{x}(t_0)$, $\dot{y}(t_0)$

Particular solutions of Equation (3-42) may be obtained if one specifies the values of the functions x, y, and their first three derivatives at some initial time $t_0$. This specification will lead to two sets of four equations, each set with four unknowns (the unknowns being $f_i$ and $g_i$, i = 1,2,3,4) as shown below.

$$x(t_0) = \sum_{i=1}^{4} v_i(t_0) f_i \qquad y(t_0) = \sum_{i=1}^{4} w_i(t_0) g_i$$

$$\dot{x}(t_0) = \sum_{i=1}^{4} \dot{v}_i(t_0) f_i \qquad \dot{y}(t_0) = \sum_{i=1}^{4} \dot{w}_i(t_0) g_i$$

$$\ddot{x}(t_0) = \sum_{i=1}^{4} \ddot{v}_i(t_0) f_i \qquad \ddot{y}(t_0) = \sum_{i=1}^{4} \ddot{w}_i(t_0) g_i$$

$$\dddot{x}(t_0) = \sum_{i=1}^{4} \dddot{v}_i(t_0) f_i \qquad \dddot{y}(t_0) = \sum_{i=1}^{4} \dddot{w}_i(t_0) g_i$$

However, it is desired to find particular solutions of Equation (3-42) that are <u>also</u> solutions of the parent equations Equation (3-25) in which the <u>only</u> initial conditions that may be specified are $x(t_0)$, $\dot{x}(t_0)$, $y(t_0)$, and $\dot{y}(t_0)$. Thus, appropriate values of $\ddot{x}(t_0)$, $\dddot{x}(t_0)$, $\ddot{y}(t_0)$, $\dddot{y}(t_0)$ must be found before the correct $f_i$ and $g_i$ may be computed from the above equations. Quite naturally, the correct values of $\ddot{x}(t_0)$, $\dddot{x}(t_0)$, $\ddot{y}(t_0)$, $\dddot{y}(t_0)$ to be inserted in the above equations for

the determination of the $f_i$ and the $g_i$ are those values of $\ddot{x}(t_0)$, $\dddot{x}(t_0)$, $\ddot{y}(t_0)$, $\dddot{y}(t_0)$ possessed by the solutions of the parent equations Equation (3-25). It follows that the remaining step is to find the initial values of the second and third x, y derivatives at $t = t_0$ possessed by the solutions of the parent equations Equation (3-25) in terms of the known quantities $x(t_0)$, $\dot{x}(t_0)$, $y(t_0)$, $\dot{y}(t_0)$. This step is accomplished by obtaining a power series solution of the parent equations for x, y and their first three derivatives at the point $t = t_0$. To this end it is convenient to transform the parent equations, Equation (3-25), into their canonical form by introducing the following notation.

$$x = x_1 \qquad \dot{x} = x_2$$

$$y = x_3 \qquad \dot{y} = x_4$$

Thus, Equation (3-25) transforms into the expressions,

$$\dot{x}_1 = x_2$$

$$\dot{x}_2 = \alpha x_1 + \beta x_2 + \gamma x_3 + \delta x_4$$

$$\dot{x}_3 = x_4$$

$$\dot{x}_4 = \mu x_1 + \nu x_2 + \theta x_3 + \varphi_4$$

where $\alpha$, $\beta$, $\gamma$, $\delta$, $\mu$, $\nu$, $\theta$, and $\varphi$ are ratios of sums and products of the original time-varying coefficients appearing in Equation (3-25). Taking as our illustrative case that in which the $\alpha$, $\beta$, $\gamma$, $\delta$, $\mu$, $\nu$, $\theta$, and $\varphi$ terms possess no singularities,* one can obtain a power

*Relaxing this assumption to discuss expansions about a regular singular point introduces more labor, by way of solving an indicial equation, but does not alter the basic technique that is demonstrated here.

series solution about any ordinary point $\eta = t-t_0$. Since $x_2 = \dot{x}_1$ and $x_4 = \dot{x}_3$ the following power series are assumed,

$$x_1 = \sum_{n=0}^{\infty} p_n \eta^n \qquad x_2 = \sum_{n=0}^{\infty} n p_n \eta^{n-1}$$

$$x_3 = \sum_{n=0}^{\infty} q_n \eta^n \qquad x_4 = \sum_{n=0}^{\infty} n q_n \eta^{n-1}$$

where as stated above, $\eta = t-t_0$. Additionally, the $\alpha$, $\beta$, $\gamma$, $\delta$, $\mu$, $\nu$, $\theta$, and $\varphi$ terms possess known expansions represented as

$$\alpha = \sum_{i=0}^{\infty} \alpha_i \eta^i \qquad \mu = \sum_{i=0}^{\infty} \mu_i \eta^i$$

$$\beta = \sum_{i=0}^{\infty} \beta_i \eta^i \qquad \nu = \sum_{i=0}^{\infty} \nu_i \eta^i$$

$$\gamma = \sum_{i=0}^{\infty} \gamma_i \eta^i \qquad \theta = \sum_{i=0}^{\infty} \theta_i \eta^i$$

$$\delta = \sum_{i=0}^{\infty} \delta_i \eta^i \qquad \varphi = \sum_{i=0}^{\infty} \varphi_i \eta^i$$

where the $\alpha_i$, $\beta_i$, $\ldots\ldots\varphi_i$ are constants.

The procedure is to now find the $p_n$ and $q_n$ in terms of the arbitrary $p_0$, $q_0$, $p_1$, and $q_1$ by means of recurrsion relations, which after some manipulation can be expressed as, for $n \geq 2$,

$$p_n = n^{-1}(\beta_0 p_{n-1} + \delta_0 q_{n-1}) + n^{-1}(n-1)^{-1} \sum_{k=0}^{n-2} \Big\{ (\alpha_{-2+n-k} p_k + \gamma_{n-k-2} q_k) + k(\beta_{n-k-1} p_k + \delta_{n-k-1} q_k) \Big\}$$

$$q_n = n^{-1}(\nu_0 p_{n-1} + \varphi_0 q_{n-1}) + n^{-1}(n-1)^{-1} \sum_{k=0}^{n-2} \left\{ (\mu_{n-k-2} p_k + \theta_{n-k-2} q_k) \right.$$

$$\left. + k(\nu_{n-k-1} p_k + \varphi_{n-k-1} q_k) \right\}$$

The series expressions for the $x_i$ and their first derivatives evaluated at $\eta = 0$ yields,

$$x(0) = p_0 \qquad \dot{x}(0) = p_1$$

$$y(0) = q_0 \qquad \dot{y}(0) = q_1$$

Since one knows the initial values $x(0)$, $\dot{x}(0)$, $y(0)$, $\dot{y}(0)$, the numerical values of $p_0$, $p_1$, $q_0$, and $q_1$ are hence determined. Furthermore, since $p_n$ and $q_n$ can be found ($n \geq 2$) in terms of $p_0$, $p_1$, $q_0$, and $q_1$ from the recurrsion relations, further differentiation of the $x_i$ series yields the following results.

$$\ddot{x}(0) = 2p_2 \qquad \dddot{x}(0) = 6p_3$$

$$\ddot{y}(0) = 2q_2 \qquad \dddot{y}(0) = 6q_3$$

Thus the second and third initial derivatives are known in terms of $p_2$, $q_2$, $p_3$, $q_3$ and hence in terms of $p_0$, $q_0$, $p_1$, $q_1$ and hence in terms of $x(0)$, $\dot{x}(0)$, $y(0)$, $\dot{y}(0)$ so one now has enough information about the initial conditions for Equation (3-42) so that the desired $f_i$ and $g_i$ may be uniquely solved for.

# APPENDIX II

## COMMENTS ON VARIABLE ALTITUDE FLIGHT

Rigorous inclusion of a non-homogenous atmosphere adds considerable difficulty to the aerodynamics problem. It is then of interest to determine an order of magnitude check on the influence of the variation of state parameters with altitude. For supersonic flight, the impulse response functions lend themselves nicely to such a check since the load due to impulsive motion must be identically zero for times after the airfoil trailing edge moves ahead of the foremost leading edge disturbance wave. For vertical flight at constant Mach number, this time is approximately

$$\Delta t \cong \frac{c}{a_\infty (M-1)}$$

and the corresponding vertical distance traveled is

$$\Delta h \cong \frac{M_c}{(M-1)}$$

Thus, except for $M \cong 1$, the change in altitude is of the order of the airfoil chord and hence negligible.* Positive acceleration reduces $\Delta h$ further. Deceleration to subsonic speeds could allow past disturbances to reach the airfoil. Solution to the latter seems out of the realm of practicability at the present, since it involves at least analysis for subsonic unsteady flow and at most inclusion of dissipation due to viscosity which is conceivably of importance here.

---

*Even Mach numbers close to M = 1 produce moderate altitude changes $\Delta h$. For example, when M = 1.05, $\Delta h$ is given by $\Delta h \cong 20c$.

Thus, since loads due to arbitrary motion can be determined from superposition of the impulse responses, one concludes that it is sufficient to use the impulse response functions developed for the homogenous atmosphere with a quasi-steady representation of the change in state variables. This, of course, holds only for the supersonic case. The subsonic case is more difficult to justify; but doe to the complexity of the problem, it is not felt that it is worthwhile proceeding along these lines at present.

As a matter of interest, the difficulty in accounting for the non-homogenous atmosphere is discussed in the following. The isentropic relation is

$$p/p_\infty = (\rho/\rho_\infty)^\gamma, \quad \gamma = 1.4$$

whereas the altitude pressure-density relation is

$$p_\infty/p_0 = (\rho_\infty/\rho_0)^K, \; K = \begin{cases} 1.23 & 0 \leq h \leq 35{,}000 \text{ (Ft.)} \\ & 35{,}000 \leq h \leq \infty \text{ (Ft.)} \end{cases}$$

Hence one cannot establish the baratropic relation $p = \rho(p)$ so that the quantity $\int dp/\rho(p)$ encountered in Kelvin's theorem and thus the Bernoulli pressure formula is not a proper integral. Thus one cannot justify the existence of a velocity potential. If one makes the approximation that $K = \gamma$, then the linearized mathematical problem can be formulated as a potential problem, the potential satisfying the wave equation with a variable speed of sound. This would of course be limited to some relatively narrow altitude band for which the above approximation is good. The solution to this latter problem is no trivial matter, particularly for the subsonic case for which its need seems most apparent.

# APPENDIX III

## OUTLINE OF THE PROCEDURES FOR OBTAINING THE UPWASH IMPULSE RESPONSES

If a finite band of upwash (width $\epsilon$) is present on the three dimensional wing planform, the planform possessing supersonic leading and trailing edges, Figure 45 depicts the regions in which the velocity potential is of interest and must be computed.

When $\epsilon \to 0$ and the upwash magnitude w is defined in general as $w = \frac{1}{\epsilon} f(\zeta, \tau)$ we have the case in which a spacewise impulse of upwash exists on the three dimensional airfoil at $\tau = 0$. Referring to Figure 46, it is seen that Regions I, II, and VI collapse onto the $\tau = 0$, $\zeta = 0$ point, Region III collapses onto the $\tau = 0$ line and all other regions collapse onto the Mach lines except IX, VII, and IV. Also points 4 and 5, and 7 and 6 merge, and point 3 coincides with the origin. Thus, if the collapsed regions yield no limiting contribution to the three dimensional wing pressure distribution, it is observed that one need calculate only the pressure in Regions IV, VII, and IX. However, since one always expects a pressure distribution to occur at the position of the applied upwash, at least Regions I, II, and III must contribute some limiting pressure distribution.

The first step in calculating the pressure distributions is to express the velocity potential $\varphi$ at some point (t,x) in terms of the wing planform geometry and the upwash w. As is well known, the velocity potential $\varphi$ is an integral* of all properly weighted upwash elements that occur in the forward Mach-cone emanating from the

---

*Consult References 71 and 72 for the details of this integral formulation of $\varphi$.

point (t,x). For any given point (t,x), this forecone will intersect the wing planform at two positions. Thus, these two positions may be on the leading edge $\tau = 0$, on the side edge $\zeta = -M_0\tau - \mathcal{F}\tau^2$ or may be on both portions of the planform. Figure 47 illustrates the possible forecone-planform intersections. The intersection points are labeled 1 and 2, the point having the largest negative value of $\zeta$ being denoted as point 2. For convenience the equations of the curves representing the wing geometry and the forward Mach-cones are also shown on Figure 47. Calculating the positions of points 1 and 2 in terms of the vertex coordinates of the forward Mach-cone and whether these points are on the leading edge $\tau = 0$ or the side edge $\zeta = -(M_0\tau + \mathcal{F}\tau^2)$ it is seen that,

$$(\tau_1, \zeta_1) = \begin{cases} (0,\ t+x); \text{ if on leading edge } \tau = 0 \\ \left(-\left[\dfrac{M_0 - 1}{2\mathcal{F}}\right] + \sqrt{\left(\dfrac{M_0 - 1}{2\mathcal{F}}\right)^2 - \dfrac{t+x}{\mathcal{F}}},\right. & \text{; if on side edge } \zeta = -(M_0\tau + \mathcal{F}\tau^2) \\ \left. t + x + \sqrt{\dfrac{M_0 - 1}{2\mathcal{F}} - \dfrac{t+x}{\mathcal{F}}}\right) & \end{cases}$$

$$(\tau_2, \zeta_2) = \begin{cases} (0,\ -t+x); \text{ if on leading edge } \tau = 0 \\ \left(-\left[\dfrac{M_0 + 1}{2\mathcal{F}}\right] + \sqrt{\left(\dfrac{M_0 + 1}{2\mathcal{F}}\right)^2 + \dfrac{t-x}{\mathcal{F}}},\right. & \text{; if on side edge } \zeta = -(M_0\tau + \mathcal{F}\tau^2) \\ \left. -t + x - \left[\dfrac{M_0 + 1}{2\mathcal{F}}\right] + \sqrt{\left(\dfrac{M_0 + 1}{2\mathcal{F}}\right)^2 + \dfrac{t-x}{\mathcal{F}}}\right) & \end{cases}$$

The values of $\varphi(t,x)$ for all nine regions are now presented in their basic form, before simplification or integration. Notice that these expressions must necessarily differ only in their integration limits providing the upwash $w(\tau,\zeta)$ is left in implicit form.

Region I

$$\varphi_I(t,x) = -\frac{1}{\pi}\int_{\tau_1}^{\tau_2}\int_{-M_0\tau-\mathcal{F}\tau^2}^{x+t-\tau}\frac{w(\tau,\zeta)d\zeta d\tau}{\sqrt{(t-\tau)^2-(x-\zeta)^2}} - \frac{1}{\pi}\int_{\tau_2}^{t}\int_{x-t+\tau}^{x+t-\tau}\frac{w(\tau,\zeta)d\zeta d\tau}{\sqrt{(t-\tau)^2-(x-\zeta)^2}}$$

where $\tau_1 = -\left(\frac{M_0-1}{2\mathcal{F}}\right) + \sqrt{\left(\frac{M_0+1}{2\mathcal{F}}\right)^2 - \left(\frac{t+x}{\mathcal{F}}\right)}$

$$\tau_2 = -\left(\frac{M_0+1}{2\mathcal{F}}\right) + \sqrt{\left(\frac{M_0+1}{2\mathcal{F}}\right)^2 + \left(\frac{t-x}{\mathcal{F}}\right)}$$

Region II

$$\varphi_{II}(t,x) = -\frac{1}{\pi}\int_{0}^{\tau_2}\int_{-M_0\tau-\mathcal{F}\tau^2}^{x+t-\tau}\frac{w(\tau,\zeta)d\zeta d\tau}{\sqrt{(t-\tau)^2-(x-\zeta)^2}} - \frac{1}{\pi}\int_{\tau_2}^{t}\int_{x-t+\tau}^{x+t-\tau}\frac{w(\tau,\zeta)d\zeta d\tau}{\sqrt{(t-\tau)^2-(x-\zeta)^2}}$$

where $\tau_2 = -\left(\frac{M_0+1}{2\mathcal{F}}\right) + \sqrt{\left(\frac{M_0+1}{2\mathcal{F}}\right)^2 + \frac{t-x}{\mathcal{F}}}$

Region III

$$\varphi_{III}(t,x) = -\frac{1}{\pi}\int_{0}^{t}\int_{x-t+\tau}^{x+t-\tau}\frac{w(\tau,\zeta)d\zeta d\tau}{\sqrt{(t-\tau)^2-(x-\zeta)^2}}$$

Region IV

$$\varphi_{IV}(t,x) = -\frac{1}{\pi}\int_0^{\epsilon}\int_{x-t+\tau}^{x+t-\tau}\frac{w(\tau,\zeta)d\zeta d\tau}{\sqrt{(t-\tau)^2-(x-\zeta)^2}}$$

Region V

$$\varphi_V(t,x) = -\frac{1}{\pi}\int_0^{\tau_2}\int_{-M_0\tau-\mathcal{J}\tau^2}^{x+t-\tau}\frac{w(\tau,\zeta)d\zeta d\tau}{\sqrt{(t-\tau)^2-(x-\zeta)^2}} - \frac{1}{\pi}\int_{\tau_2}^{\epsilon}\int_{x-t+\tau}^{x+t-\tau}\frac{w(\tau,\zeta)d\zeta d\tau}{\sqrt{(t-\tau)^2-(x-\zeta)^2}}$$

where $\tau_2 = -\left(\frac{M_0+1}{2\mathcal{J}}\right) + \sqrt{\left(\frac{M_0+1}{2\mathcal{J}}\right)^2 + \frac{t-x}{\mathcal{J}}}$

Region VI

$$\varphi_{VI}(t,x) = -\frac{1}{\pi}\int_{\tau_1}^{\tau_2}\int_{-M_0\tau-\mathcal{J}\tau^2}^{x+t-\tau}\frac{w(\tau,\zeta)d\zeta d\tau}{\sqrt{(t-\tau)^2-(x-\zeta)^2}} - \frac{1}{\pi}\int_{\tau_2}^{\epsilon}\int_{x-t+\tau}^{x+t-\tau}\frac{w(\tau,\zeta)d\zeta d\tau}{\sqrt{(t-\tau)^2-(x-\zeta)^2}}$$

where $\tau_1 = -\left(\frac{M_0 - 1}{2\mathcal{F}}\right) + \sqrt{\left(\frac{M_0 - 1}{2\mathcal{F}}\right)^2 - \frac{t + x}{\mathcal{F}}}$

$$\tau_2 = -\left(\frac{M_0 + 1}{2\mathcal{F}}\right) + \sqrt{\left(\frac{M_0 + 1}{2\mathcal{F}}\right)^2 + \frac{t - x}{\mathcal{F}}}$$

Region VII

$$\varphi_{VII}(t,x) = -\frac{1}{\pi}\int_0^{\varepsilon}\int_{-M_0\tau - \mathcal{F}\tau^2}^{x+t-\tau} \frac{w(\tau,\zeta)d\zeta d\tau}{\sqrt{(t-\tau)^2-(x-\zeta)^2}}$$

Region VIII

$$\varphi_{VIII}(t,x) = -\frac{1}{\pi}\int_{\tau_2}^{\varepsilon}\int_{-M_0\tau - \mathcal{F}\tau^2}^{x+t-\tau} \frac{w(\tau,\zeta)d\zeta d\tau}{\sqrt{(t-\tau)^2-(x-\zeta)^2}}$$

where $\tau_2 = -\left(\frac{M_0 + 1}{2\mathcal{F}}\right) + \sqrt{\left(\frac{M_0 + 1}{2\mathcal{F}}\right)^2 + \frac{t - x}{\mathcal{F}}}$

Region IX

$$\varphi_{IX}(t,x) \equiv 0$$

The second step in the analysis is to compute $\partial\varphi/\partial t$ since the pressure difference across both the two-dimensional accelerating airfoil and the three-dimensional steady flow ( $M = \sqrt{2}$ ) planform is proportional to this quantity. From this point on, the upwash is assumed to originate from a constant impulsive downwash on the two-dimensional accelerating airfoil. Thus the final quantities obtained will be $L_c$ and $M_c$. Notice that the linearly varying upwash and indeed <u>any</u> upwash proportional to $x^n$ causes no changes in the method of analysis. The validity of the following arguments would still be valid; only the actual integrations being more complex. Thus, using the upwash $w(\tau, \zeta) = \frac{1}{\epsilon}$, the $\partial\varphi/\partial t$ terms are now obtained. The two basic integrations over the dummy variable $\zeta$ are,

$$I_1(t,\tau,x) = \int_{x-t+\tau}^{x+t-\tau} [(t-\tau)^2 - (x-\zeta)^2]^{-1/2} d\zeta$$

$$I_2(t,\tau,x) = \int_{-M_0\tau-\beta\tau^2}^{x+t-\tau} [(t-\tau)^2 - (x-\zeta)^2]^{-1/2} d\zeta$$

Since the integrands are identical, both $I_1$ and $I_2$ may be computed by the same process. To this end, let $\lambda = x-\zeta$ and $B = t-\tau$ since $t-\tau$ is a constant as far as this integration is concerned. These substitutions yield the results that,

$$d\zeta = -d\lambda$$

$$\text{as } \zeta \longrightarrow -M_0\tau - \mathcal{F}\tau^2, \qquad \lambda \longrightarrow x + M_0\tau + \mathcal{F}\tau^2$$

$$\text{as } \zeta \longrightarrow x + t - \tau, \qquad \lambda \longrightarrow -t + \tau$$

$$\text{as } \zeta \longrightarrow x - t + \tau, \qquad \lambda \longrightarrow t - \tau$$

Hence, $I_1$ and $I_2$ reduce to:

$$I_1(B,x) = \int_{-B}^{B} \frac{d\lambda}{\sqrt{B^2 - \lambda^2}} = \sin^{-1}\frac{\lambda}{B}\Bigg]_{-B}^{B}$$

$$I_2(B,\tau,x) = \int_{-B}^{B} \frac{d\lambda}{\sqrt{B^2 - \lambda^2}} = \sin^{-1}\frac{\lambda}{B}\Bigg]_{-B}^{x + M_0\tau + \mathcal{F}\tau^2}$$

Evaluating the limits these integrals become,

$$I_1(B,x) = \frac{\pi}{2} - \left(-\frac{\pi}{2}\right) = \pi$$

$$I_2(B,\tau,x) = \sin^{-1}\left(\frac{x + M_0\tau + \mathcal{F}\tau^2}{B}\right) + \frac{\pi}{2}$$

Proceeding, the integrations over the $\tau$ dummy variable have the following forms,

$$I_3 = \int_0^t I_i d\tau \qquad I_4 = \int_0^{\epsilon} I_i d\tau \qquad I_5 = \int_0^{\tau_2} I_i d\tau$$

$$I_6 = \int_{\tau_1}^{\tau_2} I_i d\tau \qquad I_7 = \int_{\tau_2}^{t} I_i d\tau \qquad I_8 = \int_{\tau_2}^{\epsilon} I_i d\tau$$

where $I_i$ is either $I_1$ or $I_2$.

When $I_i = I_1$, the integrals may be written down immediately.

$$\underset{(i=1)}{I_3 = \pi t} \qquad \underset{(i=1)}{I_4 = \pi \epsilon} \qquad \underset{(i=1)}{I_5 = \pi \tau_2}$$

$$\underset{(i=1)}{I_6 = \pi(\tau_2 - \tau_1)} \qquad \underset{(i=1)}{I_7 = \pi(t - \tau_2)} \qquad \underset{(i=1)}{I_8 = \pi(\epsilon - \tau_2)}$$

When $I_i = I_2$ it is most advantageous <u>not</u> to compute $I_3$ through $I_7$, but to instead compute $\partial/\partial t(I_3)$ through $\partial/\partial t(I_7)$ immediately. These relations are now determined using Leibnitz's rule which states,

$$\frac{\partial}{\partial t}\int_{P(t)}^{Q(t)} f(t,\tau)d\tau = \int_{P(t)}^{Q(t)} \frac{\partial f(t,\tau)}{\partial t} d\tau + f(t,Q(t))\frac{dQ(t)}{dt} - f(t,P(t))\frac{dP(t)}{dt}.$$

Thus, noting that $\partial/\partial t(I_3)_{(i=2)}$ and $\partial/\partial t(I_7)_{(i=2)}$ need not be computed, the remaining quantities are given by,

$$\frac{\partial}{\partial t}(I_4)_{(i=2)} = \int_0^{\epsilon} \frac{\partial}{\partial t}\left[\sin^{-1}\left(\frac{x + M_0\tau + \mathcal{J}\tau^2}{t-\tau}\right)\right]d\tau$$

$$\frac{\partial}{\partial t}(I_5)_{(i=2)} = \int_0^{\tau_2} \frac{\partial}{\partial t}\left[\sin^{-1}\left(\frac{x+M_0\tau+\mathcal{J}\tau^2}{t-\tau}\right)\right]d\tau + \frac{\pi}{2}\frac{\partial \tau_2}{\partial t} + \sin^{-1}\left(\frac{x+M_0\tau_2+\mathcal{J}\tau_2^2}{t-\tau_2}\right)\frac{\partial \tau_2}{\partial t}$$

$$\frac{\partial}{\partial t}(I_6)_{(i=2)} = \int_{\tau_1}^{\tau_2} \frac{\partial}{\partial t}\left[\sin^{-1}\left(\frac{x+M_0\tau+\mathcal{J}\tau^2}{t-\tau}\right)\right]d\tau + \frac{\pi}{2}\left[\frac{\partial \tau_2}{\partial t}\right] + \sin^{-1}\left(\frac{x+M_0\tau_2+\mathcal{J}\tau_2^2}{t-\tau_2}\right)\frac{\partial \tau_2}{\partial t}$$

$$- \sin^{-1}\left(\frac{x+M_0\tau_1+\mathcal{J}\tau_1^2}{t-\tau_1}\right)\frac{\partial \tau_1}{\partial t} - \frac{\pi}{2}\left[\frac{\partial \tau_1}{\partial t}\right]$$

$$\frac{\partial}{\partial t}(I_8)_{(i=2)} = \int_{\tau_2}^{\epsilon} \frac{\partial}{\partial t}\left[\sin^{-1}\left(\frac{x+M_0\tau+\mathcal{J}\tau^2}{t-\tau}\right)\right]d\tau - \frac{\pi}{2}\frac{\partial \tau_2}{\partial t} - \sin^{-1}\left(\frac{x+M_0\tau_2+\mathcal{J}\tau_2^2}{t-\tau_2}\right)\frac{\partial \tau_2}{\partial t}$$

By explicitly denoting $\tau_1$ and $\tau_2$ in terms of $M_0$, $\mathcal{J}$, t and x the arcsin terms reduce to the following values.

$$\sin^{-1}\left(\frac{x + M_0\tau_2 + \mathcal{F}\tau_2^2}{t-\tau_2}\right) = \frac{\pi}{2}$$

$$\sin^{-1}\left(\frac{x + M_0\tau_1 + \mathcal{F}\tau_1^2}{t-\tau_1}\right) = -\frac{\pi}{2}$$

Using the accumulated information above, the $\partial\varphi/\partial t$ terms for all regions may now be presented.

$$\frac{\partial}{\partial t}\varphi_I = -\frac{1}{\epsilon} - \frac{1}{\epsilon\pi}\int_{\tau_1}^{\tau_2} \frac{\partial}{\partial t}\left[\sin^{-1}\left(\frac{x + M_0\tau + \mathcal{F}\tau^2}{t-\tau}\right)\right]d\tau$$

$$\frac{\partial}{\partial t}\varphi_{II} = -\frac{1}{\epsilon} - \frac{1}{\epsilon\pi}\int_{0}^{\tau_2} \frac{\partial}{\partial t}\left[\sin^{-1}\left(\frac{x + M_0\tau + \mathcal{F}\tau^2}{t-\tau}\right)\right]d\tau$$

$$\frac{\partial}{\partial t}\varphi_{III} = -\frac{1}{\epsilon}$$

$$\frac{\partial}{\partial t}\varphi_{IV} = 0$$

$$\frac{\partial}{\partial t}\varphi_V = -\frac{1}{\epsilon\pi}\int_{0}^{\tau_2} \frac{\partial}{\partial t}\left[\sin^{-1}\left(\frac{x + M_0\tau + \mathcal{F}\tau^2}{t-\tau}\right)\right]d\tau$$

$$\frac{\partial}{\partial t}\varphi_{VI} = -\frac{1}{\epsilon\pi}\int_{\tau_1}^{\tau_2}\frac{\partial}{\partial t}\left[\sin^{-1}\left(\frac{x + M_0\tau + \mathcal{J}\tau^2}{t-\tau}\right)\right]d\tau$$

$$\frac{\partial}{\partial t}\varphi_{VII} = -\frac{1}{\epsilon\pi}\int_{0}^{\epsilon}\frac{\partial}{\partial t}\left[\sin^{-1}\left(\frac{x + M_0\tau + \mathcal{J}\tau^2}{t-\tau}\right)\right]d\tau$$

$$\frac{\partial}{\partial t}\varphi_{VIII} = -\frac{1}{\epsilon\pi}\int_{\tau_1}^{\epsilon}\frac{\partial}{\partial t}\left[\sin^{-1}\left(\frac{x + M_0\tau + \mathcal{J}\tau^2}{t-\tau}\right)\right]d\tau$$

$$\frac{\partial}{\partial t}\varphi_{IX} = 0$$

Since the lift at any station t is proportional to the chordwise integration of the $\partial\varphi/\partial t$ terms, the method for determining whether limiting (as $\epsilon \longrightarrow 0$) values of lift remain due to the collapsed regions is now obvious. It is required that several carefully chosen chordwise integrations be made and then take the limit as $\epsilon \longrightarrow 0$. The collapsed regions may then be inspected for lift contributions. The same procedure is then used to compute a quantity proportional to the moment. Notice that this same technique, when the proper constants of proportionality are supplied, determines the lift and the moment contributions of the non-collapsed regions also. Furthermore, this method can be used when the upwash is any power in the variable x.

In order to facilitate these proposed integrations Figure 48 presents the equations of the various curves of importance and the following tabulation gives the t stations at which various regions begin and end, these t stations being denoted by the t coordinate of points 3 through 7 shown in Figure 48.

$$t_3 = \frac{\epsilon}{2}\left[M_0 + 1 + \mathcal{F}\epsilon\right]$$

$$t_4 = -\left(\frac{M_0 + 1}{2\mathcal{F}}\right) + \sqrt{\left(\frac{M_0 + 1}{2\mathcal{F}}\right)^2 + \frac{1}{\mathcal{F}}}$$

$$t_5 = -\left(\frac{M_0 + 1}{2\mathcal{F}}\right) + \sqrt{\left(\frac{M_0 + 1}{2\mathcal{F}}\right)^2 + \left[\epsilon(M_0 + 1 + \mathcal{F}\epsilon) + 1\right]/\mathcal{F}}$$

$$t_6 = -\left(\frac{M_0 - 1}{2\mathcal{F}}\right) + \sqrt{\left(\frac{M_0 - 1}{2\mathcal{F}}\right)^2 + \frac{1}{\mathcal{F}}}$$

$$t_7 = -\left(\frac{M_0 - 1}{2\mathcal{F}}\right) + \sqrt{\left(\frac{M_0 - 1}{2\mathcal{F}}\right)^2 + \left[1 + \epsilon(M_0 - 1 + \mathcal{F}\epsilon)\right]/\mathcal{F}}$$

The first integration to be carried out will be for the regions $0 \leq t \leq \epsilon$. Thus choosing some t between 0 and $\epsilon$, the lift is proportional to the following expression.

$$L_c \sim \int_{-M_0 t - \mathcal{F} t^2}^{-t} \frac{\partial}{\partial t} \varphi_I \, dx + \int_{-t}^{t} \frac{\partial}{\partial t} \varphi_{II} dx + \int_{t}^{1 - M_0 t - \mathcal{F} t^2} \frac{\partial}{\partial t} \varphi_{III} \, dx$$

Since all three integrands contain $-\frac{1}{\epsilon}$, and in fact $\partial/\partial t \, \varphi_{III}$ is identically equal to $-\frac{1}{\epsilon}$, this $-\frac{1}{\epsilon}$ term can be removed and treated as a single integration across the planform. Utilizing this equivalent expression and writing out the remainder of the integrands explicitly yields the following.

$$L_c \sim -\frac{1}{\epsilon} \int_{-M_0 t - \mathcal{F} t^2}^{1 - M_0 t - \mathcal{F} t^2} dx \; - \frac{1}{\epsilon \pi} \int_{-M_0 t - \mathcal{F} t^2}^{-t} dx \int_{\tau_1}^{\tau_2} \frac{\partial}{\partial t} \sin^{-1} \left( \frac{x + M_0 \tau + \mathcal{F} \tau^2}{t - \tau} \right) d\tau$$

$$- \frac{1}{\epsilon \pi} \int_{-t}^{t} dx \int_{0}^{\tau_2} \frac{\partial}{\partial t} \sin^{-1} \left( \frac{x + M_0 \tau + \mathcal{F} \tau^2}{t - \tau} \right) d\tau$$

As presently written, the double integrals are to be evaluated by first holding x constant, integrating over the appropriate $\tau$ interval and then integrating over the indicated x interval. This integration is difficult to do by this sequence of operations, thus a change in the order of integration is appropriate. Referring to Figure 49, which illustrates the $\tau$, x region of integration, the expression proportional to $L_c$ is given as,

$$L_c \sim -\frac{1}{\epsilon} - \frac{1}{\epsilon\pi}\int_0^t d\tau \int_{x(\tau_1)}^{x(\tau_2)} \frac{\partial}{\partial t} \sin^{-1}\left(\frac{x + M_0\tau + \mathcal{J}\tau^2}{t-\tau}\right)dx$$

$$= -\frac{1}{\epsilon} - \frac{1}{\epsilon\pi}\int_0^t d\tau \int_{-M_0\tau-\mathcal{J}\tau^2-t+\tau}^{-M_0\tau-\mathcal{J}\tau^2+t-\tau} \frac{x + M_0\tau + \mathcal{J}\tau^2}{\sqrt{(t-\tau)^2-(x+M_0\tau+\mathcal{J}\tau^2)^2}}\,dx\,.$$

Carrying out the integration, $L_c \sim -\frac{1}{\epsilon}$.

Noting that the upwash $w = \frac{1}{\epsilon}$ or that $w\epsilon = 1$ even as the $\epsilon \rightarrow 0$ limit is taken, it is seen that $L_c$ is proportional to a unit delta function at $t = 0$. Therefore, $L_c \sim \delta(t - 0)$ when $t = 0$. This value is in fact proportional to the zero-thickness second-order piston theory value as should be expected.

Observing that the distance between some point x and the planform leading edge, at some time t, is equal to $x + M_0 t + \mathcal{J}t^2$, the expression proportional to the moment for $0 \leq t \leq \epsilon$ is given by

$$M_c \sim \frac{1}{2\epsilon} - \frac{1}{\epsilon\pi}\int_0^t \frac{d\tau}{(t-\tau)} \int_{-(M_0\tau+\mathcal{J}\tau^2)-t+\tau}^{-(M_0\tau+\mathcal{J}\tau^2)+t-\tau} \frac{(x + M_0\tau + \mathcal{J}\tau^2)(x + M_0 t + \mathcal{J}t^2)}{\sqrt{(t-\tau)^2 - (x + M_0\tau + \mathcal{J}\tau^2)^2}}\,dx$$

Using the identity that $x + M_0 t + \mathcal{J}t^2 = x + M_0\tau + \mathcal{J}\tau^2 + M_0(t-\tau) + \mathcal{J}(t-\tau)^2 + 2\tau(t-\tau)$, the integration is easily executed and yields the following result.

$$M_c \sim \frac{1}{2\epsilon} - \frac{1}{4\epsilon}\,t^2$$

As $\epsilon \rightarrow 0$ the product $\frac{t^2}{\epsilon} \rightarrow 0$, since $t \leq \epsilon$. Thus $M_c$ is also impulsive, as should be expected, at $t = 0$.

$$M_c \sim \frac{1}{2}\ \delta(t - 0);\ t = 0$$

The second integration to be carried out is for $\epsilon < t \leq t_3$. Making use of Figure 50, the integrals for the lift and moment proportionals become,

$$L_c \sim \frac{1}{\epsilon\pi} \int_0^{\epsilon} \frac{d\tau}{(t-\tau)} \int_{-(M_0\tau+\mathcal{J}\tau^2)-t+\tau}^{-(M_0\tau+\mathcal{J}\tau^2)+t-\tau} \frac{(x + M_0\tau + \mathcal{J}\tau^2)dx}{[(t-\tau)^2 - (x + M_0\tau + \mathcal{J}\tau^2)^2]^{1/2}} \equiv 0$$

$$M_c \sim \frac{1}{\epsilon\pi} \int_0^{\epsilon} \frac{\pi(t-\tau)}{2}\, d\tau = \frac{1}{2}\left(t - \frac{\epsilon}{2}\right)$$

Now as $\epsilon \rightarrow 0$, $t \rightarrow 0$ if $t \leq t_3$ so that $M_c$ for this $\tau$ region goes to zero. In a similar fashion the lifts and moments can be computed for the limiting case of $\epsilon \rightarrow 0$. The results of these calculations have been presented in Section 6.4 of this thesis, and reflect the results that no singularities occur across the collapsed regions except those regions that contribute to the impulse functions at $t = 0$.

# APPENDIX IV

## APPROXIMATE TIMES ON THE 704 FOR THE FOLLOWING PROGRAMS

| | Time |
|---|---|
| 1. Compute GJ(t) (one k)<br>$0 \leq t \leq 23.26$ sec.<br>ng = 9g | 9 mins. |
| 2. Compute GJ(t) (one k)<br>$23.26 \leq t \leq 1200$ sec.<br>ng = 9g | 3.5 mins. |
| 3. Piston theory differential equations<br>ng = 270 (1-cos.2513t)<br>$0 \leq t \leq 1.0$ sec., $\Delta t = .001$ sec. | 8 mins. |
| 4. Unsteady Aerodynamics Difference Equations<br>ng = 270 (1-cos.2513t) | |
| $0 \leq t \leq .500$ sec., $t_0 = 0$ sec. | 110 mins. |
| $8 \leq t \leq 8.5$ sec., $t_0 = 8$ sec. | 7 mins. |

It is to be noted that the computing time factor from computation (3) to (4) is about 20 for the early time calculations $0 \leq t_0 \leq 4$ sec.

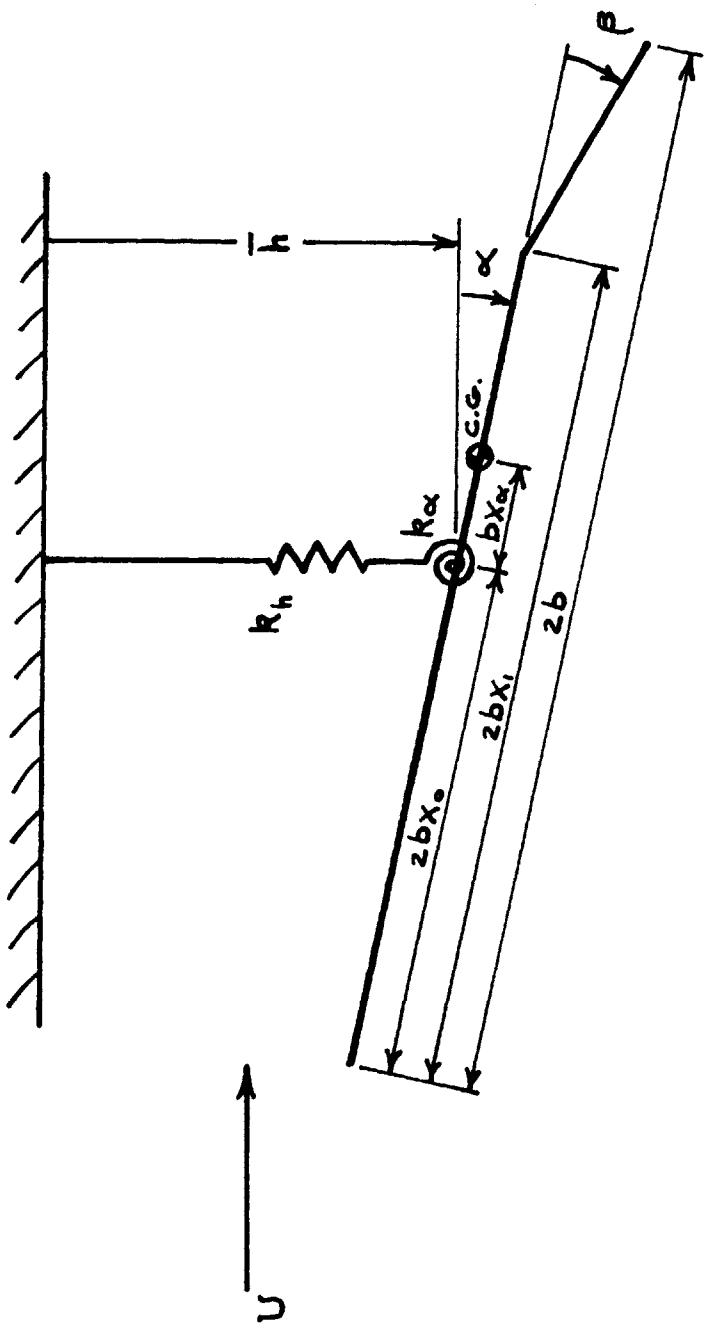


Figure 1 Zero Thickness Typical Section

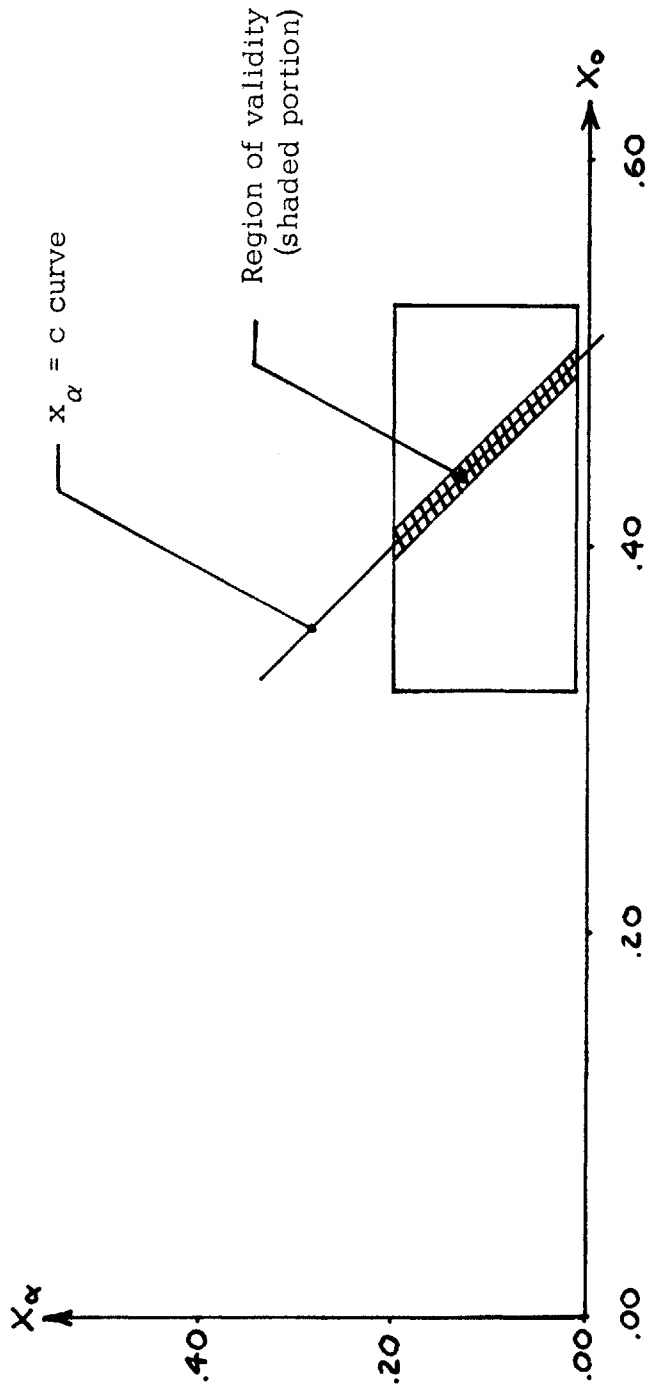


Figure 2 Region of Validity for Zero-Damping Analysis of Bending-Torsion Supersonic Flutter.

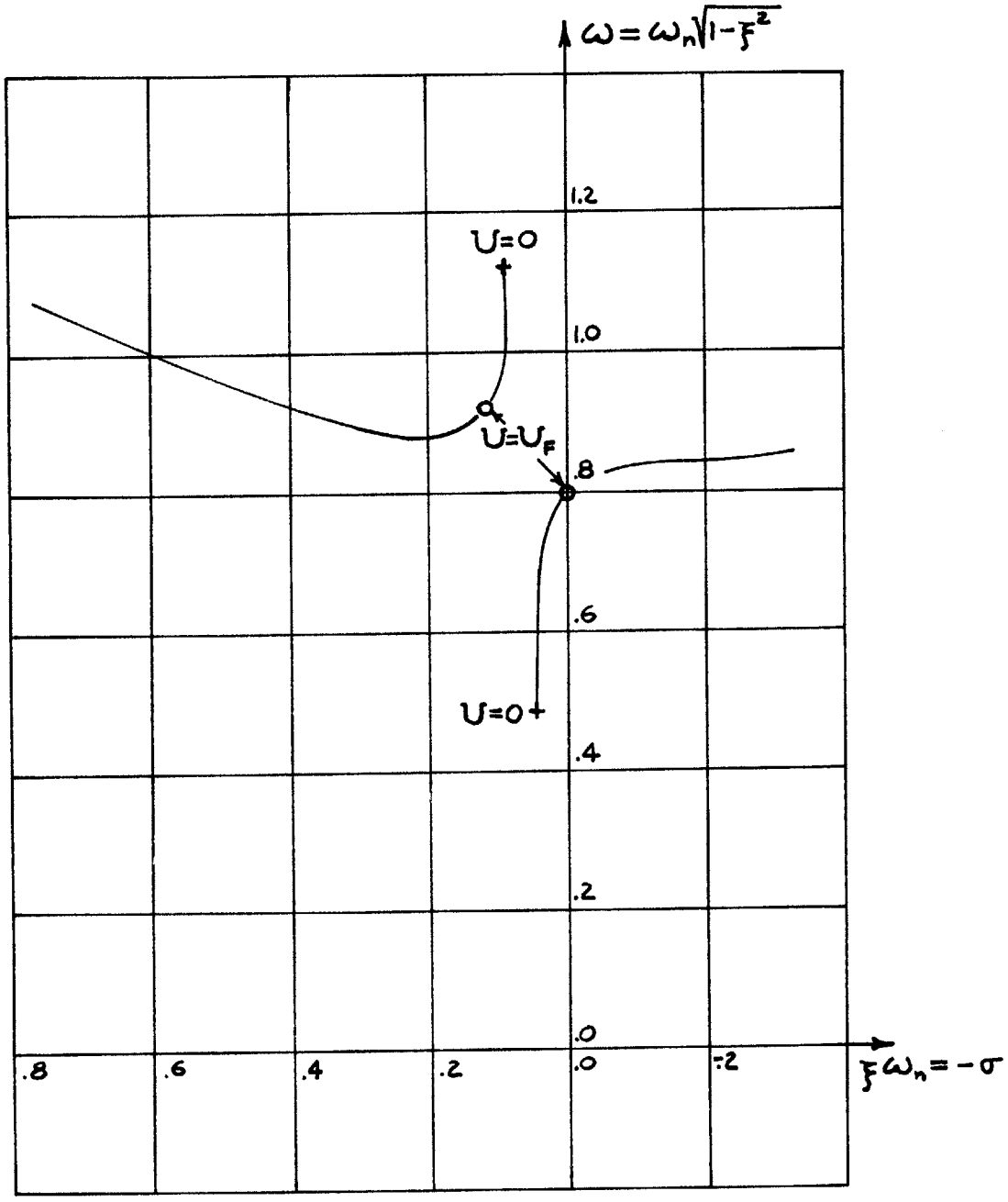


Figure 3 System A Root Locus Plot

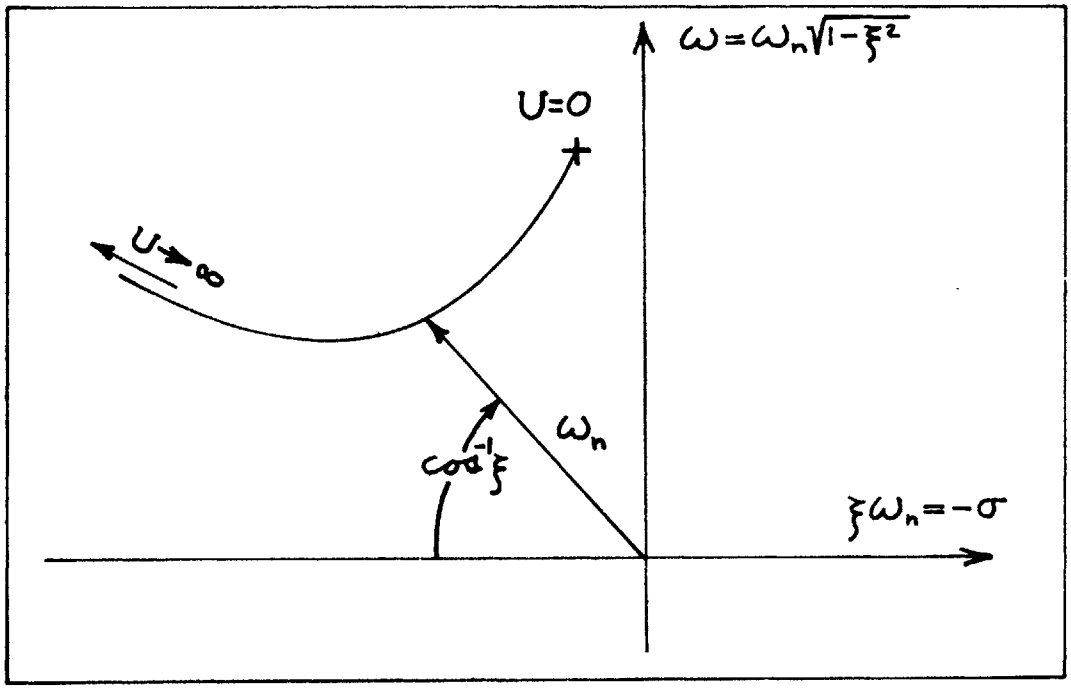


Figure 4 Quantities Described by the Complex Plane Plot

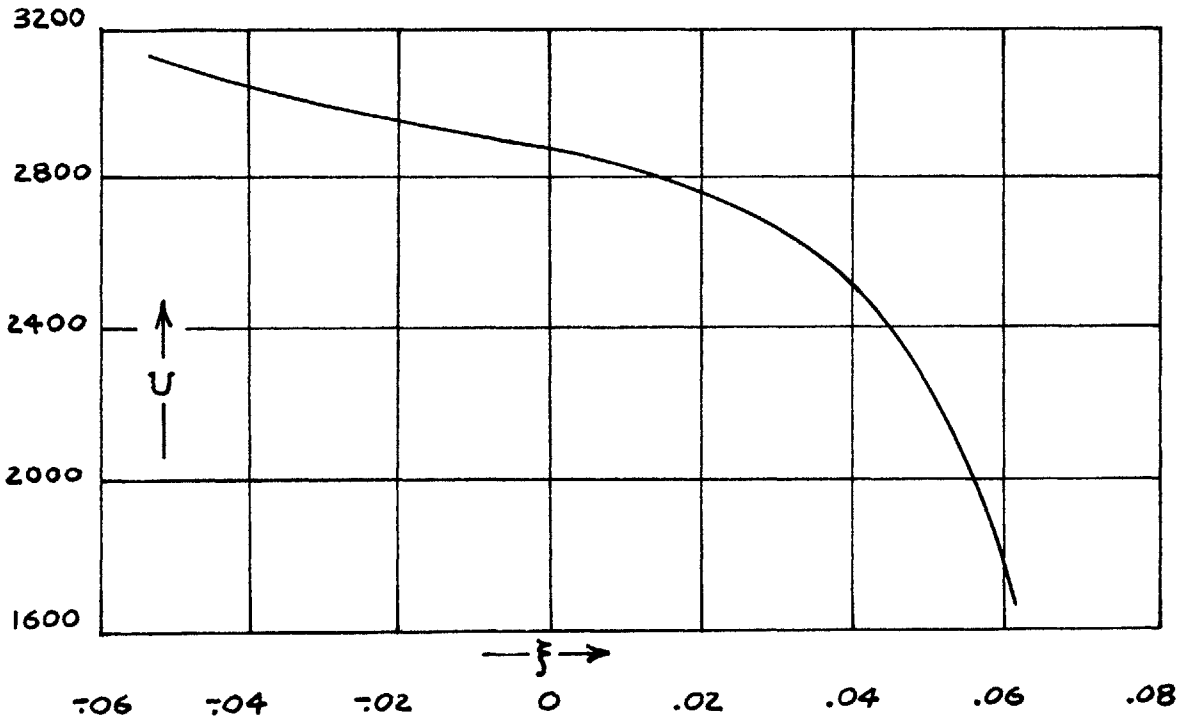


Figure 5 Airspeed U Versus Damping Ratio $\zeta$ for System A

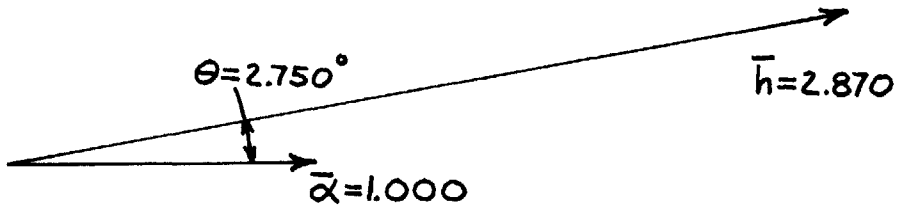


Mode Shape before Flutter Speed is Reached

U = 1950 FT/SEC.

p = -.035 + .689i

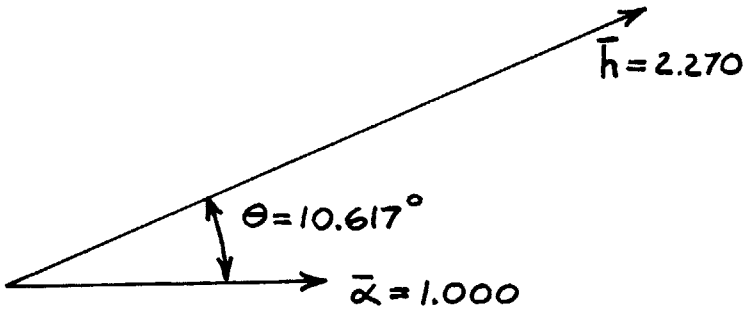


Mode Shape at Flutter Speed

$U = U_F = 2840$ FT/SEC

p = .802i

Figure 6 Mode Shape of the Eventually Unstable Locus of Figure 2 for Two Values of Airspeed U

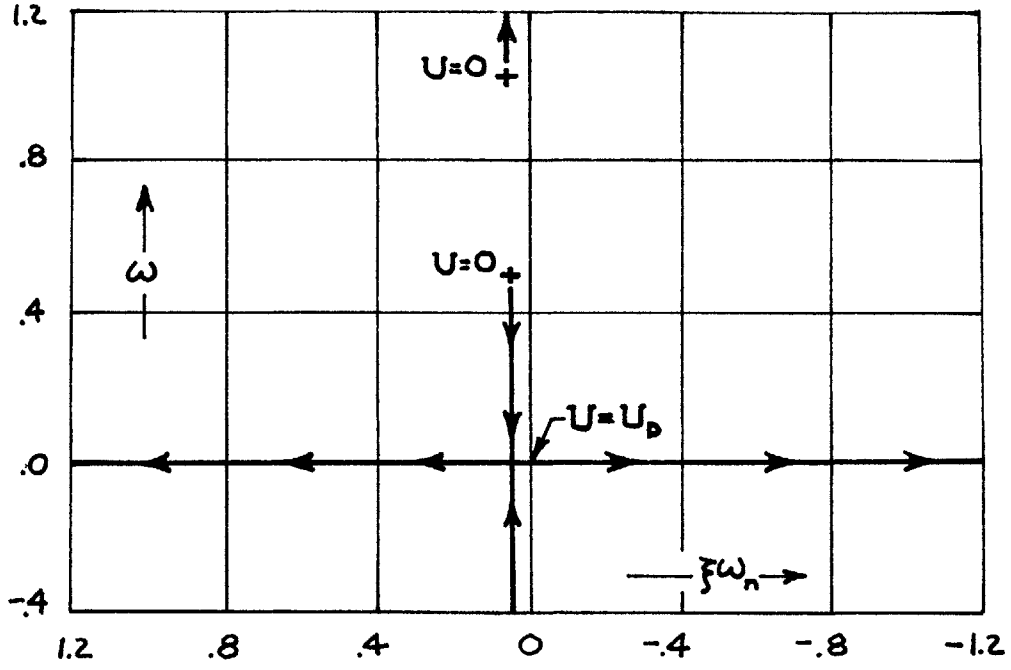


Figure 7 System B Root Locus Plot

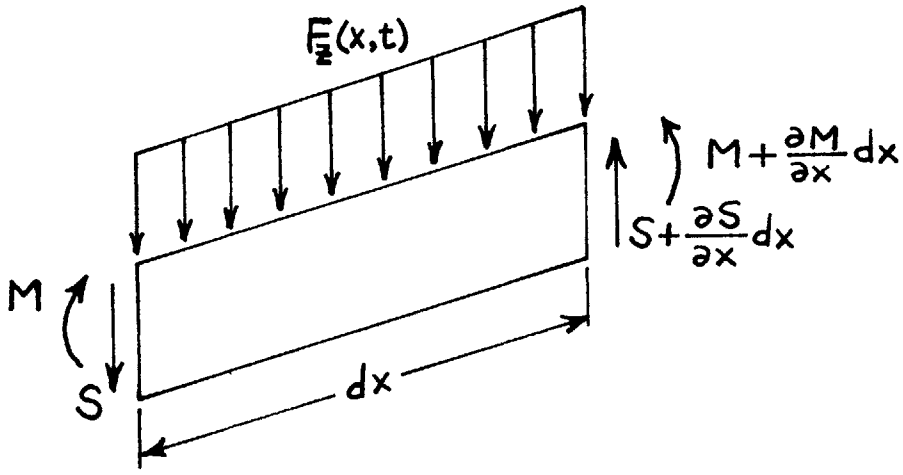


Figure 8 Beam Element in Combined Shear and Bending

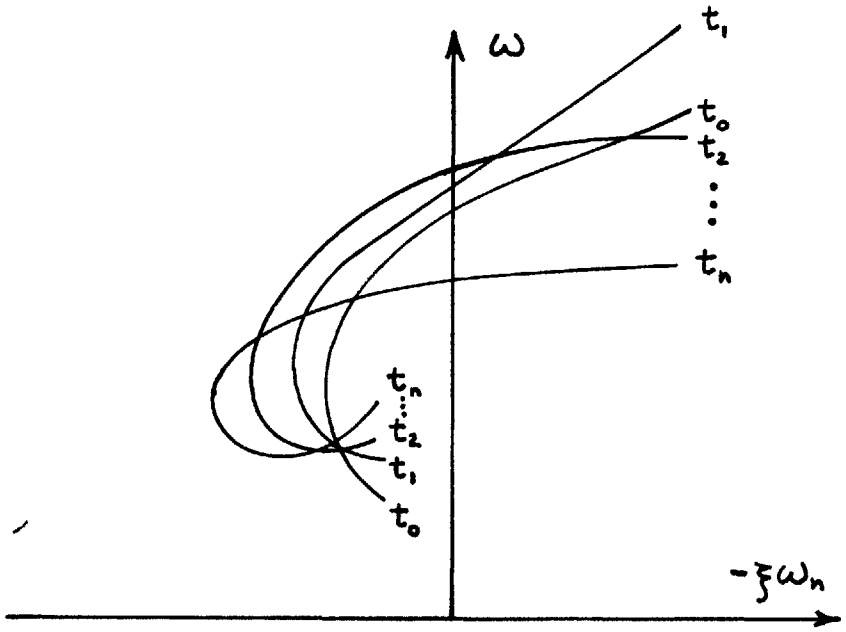


Figure 9 A Quasi-Steady System Locus for Times $t_o, t_1, t_2 \ldots, t_n$

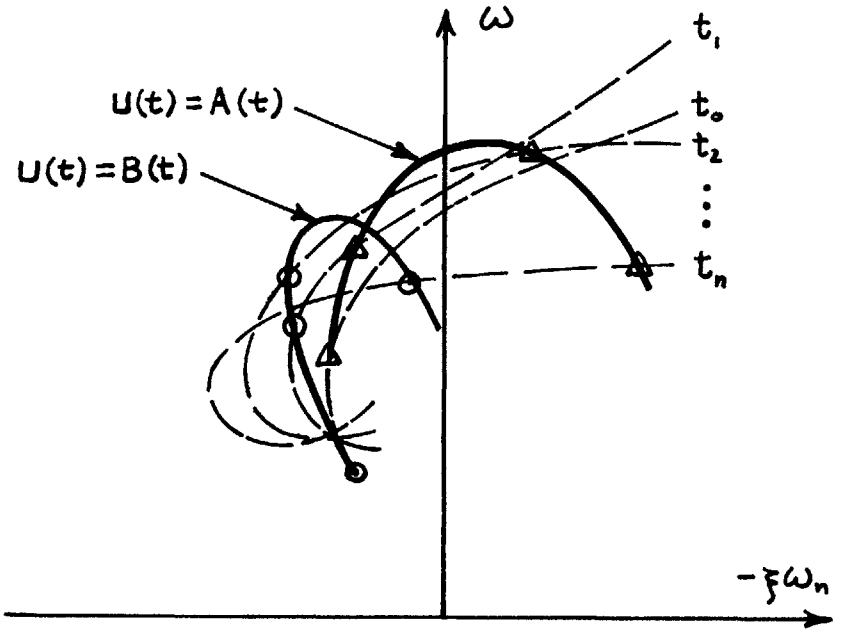


Figure 10 Actual Quasi-Steady System Locus Corresponding to Two Parameter Time Histories U(t)

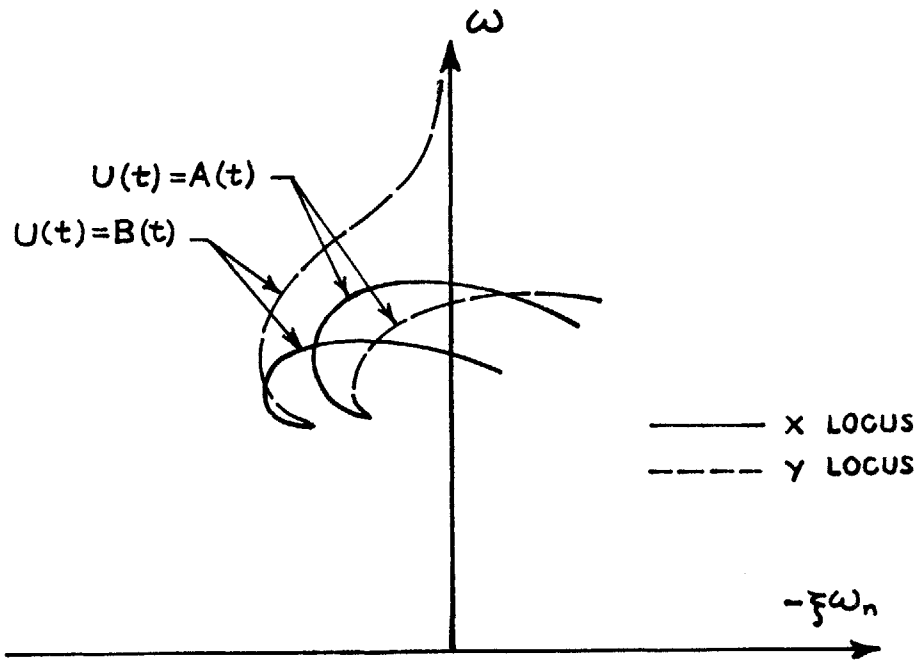


Figure 11 Actual Discrete-Time System Loci Corresponding to Two Parameter Time Histories U(t)

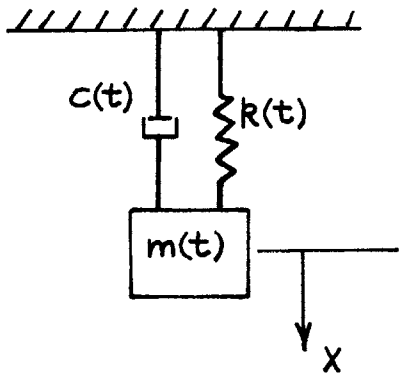


Figure 12 A Simple Time-Varying Mechanical System

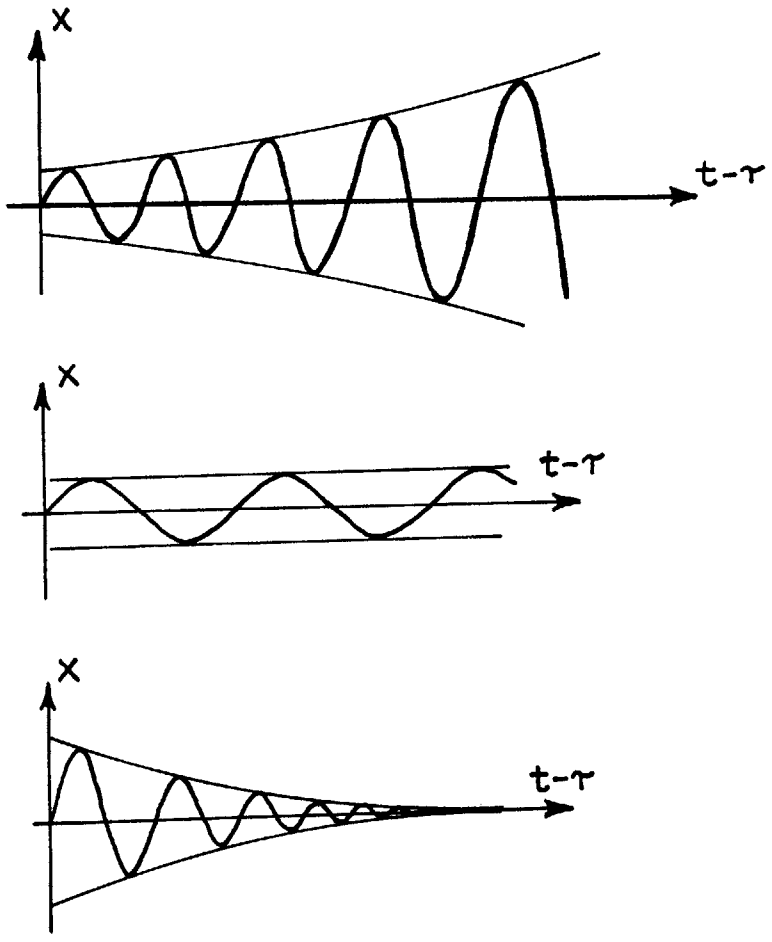


Figure 13 Admissible Types of Quasi-Steady Oscillatory Homogeneous Behavior

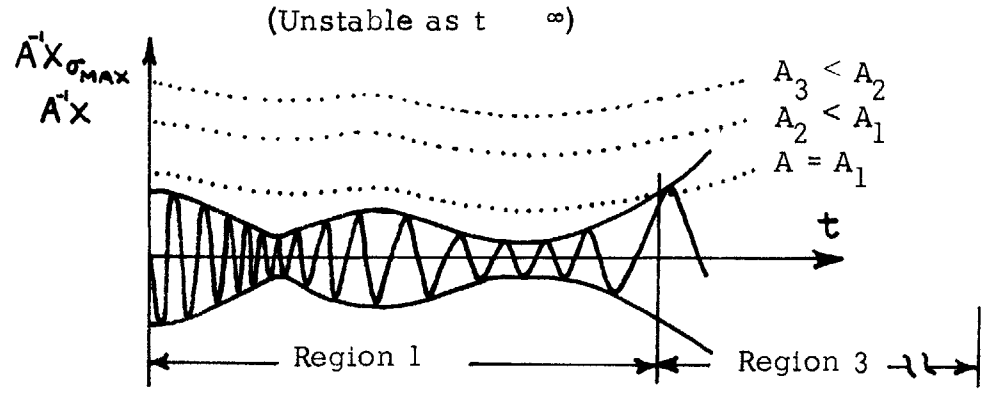


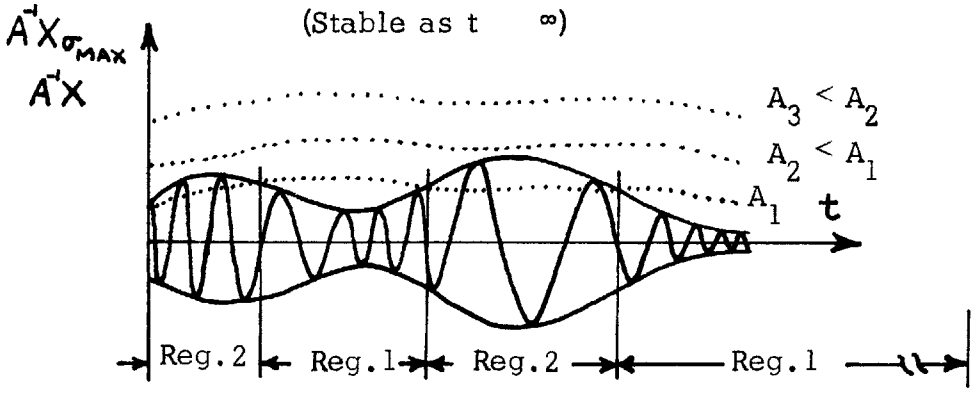


Figure 14 Possible Types of Non-Monotonic Oscillatory Homogeneous Behavior

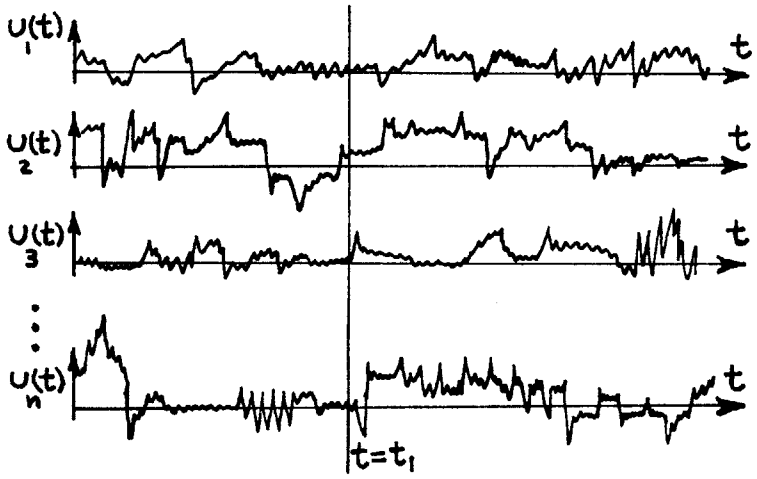


Figure 15 Ensemble of a Given Non-Stationary Random Process

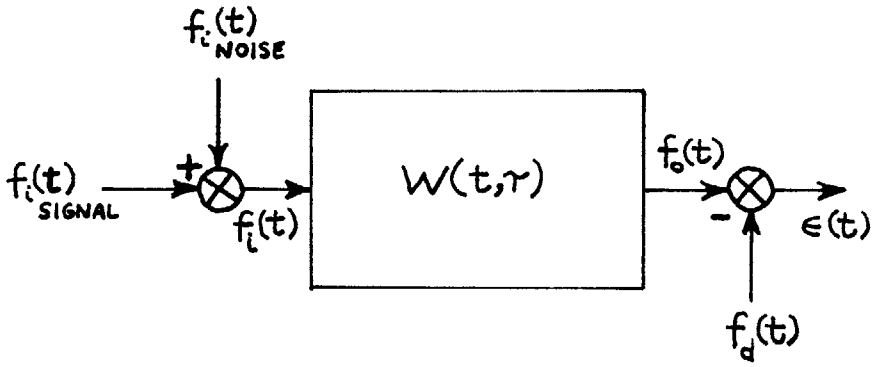


$f_i(t)$ = INPUT = $f_{i\,NOISE}(t) + f_{i\,SIGNAL}(t)$

$f_o(t)$ = SYSTEM OUTPUT

$f_d(t)$ = DESIRED SYSTEM OUTPUT

$\epsilon(t)$ = SYSTEM OUTPUT ERROR = $f_o(t) - f_d(t)$

Figure 16 A General Non-Stationary Random System

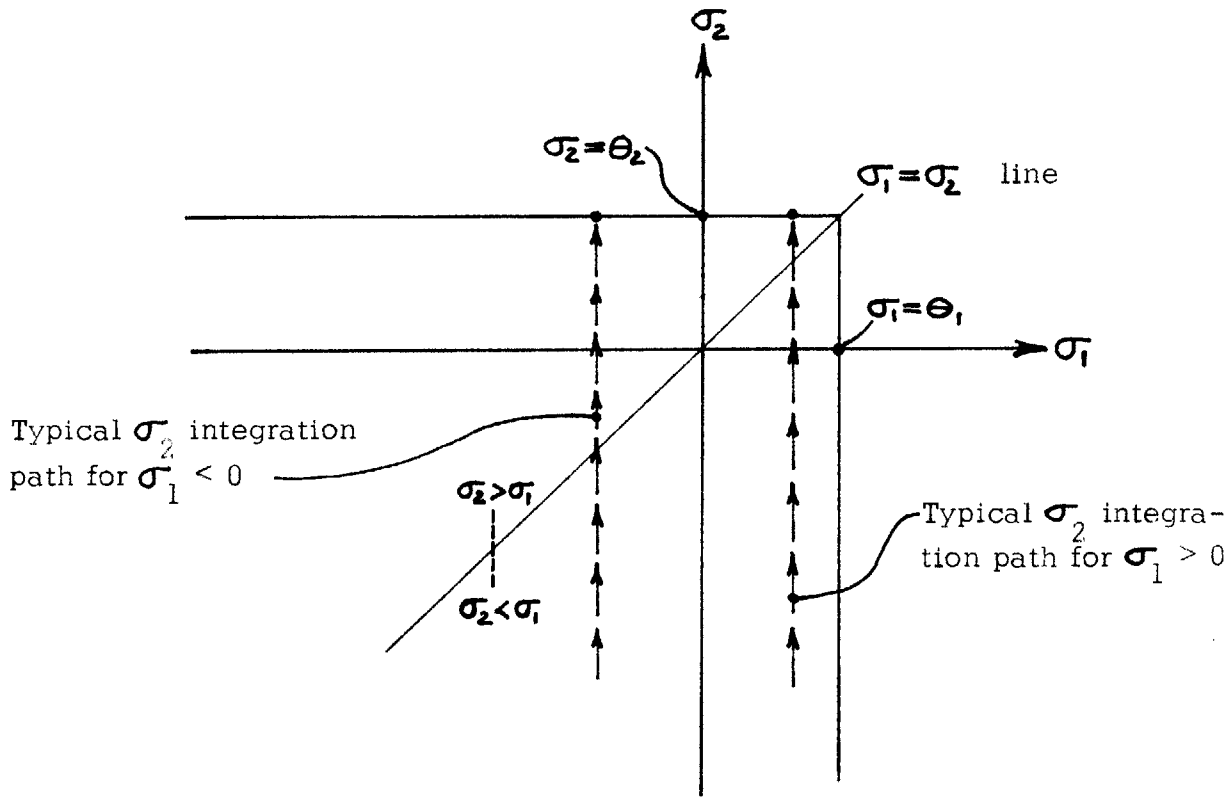


Figure 17 The Domain of Integration and Two Typical Integration Paths of $F(\theta_1, \theta_2, \beta, \mathcal{F})$.

155

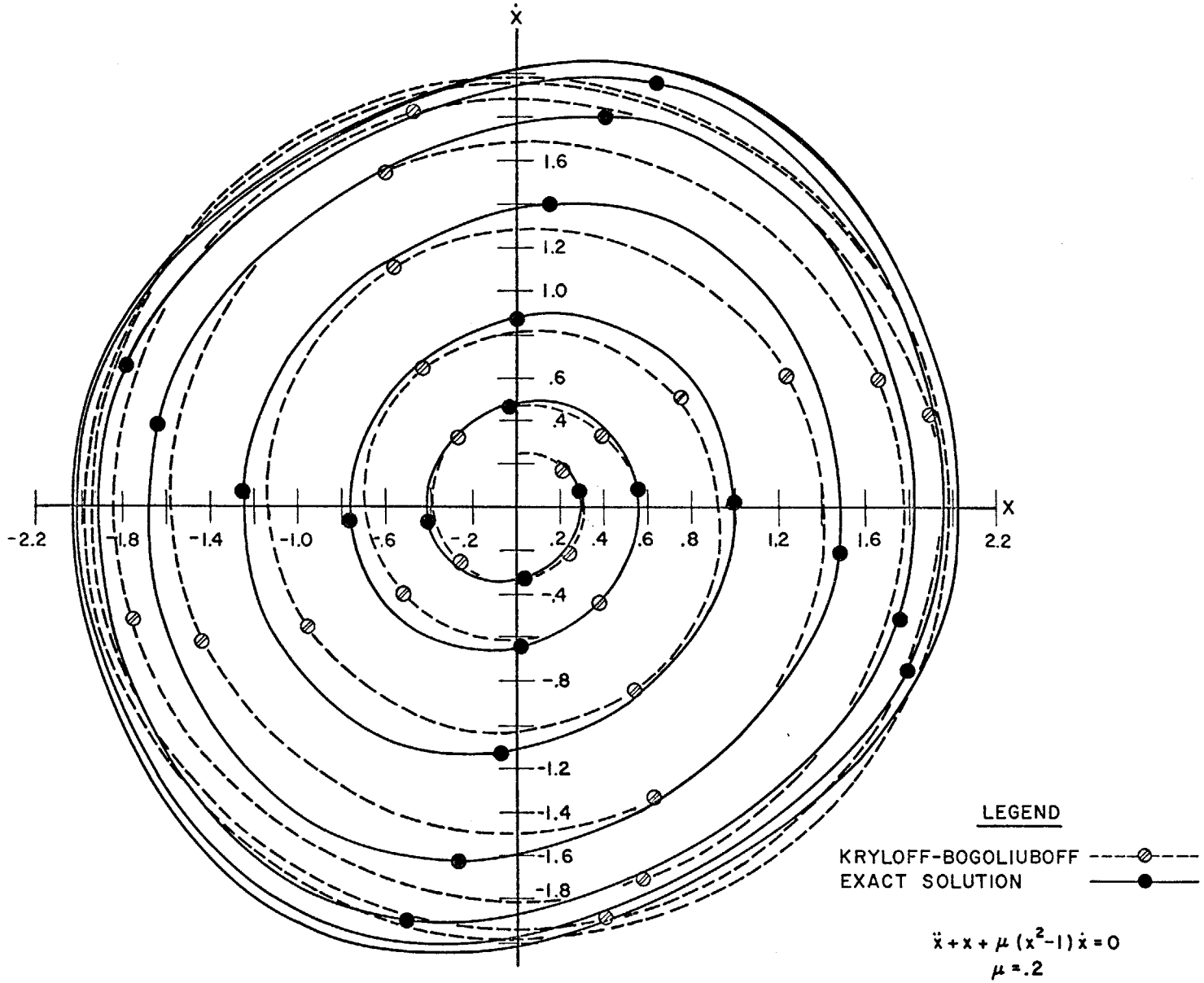


FIG. 18 COMPARISON OF THE KRYLOFF-BOGOLIUBOFF AND THE EXACT PHASE PLANE SOLUTIONS OF THE VAN DER POL EQUATION FOR $\mu = .2$

156

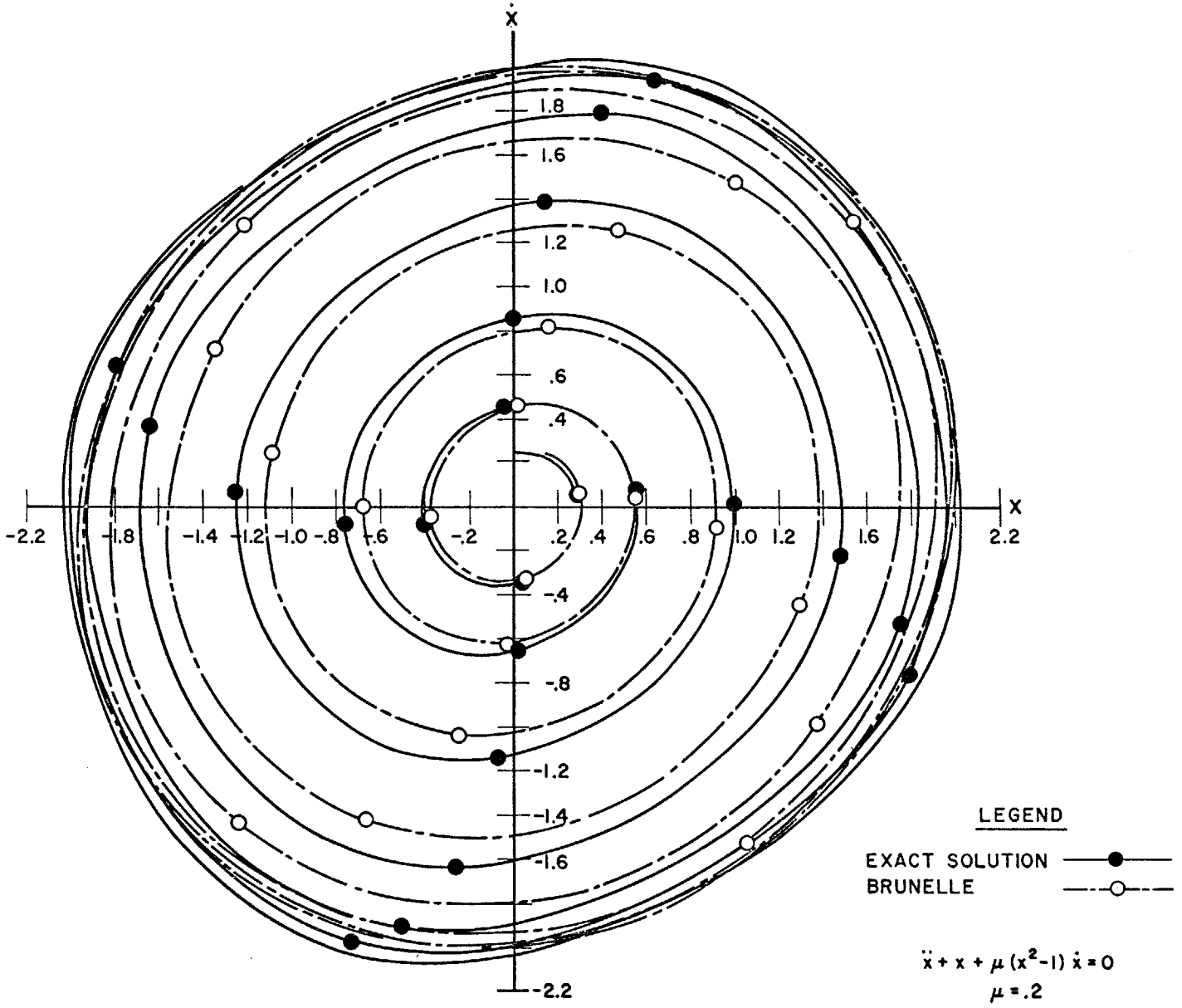


FIG. 19 COMPARISON OF THE BRUNELLE AND THE EXACT PHASE PLANE SOLUTIONS OF THE VAN DER POL EQUATION FOR $\mu = .2$

157

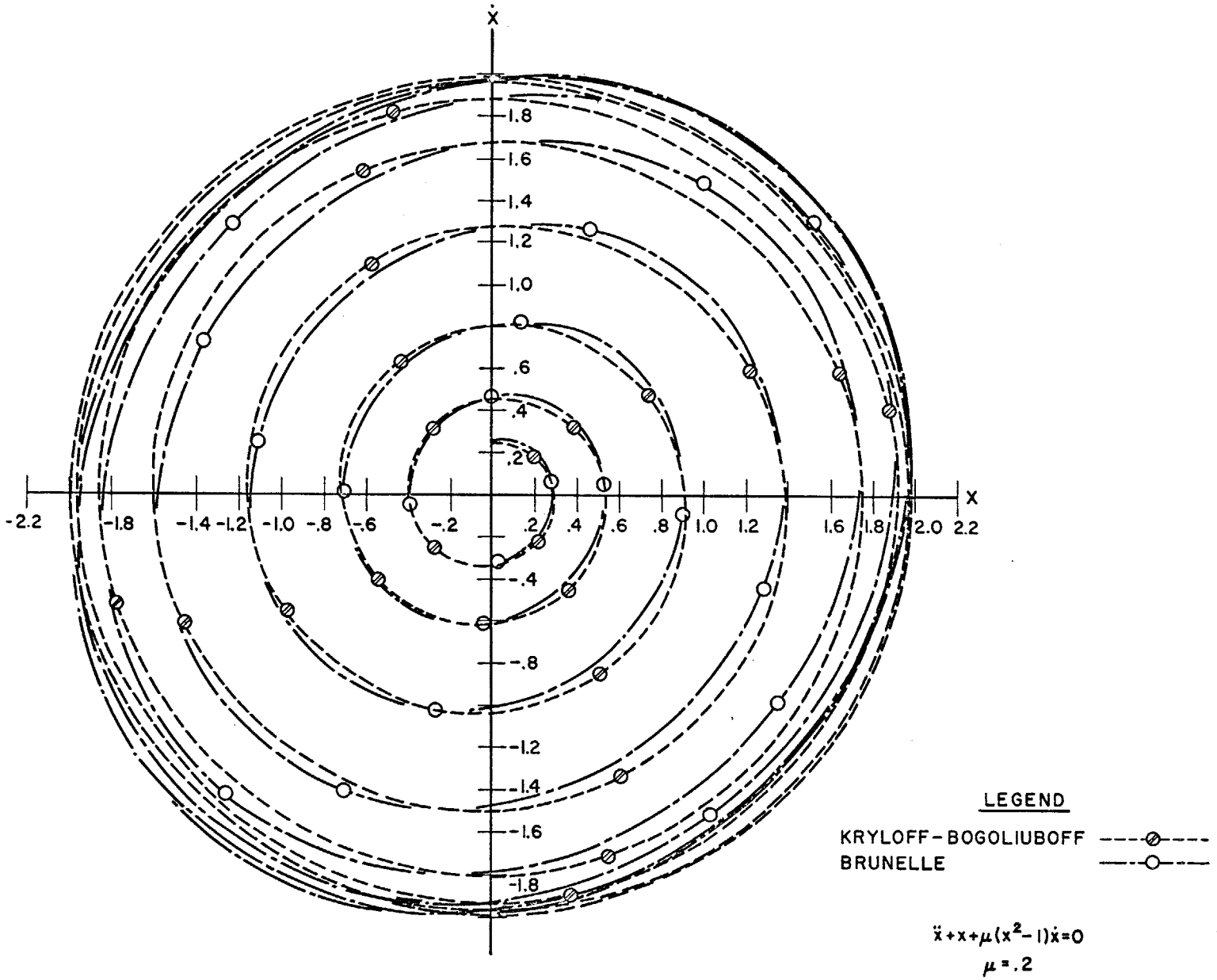


FIG.20 COMPARISON OF THE BRUNELLE AND THE KRYLOFF-BOGOLIUBOFF PHASE PLANE SOLUTIONS OF THE VAN DER POL EQUATION FOR $\mu = .2$

158

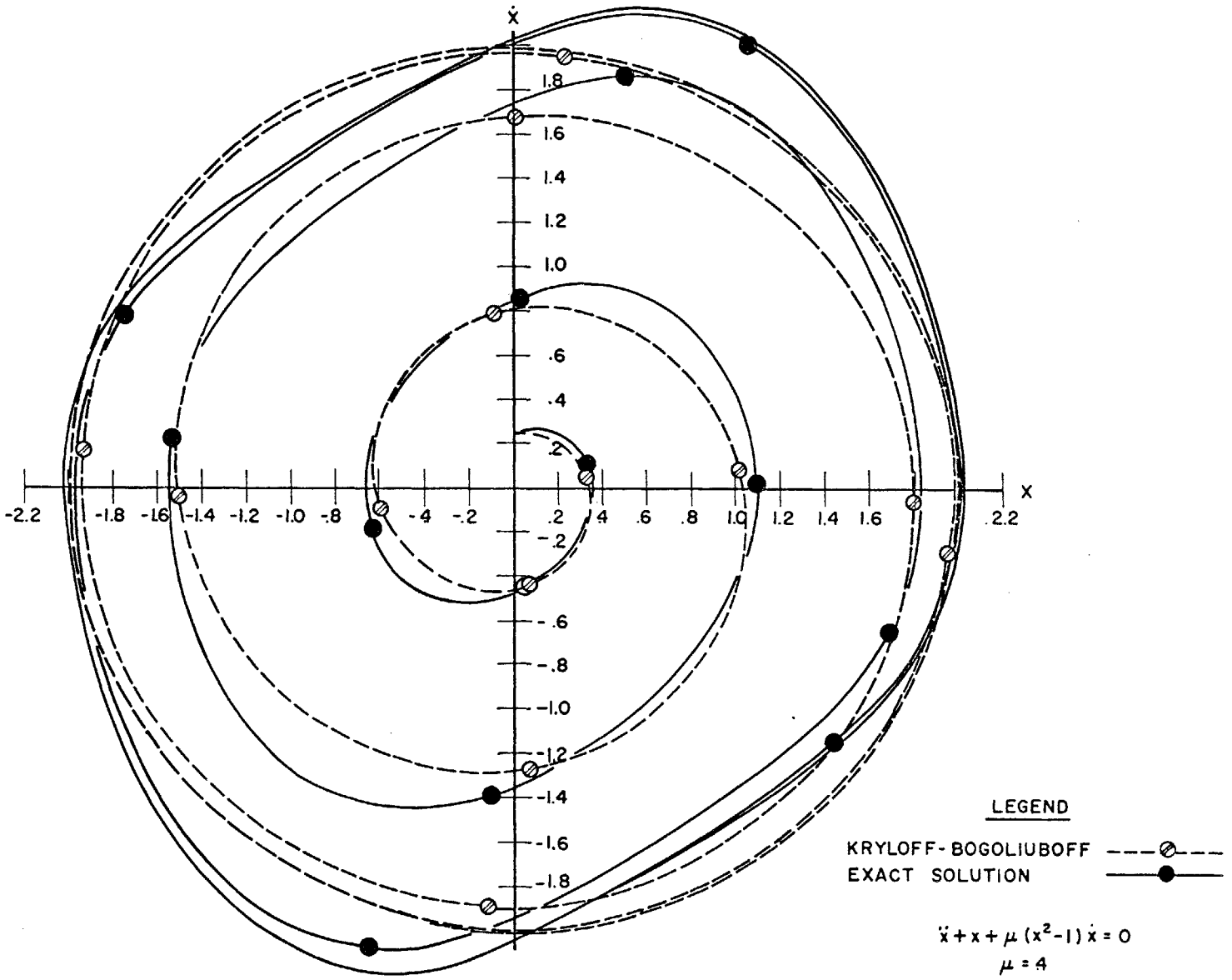


FIG. 21 COMPARISON OF THE KRYLOFF-BOGOLIUBOFF AND THE EXACT PHASE PLANE SOLUTIONS OF THE VAN DER POL EQUATION FOR $\mu = .4$

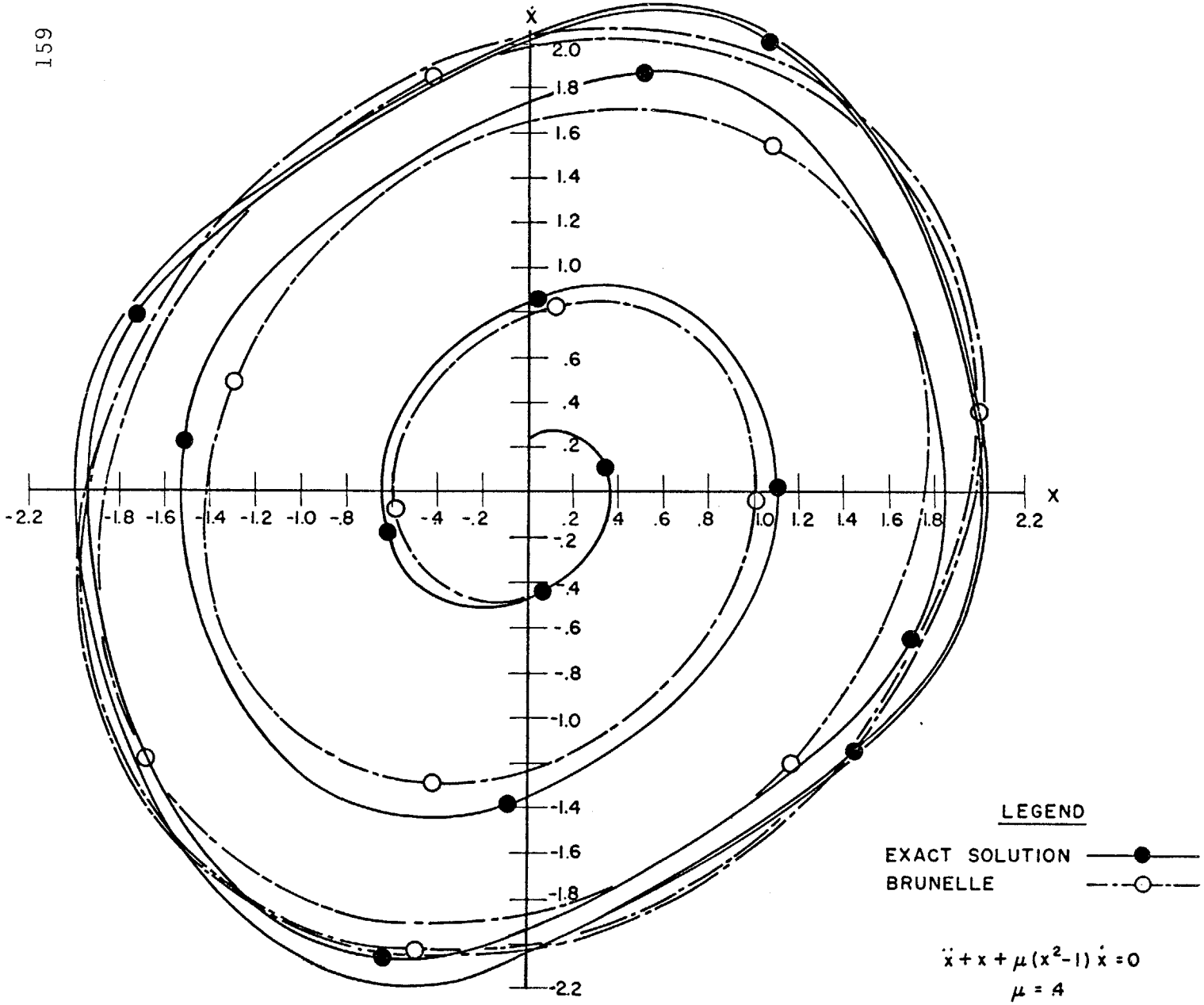


LEGEND

EXACT SOLUTION

BRUNELLE

$\ddot{x} + x + \mu(x^2-1)\dot{x} = 0$

$\mu = .4$

FIG. 22 COMPARISON OF THE BRUNELLE AND THE EXACT PHASE PLANE SOLUTIONS OF THE VAN DER POL EQUATION FOR $\mu = .4$

160

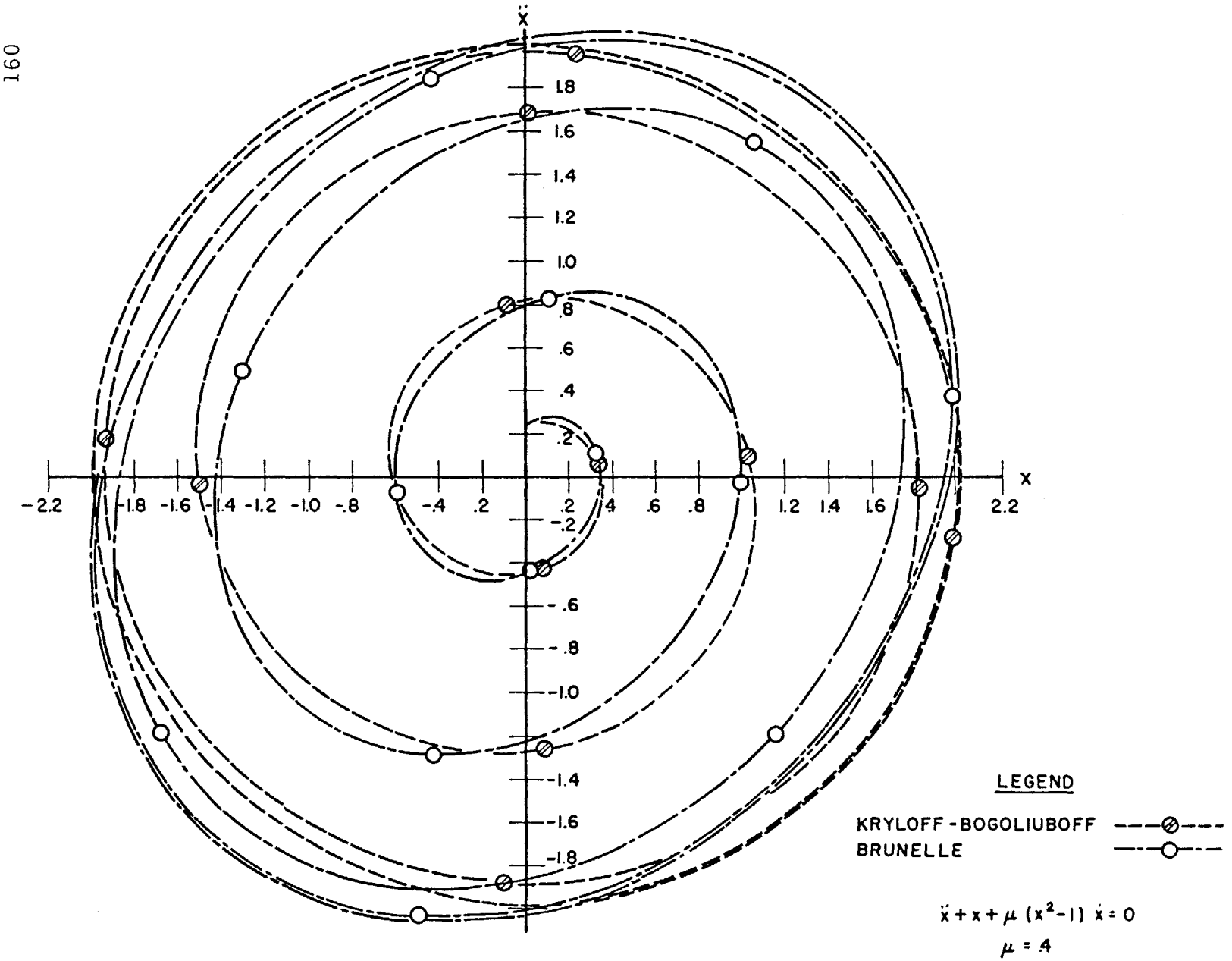


FIG. 23 COMPARISON OF THE BRUNELLE AND THE KRYLOFF-BOGOLIUBOFF PHASE PLANE SOLUTIONS OF THE VAN DER POL EQUATION FOR $\mu = 4$

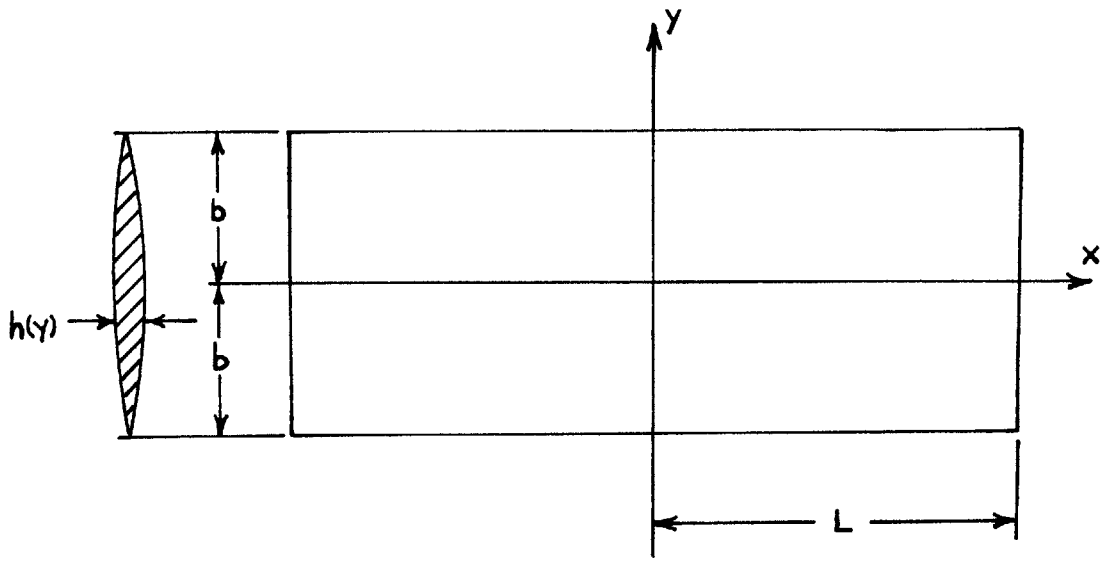


Figure 24 Wing Planform and Cross-Section

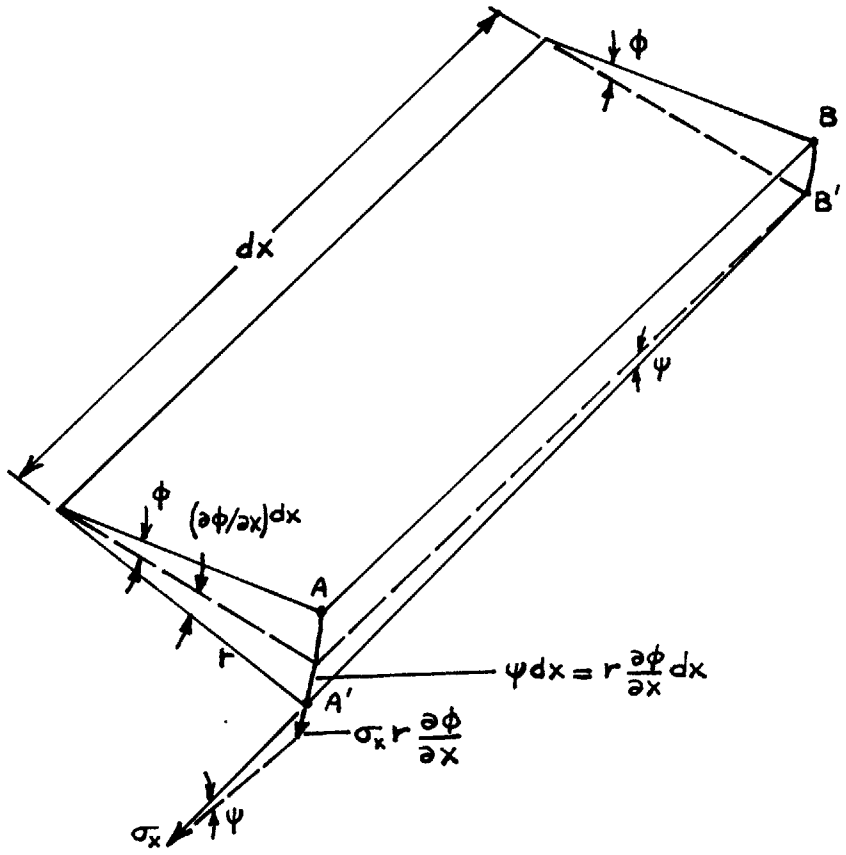


Figure 25 Segment of Twisted Wing

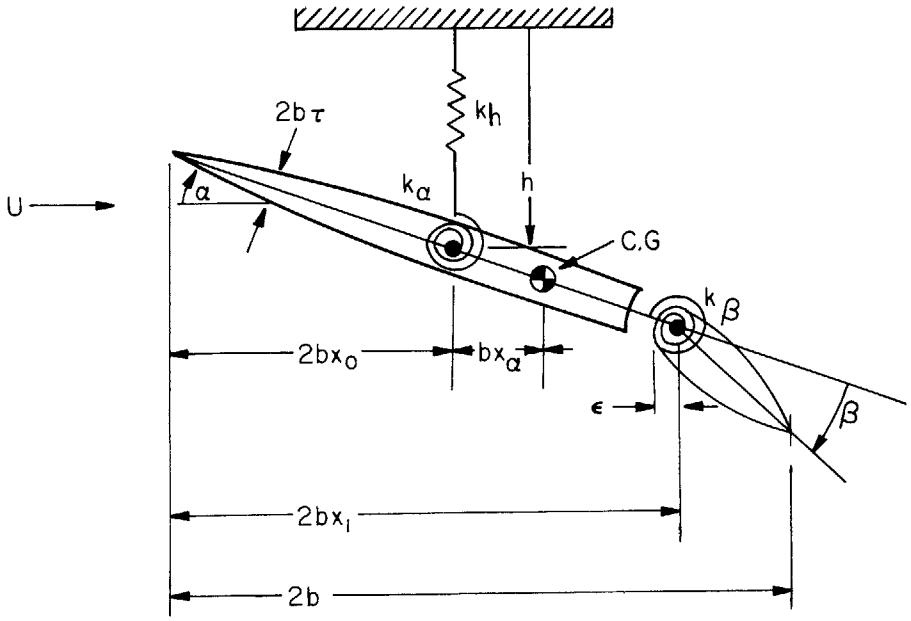


Fig. 26 Non-Zero-Thickness Typical Section

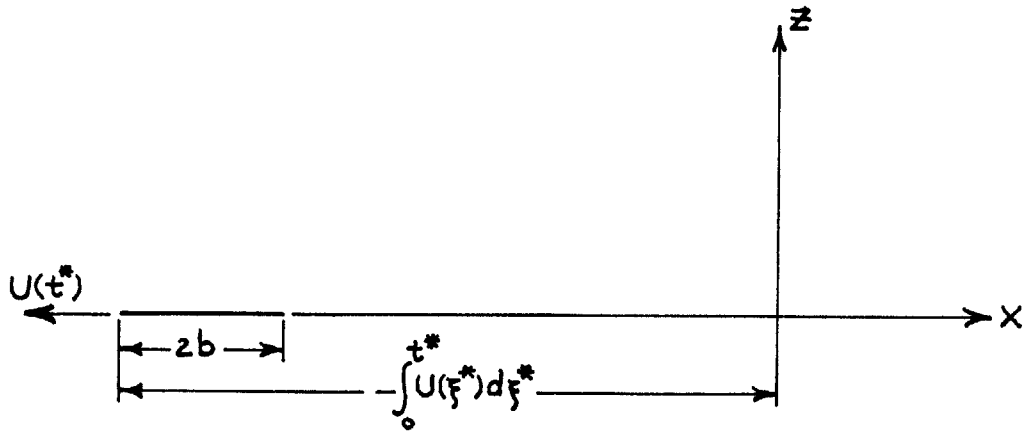


$$\varphi_{tt} - \varphi_{xx} - \varphi_{zz} = 0$$

$$\varphi_z \Big]_{z=0^{\pm}} = W_a(x,t) \qquad \text{on the airfoil}$$

$$\varphi_t = 0 \qquad \text{off the airfoil}$$

$$-\frac{1}{a_\infty}\int_0^t U(\zeta)d\zeta \leq x \leq 2b - \frac{1}{a_\infty}\int_0^t U(\zeta)d\zeta$$

$$p_L - p_u = 2\rho_\infty a_\infty \varphi_t$$

$$t = a_\infty t^*$$

$t^*$ is real time

Figure 27 Two Dimensional Accelerating Airfoil and Related Equations

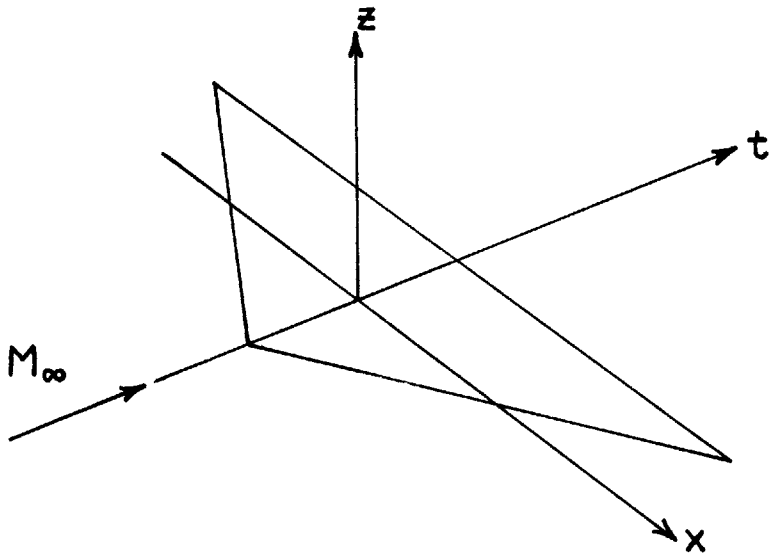


$$(M^2 - 1)\,\varphi_{tt} - \varphi_{xx} - \varphi_{zz} = 0$$

$$\varphi_z\Big]_{z=0\pm} = W_a(t,x) \quad \text{on the airfoil}$$

$$\varphi_t = 0 \qquad \text{off the airfoil}$$

$$p_L - p_u = 2\rho_\infty U \varphi_t$$

$$U = Ma_\infty$$

t is axial space coordinate

M is to be fixed at $\sqrt{2}$

Figure 28 Three Dimensional Steady State Airfoil and Related Equations

165

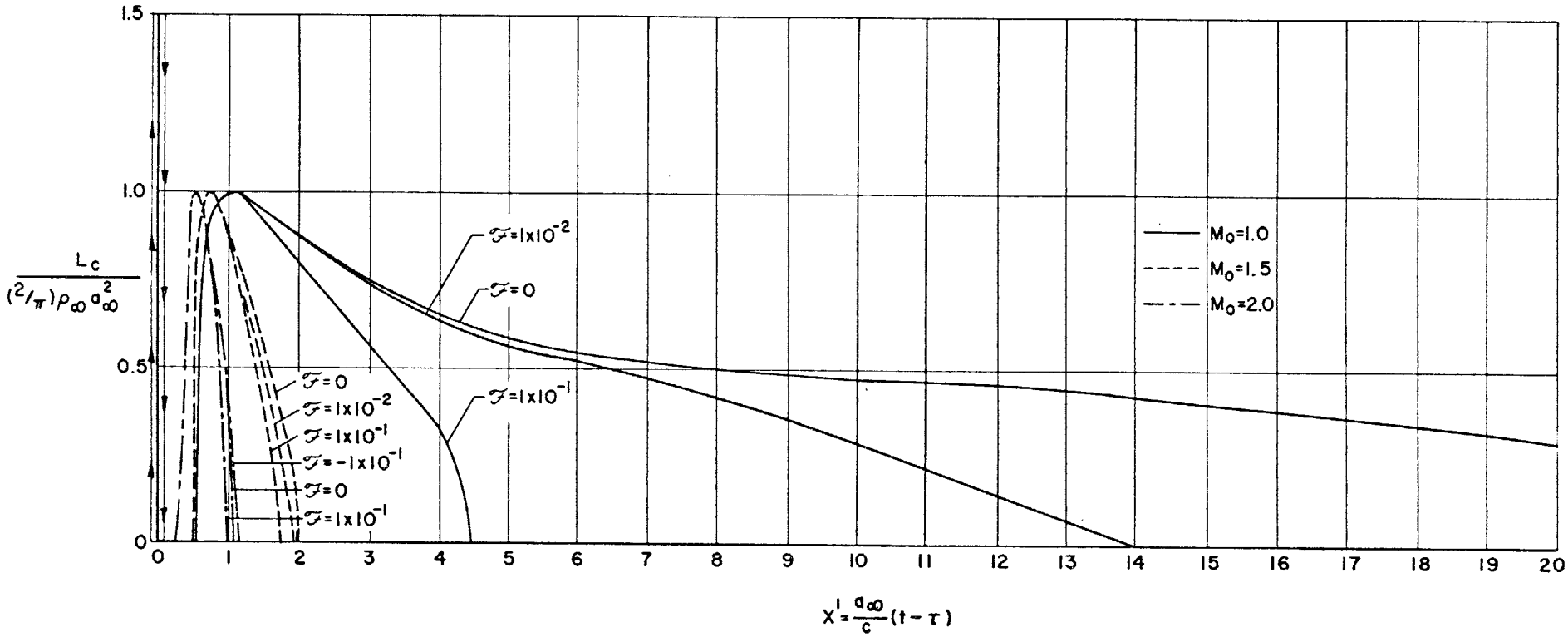


FIG. 29 LIFT DUE TO IMPULSIVE PLUNGING MOTION FOR CONSTANT $\mathcal{F}$'S

166

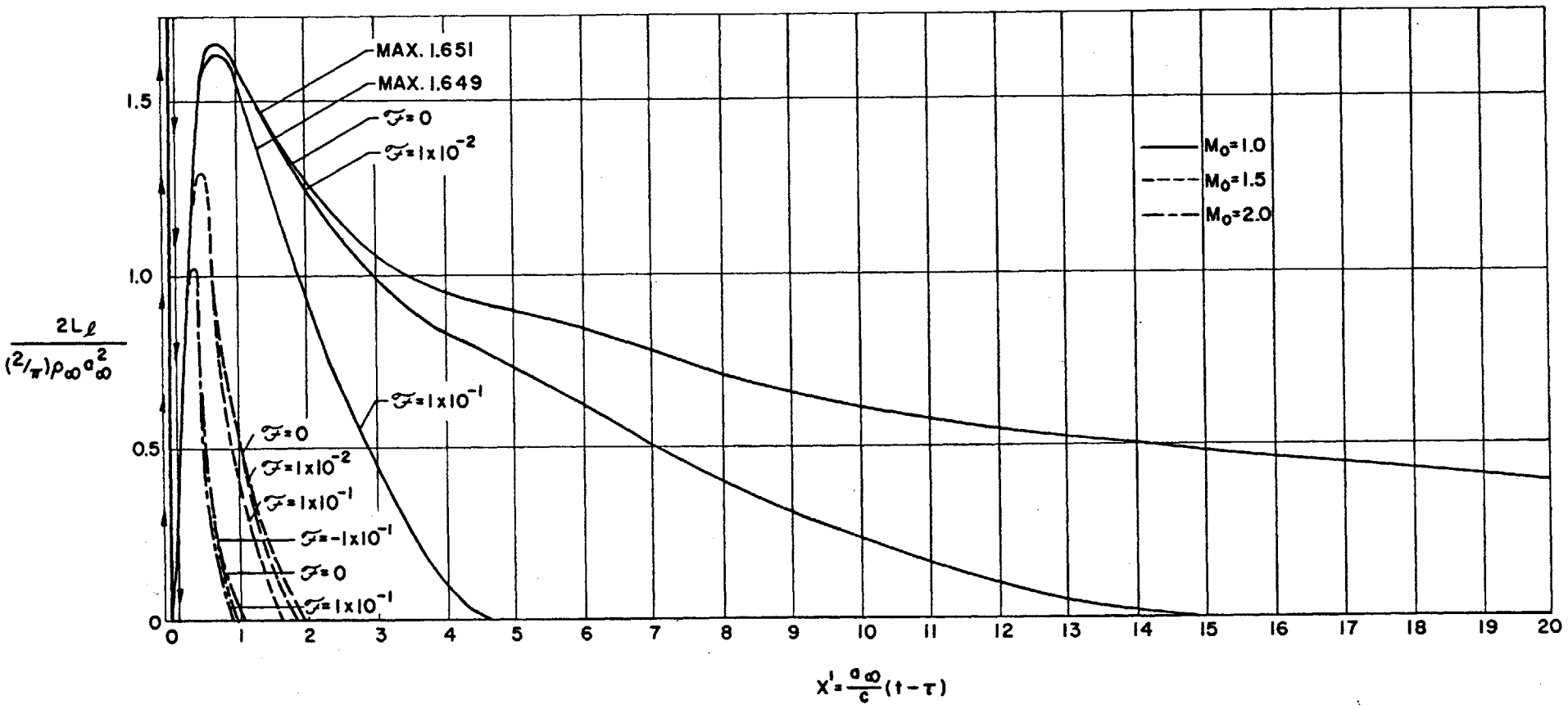


FIG. 30 LIFT DUE TO IMPULSIVE PITCH RATE ABOUT THE AIRFOIL LEADING EDGE FOR CONSTANT $\mathcal{F}$'S

167

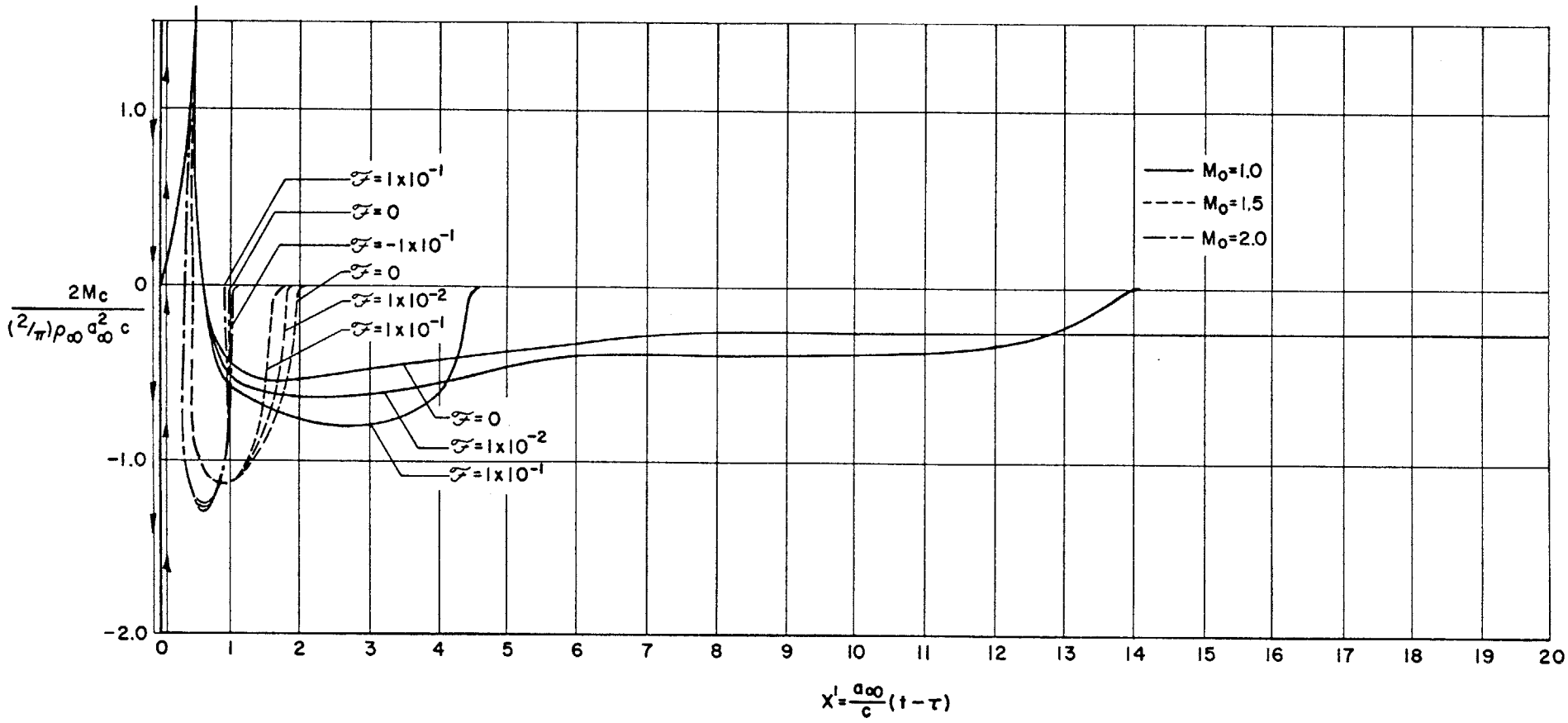


FIG. 31 PITCHING MOMENT DUE TO IMPULSIVE PLUNGING MOTION FOR CONSTANT $\mathscr{F}$'S

168

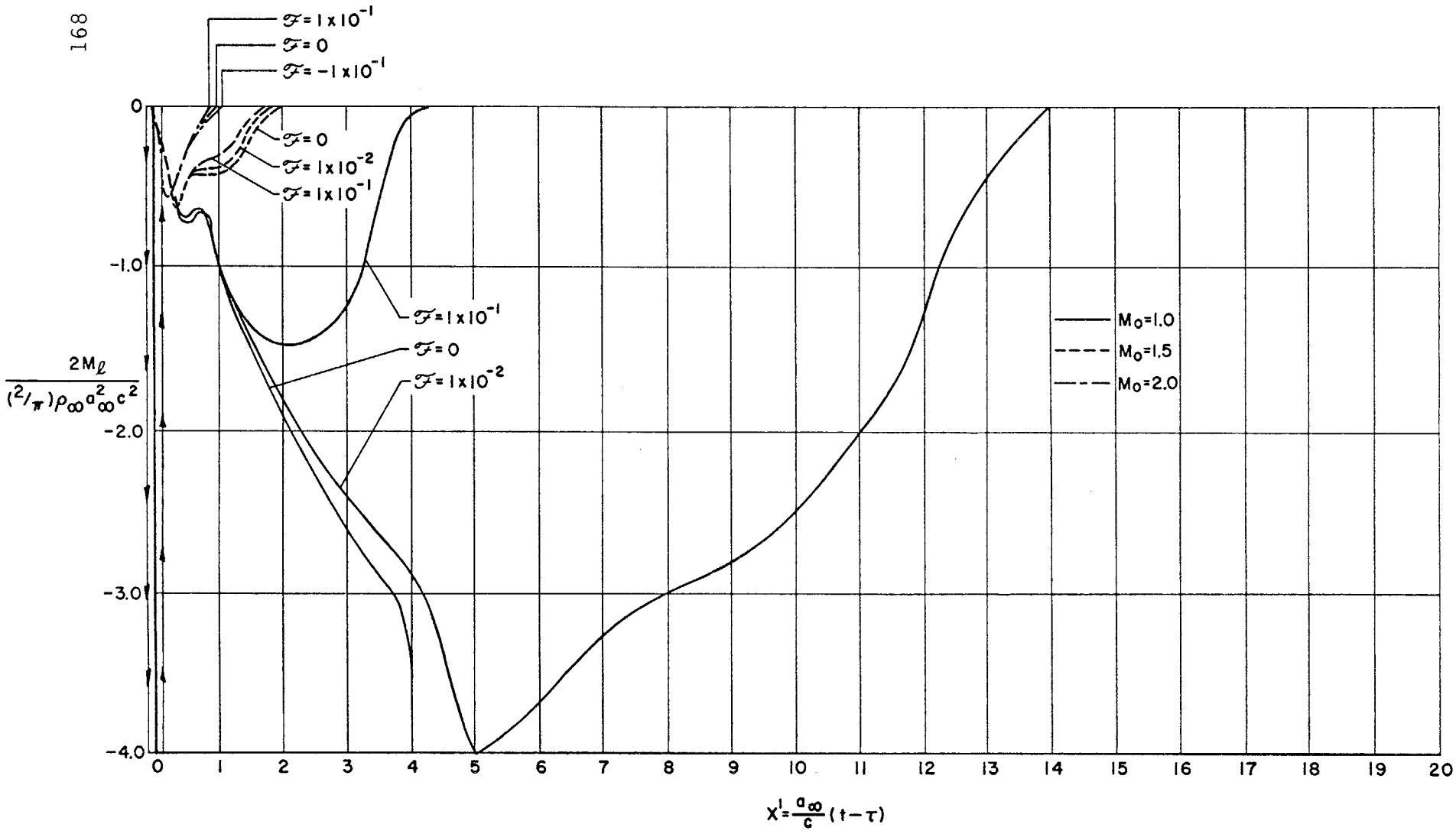


FIG. 32 PITCHING MOMENT DUE TO IMPULSIVE PITCH RATE ABOUT THE AIRFOIL LEADING EDGE FOR CONSTANT $\mathcal{F}$'S

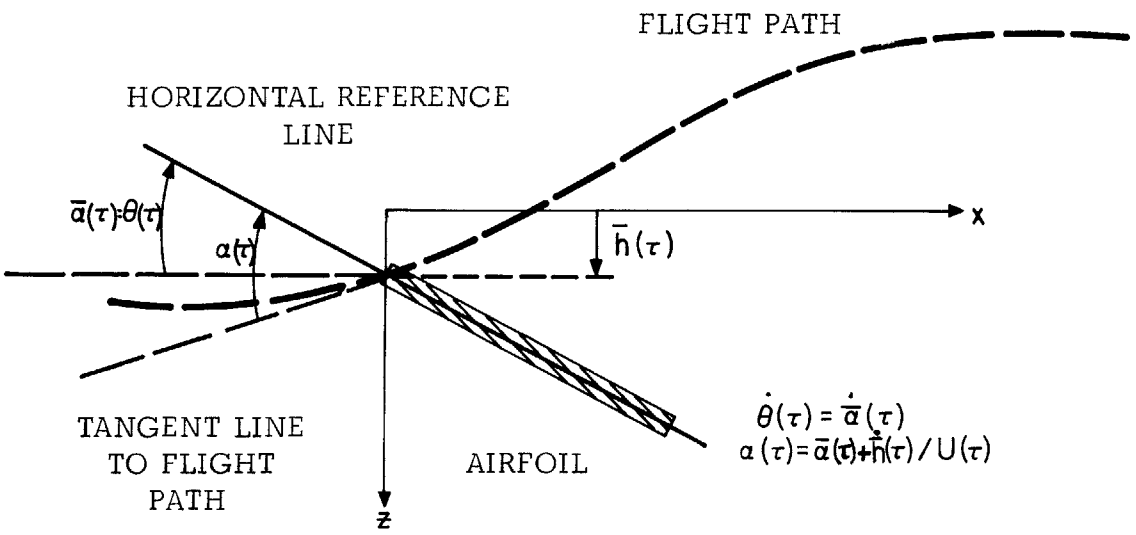


Fig. 33 Flight Path Variables

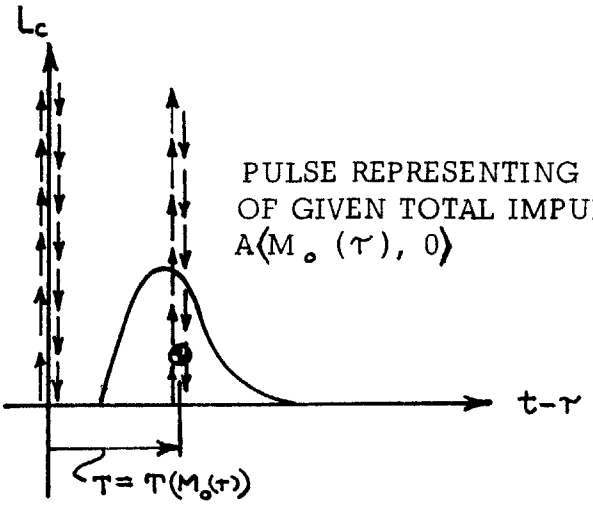


Fig. 34 Pulse Representation

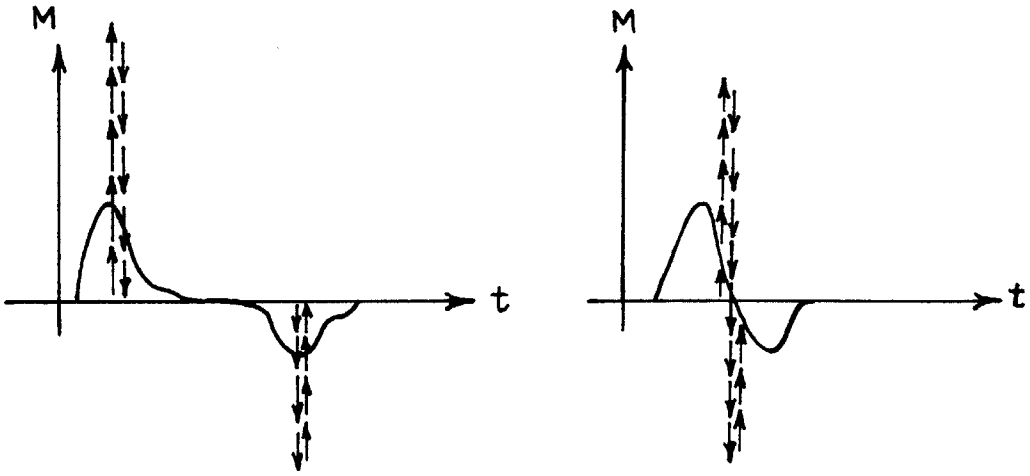


Fig. 35 Moment Pulse and Doublet Representation

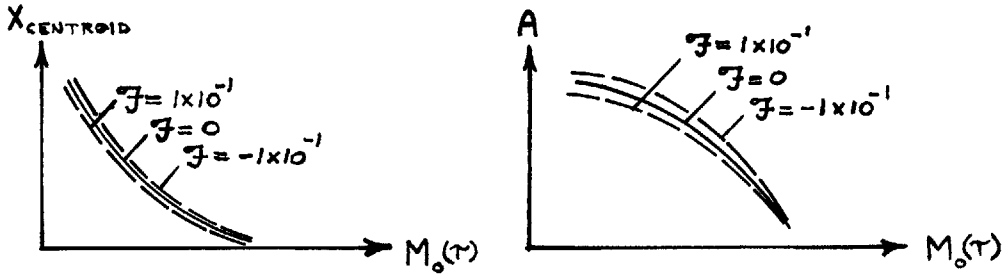


Fig. 36 Typical Pulse Strength and Pulse Centroid Plots

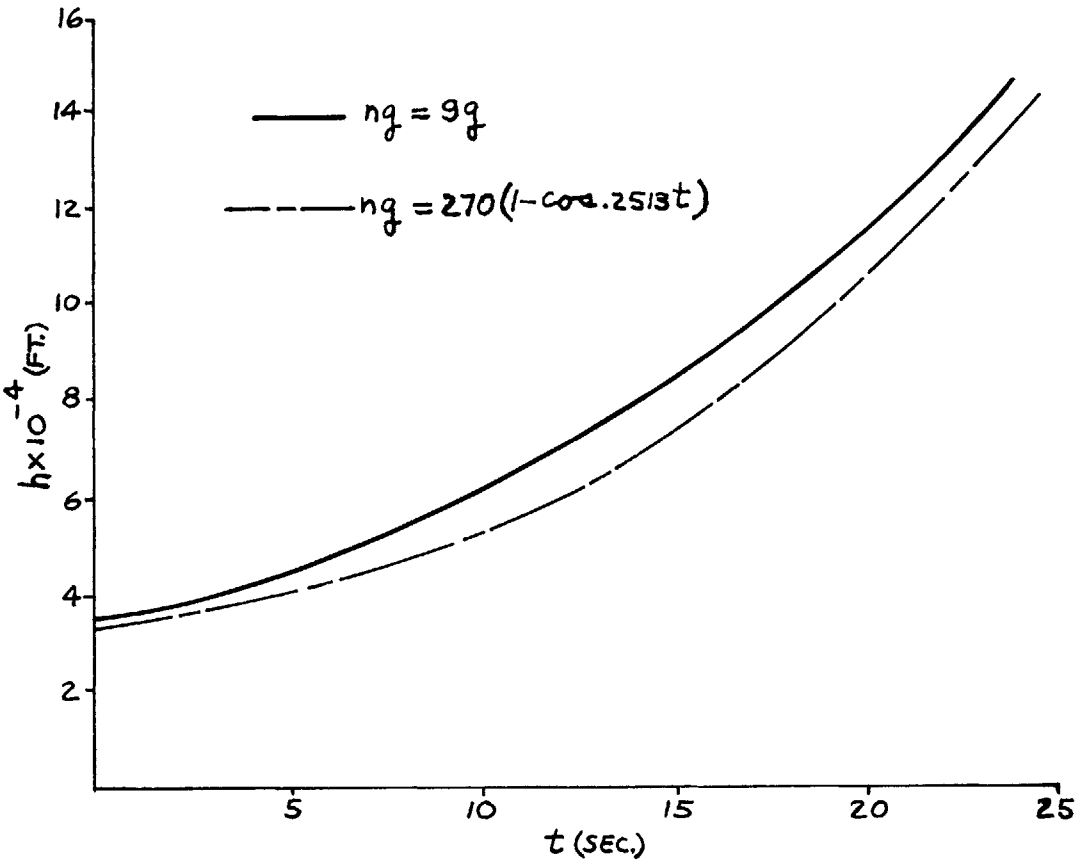


Fig. 37 Altitude versus Time for the Chosen Flight Missions

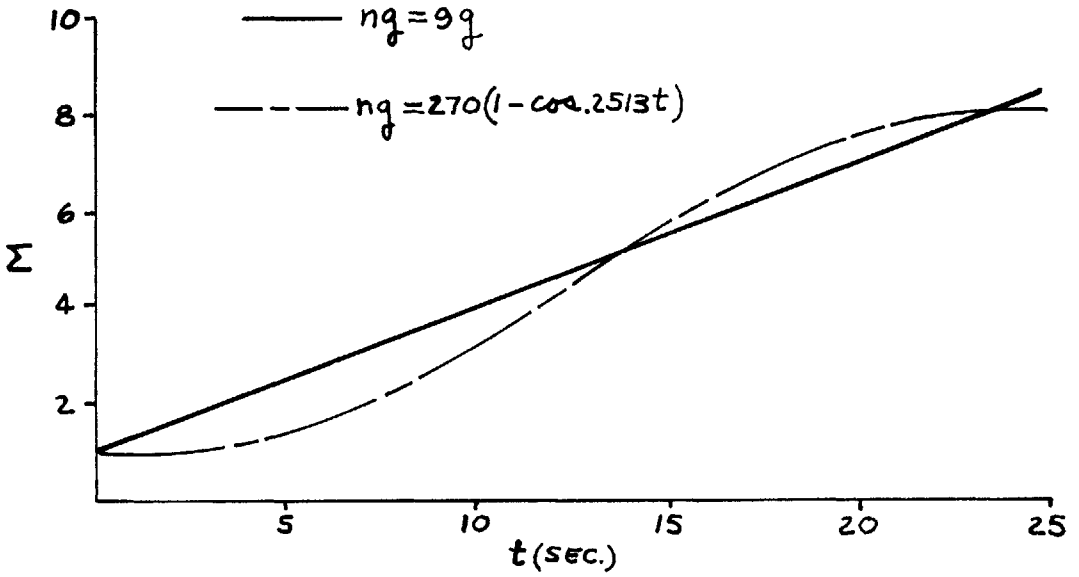


Fig. 38 Mach Number versus Time for the Chosen Flight Missions

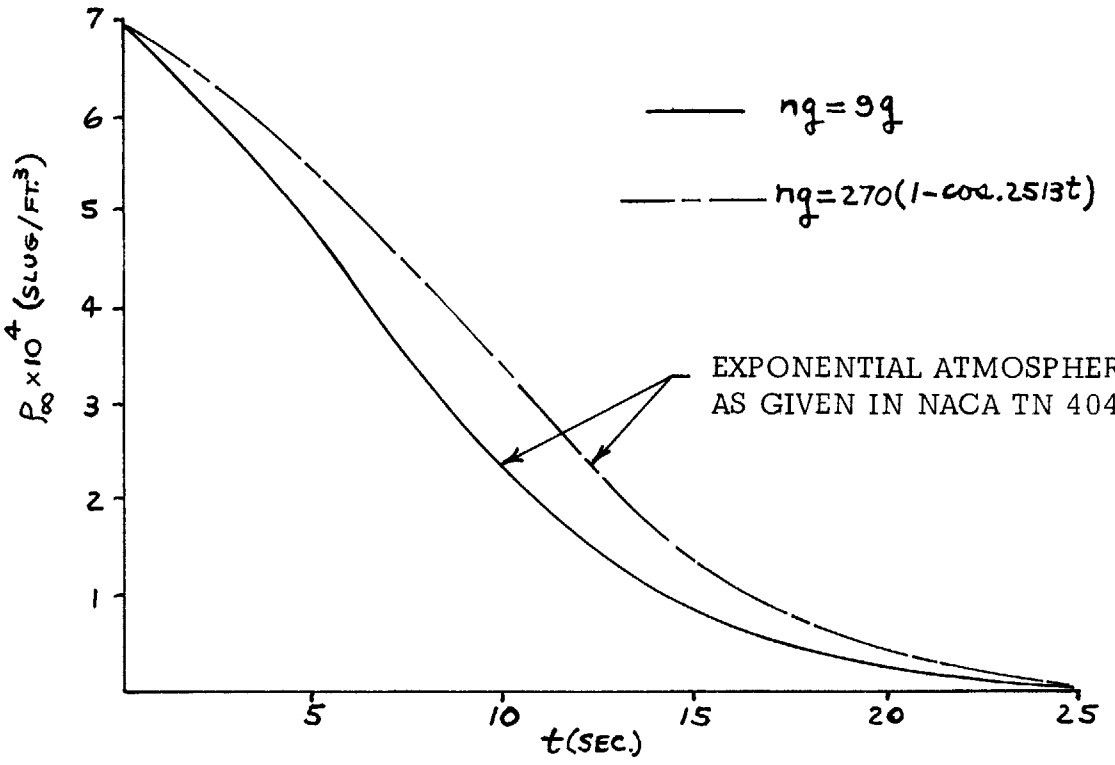


Fig. 39 Ambient Density versus Time for the Chosen Flight Missions

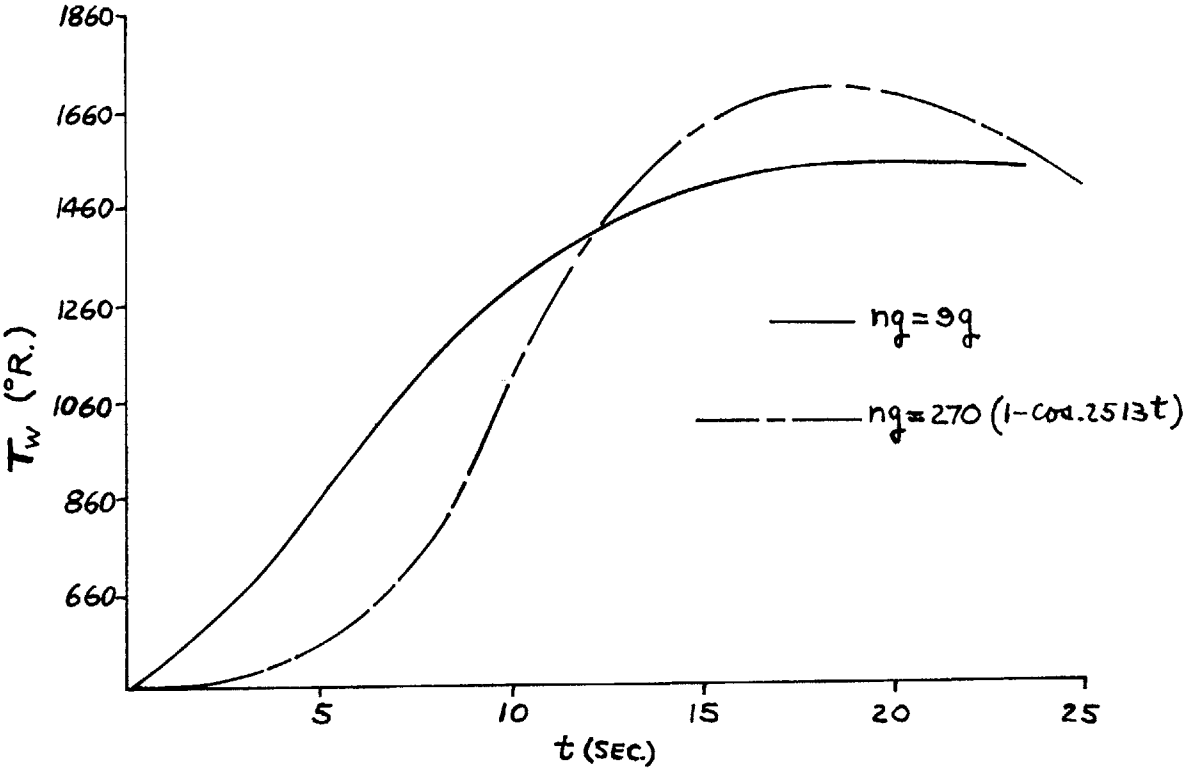


Fig. 40 Wall Temperature versus Time for the Chosen Flight Missions

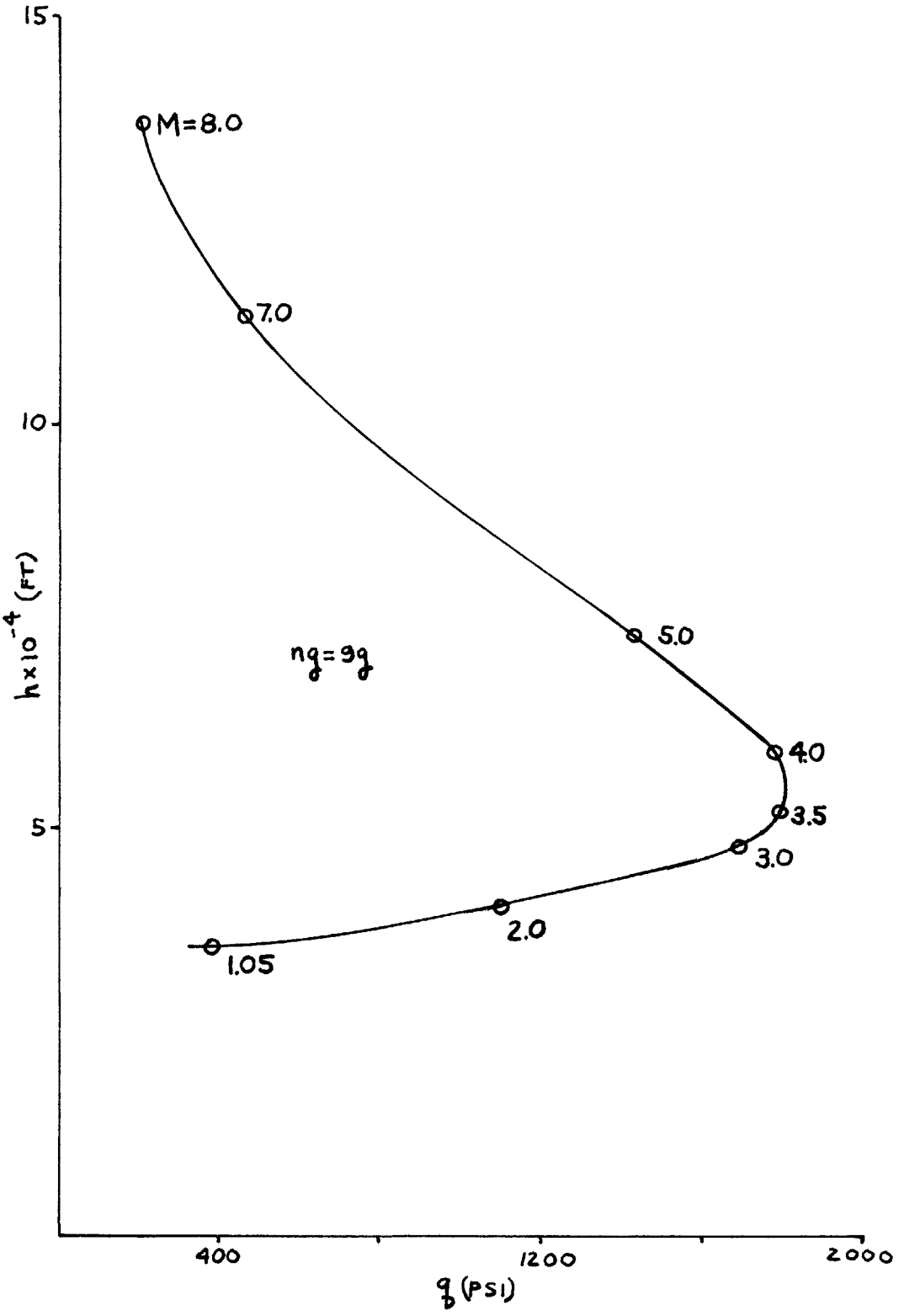


Fig. 41 Dynamic Pressure versus Altitude for the 9g Accelerated Flight Mission

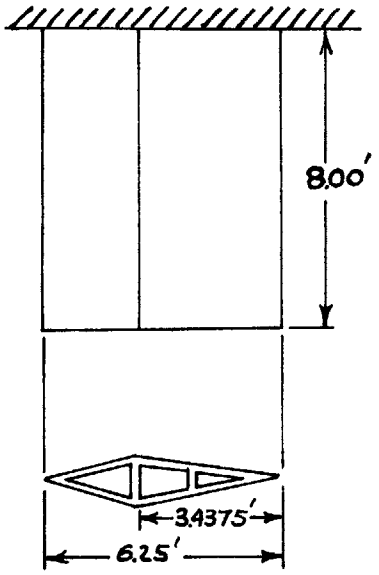


WING AREA = 50 FT.$^2$ WING WEIGHT/FT.$^2$ = 30#/FT.$^2$
3% UNSYMMETRICAL DOUBLE WEDGE STAINLESS STEEL HOLLOW n-CELL WING. THE NUMBER n IS NOT SPECIFIED SO THAT $\omega_{\alpha}$ ISO-THERMAL MAY BE CONVENIENTLY CHOSEN.

Fig. 42 Wing Geometry of the Vehicle Performing the Flight Missions

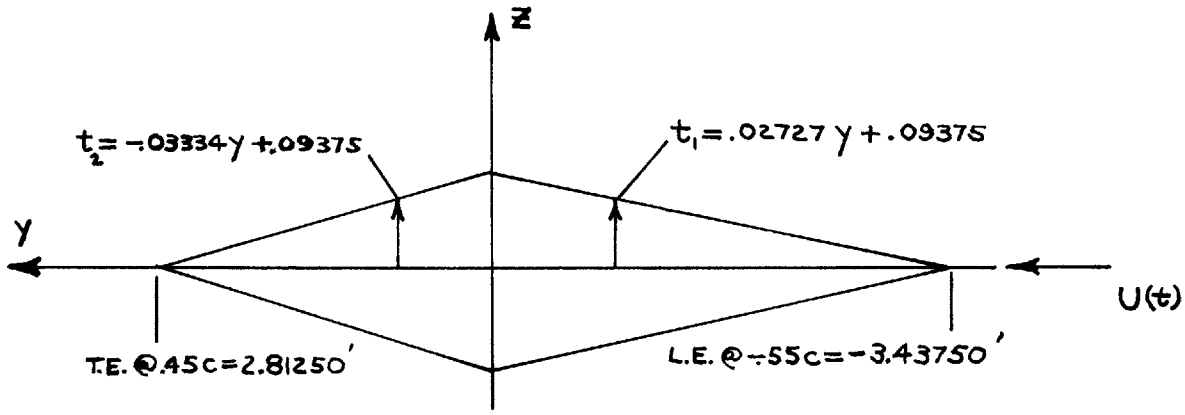


Fig. 43 External Wing Cross-Section Geometry of the Vehicle Performing the Flight Missions

175

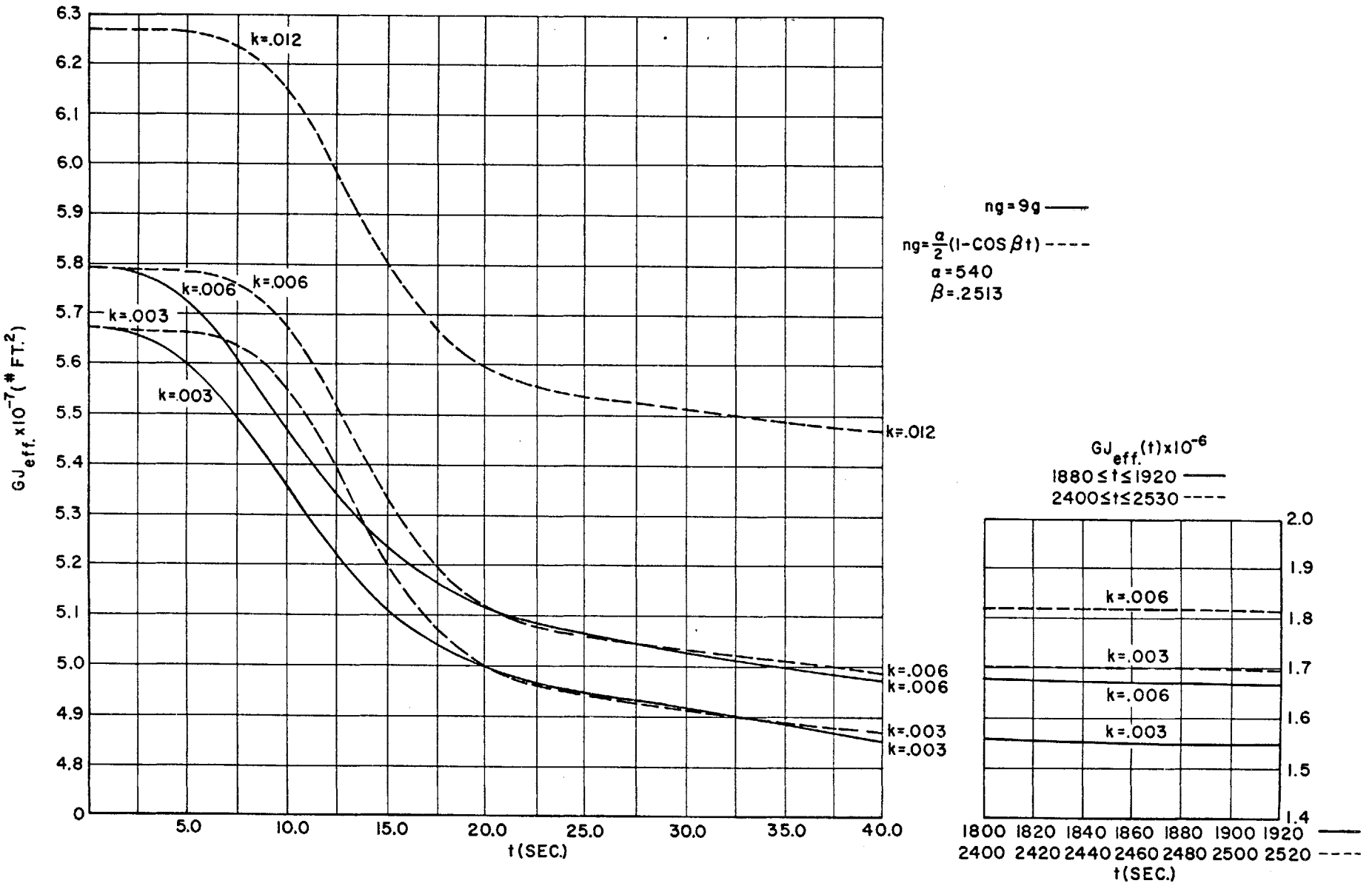


FIG. 44 EFFECTIVE TORSIONAL WING STIFFNESS VERSUS TIME FOR THE CHOSEN FLIGHT MISSIONS AND SEVERAL VALUES OF THE PARAMETER k

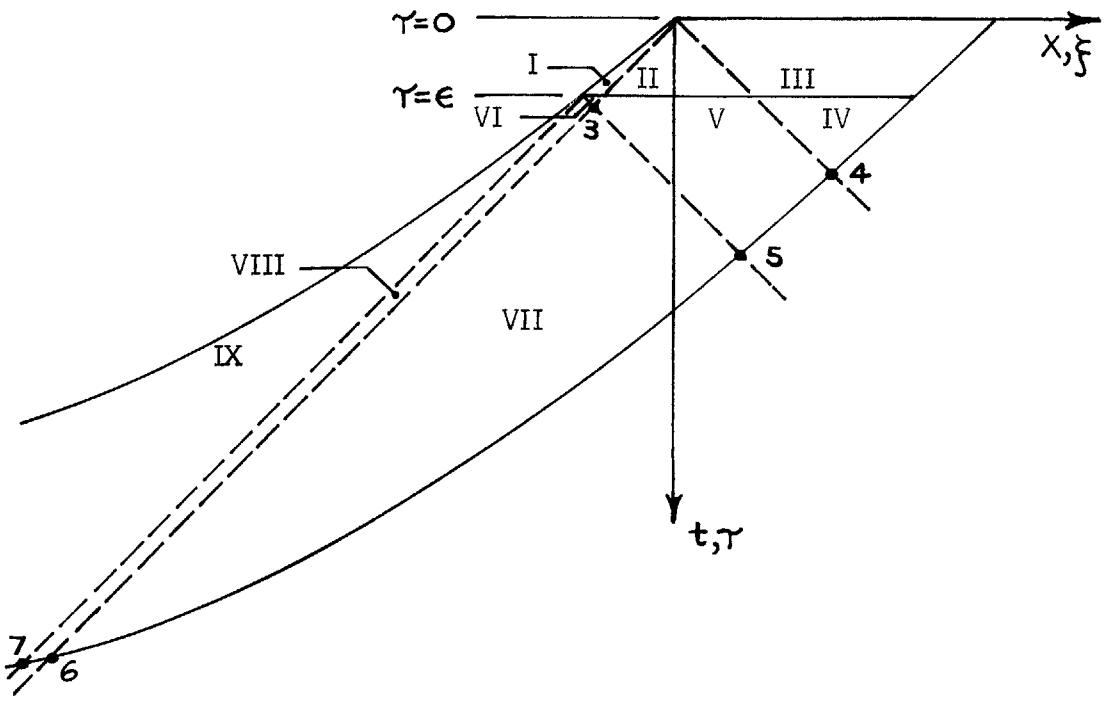


Fig. 45 Supersonic Three-Dimensional Analogy Planform with a Finite Band of Upwash on the Airfoil Between $0 \le t \le \epsilon$

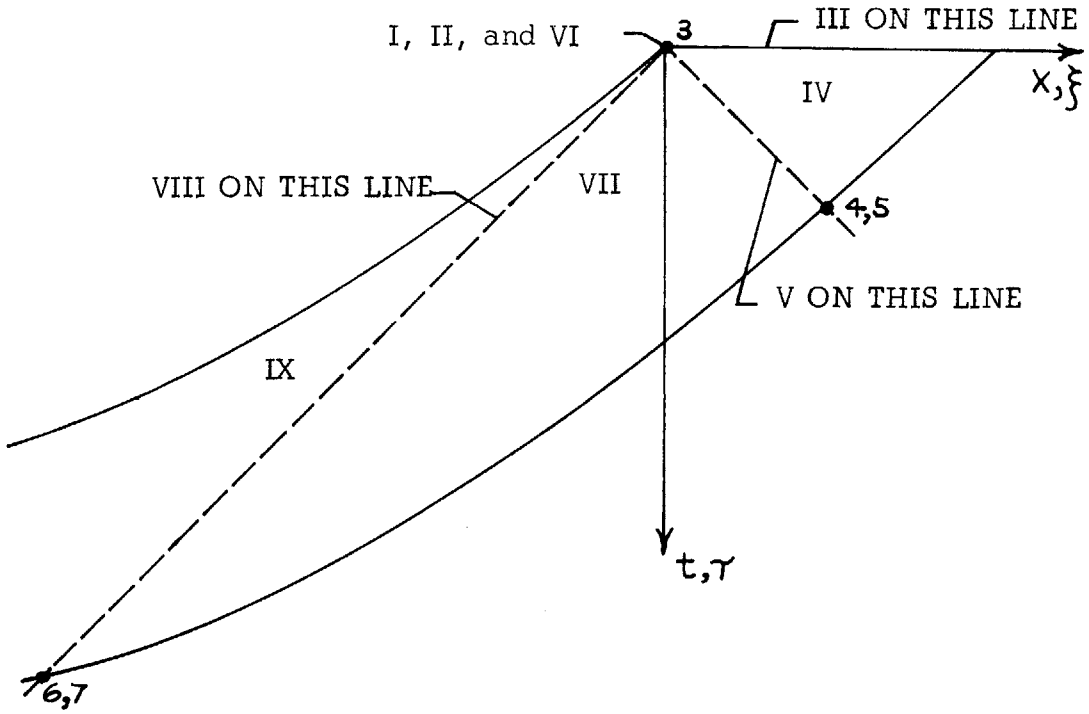


Fig. 46 Supersonic Three-Dimensional Analogy Planform with an Impulsive Upwash Along the Leading Edge

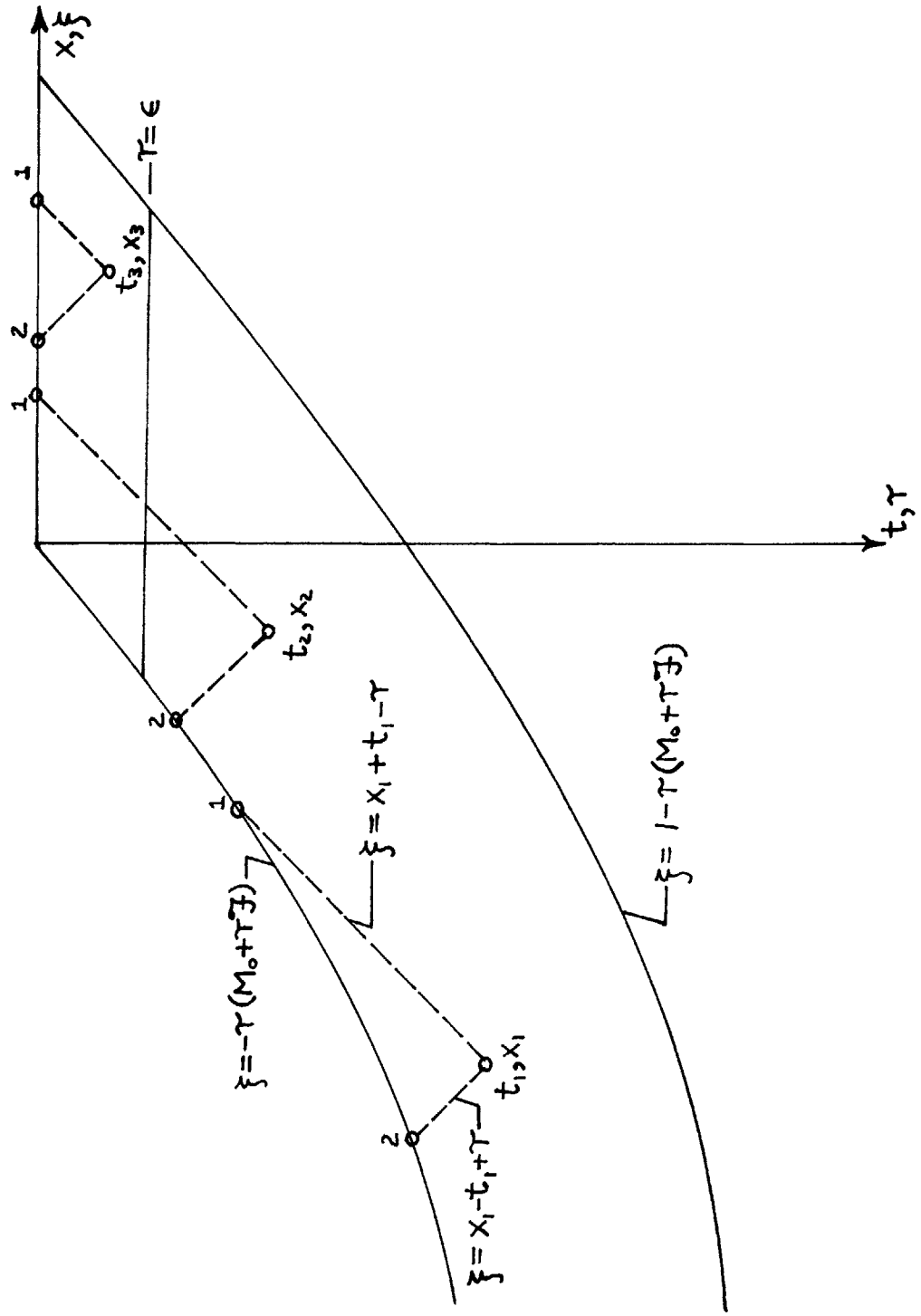


Fig. 47 Wing Geometry and Forward Mach Cone Representations

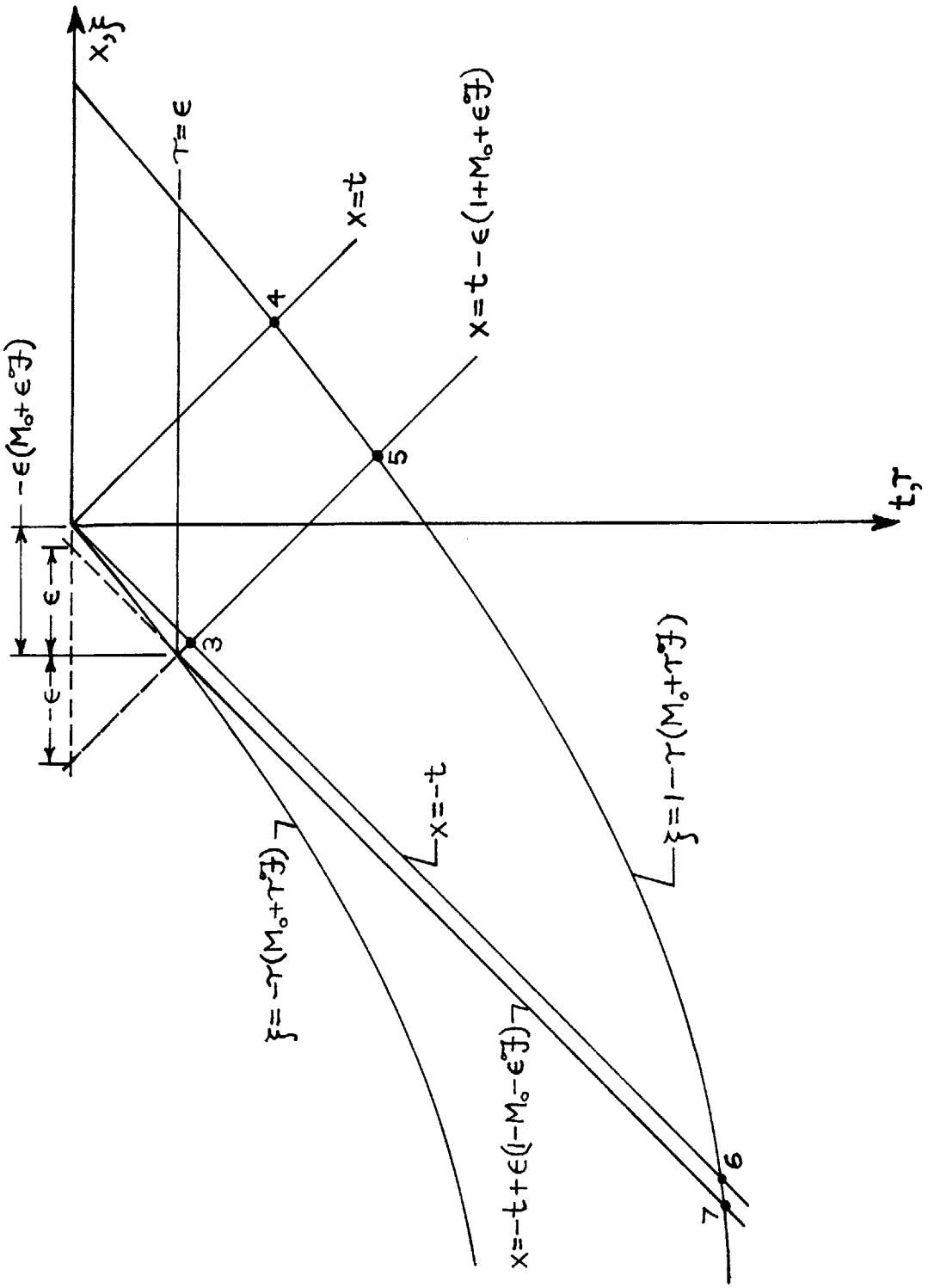


Fig. 48 Equations Representing the Various Planform Curves and the Mach Lines

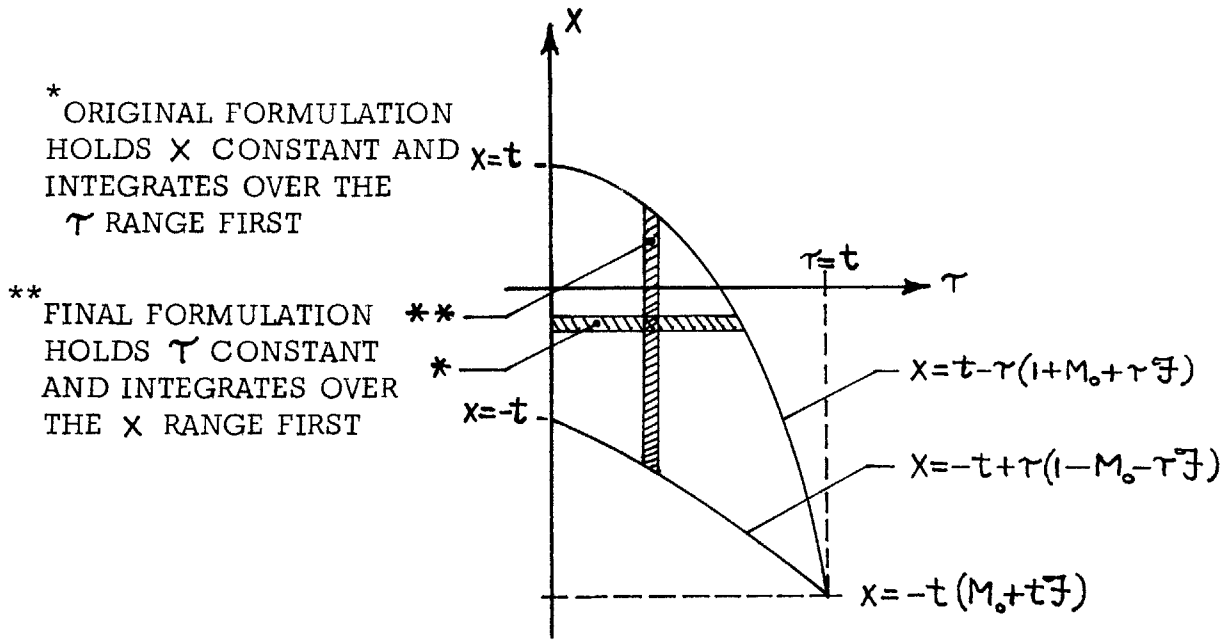


Fig. 49 Integration Region for $0 \le t \le \epsilon$

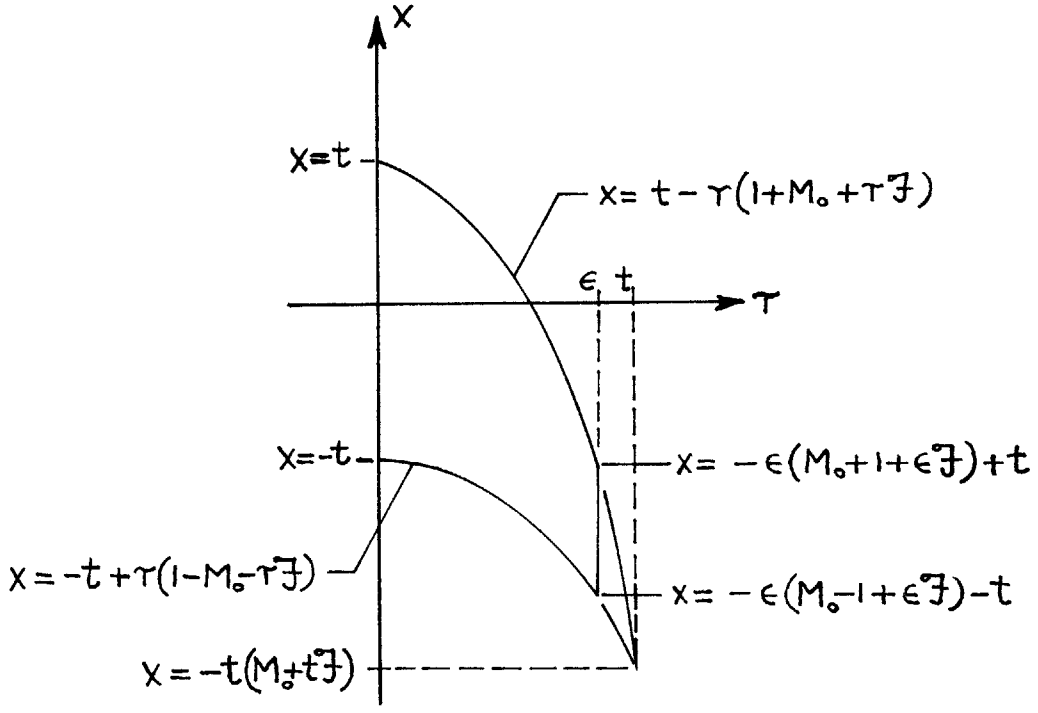


Fig. 50 Integration Region for $\epsilon \le t \le t_3$

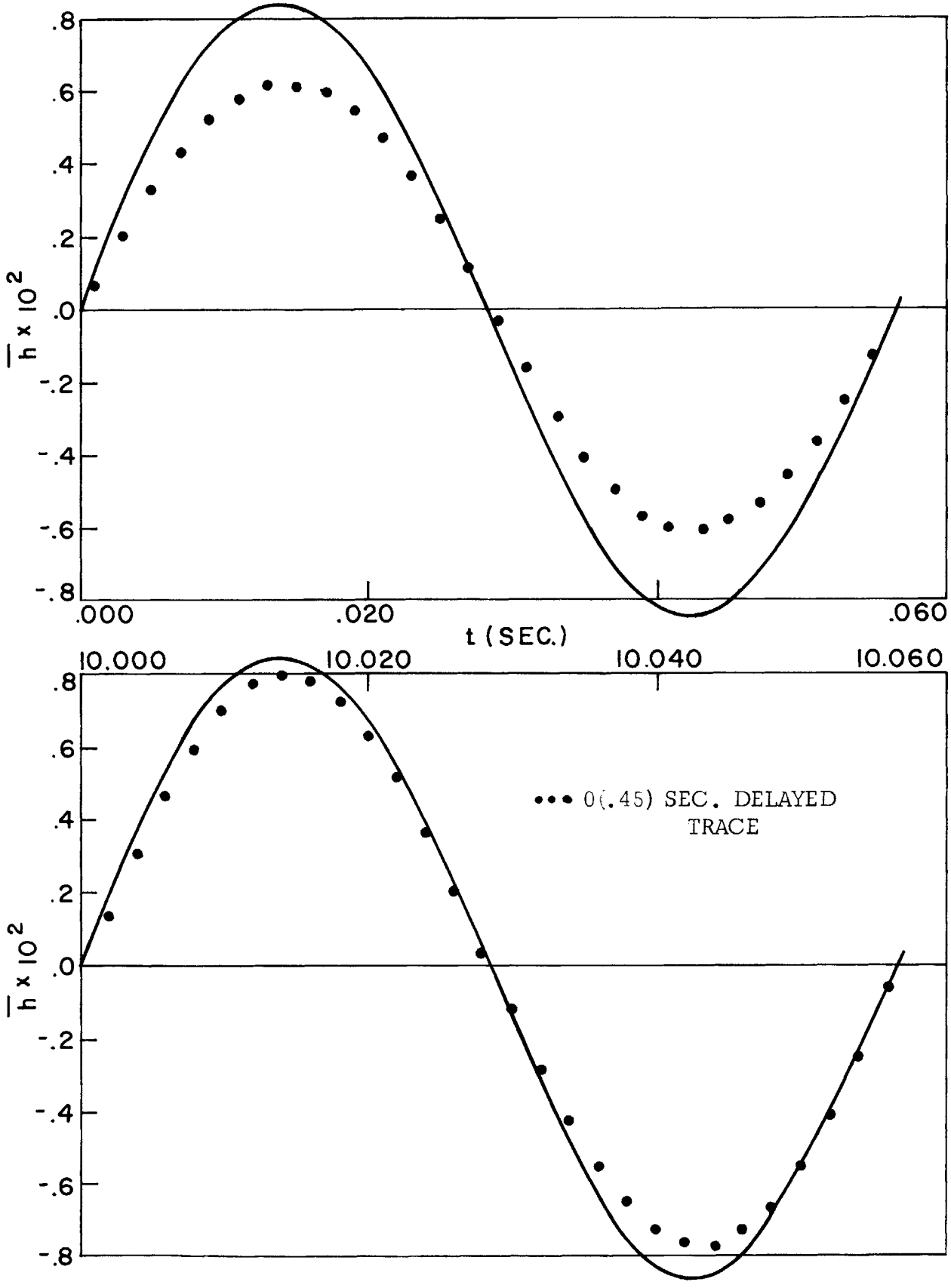


Fig. 51 $\bar{h}$ Time History Due to Case 1 Initial Conditions Applied at t = 0 and 10 Seconds Compared with Itself Approximately .45 Seconds Later; ng = 9g

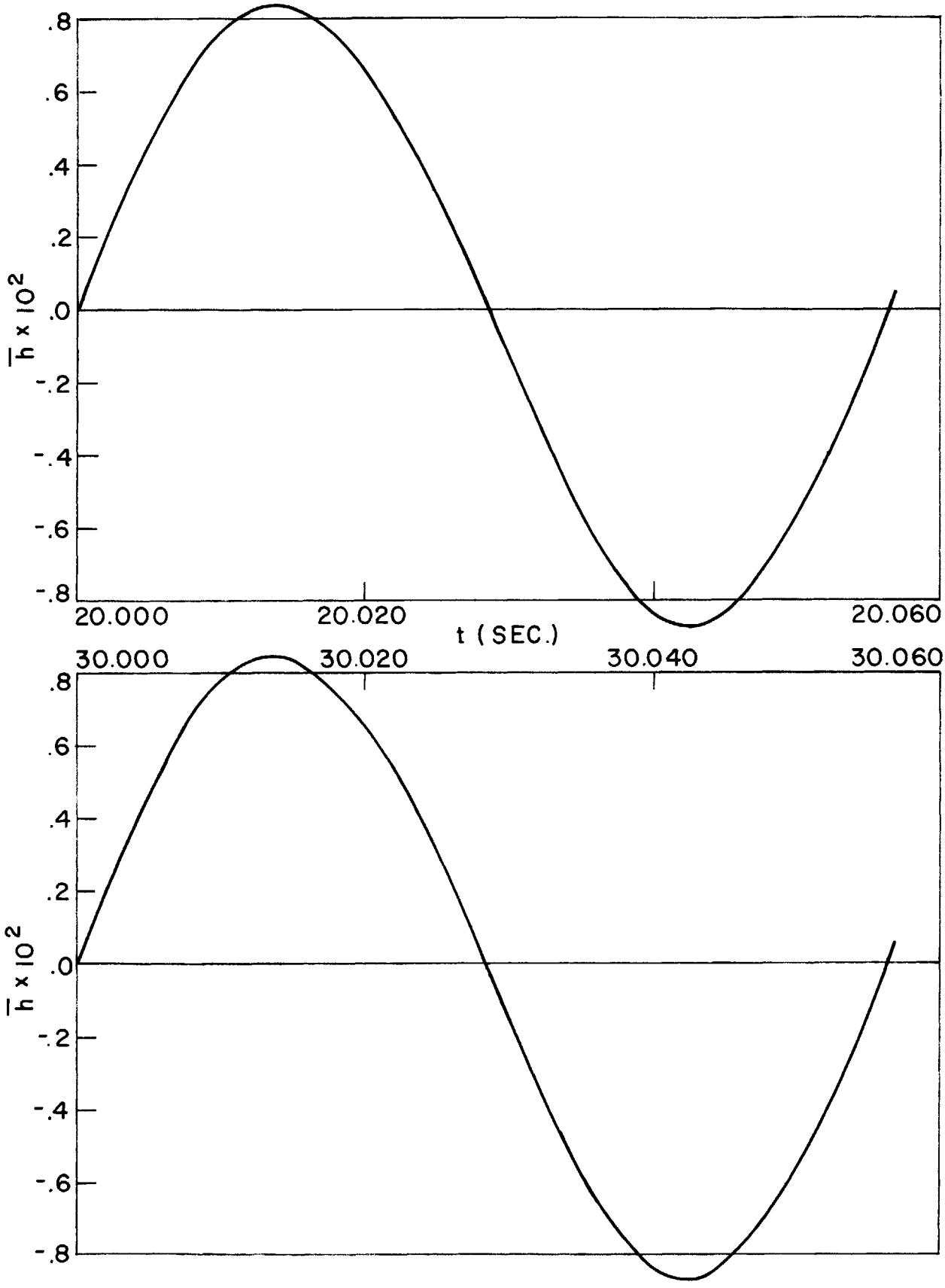


Fig. 52 $\bar{h}$ Time History Due to Case 1 Initial Conditions Applied at t = 20 and 30 Seconds; ng = 9g

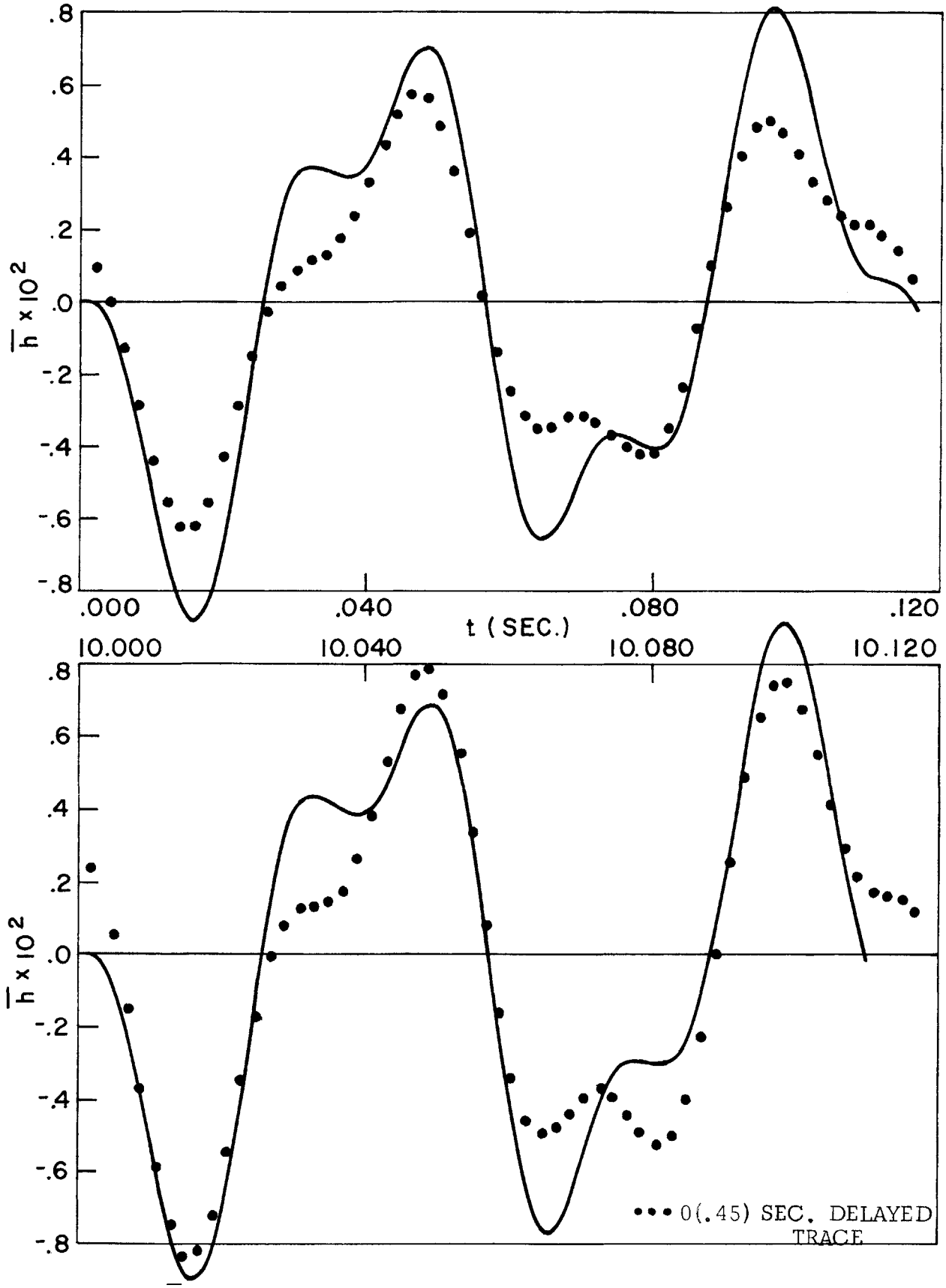


Fig. 53 $\bar{h}$ Time History Due to Case 2 Initial Conditions Applied at t = 0 and 10 Seconds Compared with Itself Approximately .45 Seconds Later; ng = 9g

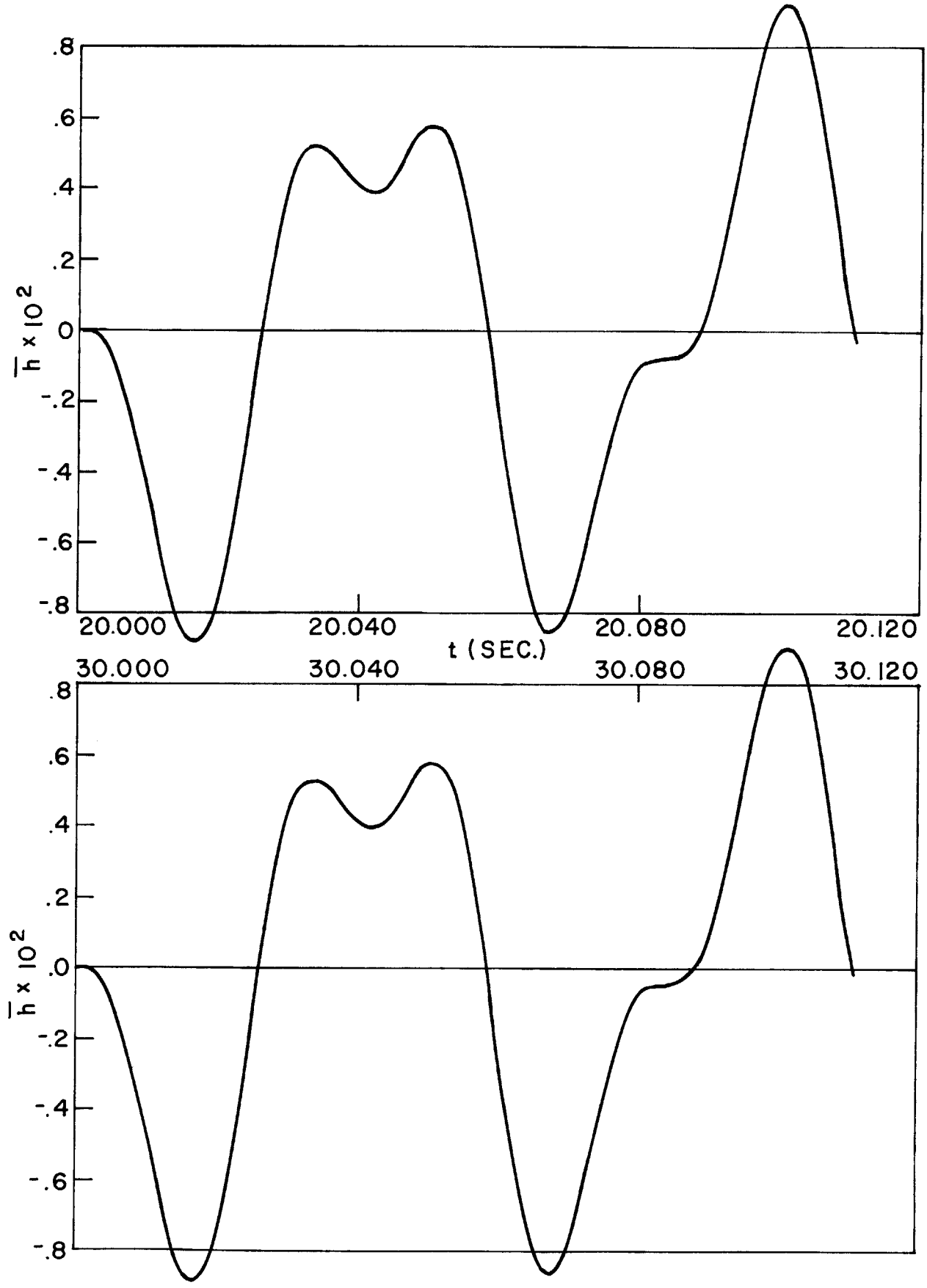


Fig. 54 $\bar{h}$ Time History Due to Case 2 Initial Conditions Applied at t = 20 and 30 Seconds; ng = 9g

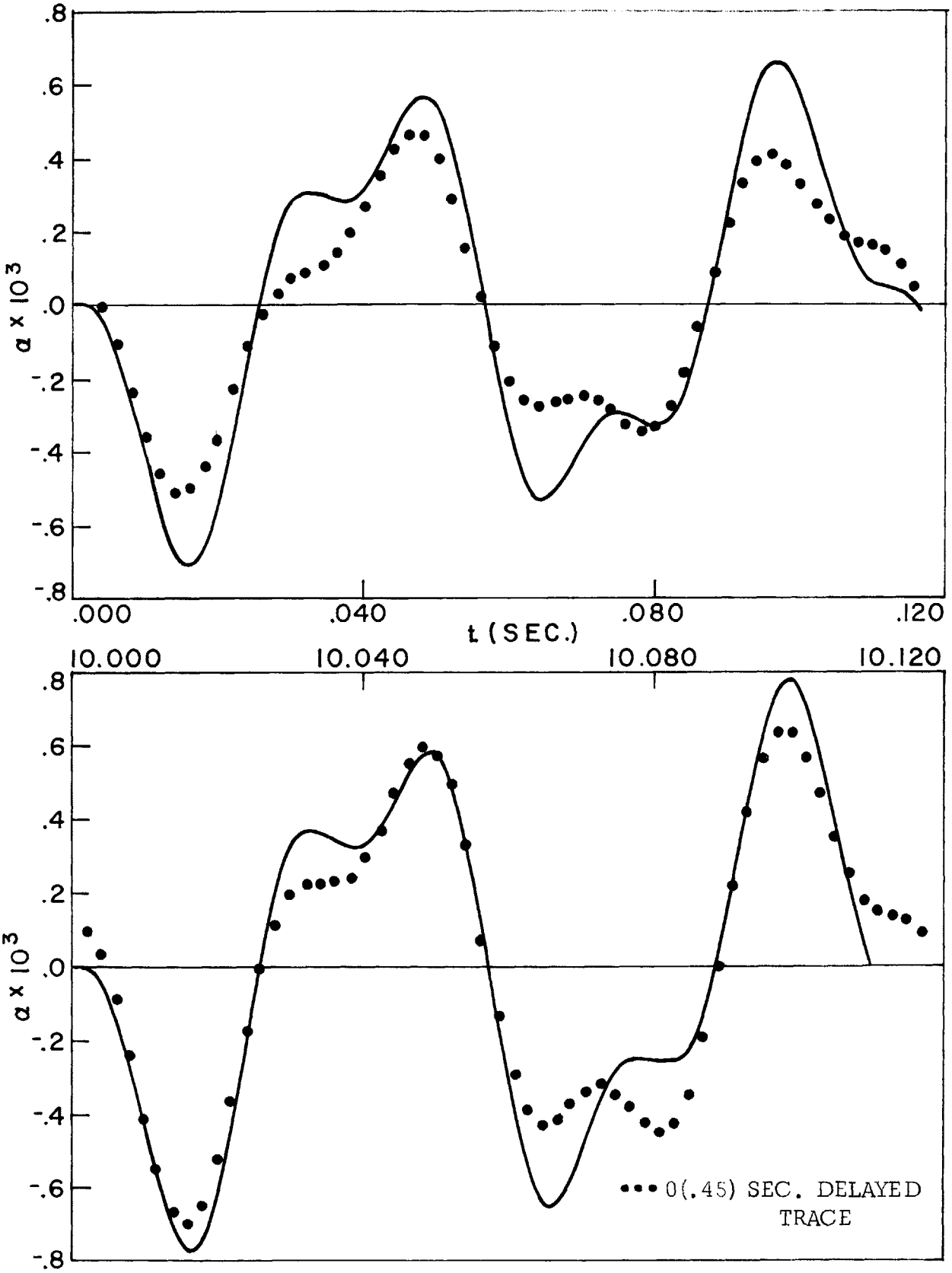


Fig. 55 $\alpha$ Time History Due to Case 1 Initial Conditions Applied at t = 0 and 10 Seconds Compared with Itself Approximately .45 Seconds Later; ng = 9g

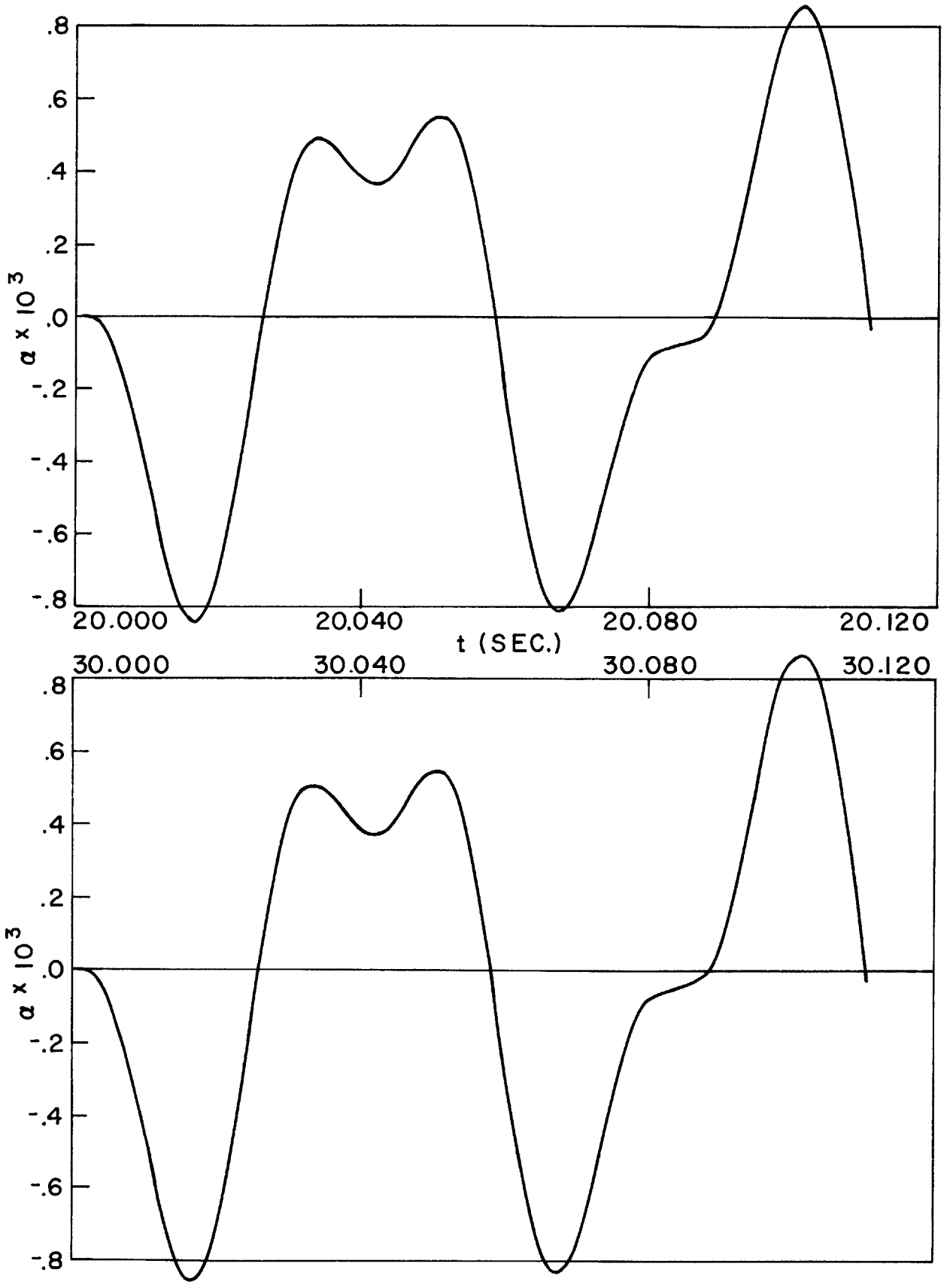


Fig. 56 $\alpha$ Time History Due to Case 1 Initial Conditions Applied at t = 20 and 30 Seconds; ng = 9g

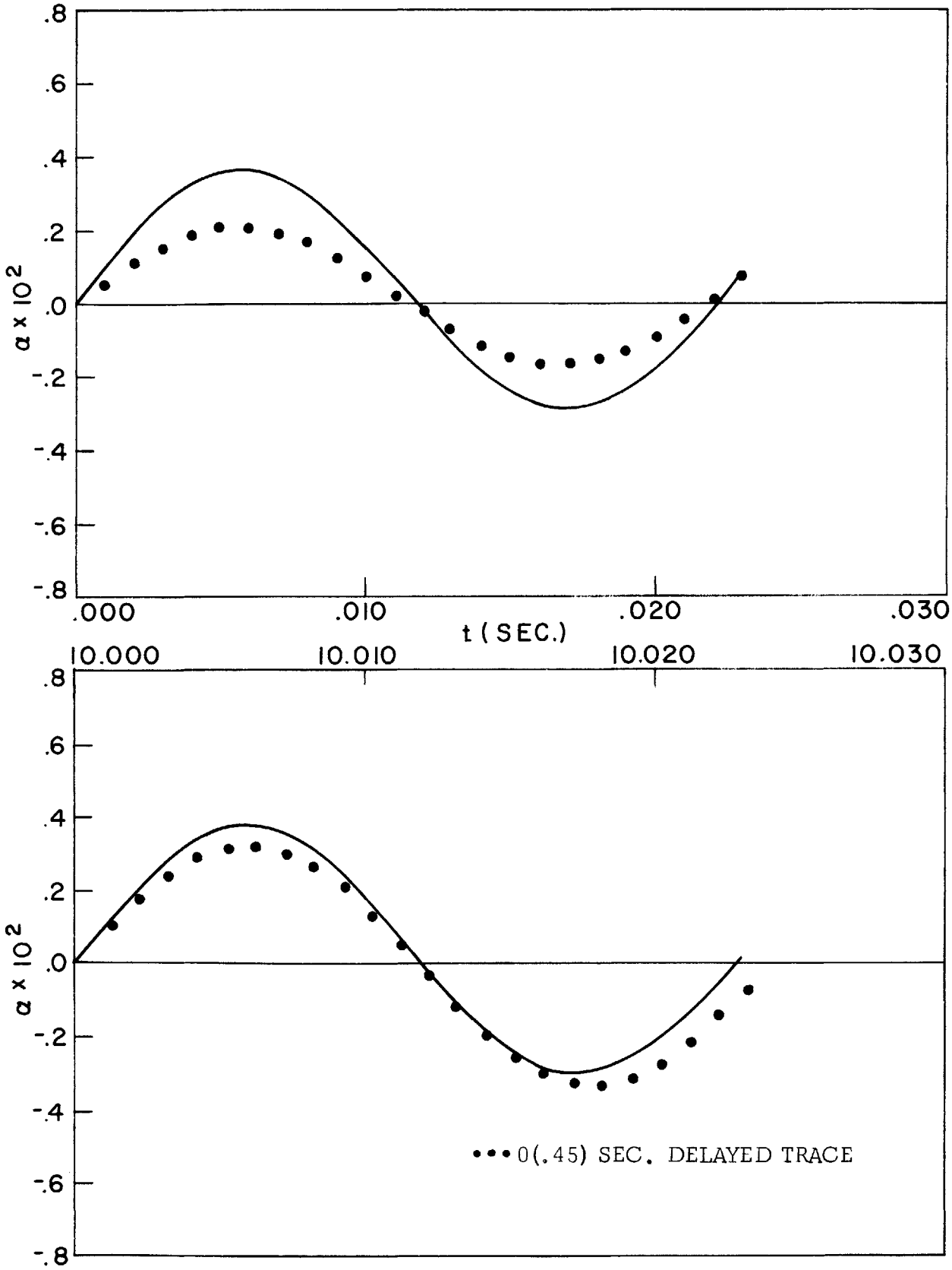


Fig. 57 $\alpha$ Time History Due to Case 2 Initial Conditions Applied at t = 0 and 10 Seconds Compared with Itself Approximately .45 Seconds Later; ng = 9g

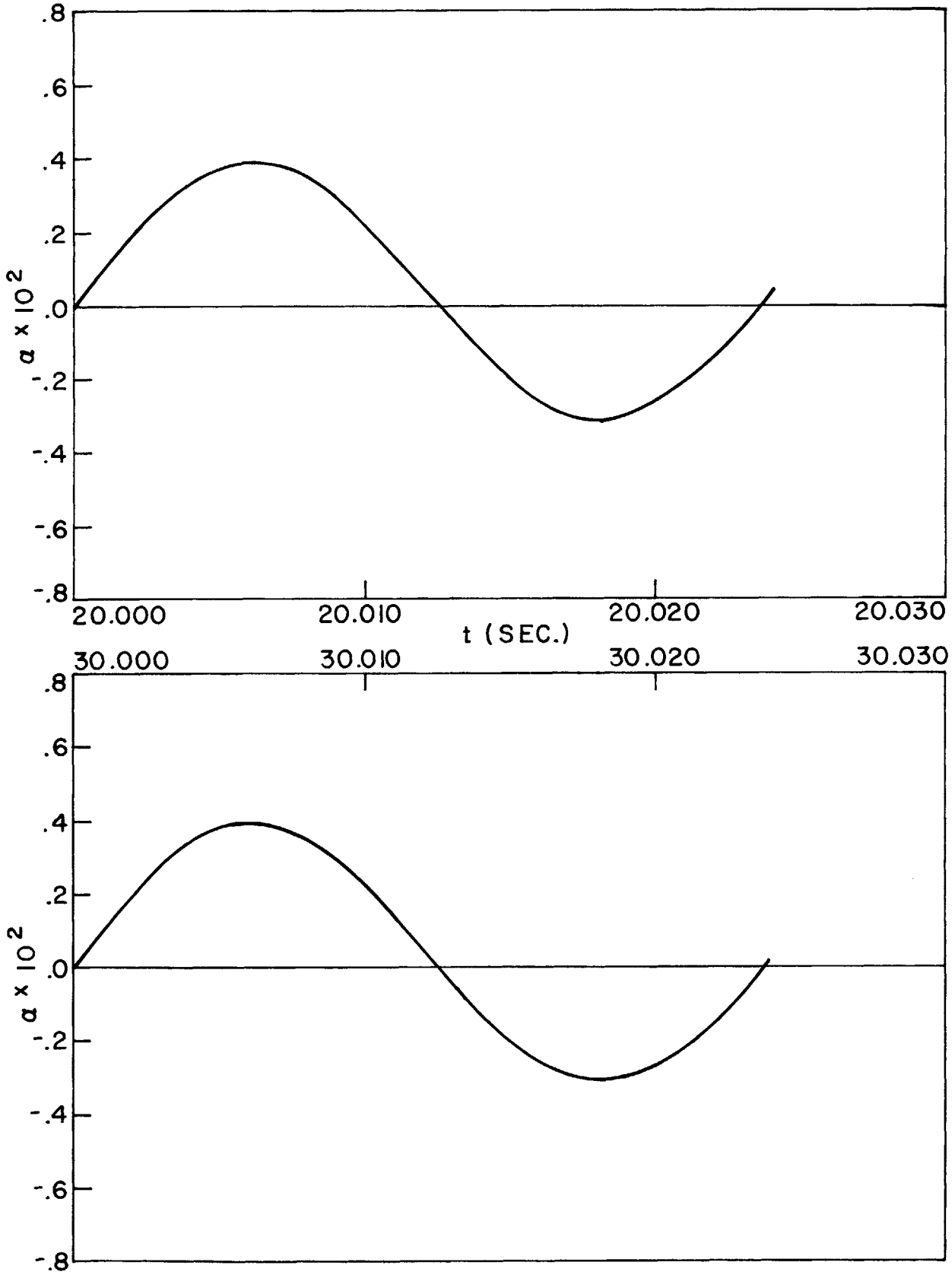


Fig. 58 $\alpha$ Time History Due to Case 2 Initial Conditions Applied at t = 20 and 30 Seconds; ng = 9g

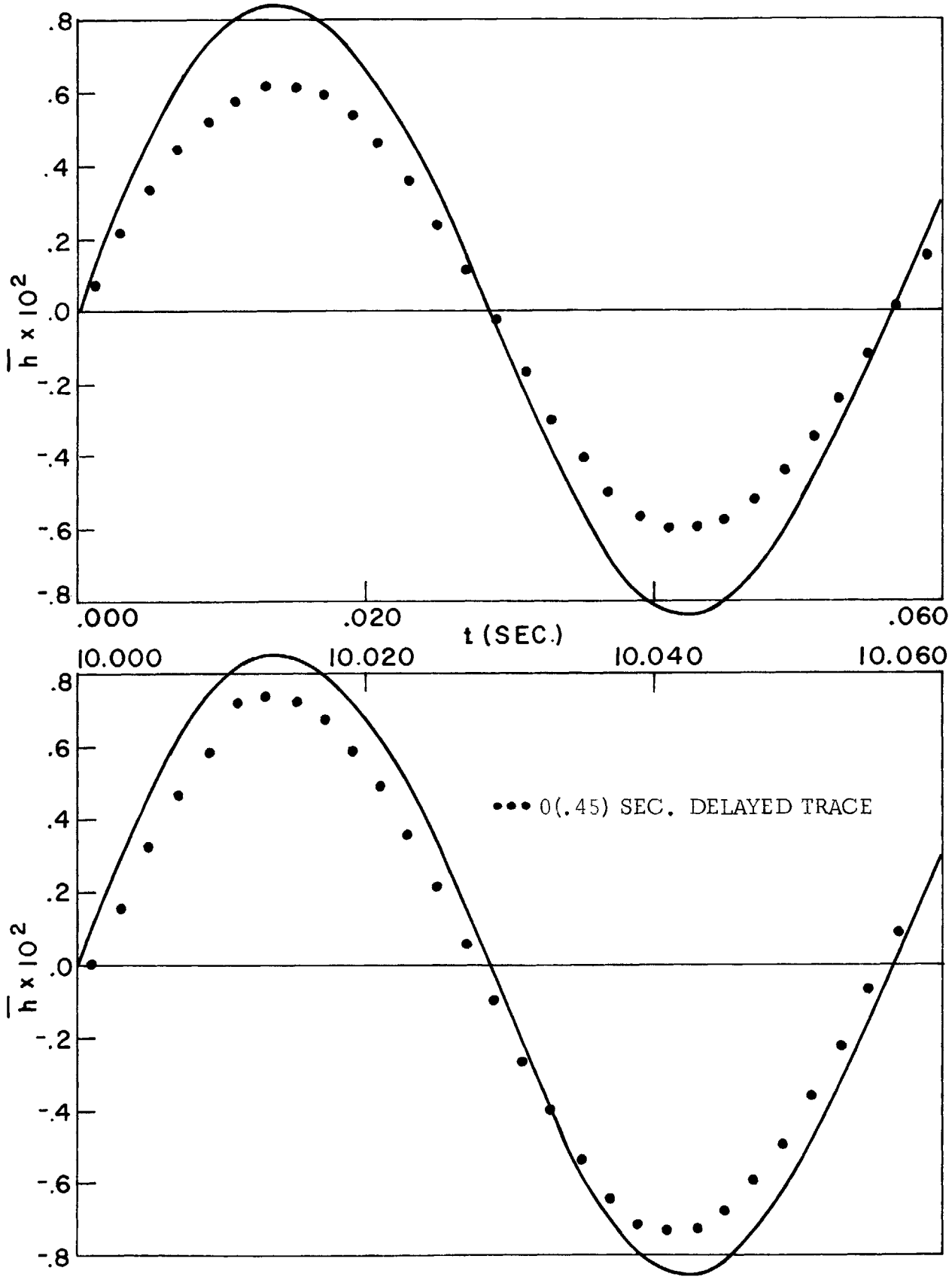


Fig. 59 $\bar{h}$ Time History Due to Case i Initial Conditions Applied at t = 0 and 10 Seconds Compared with Itself Approximately .45 Seconds Later; ng = 270 (1-cos.2513t)

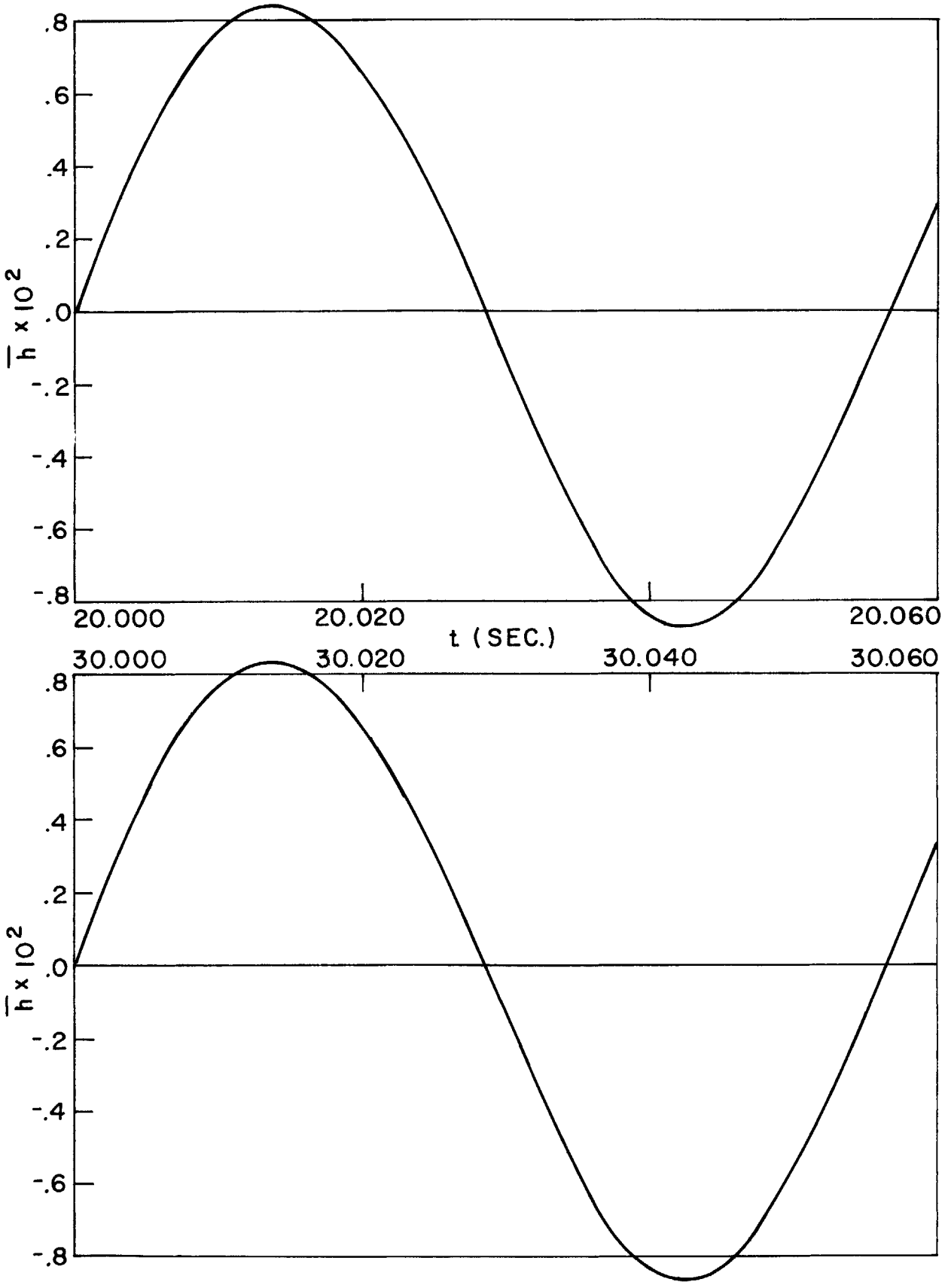


Fig. 60 $\bar{h}$ Time History Due to Case 1 Initial Conditions Applied at t = 20 and 30 Seconds; ng = 270 (1-cos.2513t)

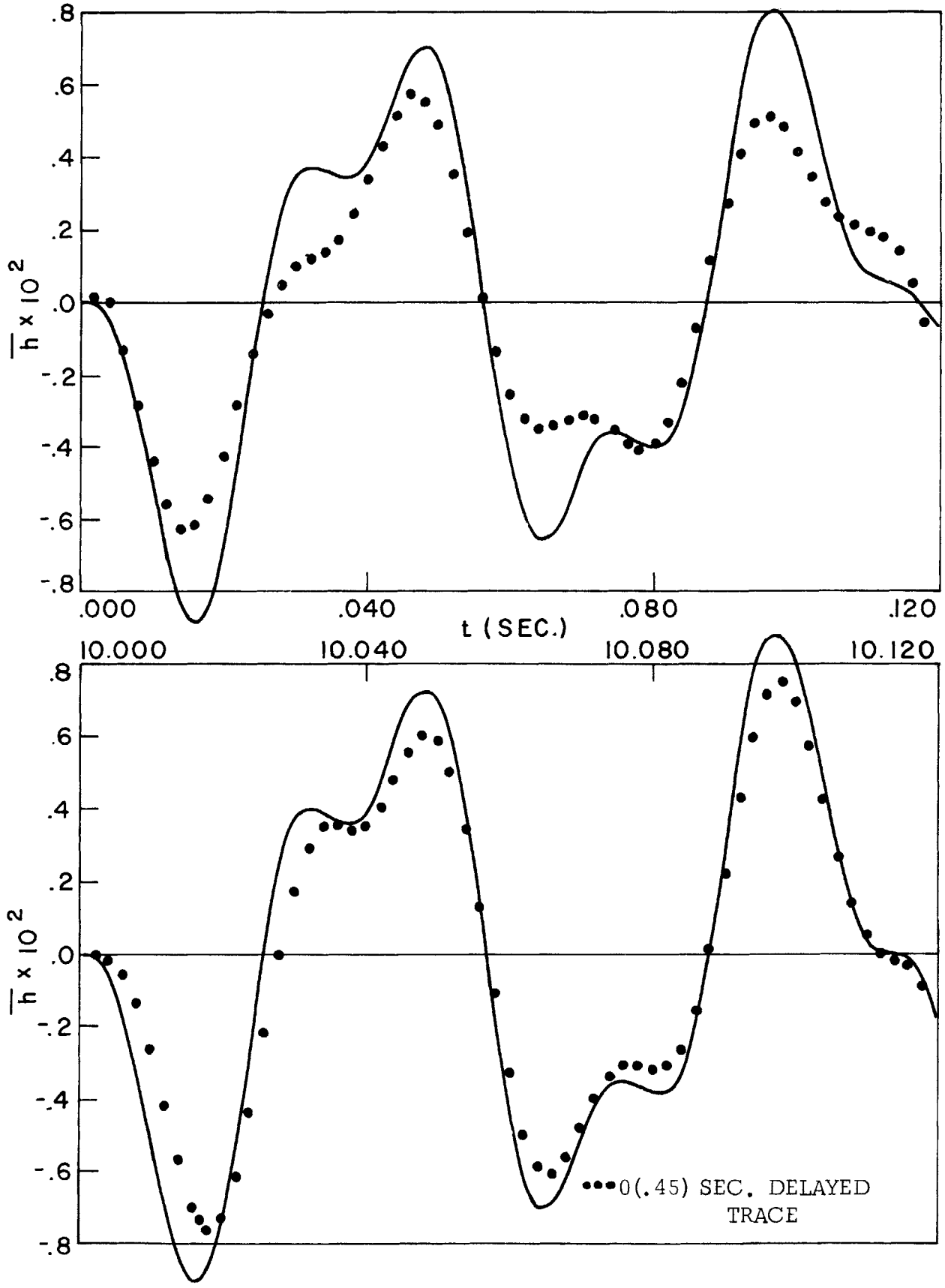


Fig. 61 $\bar{h}$ Time History Due to Case 2 Initial Conditions Applied at t = 0 and 10 Seconds Compared with Itself Approximately .45 Seconds Later; ng = 270 (1-cos.2513t)

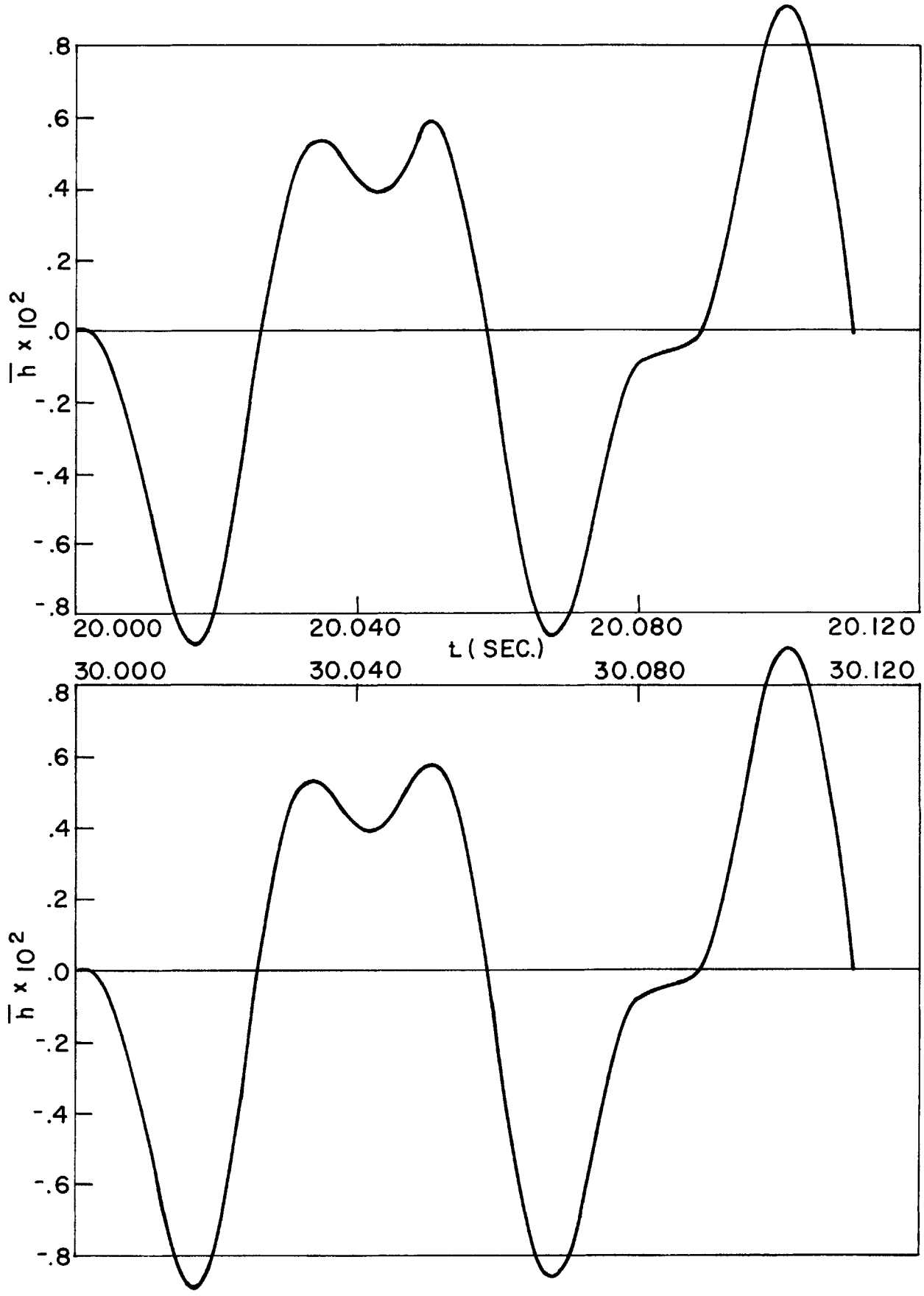


Fig. 62 $\bar{h}$ Time History Due to Case 2 Initial Conditions Applied at t = 20 and 30 Seconds; ng = 270 (1-cos.2513t)

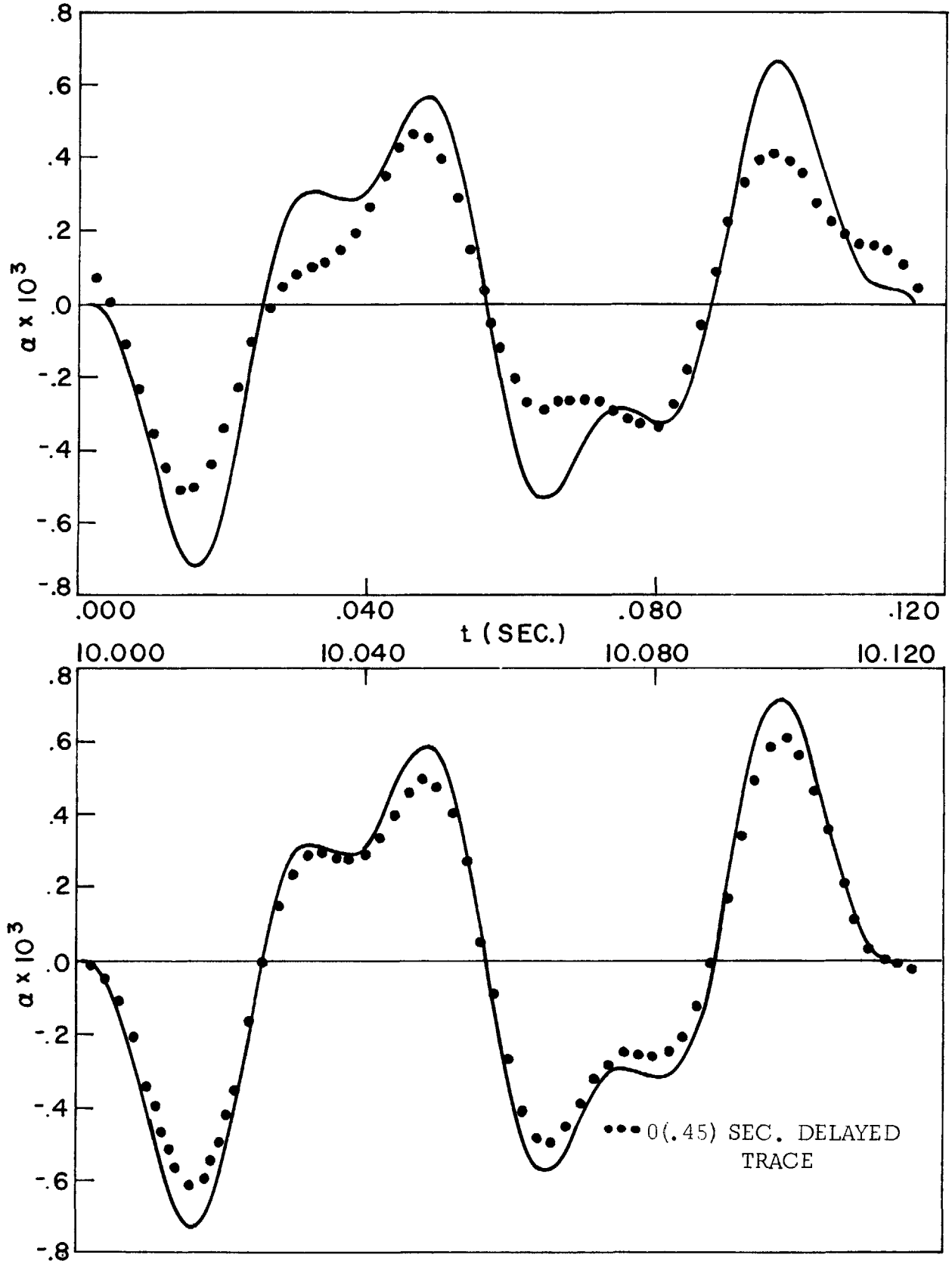


Fig. 63 $\alpha$ Time History Due to Case 1 Initial Conditions Applied at t = 0 and 10 Seconds Compared with Itself Approximately .45 Seconds Later; ng = 270 (1-cos.2513t)

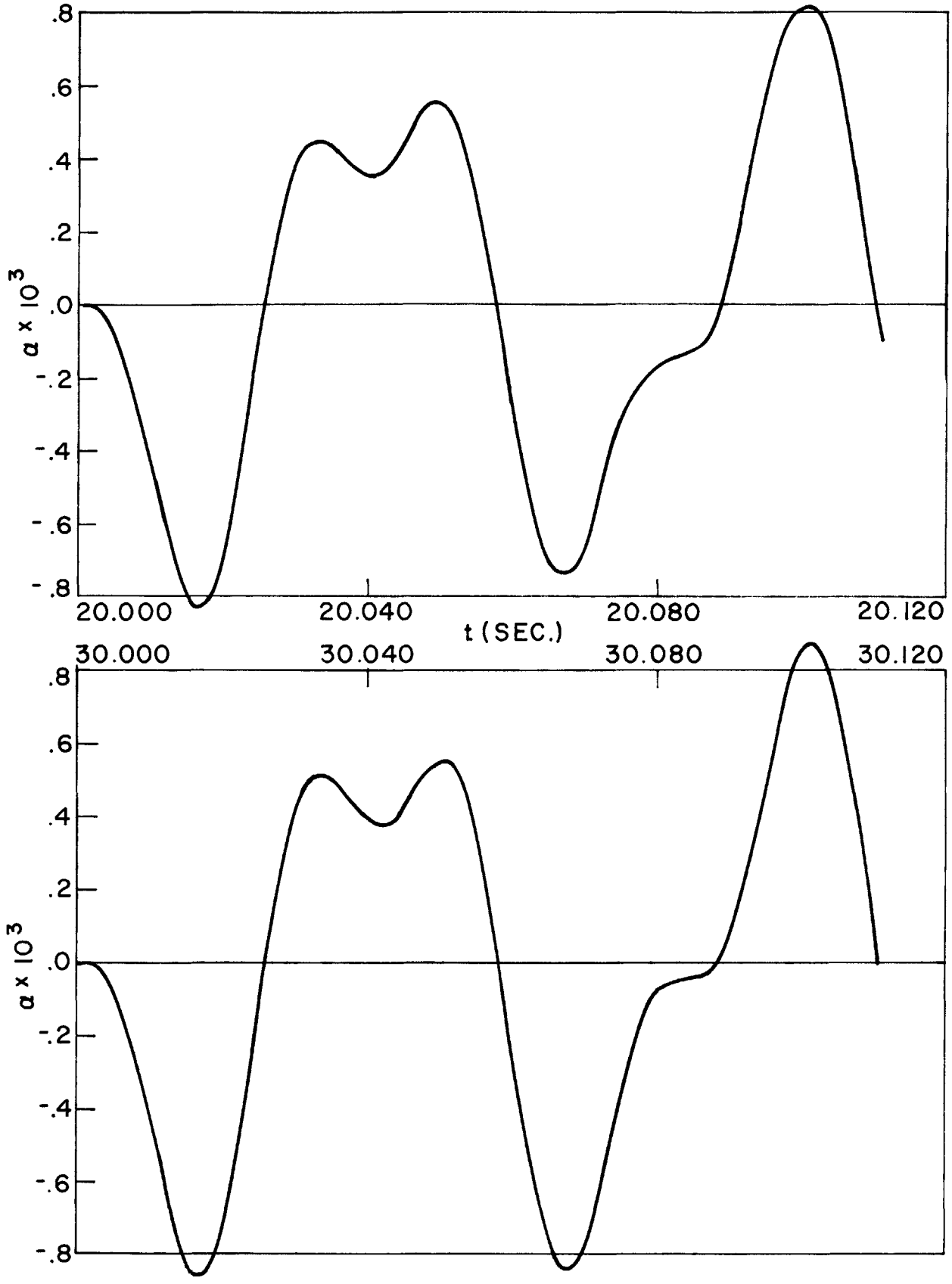


Fig. 64 $\alpha$ Time History Due to Case 1 Initial Conditions Applied at t = 20 and 30 Seconds; $n_g$ = 270 (1-cos.2513t)

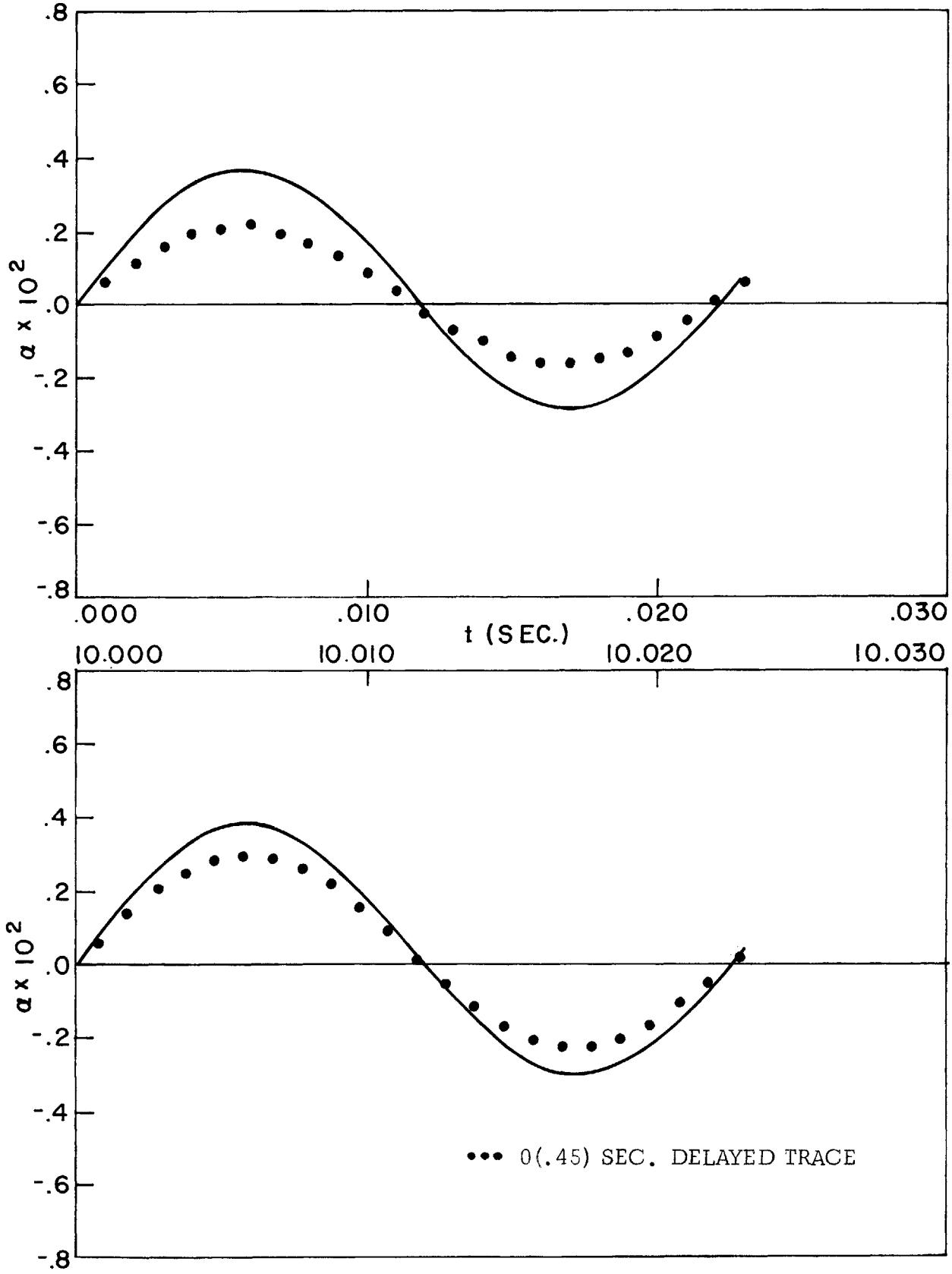


Fig. 65 $\alpha$ Time History Due to Case 2 Initial Conditions Applied at t = 0 and 10 Seconds Compared with Itself Approximately .45 Seconds Later; ng = 270 (1-cos.2513t)

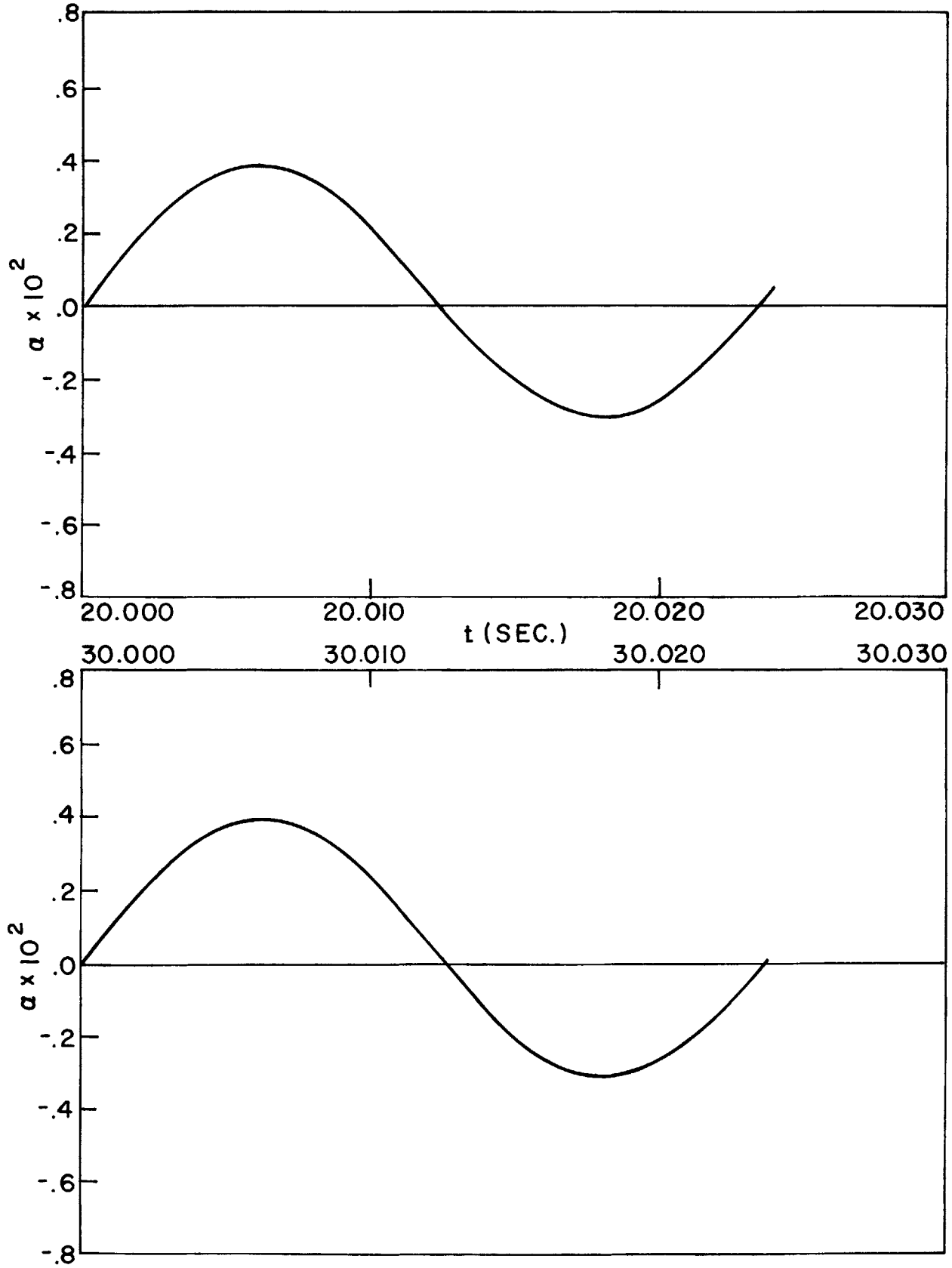


Fig. 66 $\alpha$ Time History Due to Case 2 Initial Conditions Applied at t = 20 and 30 Seconds; ng = 270 (1-cos.2513t)

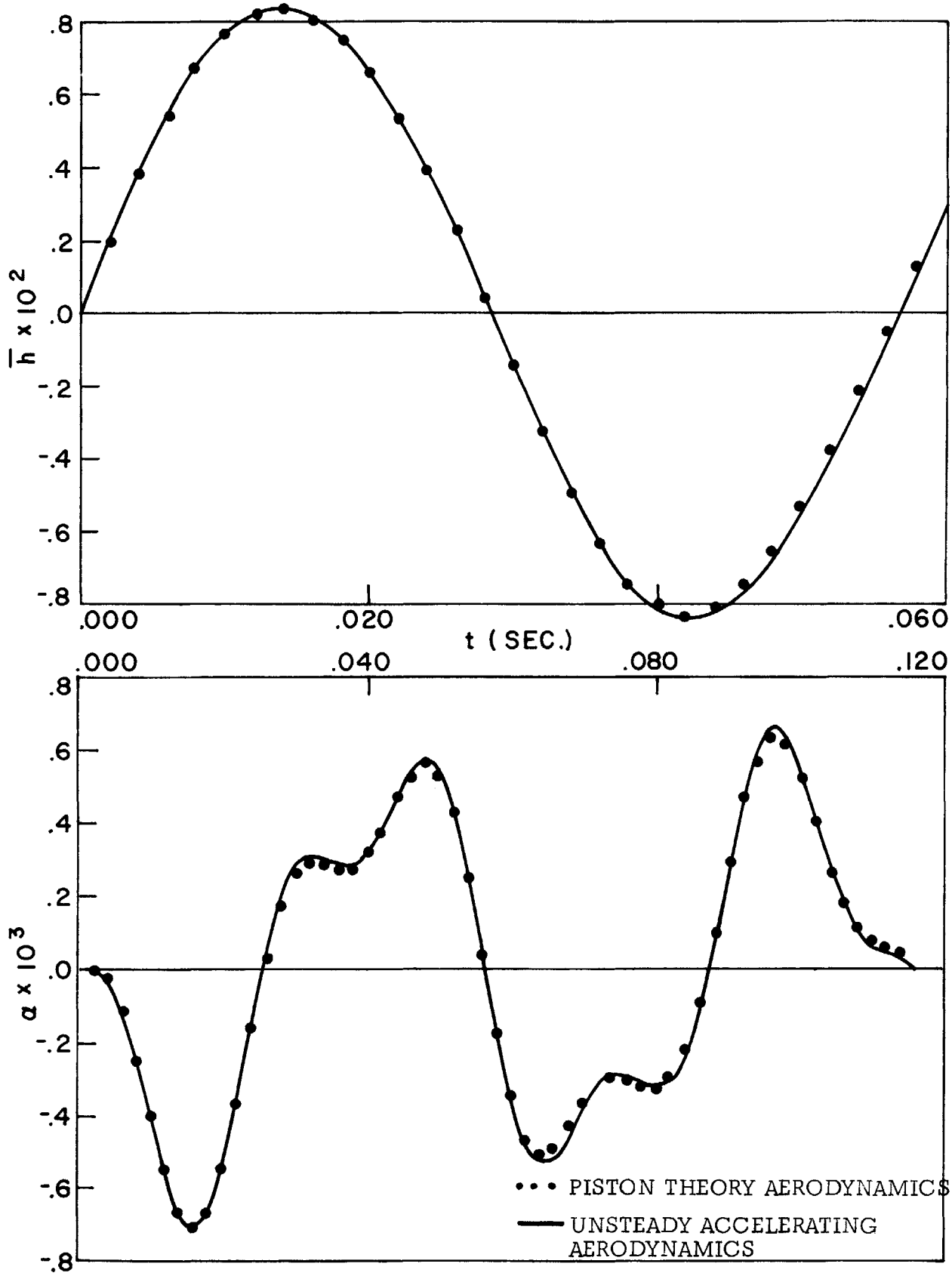


Fig. 67 $\bar{h}$ and $\alpha$ Time Histories Observed First at t = 0 Seconds Due to Case 1 Initial Conditions Applied at t = 0 Seconds; ng = 270 (1-cos.2513t)

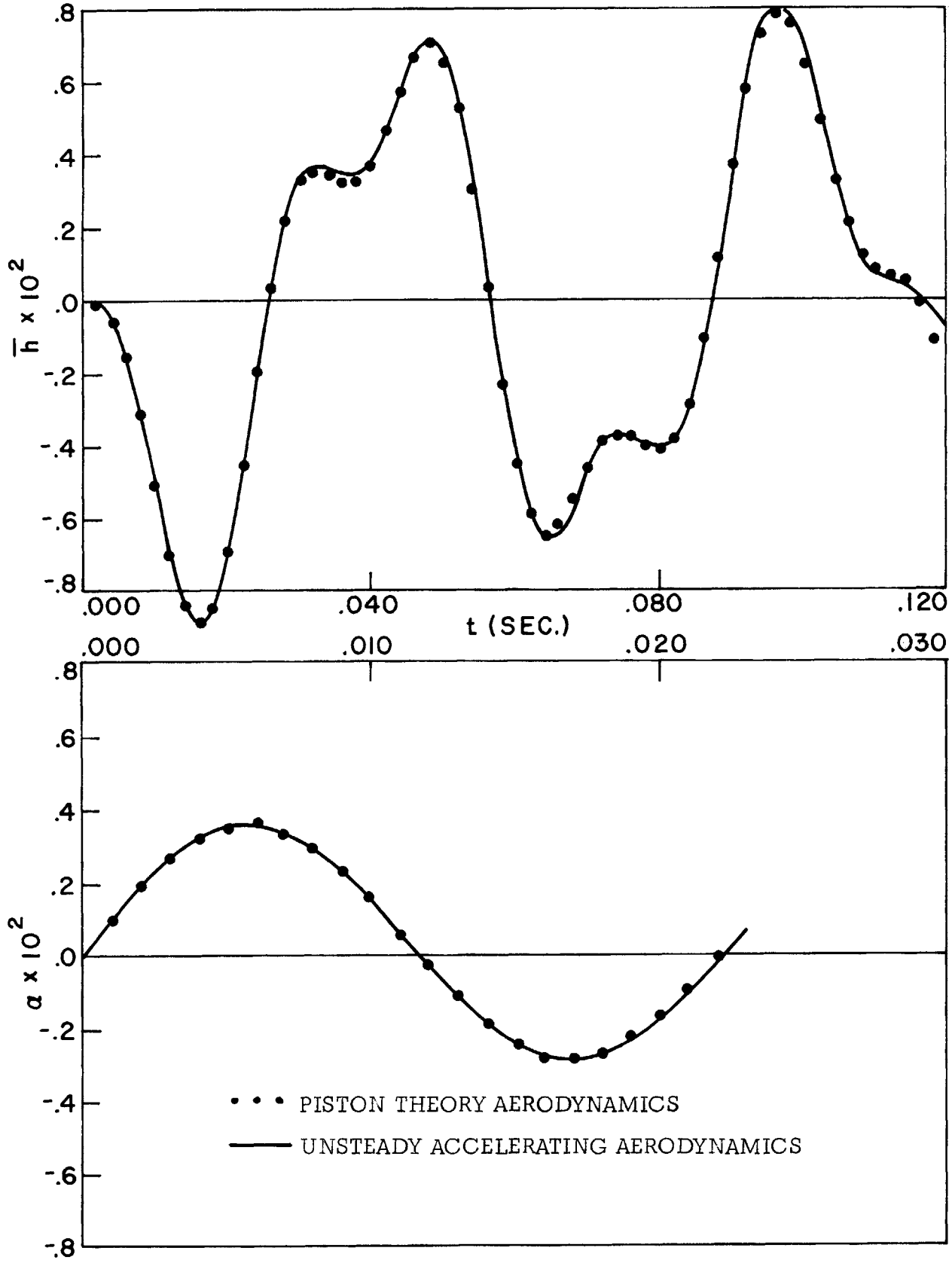


Fig. 68 $\bar{h}$ and $\alpha$ Time Histories Observed First at t = 0 Seconds Due to Case 2 Initial Conditions Applied at t = 0 Seconds; ng = 270 (1-cos.2513t)

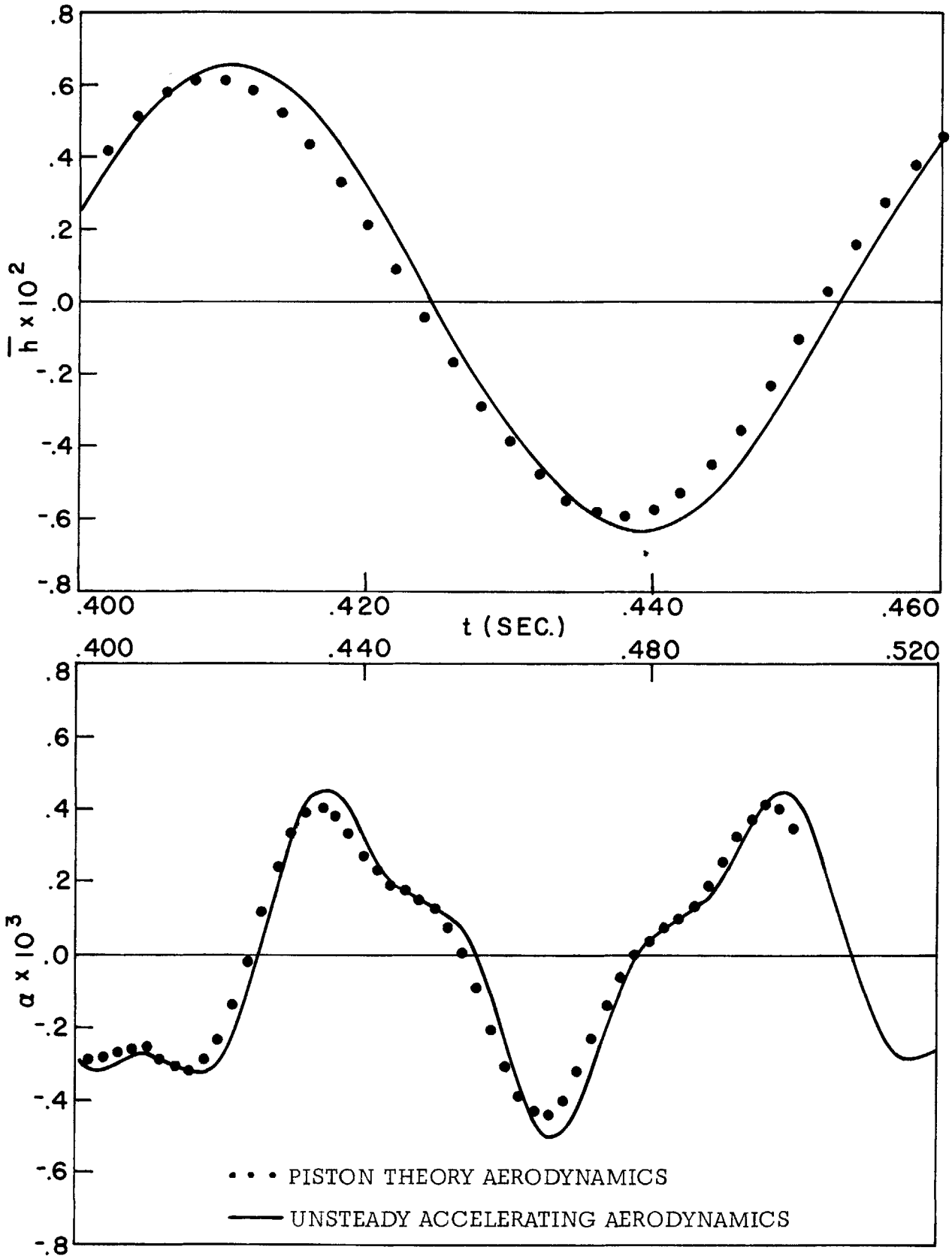


Fig. 69 $\bar{h}$ and $\alpha$ Time Histories Observed First at t = .4 Seconds Due to Case 1 Initial Conditions Applied at t = 0 Seconds; ng = 270 (1-cos.2513t)

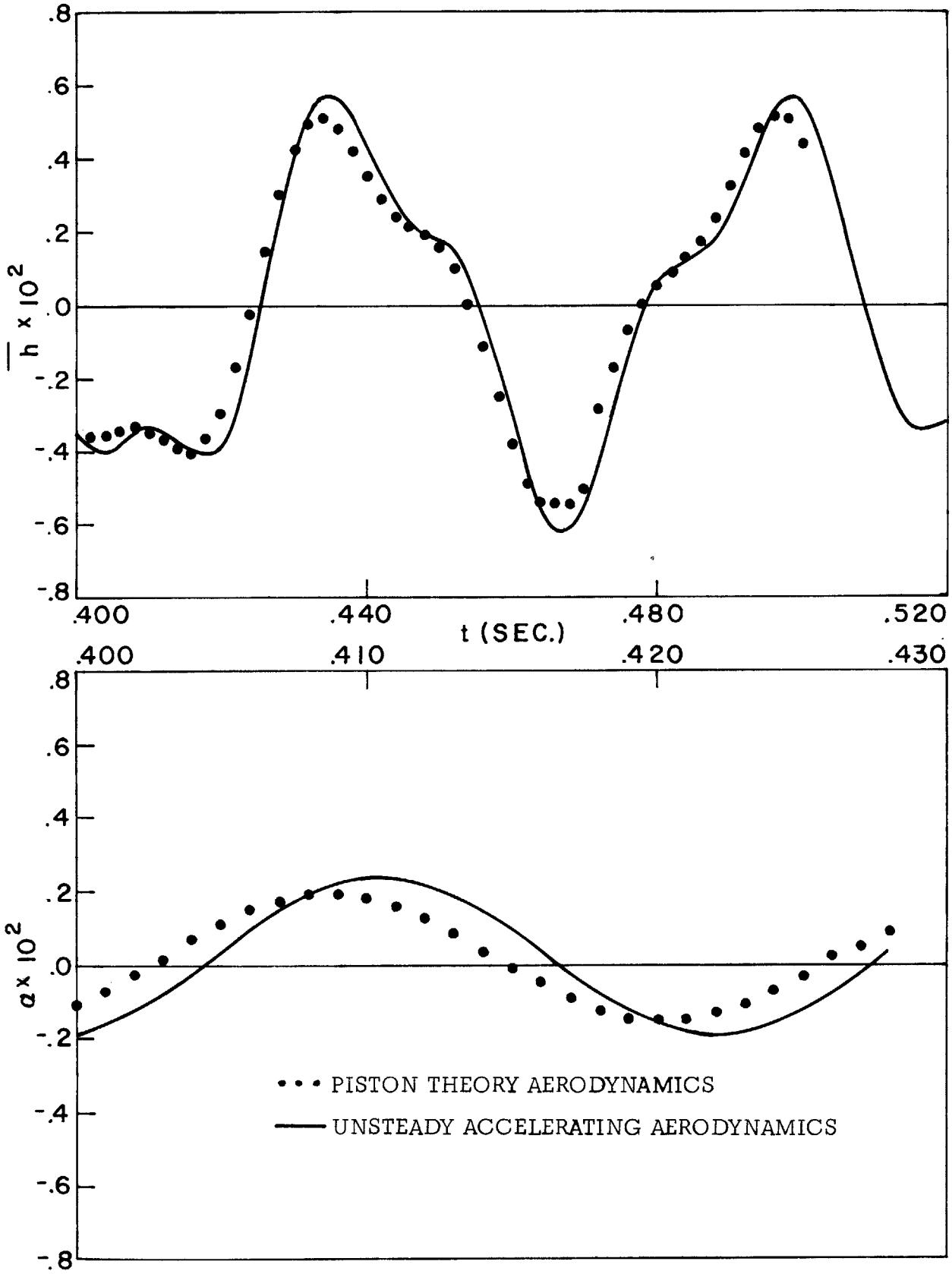


Fig. 70 $\bar{h}$ and $\alpha$ Time Histories Observed First at t = .4 Seconds Due to Case 2 Initial Conditions Applied at t = 0 Seconds; ng = 270 (1-cos.2513t)

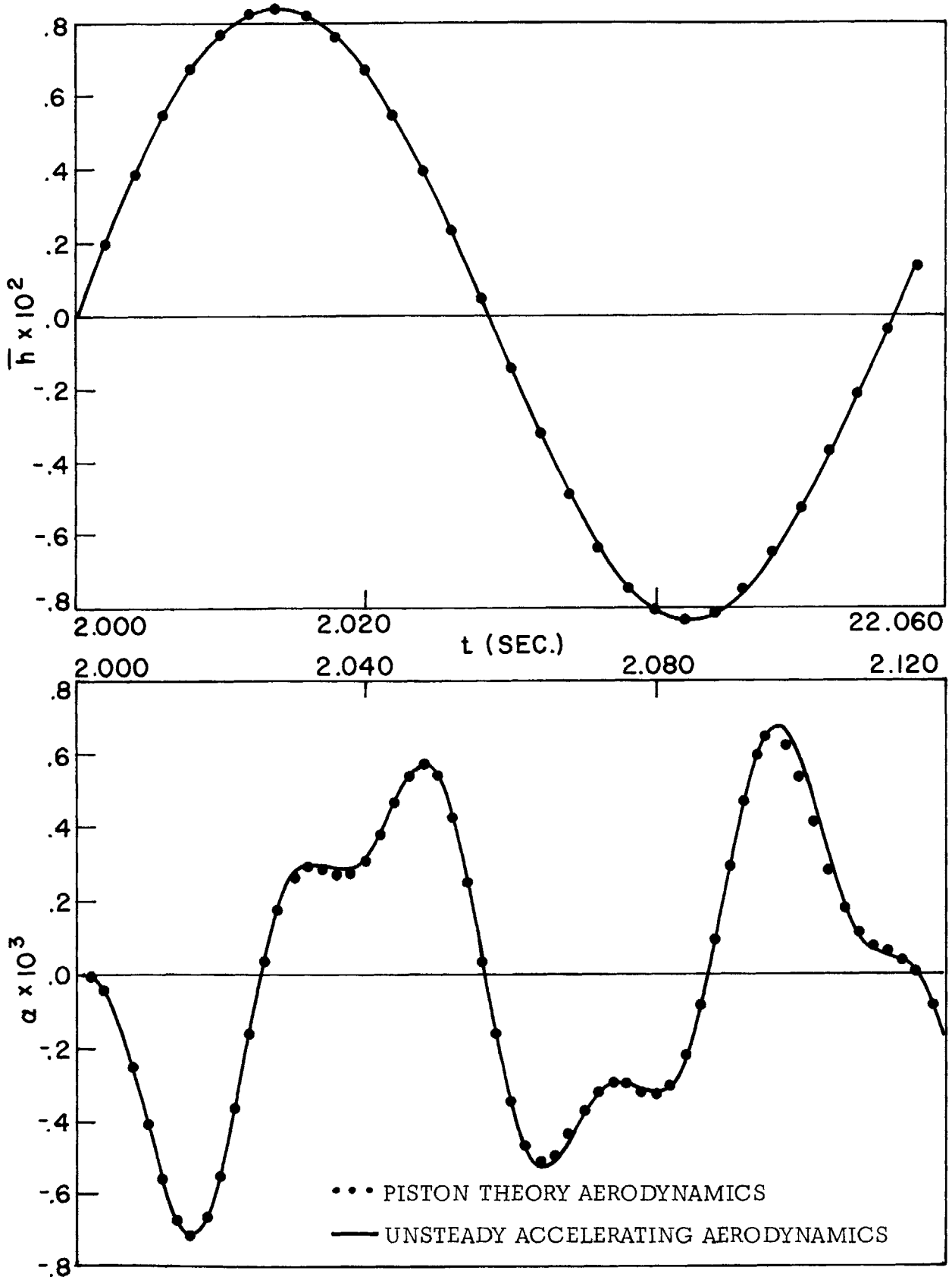


Fig. 71 $\bar{h}$ and $\alpha$ Time Histories Observed First at t = 2.0 Seconds Due to Case 1 Initial Conditions Applied at t = 2.0 Seconds; ng = 270 (1-cos.2513t)

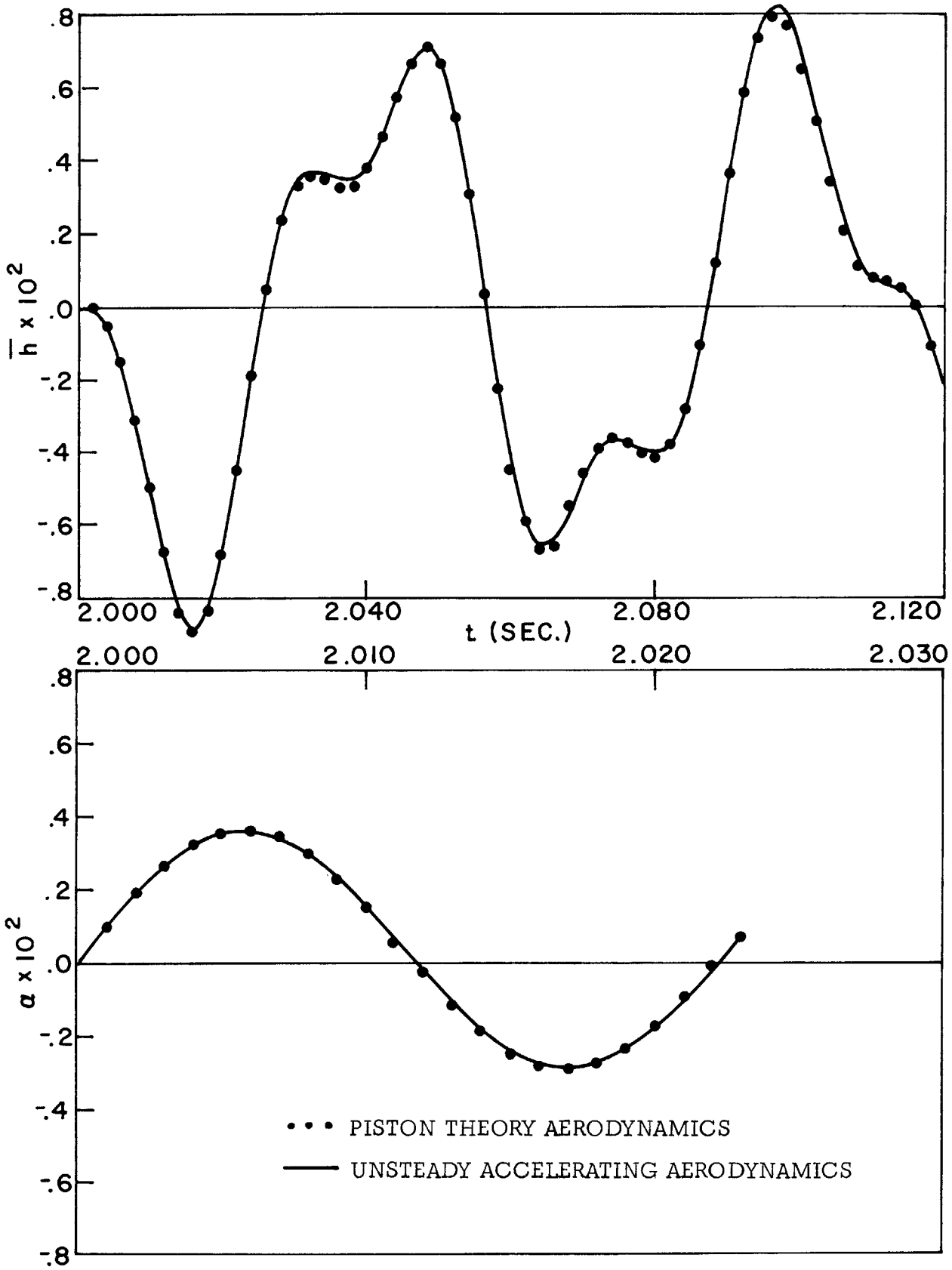


Fig. 72 $\bar{h}$ and $\alpha$ Time Histories Observed First at t = 2.0 Seconds Due to Case 2 Initial Conditions Applied at t = 2.0 Seconds; ng = 270 (1-cos.2513t)

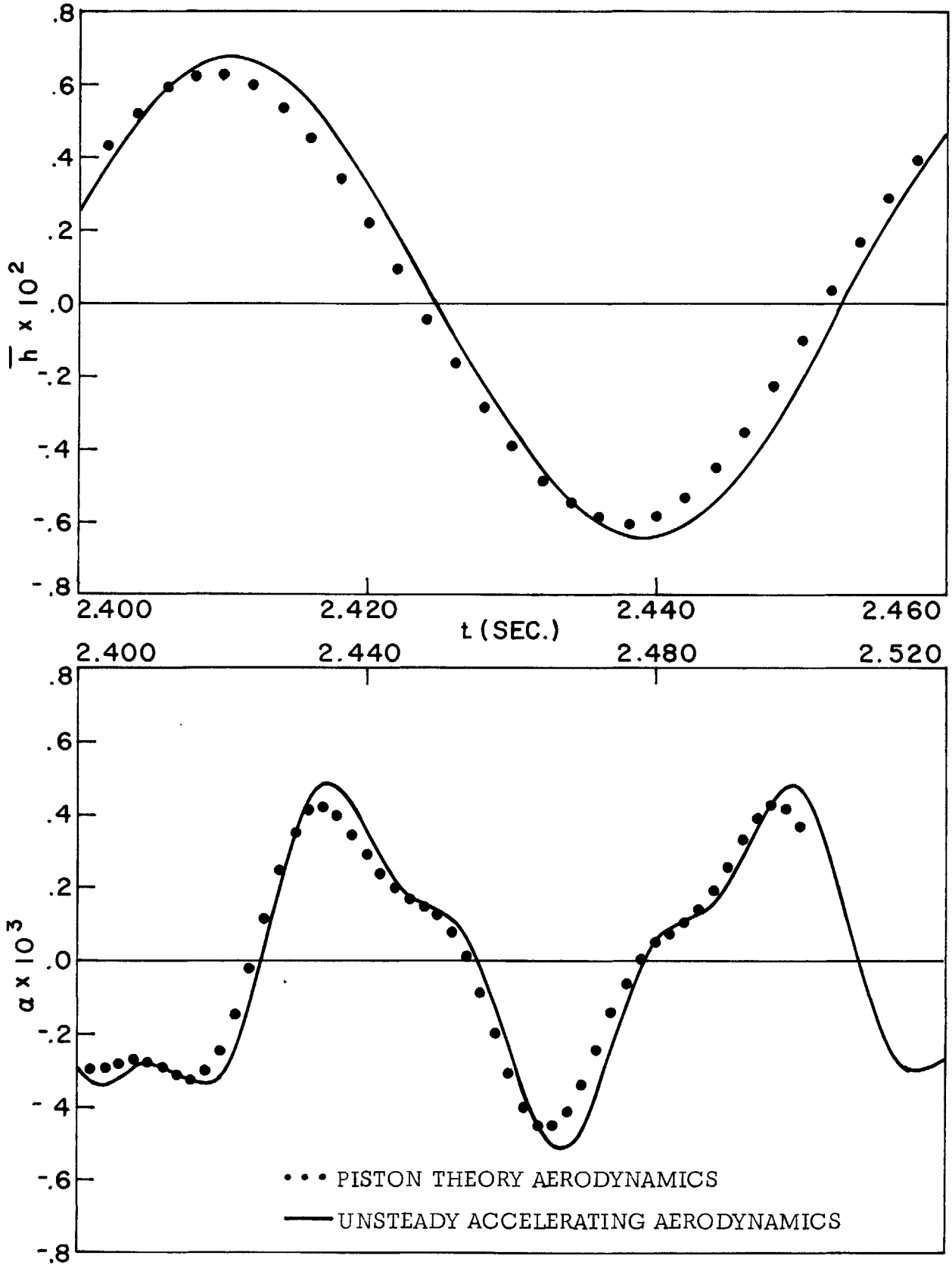


Fig. 73 $\bar{h}$ and $\alpha$ Time Histories Observed First at t = 2.4 Seconds Due to Case 1 Initial Conditions Applied at t = 2.0 Seconds; ng = 270 (1-cos.2513t)

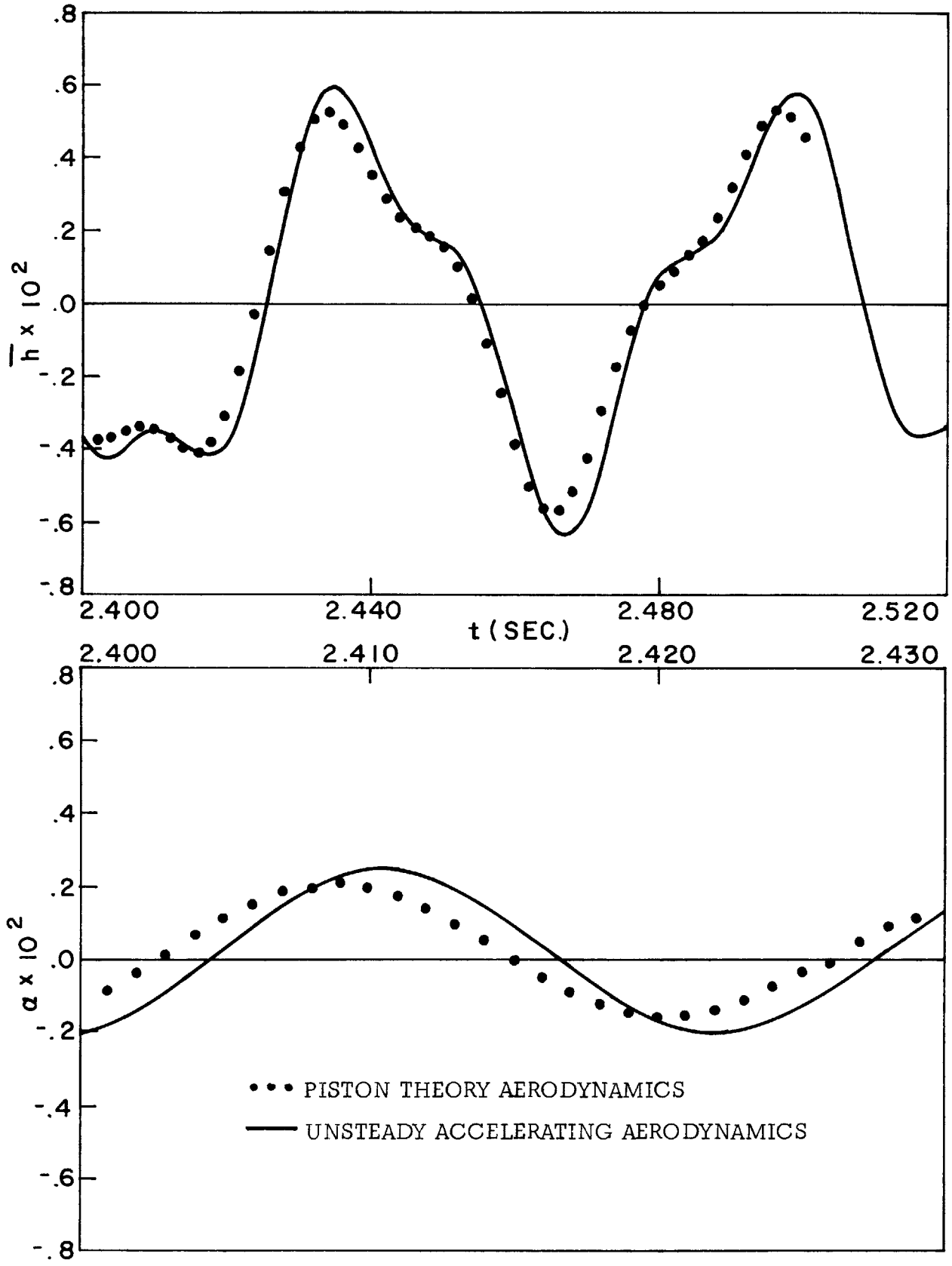


Fig. 74 $\bar{h}$ and $\alpha$ Time Histories Observed First at t = 2.4 Seconds Due to Case 2 Initial Conditions Applied at t = 2.0 Seconds; ng = 270 (1-cos.2513t)

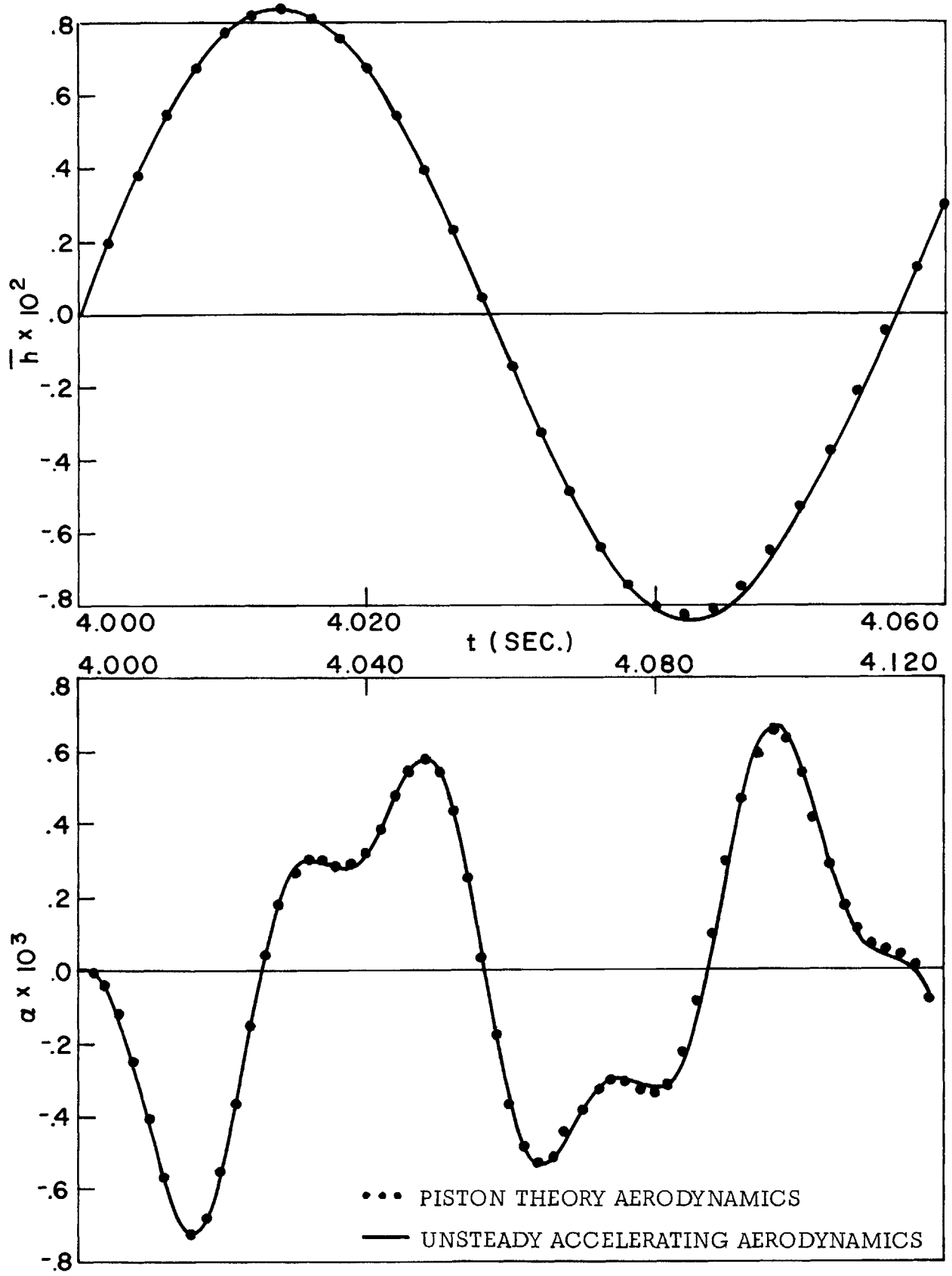


Fig. 75 $\bar{h}$ and $\alpha$ Time Histories Observed First at t = 4.0 Seconds Due to Case 1 Initial Conditions Applied at t = 4.0 Seconds; ng = 270 (1-cos.2513t)

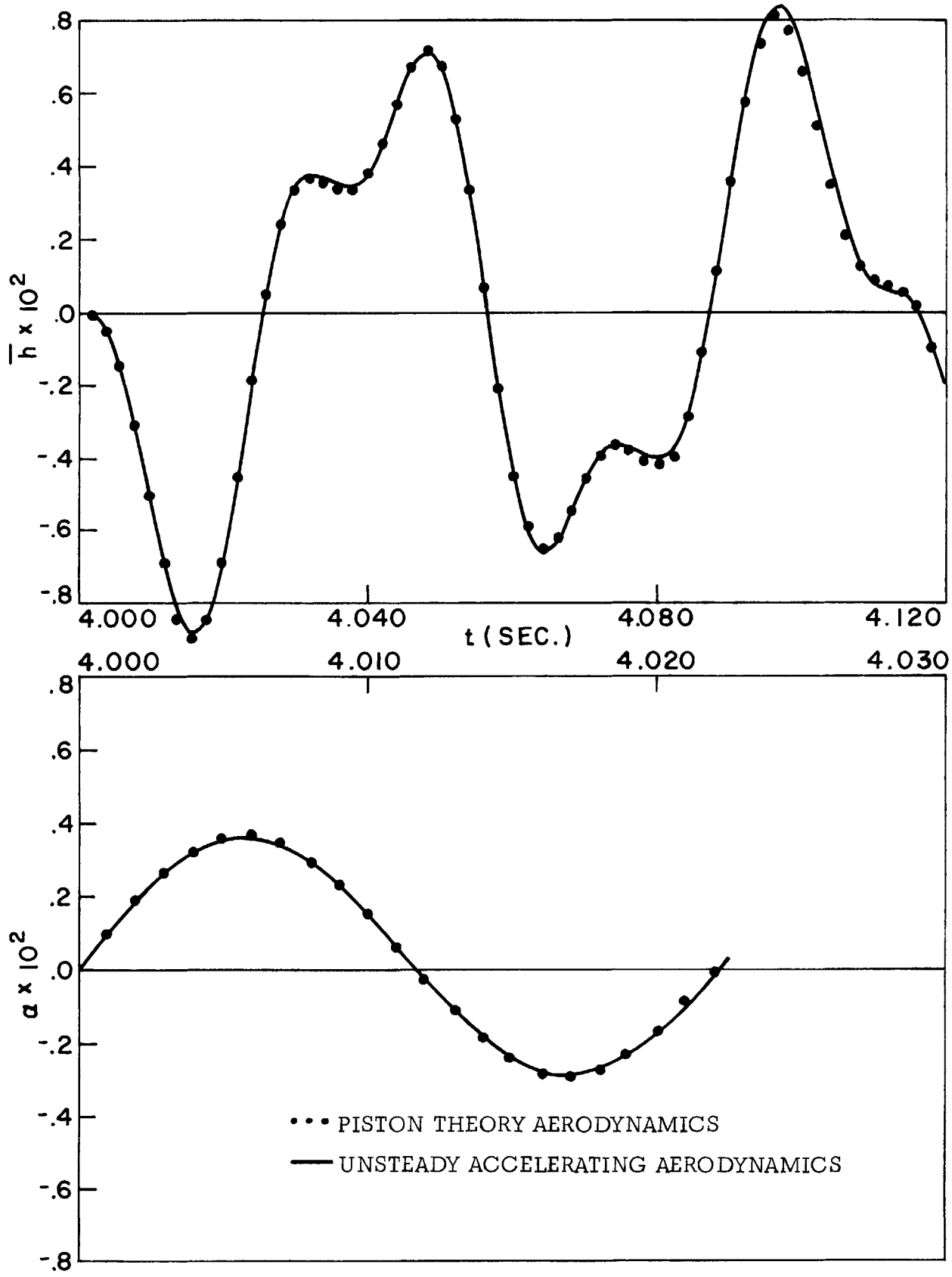


Fig. 76 $\bar{h}$ and $\alpha$ Time Histories Observed First at t = 4.0 Seconds Due to Case 2 Initial Conditions Applied at t = 4.0 Seconds; ng = 270 (1-cos.2513t)

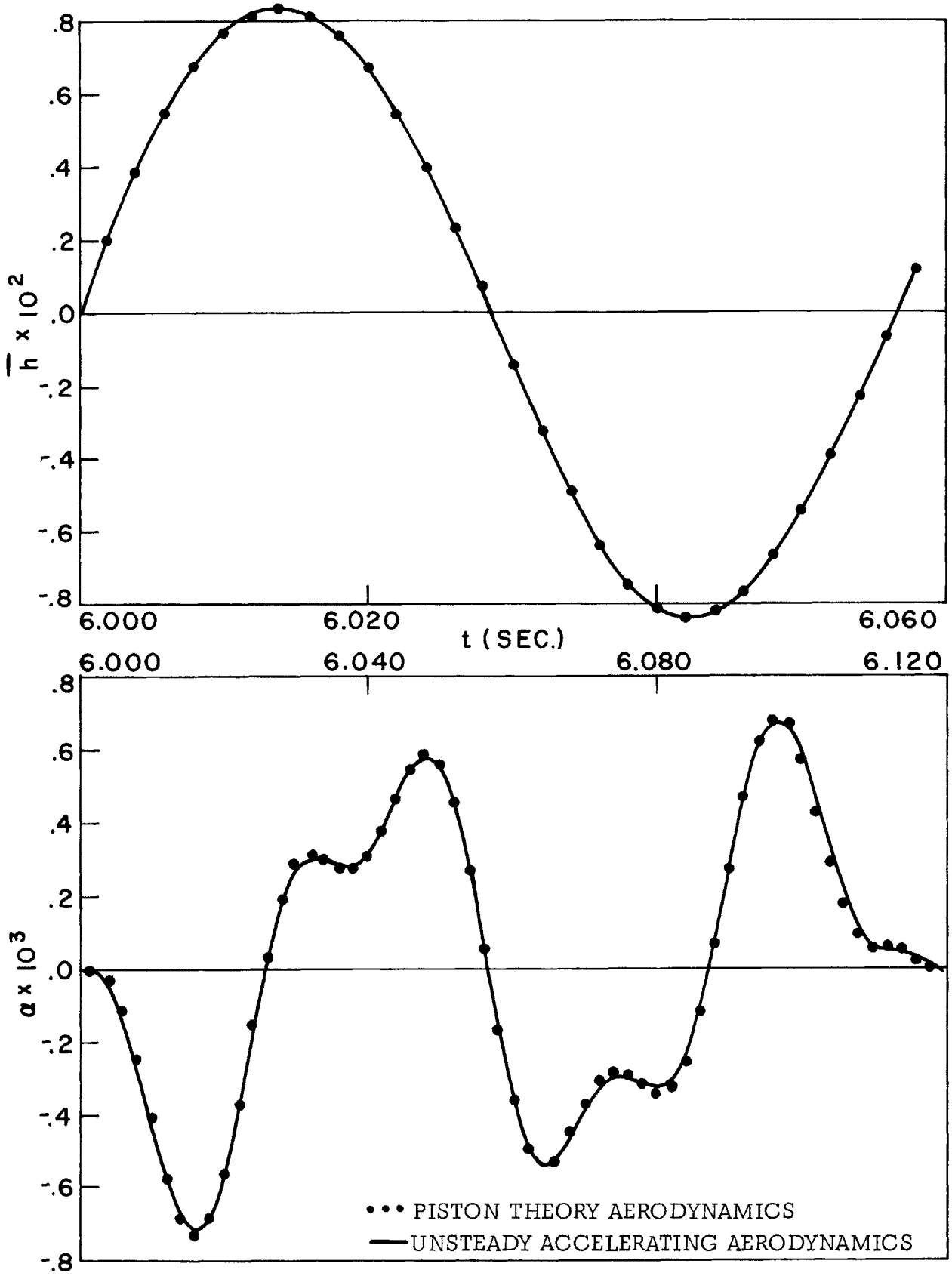


Fig. 77 $\bar{h}$ and $\alpha$ Time Histories Observed First at t = 6.0 Seconds Due to Case 1 Initial Conditions Applied at t = 6.0 Seconds; ng = 270 (1-cos.2513t)

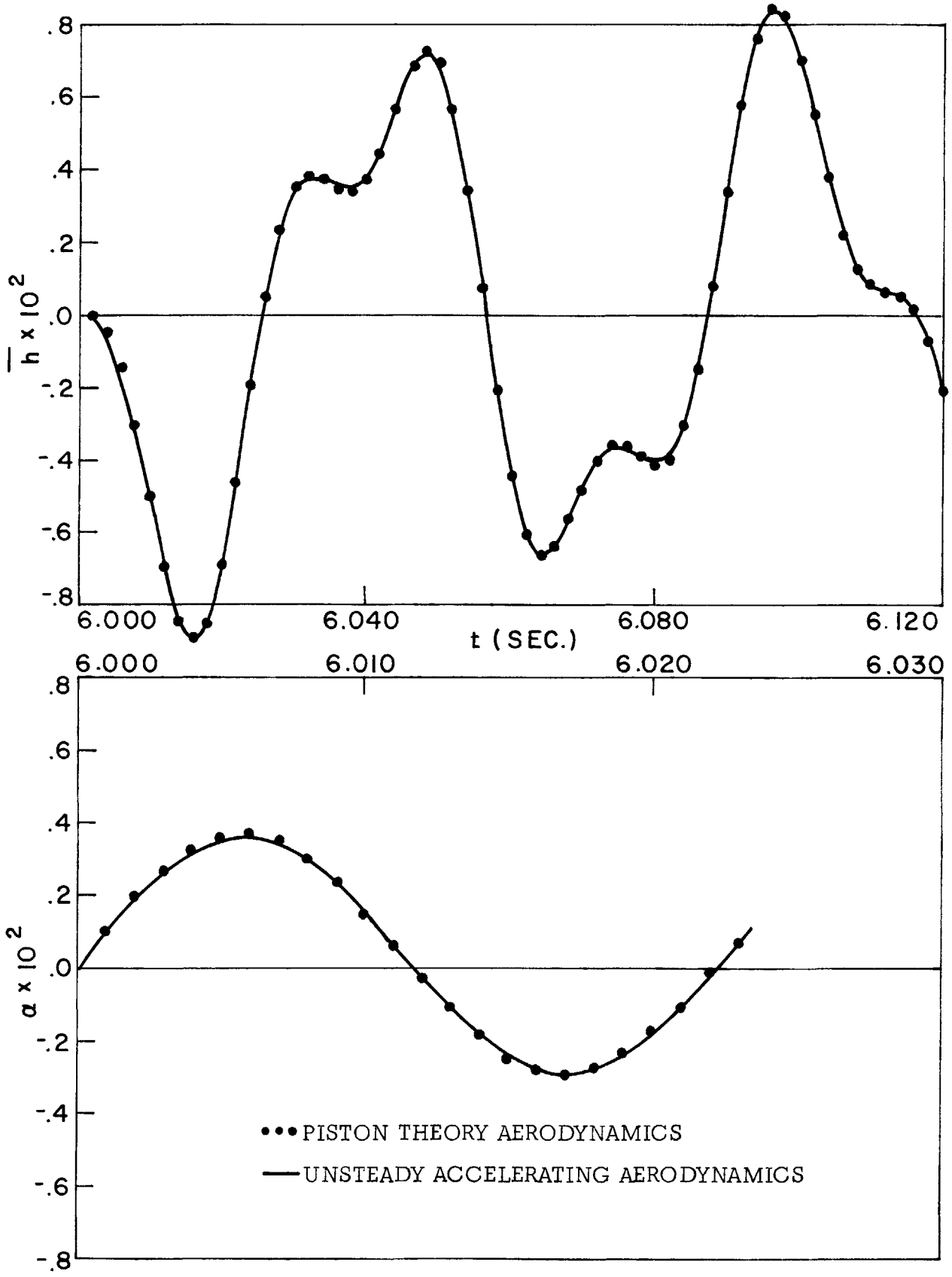


Fig. 78 $\bar{h}$ and $\alpha$ Time Histories Observed First at t = 6.0 Seconds Due to Case 2 Initial Conditions Applied at t = 6.0 Seconds; ng = 270 (1-cos.2513t)

Table 1 Comparison of Exact and Zero-Damping Flutter and Divergence Calculation

| CASE | $X_o$ | $X_\alpha$ | $U_{F_{exact}}$ (ft/sec) | $U_{F_{zero\text{-}damping}}$ (ft/sec) | $(\omega_F/\omega_\alpha)_{exact}$ | $(\omega_F/\omega_\alpha)_{zero\text{-}damping}$ | $U_{D_{exact}}$ (ft/sec) | $U_{D_{zero\text{-}damping}}$ (ft/sec) |
|---|---|---|---|---|---|---|---|---|
| 1 | .40 | .10 | ∞ | ∞ | ∞ | ∞ | ∞ | ∞ |
| 2 | .40 | .20 | 2844 | 3526 | .81 | .85 | ∞ | ∞ |
| 3 | .40 | .30 | 1852 | 2821 | .84 | .88 | ∞ | ∞ |
| 4 | .55 | -.30 | ∞ | 3080 | ∞ | .73 | 6990 | ∞ |
| 5 | .55 | -.20 | ∞ | ∞ | ∞ | ∞ | 6880 | ∞ |
| 6 | .55 | -.10 | ∞ | 4555 | ∞ | .80 | 6612 | ∞ |
| 7 | .55 | .00 | 3075 | 1193 | .74 | .74 | 6329 | ∞ |
| *8 | .55 | .10 | 1209 | 781 | .74 | .73 | ∞ | ∞ |
| *9 | .55 | .20 | 865 | 800 | .74 | .76 | ∞ | ∞ |
| *10 | .55 | .30 | 855 | 1103 | .74 | .81 | ∞ | ∞ |

*Piston theory not applicable for these cases when $\gamma \cong 1.4$

Table 2 Comparison of System Frequencies (cycles/sec.) Obtained by Various Methods of Analysis Due to Case 1 Inputs for the Time Interval $0 \leq t_o \leq 8$ Seconds; ng = 270 (1-cos.2513t)

| $t_o$ (sec) | $t_{ref}$ (sec) | $\bar{h}$ | | | $\alpha$ | | |
|---|---|---|---|---|---|---|---|
| | | Q.S. | P.T. | U.A.A. | Q.S. | P.T. | U.A.A. |
| 0 | 0 | 17.65 | 17.7 | 17.72 | 17.65 | 17.2 | 17.26 |
| 0 | 0.5 | | | 17.71 | | | 17.61 |
| 0 | 1.0 | | 17.7 | | | 17.7 | |
| 2 | 2.0 | 17.67 | 17.7 | 17.72 | 17.67 | 17.2 | 17.27 |
| 2 | 2.5 | | | 17.71 | | | 17.63 |
| 2 | 3.0 | | | 17.7 | | 17.7 | |
| 4 | 4.0 | 17.65 | 17.7 | 17.70 | 17.65 | 17.2 | 17.26 |
| 4 | 4.5 | | | 17.70 | | | 17.59 |
| 4 | 5.0 | | 17.7 | | | 17.7 | |
| 6 | 6.0 | 17.65 | 17.7 | 17.66 | 17.65 | 17.2 | 17.16 |
| 6 | 6.5 | | | 17.65 | | | 17.62 |
| 6 | 7.0 | | 17.6 | | | 17.7 | |
| 8 | 8.0 | 17.63 | 17.6 | 17.65 | 17.63 | 17.2 | 17.14 |
| 8 | 8.5 | | | 17.64 | | | 17.61 |
| 8 | 9.0 | | 17.6 | | | 17.7 | |

Q.S. = Quasi-Steady
P.T. = Piston Theory with time-varying coefficients
U.A.A. = Unsteady Accelerating Aerodynamics with time-varying coefficients

Table 3 Comparison of System Frequencies (cycles/second) Obtained by Various Methods of Analysis Due to Case 1 Inputs for the Time Interval $10 \leq t_o \leq 30$ Seconds; ng = 270 (1-cos.2513t)

| $t_o$ (sec) | $t_{ref}$ (sec) | $\bar{h}$ | | $\alpha$ | |
|---|---|---|---|---|---|
| | | Q.S. | P.T. | Q.S. | P.T. |
| 10 | 10.0 | 17.62 | 17.6 | 17.62 | 17.5 |
| 10 | 11.0 | | 17.6 | | 17.6 |
| 12 | 12.0 | 17.60 | 17.6 | 17.60 | 18.2 |
| 12 | 13.0 | | 17.6 | | 17.5 |
| 14 | 14.0 | 17.62 | 17.6 | 17.62 | 18.2 |
| 14 | 15.0 | | 17.6 | | 17.5 |
| 16 | 16.0 | 17.62 | 17.6 | 17.62 | 18.2 |
| 16 | 17.0 | | 17.6 | | 17.3 |
| 18 | 18.0 | 17.63 | 17.6 | 17.63 | 18.1 |
| 18 | 19.0 | | 17.7 | | 17.2 |
| 20 | 20.0 | 17.65 | 17.6 | 17.65 | 18.1 |
| 20 | 21.0 | | 17.6 | | 18.4 |
| 22 | 22.0 | 17.65 | 17.6 | 17.65 | 18.1 |
| 22 | 23.0 | | 17.6 | | 18.9 |
| 24 | 24.0 | 17.65 | 17.6 | 17.65 | 18.1 |
| 24 | 25.0 | | 17.6 | | 18.8 |
| 26 | 26.0 | 17.65 | 17.6 | 17.65 | 18.05 |
| 26 | 27.0 | | 17.6 | | 18.6 |
| 28 | 28.0 | 17.65 | 17.6 | 17.65 | 18.0 |
| 28 | 29.0 | | 17.6 | | 17.7 |
| 30 | 30.0 | 17.65 | 17.6 | 17.65 | 18.0 |
| 30 | 31.0 | | 17.6 | | 17.4 |

Table 4 Comparison of System Frequencies (cycles/second) Obtained by Various Methods of Analysis Due to Case 2 Inputs for the Time Interval $0 \leq t_o \leq 8$ Seconds; ng = 270 (1-cos.25$\pi$3t)

| $t_o$ (sec) | $t_{ref}$ (sec) | $\bar{h}$ | | | $\alpha$ | | |
|---|---|---|---|---|---|---|---|
| | | Q.S. | P.T. | U.A.A. | Q.S. | P.T. | U.A.A. |
| 0 | 0 | 17.65 | 17.2 | 17.26 | 44.47 | 44.1 | 44.22 |
| 0 | 0.5 | | | 17.62 | | | 44.23 |
| 0 | 1.5 | | 17.7 | | | 45.2 | |
| 2 | 2.0 | 17.67 | 17.2 | 17.25 | 44.45 | 44.1 | 44.20 |
| 2 | 2.5 | | | 17.63 | | | 44.24 |
| 2 | 3.0 | | 17.7 | | | 45.1 | |
| 4 | 4.0 | 17.65 | 17.2 | 17.22 | 44.45 | 44.1 | 44.17 |
| 4 | 4.5 | | | 17.58 | | | 44.20 |
| 4 | 5.0 | | 17.7 | | | 45.1 | |
| 6 | 6.0 | 17.65 | 17.2 | 17.15 | 44.43 | 44.1 | 44.11 |
| 6 | 6.5 | | | 17.61 | | | 44.24 |
| 6 | 7.0 | | 17.7 | | | 45.0 | |
| 8 | 8.0 | 17.63 | 17.2 | 17.13 | 44.34 | 44.0 | 44.05 |
| 8 | 8.5 | | | 17.61 | | | 44.16 |
| 8 | 9.0 | | 17.7 | | | 44.8 | |

Table 5 Comparison of System Frequencies (cycles/second) Obtained by Various Methods of Analysis Due to Case 2 Inputs for the Time Interval $10 \leq t_o \leq 30$ Seconds; ng = 270 (1-cos.2513t)

| $t_o$ (sec) | $t_{ref}$ (sec) | $\bar{h}$ | | $\alpha$ | |
|---|---|---|---|---|---|
| | | Q.S. | P.T. | Q.S. | P.T. |
| 10 | 10.0 | 17.62 | 17.5 | 44.07 | 43.7 |
| 10 | 11.0 | | 17.6 | | 43.3 |
| 12 | 12.0 | 17.60 | 18.0 | 43.61 | 43.2 |
| 12 | 13.0 | | 17.5 | | 44.0 |
| 14 | 14.0 | 17.62 | 18.2 | 43.05 | 42.6 |
| 14 | 15.0 | | 17.5 | | 42.3 |
| 16 | 16.0 | 17.62 | 18.2 | 42.52 | 42.1 |
| 16 | 17.0 | | 17.3 | | 43.7 |
| 18 | 18.0 | 17.63 | 18.1 | 42.14 | 41.8 |
| 18 | 19.0 | | 17.2 | | 42.2 |
| 20 | 20.0 | 17.65 | 18.1 | 41.89 | 41.5 |
| 20 | 21.0 | | 18.5 | | 41.4 |
| 22 | 22.0 | 17.65 | 18.1 | 41.73 | 41.4 |
| 22 | 23.0 | | 18.9 | | 41.4 |
| 24 | 24.0 | 17.65 | 18.1 | 41.65 | 41.3 |
| 24 | 25.0 | | 18.8 | | 41.4 |
| 26 | 26.0 | 17.65 | 18.05 | 41.60 | 41.2 |
| 26 | 27.0 | | 18.6 | | 41.4 |
| 28 | 28.0 | 17.65 | 18.0 | 41.57 | 41.2 |
| 28 | 29.0 | | 17.7 | | 41.4 |
| 30 | 30.0 | 17.65 | 18.0 | 41.54 | 41.2 |
| 30 | 31.0 | | 17.4 | | 41.4 |

Table 6 Comparison of System Frequencies (cycles/second) Obtained by Various Methods of Analysis Due to Both Case 1 and Case 2 Inputs for the Time Interval $0 \leq t_o \leq 30$ Seconds; ng = 9g

| | | Case 1 | | | | Case 2 | | | |
|---|---|---|---|---|---|---|---|---|---|
| | | $\bar{h}$ | | $\alpha$ | | $\bar{h}$ | | $\alpha$ | |
| $t_o$ (sec) | $t_{ref}$ (sec) | Q.S. | P.T. | Q.S. | P.T. | Q.S. | P.T. | Q.S. | P.T. |
| 0 | 0 | 17.65 | 17.7 | 17.65 | 17.2 | 17.65 | 17.2 | 44.47 | 44.1 |
| 0 | 1 | | 17.7 | | 17.7 | | 17.7 | | 45.2 |
| 2 | 2 | 17.63 | 17.6 | 17.63 | 17.2 | 17.63 | 17.2 | 44.47 | 44.1 |
| 2 | 3 | | 17.6 | | 17.7 | | 17.7 | | 45.2 |
| 4 | 4 | 17.62 | 17.6 | 17.62 | 17.2 | 17.62 | 17.2 | 44.37 | 44.0 |
| 4 | 5 | | 17.6 | | 17.6 | | 17.7 | | 44.9 |
| 6 | 6 | 17.60 | 17.6 | 17.60 | 17.3 | 17.60 | 17.3 | 44.12 | 43.7 |
| 6 | 7 | | 17.6 | | 17.6 | | 17.6 | | 44.2 |
| 8 | 8 | 17.60 | 17.6 | 17.60 | 18.1 | 17.60 | 18.1 | 43.73 | 43.3 |
| 8 | 9 | | 17.6 | | 17.6 | | 17.6 | | 43.1 |
| 10 | 10 | 17.62 | 17.6 | 17.62 | 18.2 | 17.62 | 18.2 | 43.30 | 42.9 |
| 10 | 11 | | 17.6 | | 17.5 | | 17.5 | | 43.5 |
| 12 | 12 | 17.62 | 17.6 | 17.62 | 18.2 | 17.62 | 18.2 | 42.88 | 42.5 |
| 12 | 13 | | 17.6 | | 18.4 | | 18.5 | | 42.3 |
| 14 | 14 | 17.63 | 17.6 | 17.63 | 18.2 | 17.63 | 18.2 | 42.51 | 42.1 |
| 14 | 15 | | 17.6 | | 17.3 | | 17.3 | | 42.8 |
| 16 | 16 | 17.63 | 17.6 | 17.63 | 18.1 | 17.63 | 18.1 | 42.21 | 41.8 |
| 16 | 17 | | 17.7 | | 17.3 | | 17.3 | | 42.4 |
| 18 | 18 | 17.65 | 17.6 | 17.65 | 18.1 | 17.65 | 18.1 | 42.00 | 41.7 |
| 18 | 19 | | 17.6 | | 17.3 | | 17.3 | | 41.5 |
| 20 | 20 | 17.65 | 17.6 | 17.65 | 18.1 | 17.65 | 18.1 | 41.84 | 41.5 |
| 20 | 21 | | 17.6 | | 18.7 | | 18.7 | | 41.4 |
| 22 | 22 | 17.65 | 17.6 | 17.65 | 18.1 | 17.65 | 18.1 | 41.75 | 41.4 |
| 22 | 23 | | 17.6 | | 18.9 | | 18.9 | | 41.4 |

Table 6 (continued)

| | | Case 1 | | | | Case 2 | | | |
|---|---|---|---|---|---|---|---|---|---|
| | | $\bar{h}$ | | $\alpha$ | | $\bar{h}$ | | $\alpha$ | |
| $t_o$ (sec) | $t_{ref}$ (sec) | Q.S. | P.T. | Q.S. | P.T. | Q.S. | P.T. | Q.S. | P.T. |
| 24 | 24 | 17.65 | 17.6 | 17.65 | 18.1 | 17.65 | 18.1 | 41.3 | 41.68 |
| 24 | 25 | | 17.6 | | 18.9 | | 18.9 | 41.4 | |
| 26 | 26 | 17.65 | 17.6 | 17.65 | 18.1 | 17.65 | 18.1 | 41.3 | 41.63 |
| 26 | 27 | | 17.6 | | 18.7 | | 18.7 | 41.4 | |
| 28 | 28 | 17.65 | 17.6 | 17.65 | 18.1 | 17.65 | 18.1 | 41.2 | 41.59 |
| 28 | 29 | | 17.6 | | 18.4 | | 18.4 | 41.4 | |
| 30 | 30 | 17.65 | 17.6 | 17.65 | 18.0 | 17.65 | 18.0 | 41.2 | 41.54 |
| 30 | 31 | | 17.6 | | 17.4 | | 17.4 | 41.4 | |

## BIOGRAPHICAL SKETCH

E. J. Brunelle, Jr. was born on 17 March 1932 in Montpelier, Vermont. He was educated by the Montpelier School system and then entered the University of Michigan in 1949 where he received the B.S.E. (Aero.) and M.S.E. (Aero.) in 1954 and 1955 respectively. After working 15 months for the Bell Aircraft Corporation (Buffalo, N. Y.) as a structural research engineer, he entered M.I.T. in 1956 as a hopeful doctoral candidate. During the time he was studying and doing thesis research work as a research assistant and later as a project engineer he held, at various times, several additional jobs. These included, instructor in the evening school at Boston University, senior staff member at Allied Research Associates (a subsidiary of Boeing Aircraft Corporation), and consultant for Raytheon Manufacturing Company and Helioplane Aircraft Corporation. During this period he published four papers and/or reports in the areas of unsteady helicopter aerodynamics, differential equation systems with either time-varying coefficients or weak nonlinearities, and aerothermoelasticity.

At present he holds the rank of Assistant Professor of Aeronautical Engineering at Princeton University.

# BIBLIOGRAPHY


1. Ashley, H. and Zartarian, G., "Piston Theory - A New Aerodynamic Tool for the Aeroelastician," Journal of the Aeronautical Sciences, Vol. 23, No. 13, pp. 1109-1118, December 1956.
2. Evans, W. R., Control System Dynamics. McGraw-Hill Book Company, Inc., New York, New York, 1954, pp. 96-121.
3. Hedgepeth, J. M., "Flutter of Rectangular Simply Supported Panels at High Supersonic Speeds." Journal of the Aeronautical Sciences Vol. 24, No. 8, August 1957, pp. 563-573.
4. Pines, S., "An Elementary Explanation of the Flutter Mechanism." Proc. of the National Specialists Meeting on Dynamics and Aeroelasticity, pp. 52-56.
5. Dugundji, J., and Crisp, J. D. C., On the Aeroelastic Characteristics of Low Aspect Ratio Wings with Chordwise Deformations. OSR Technical Note No. 59-787. Office of Scientific Research, United States Air Force, July 1959, pp. 54-59.
6. Hildebrand, F. B., Advanced Calculus for Engineers. Prentice-Hall, Inc., Englewood Cliffs, N. J., 1949, pp. 196-197.
7. Garber, T. B., "On the Rotational Motion of a Body Re-Entering the Atmosphere." Journal of the Aero/Space Sciences. Vol. 26, No. 7, July 1959, pp. 443-449.
8. Kelly, R. E., The Response of Aircraft Structural Systems with Time-Variant Parameters. Aero. Eng. Thesis, Department of Aeronautics and Astronautics, Mass. Inst. of Technology, Cambridge, Mass., June 1959.
9. Collar, A. R., "On the Stability of Accelerated Motion; Some Thoughts on the Evaluation of Linear Differential Equations with Variable Coefficients." Aeronautical Quarterly, Vol. VIII, Nov. 1957, pp. 315-317.

10. Squire, W., "Approximate Solution of Linear Second-Order Differential Equations." Journal of the Royal Aeronautical Society, Vol. 63, No. 582, June 1959, pp. 368-369.

11. Reed, W. H., III, "Effects of a Time-Varying Test Environment on the Evaluation of Dynamic Stability with Application to Flutter Testing." Journal of the Aero/Space Sciences, Vol. 25, No. 7, July 1958, pp. 437-439.

12. Brunelle, E. J., Jr., Transient and Non-Linear Effects on High Speed, Vibratory Thermoelastic Instability Phenomena, WADD Technical Report 60-484 Part I - Theoretical Considerations, July 1960.

13. Zadeh, L., "Frequency Analysis of Variable Networks." Proceedings of the I.R.E., March 1950, p. 295.

14. Merrick, V. K., "The Influence of Rate of Change of Altitude and Acceleration on the Longitudinal Dynamic Stability of Aircraft and Missiles." Proc. of the National Specialists Meeting on Dynamics and Aeroelasticity, pp. 121-123.

15. Laning, J. H., and Battin, R. H., Random Processes in Automatic Control, McGraw-Hill Book Company, Inc., New York, 1956, pp. 225-239.

16. Tsien, H. S., Engineering Cybernetics, McGraw-Hill Book Company, Inc., New York, 1954, pp. 123-127.

17. Cramér, H., The Elements of Probability Theory, John Wiley and Sons, New York, 1955, pp. 81-82.

18. Rice, S. O., "Mathematical Analysis of Random Noise." Selected Papers on Noise and Stochastic Processes, edited by Nelson Wax, Dover Publications, Inc., New York, 1954, pp. 184-246.

19. Mott-Smith, H. M., "The Solution of the Boltzmann Equation for a Shock Wave," The Physical Review, Vol. 82, No. 6, June 1951, pp. 885-892.

20. Bisplinghoff, R. L., Ashley, H., Halfman, R. L., Aeroelasticity, Addison-Wesley Publishing Company, Inc., Cambridge 42, Mass., 1955, pp. 685-694.

21. Bisplinghoff, R. L. Pian, T. H. H., Foss, K. A., Response of Elastic Aircraft to Continuous Turbulence, Rept. 117, Advisory Group for Aeronautical Research and Development, North Atlantic Treaty Organization, Palais de Chaillot, Paris 16, April-May 1957.

22. Fung, Y. C., The Theory of Aeroelasticity, John Wiley and Sons, Inc., New York, 1955, pp. 283-309.

23. Fung, Y. C., "Statistical Aspects of Dynamic Loads," Journal of the Aeronautical Sciences, Vol. 20, No. 5, May 1953, pp. 319-330.

24. Fung, Y. C., "Dynamic Stresses in Aircraft Landing," Journal of Applied Mechanics, Vol. 22, No. 4, Dec. 1955, pp. 449-457.

25. Thorson, K. R., Bohne, Q. R., "Application of Power Spectral Methods in Airplane and Missile Design," Journal of the Aerospace Sciences, Vol. 27, No. 2, Feb. 1960, pp. 107-116.

26. Bieber, R. E., "Missile Structural Loads by Nonstationary Statistical Methods," Journal of the Aerospace Sciences, Vol. 28, No. 4, April 1961, pp. 284-294.

27. Acker, C., An Analysis of the Vertical Acceleration Response of a Two-Dimensional Wing to a Non-Stationary Random Gust Input. Master's Thesis, Department of Aeronautics, Princeton University, Princeton, New Jersey, Sept. 1961.

28. Liepmann, H. W., "On the Application of Statistical Concepts to the Buffeting Problem," Journal of the Aeronautical Sciences, Vol. 19, No. 12, Dec. 1952, pp. 793-800, 822.

29. Lindstedt, A., "Differentialgleichungen der Storungstheorie," Mémoires de l'Academie Impériale des Sciences de St.Péterbourg, Vol. 31, No. 4, 1883.

30. Poincaré, H., "Sur les courbes définies par une équation différentielle," Journal de Mathématiques, 8, 1882.

31. Poincaré, H., Les Methodes Nouvelles de la Mécanique Céleste, Vols. I, II, Gauthier-Villars, Paris, 1892, 1893.

32. Liapounoff, M. A., "Problème général de la stabilité du mouvement," Communications de la Societé Mathématique de Kharkow, 1893.

33. Bendixon, I., "Sur les courbes définies par les équations différentielles," Acta Mathematica, 24, 1901, pp. 1-88.

34. van der Pol, B., "On Relaxation Oscillations," Philosophical Magazine, Sec. 7, 2, 1926, pp. 978-992.

35. Liénard, A., "Étude des oscillations entretenues," Revue Générale de l'Électricité, 23, 1928, pp. 901-946.

36. Kryloff, N., Bogoliuboff, "Quelques exemples d'oscillations non-linéaires," Comptes rendus des seances de l'Académie des Sciences de Paris, t. 194, 1932, pp. 957-960.

37. Kryloff, N., Bogoliuboff, "Problèmes fondamentaux de la mécanique non linéaire" (en russe), Bulletin de l"Académie des Sciences de l'URSS, 1933, pp. 475-498.

38. Kryloff, N., Bogoliuboff, "L'application des méthodes de la mécanique non linéaire à la théorie des perturbations des systèmes canoniques" (Monographie en francais), Ukrainska akad. nauk, Inst. mécanique, Rapport No. 4., Kieff, 1934.

39. Kryloff, N., Bogoliuboff, "Sur quelques développments formels en séries dans la mécanique non linéaire" (Monographie en ukrainien avec un résumé en francais), Ukrainska akad. nauk, Inst. mécanique, Rapport No. 5, Kieff, 1934.

40. Kryloff, N., Bogoliuboff, "Méthodes de la mécanique non linéaire appliquées a l'étude des oscillations stationnaires." (Monographie en russe avec un résumé en francais), Ukrainska akad. nauk, Inst. mécanique, Rapport No. 8, Kieff, 1934.

41. Kryloff, N., Bogoliuboff, "Méthodes approchées de la mécanique non linéaire dans leur application à l'étude de la perturbation des mouvements périodiques et le divers phénomènes de résonance s'y rapportant" (Monographie en francais), Ukrainska akad. nauk, Inst. mécanique, Rapport No. 14, Kieff, 1935.

42. Kryloff, N., Bogoliuboff, "Introduction à la mécanique non-linéaire: les méthodes approchées et asymptotiques" Ukrainska akad. nauk, Inst. de la mécanique, Chaire de phys. math. Annales, t. 1-2, 1937.

43. Mandelstam, L., Papalexi, N., "Uber Resonanzerscheinungen bei Frequenzteilung," Zeitschrift fur Physik, Vol. 73, 1932.

44. Mandelstam, L., Papalexi, N., et al., "Exposé des recherches récentes sur les oscillations non linéaires," Journal Tekhnitcheskoi Fisiki, 5, Moscow, USSR, 1935, pp. 81-134.

45. Lefschetz, S., Contributions to the Theory of Nonlinear Oscillations, Vols. I through V, Princeton University Press, Princeton, New Jersey.

46. Ku, Y. H., Analysis and Control of Nonlinear Systems, The Ronald Press Company, New York, 1958, pp. 323-350.

47. Minorsky, N., Introduction to Non-Linear Mechanics, J. W. Edwards, Ann Arbor, Michigan, 1947.

48. Proskuriakov, A. P., "On the Construction of Periodic Solutions of Autonomous Systems with One Degree of Freedom," PMM, Vol. 21, No. 4, 1957, pp. 585-590.

49. Laricheva, V. V., "Nonlinear Damping of the Natural Vibrations of Systems of Arbitrary Order," PMM, Vol. 22, No. 4, 1958, pp. 536-538.

50. Proskuriakov, A. P., "On Ways of Introducing a Small Parameter into Equations of Nonlinear Vibrations," PMM, Vol. 22, No. 5, 1958, pp. 711-713.

51. Aizerman, M. A., Gantmakher, F. R., "On the Stability of Periodic Motions," PMM, Vol. 22, No. 6, 1958, pp. 750-758.

52. Kharasakhal, V. Kh., "Almost-Periodic Solutions of Non-Linear Systems of Differential Equations," PMM, Vol. 24, No. 3, 1960.

53. Plotnikova, G. V., "On the Construction of Periodic Solutions of a Nonautonomous Quasi-Linear System with Two Degrees of Freedom," PMM, Vol. 24, No. 5, 1960, pp. 933-937.

54. Proskuriakov, A. P., "Periodic Oscillations of Quasilinear Autonomous Systems with Two Degrees of Freedom," PMM, Vol. 24, No. 6, 1960, pp. 1103-1109.

55. Cesari, L., Asymptotic Behavior and Stability Problems in Ordinary Differential Equations, Ergbn. d. Mathematik und ih. Grenzgebiete, Heft, 16, 1959.

56. Malkin, I. G., Certain Problems in the Theory of Nonlinear Oscillations, (in Russian) Gostekhizdat, 1956.

57. Bogoliuboff, N., Mitropolsky, Yu. A., Asymptotic Methods in the Theory of Nonlinear Oscillations, (in Russian) Gostekhizdat, 1955.

58. Fung, Y. C., "On Two-Dimensional Panel Flutter," Journal of the Aeronautical Sciences, Vol. 25, No. 3, March 1958, pp. 145-160.

59. Shen, S. F., "An Approximate Analysis of Nonlinear Flutter Problems," Journal of the Aero/Space Sciences, Vol. 26, No. 1, January 1959, pp. 25-32, 45.

60. Woolston, D. S., Runyan, H. L., Andrews, R. E., "An Investigation of Effects of Certain Types of Structural Nonlinearities on Wing and Control Surface Flutter," Journal of the Aeronautical Sciences, Vol. 24, No. 1, January 1957, pp. 57-63.

61. Cesari, L., Existence Theorems for Periodic Solutions of Nonlinear Differential Systems, RIAS Technical Report 60-8, March 1960.

62. Hale, J. K., On the Method of Kylov-Bogoliubov-Mitropolski for the Existence of Integral Manifolds of Perturbed Differential Systems, RIAS Technical Report 60-1, January 1960.

63. Hale, J. K., Behavior of Solutions Near Integral Manifolds, RIAS Technical Report 60-10, March 1960.

64. Hale, J. K., On the Method of Averaging, RIAS Technical Report 60-13, May 1960.

65. Budiansky, B., and Mayers, J., "Influence of Aerodynamic Heating on the Effective Torsional Stiffness of Thin Wings," pp. 1081-1093, Vol. 23, No. 12, December 1956, Journal of the Aeronautical Sciences.

66. Bisplinghoff, R. L., and Dugundji, J., "Influence of Aerodynamic Heating on Aeroelastic Phenomena." Monograph reprinted from High Temperature Effects in Aircraft Structures, AGARDograph No. 28, N. J. Hoff editor, Pergamon Press, London, 1959.

67. Singer, J., "Thermal Buckling of Solid Wings of Arbitrary Aspect Ratio," pp. 573-580, Journal Aero/Space Sciences, Vol. 25, No. 9, September 1958.

68. Runyan, H. L., and Morgan, H. G., "Flutter at Very High Speeds," NASA TN D-942, August 1961.

69. Hayes, W. D., "On Hypersonic Similitude," Quarterly Journal of Applied Mathematics, Vol. 5, No. 1, April 1947, pp. 105-106.

70. Lighthill, M. J., "Oscillating Airfoils at High Mach Number," Journal of the Aeronautical Sciences, Vol. 20, No. 6, June 1953, pp. 402-406.

71. Lomax, H., Heaslet, M. A., Fuller, F. B., and Sluder, L., "Two and Three-Dimensional Unsteady Lift Problems in High Speed Flight," NACA Report 1077, 1952.

72. Miles, J. W., "Unsteady Supersonic Flow," Chapter 13, Monograph prepared for the Air Research and Development Command, U.S.A.F., March 1955.

73. Evvard, J., "Use of Source Distributions for Evaluating Theoretical Aerodynamics of Thin Finite Wings at Supersonic Speeds," NACA TR 951, 1950.

74. Krasil-shchikova, E. A., "Effect of the Tip Edge on the Motion of a Wing at Supersonic Speeds," D.A.N., Vol. LVIII, No. 4, 1947 and "Effect of the Vortex Sheet for Steady Motion of a Wing at Supersonic Speeds," D.A.N., Vol. LVIII, No. 6, 1947.

75. Rogers, M., "Aerothermoelasticity," Journal of Aero/Space Engineering, Vol. 17, No. 10, October 1958, p. 35.

76. Space Handbook - Astronautics and its Applications, by Robert W. Buchhiem and the Staff of The Rand Corporation, Random House, New York, 1959.